6-1979

An Investigation of High Order and Low Order Dynamic Modeling of a Complete Pressurized Water Reactor Nuclear Power Plant

James Downing Freels
University of Tennessee - Knoxville

To the Graduate Council:

I am submitting herewith a thesis written by James Downing Freels entitled "An Investigation of High Order and Low Order Dynamic Modeling of a Complete Pressurized Water Reactor Nuclear Power Plant." I have examined the final electronic copy of this thesis for form and content and recommend that it be accepted in partial fulfillment of the requirements for the degree of Master of Science, with a major in Nuclear Engineering.

T. W. Kerlin, Major Professor

We have read this thesis and recommend its acceptance:

P. F. Pasqua, E. M. Katz, T. W. Reddoch

Accepted for the Council:
Carolyn R. Hodges

Vice Provost and Dean of the Graduate School

(Original signatures are on file with official student records.)

To the Graduate Council:

I am submitting herewith a thesis written by James Downing Freels entitled "An Investigation of High Order and Low Order Dynamic Modeling of a Complete Pressurized Water Reactor Nuclear Power Plant." I recommend that it be accepted in partial fulfillment of the requirements for the degree of Master of Science, with a major in Nuclear Engineering.

T. W. Kerlin, Major Professor

We have read this thesis
and recommend its acceptance:

Accepted for the Council:

Vice Chancellor
Graduate Studies and Research

AN INVESTIGATION OF HIGH ORDER AND LOW ORDER DYNAMIC MODELING OF A COMPLETE PRESSURIZED WATER REACTOR NUCLEAR POWER PLANT

A Thesis

Presented for the

Master of Science

Degree

The University of Tennessee, Knoxville

James Downing Freels

June 1979

ACKNOWLEDGEMENTS

The author would like to thank Dr. T. W. Kerlin, the major professor, and Dr. E. M. Katz, the research advisor, for their guidance, encouragement, and valuable suggestions during the development of this thesis.

He wishes to thank Dr. P. F. Pasqua, head of the Nuclear Engineering Department, for making the research for this thesis possible through a graduate research assistantship.

A special thanks is given to Dr. T. W. Reddoch, of the Electrical Engineering Department, for his teaching which made the understanding and incorporation of the megawatt-frequency controller model possible.

Much appreciation is given to Mrs. Gail Colson for her skills and effort in typing this thesis.

The members of the staff of the University of Tennessee Computing Center are appreciated for their constant advice and the use of their facilities.

The author would like to express extreme gratitude to his wife, Elizabeth Freels, for her patience and understanding during the course of this graduate study.

ABSTRACT

A reference high order PWR system model was developed resulting in a 57th order, lumped parameter, state variable dynamic model. Included in the model are representations of the reactor core, pressurizer, U-tube recirculation type steam generator, connecting piping, and turbine-feedwater heaters. Also included are the models of three-element feedwater flow control, nonlinear reactor control, pressurizer pressure control, and megawatt-frequency turbine control systems.

A low order PWR system model was developed by reducing the 57th order model to a 25th order model by physical methods.

A further reduction on the low order model was demonstrated by a numerical method called the "pole-zero deletion method."

The results of the physically reduced low order model were compared to the results of the reference high order model. This comparison showed that the low order model could simulate the desired output of turbine shaft power equally as well as the reference high order model. Other intermediate system outputs were also shown to give good results for the low order model as compared to the reference high order model.

TABLE OF CONTENTS

LIST OF TABLES

LIST OF FIGURES

CHAPTER I

INTRODUCTION

I.1 Purpose of This Research

The purpose of a pressurized water reactor (hereafter referred to as PWR) nuclear power plant is to produce electrical power and inject this power into an electrical system grid. During the process of electricity production, it is desirable for a PWR to help maintain stability within the total system, and operate as economically as possible, under normal and abnormal conditions. It is not feasible to examine PWR system behavior by creating major power system disturbances. Thus the need arises for modeling and simulation of a complete PWR system.

The Electric Power Research Institute (hereafter referred to as EPRI), which was the sponsors of this research, has developed a computer code called LOTDYS. LOTDYS stands for "long term system dynamics." LOTDYS simulates a complete electrical system grid. The intent of LOTDYS is to examine the effect of slow boiler dynamics (both conventional and nuclear) on the much faster electrical system dynamics. The current version of LOTDYS does not include a representation of a PWR. The goal of this project is to develop a PWR model suitable for use by the LOTDYS program.

I.2 General Considerations and Previous Development

The LOTDYS program is a very large code which includes representations for generating units (hydro, coal fired, and boiling water reactors), transmission systems, transformers, loads, etc. LOTDYS presently requires a great deal of computer memory. A new addition to the LOTDYS program should require as little additional computer memory as possible, while still correctly simulating the operating features of a PWR. This is equivalent to saying that the PWR representation should be a low order model.

The inputs available to the PWR model from the LOTDYS program include the electrical system frequency and the automatic generation control signal (power control signal). The only output necessary from the PWR model to the LOTDYS program is the turbine mechanical shaft power. However other intermediate outputs from the PWR model might be desirable such as reactor power, steam generator pressure, etc.

At the Department of Nuclear Engineering of The University of Tennessee, previous research has been done in PWR power plant dynamics.[2,6,13,17,18,35,37] This work has resulted in representations for the reactor core, piping, pressurizer, steam generators, and feedwater flow control systems. This thesis will include the results similar to previous work with development of additional models necessary to couple the PWR model with LOTDYS.

I.3 Organization of the Text

Following this introductory chapter, a reference high order PWR system model is presented in Chapter II. Two methods of reducing the high order model are presented in Chapter III. The first method reduces the high order model by "physical methods." The second method reduces the order of the system by a numerical development called the "pole-zero deletion method." In Chapter IV, a comparison is made between the reference high order model and the physically reduced low order model results. Some overall conclusions and recommendations for further research in low order modeling are discussed in Chapter V.

In the appendixes, three major areas are discussed. Two computer codes, which were developed, or modified during the course of this research, are described and instructions for their operation are included. All the dynamic model derivations, which are new to the Department of Nuclear Engineering of the University of Tennessee, are presented. In addition, some figures, which have been referred to in the main body of the text, are included in the appendix for clarity.

CHAPTER II

THE HIGH ORDER MODEL

II.1 The Reactor Core

The reactor core model used in this development is a typical representation of PWRs manufactured today. A typical reactor core and vessel internals are shown in Figure 2.1. The reactor coolant enters the vessel from the cold leg piping, through nozzles which are slightly above the core, and flows down through the annular region between the vessel wall and the core barrel, and into the lower plenum. The coolant enters the core at the bottom and flows up through the core. All the coolant, upon leaving the core, is then mixed together in the upper plenum before leaving the reactor vessel through nozzles and flowing into the hot leg piping.

The theoretical model representing a typical PWR reactor core consists of a set of first order linear differential equations. The equations represent the reactor kinetics, the core heat transfer, and the transport of coolant in the piping connecting the core to the steam generators and pressurizer. The coolant is assumed to be well mixed at each node in the model. The coolant flow rate is assumed to be constant. The reader should refer to Katz[13] and Kerlin[16] for additional information on the derivation of these equations. The equations for the reactor core are given below.

$$\frac{d\,\delta P/P_0}{dt} = -\frac{\beta_T}{\Lambda}\frac{\delta P}{P_0} + \sum_{i=1}^{6}\lambda_i\,\delta C_i + \frac{\beta_T}{\Lambda}\delta\rho_{ext} + \frac{\alpha_c}{2\Lambda}(\delta\Theta_1 + \delta\Theta_2) + \frac{\alpha_F}{\Lambda}\delta T_F + \frac{\alpha_P}{\Lambda}\delta P_P \tag{II.1}$$

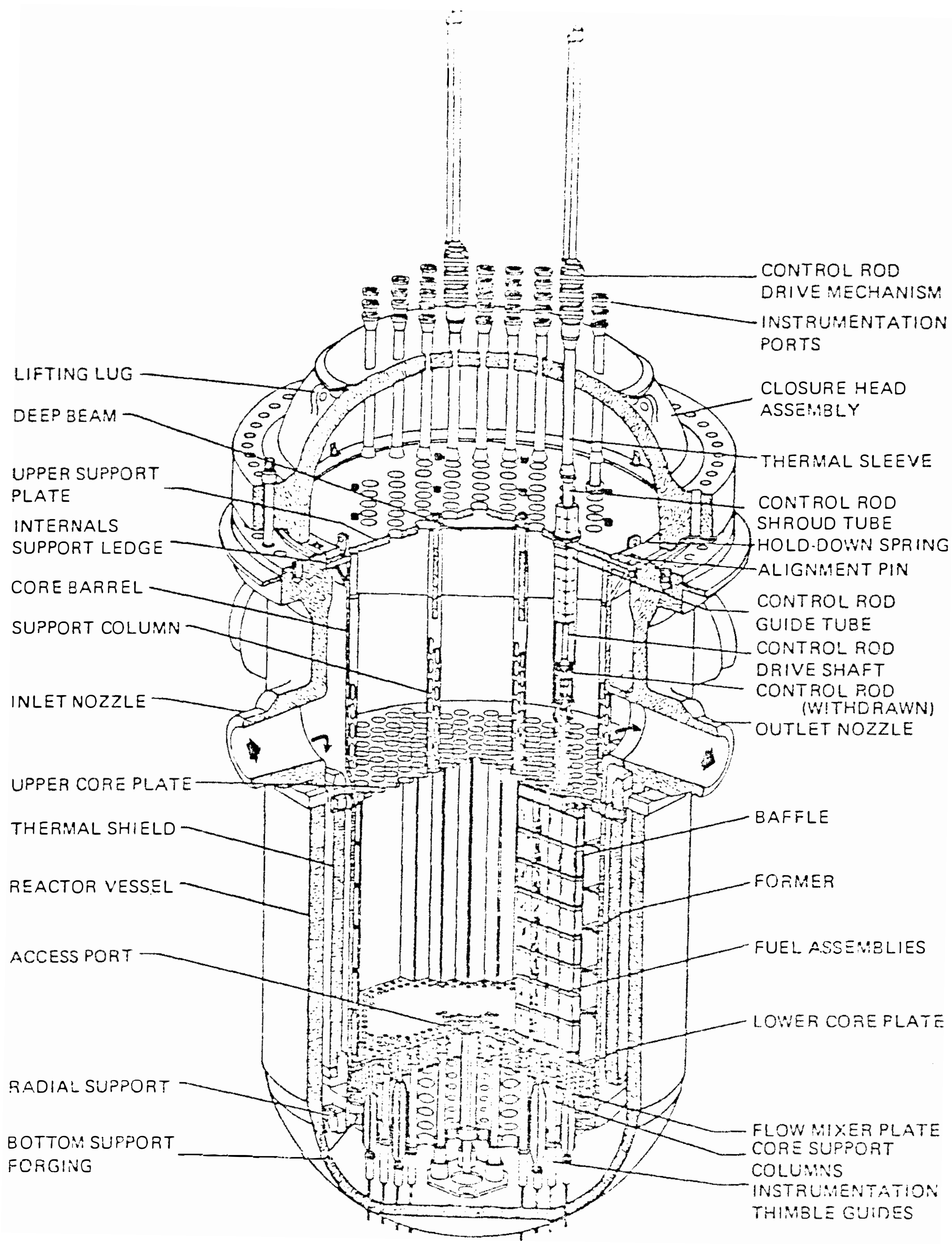

Figure 2.1 A typical PWR reactor core and vessel internals.

(II.2) $$\frac{d\,\delta C_1}{dt} = \frac{\beta_1}{\Lambda}\,\frac{\delta P}{P_0} - \lambda_1\,\delta C_1$$

(II.3) $$\frac{d\,\delta C_2}{dt} = \frac{\beta_2}{\Lambda}\,\frac{\delta P}{P_0} - \lambda_2\,\delta C_2$$

(II.4) $$\frac{d\,\delta C_3}{dt} = \frac{\beta_3}{\Lambda}\,\frac{\delta P}{P_0} - \lambda_3\,\delta C_3$$

(II.5) $$\frac{d\,\delta C_4}{dt} = \frac{\beta_4}{\Lambda}\,\frac{\delta P}{P_0} - \lambda_4\,\delta C_4$$

(II.6) $$\frac{d\,\delta C_5}{dt} = \frac{\beta_5}{\Lambda}\,\frac{\delta P}{P_0} - \lambda_5\,\delta C_5$$

(II.7) $$\frac{d\,\delta C_6}{dt} = \frac{\beta_6}{\Lambda}\,\frac{\delta P}{P_0} - \lambda_6\,\delta C_6$$

(II.8) $$\frac{d\,\delta T_F}{dt} = \frac{f P_0}{(mc_p)_F}\,\frac{\delta P}{P_0} + \frac{hA}{(mc_p)_F}\left(\delta\Theta_1 - \delta T_F\right)$$

(II.9) $$\frac{d\,\delta\Theta_1}{dt} = \frac{(1-f)P_0}{(mc_p)_c}\,\frac{\delta P}{P_0} + \frac{hA}{(mc_p)_c}\left(\delta T_F - \delta\Theta_1\right) + \left(\frac{\dot m}{m}\right)_c\left(\delta\Theta_{LP} - \delta\Theta_1\right)$$

(II.10) $$\frac{d\,\delta\Theta_2}{dt} = \frac{(1-f)P_0}{(mc_p)_c}\,\frac{\delta P}{P_0} + \frac{hA}{(mc_p)_c}\left(\delta T_F - \delta\Theta_1\right) + \left(\frac{\dot m}{m}\right)_c\left(\delta\Theta_1 - \delta\Theta_2\right)$$

(II.11) $$\frac{d\,\delta\Theta_{UP}}{dt} = \left(\frac{\dot m}{m}\right)_{UP}\left(\delta\Theta_2 - \delta\Theta_{UP}\right)$$

$$\frac{d\delta T_{HL}}{dt} = \left(\frac{\dot{M}}{M}\right)_{HL} \left(\delta\Theta_{UP} - \delta T_{HL}\right) \tag{II.12}$$

$$\frac{d\delta\Theta_{LP}}{dt} = \left(\frac{\dot{M}}{M}\right)_{LP} \left(\delta T_{CL} - \delta\Theta_{LP}\right) \tag{II.13}$$

$$\frac{d\delta T_{CL}}{dt} = \left(\frac{\dot{M}}{M}\right)_{CL} \left(\delta T_{PL_o} - \delta T_{CL}\right). \tag{II.14}$$

The essential design parameters needed to generate the model coefficients are given in Table I. The numerical value of the parameters listed in this table are typical of a Westinghouse PWR plant. However, a PWR of another manufacturer could also be modeled given these essential design parameters. A computer program for generating the coefficients of these equations has been written and is described in Appendix A.

The resulting equations will describe the dynamics of the reactor core with 14 state variables. Table II is a list and description of these state variables. The reactor core equations will also have 2 disturbance or forcing terms appearing in equation (II.1), describing the fractional change in power, and equation (II.14), which describes the change in cold leg temperature. These forcing terms are listed below.

$$f(1) = \frac{\beta_T}{\Lambda} \delta\rho_{ext} \tag{II.15}$$

$$f(14) = \left(\frac{\dot{M}}{M}\right)_{CL} \delta T_{PL_o} \tag{II.16}$$

TABLE I

ESSENTIAL DESIGN PARAMETERS FOR THE REACTOR CORE MODEL

1.	1st Delayed Neutron Group Fraction β_1	0.000209
2.	2nd Delayed Neutron Group Fraction β_2	0.001414
3.	3rd Delayed Neutron Group Fraction β_3	0.001309
4.	4th Delayed Neutron Group Fraction β_4	0.002727
5.	5th Delayed Neutron Group Fraction β_5	0.000925
6.	6th Delayed Neutron Group Fraction β_6	0.000314
7.	Total Delayed Neutron Group Fraction β_T	0.006898
8.	1st Group Decay Constant (1/sec) λ_1	0.0125
9.	2nd Group Decay Constant (1/sec) λ_2	0.0308
10.	3rd Group Decay Constant (1/sec) λ_3	0.1140
11.	4th Group Decay Constant (1/sec) λ_4	0.3070
12.	5th Group Decay Constant (1/sec) λ_5	1.1900
13.	6th Group Decay Constant (1/sec) λ_6	3.1900
14.	Neutron Generation Time (sec) Λ	17.9×10^{-6}
15.	Fuel Coefficient of Reactivity (1/°F) α_F	-1.1×10^{-5}
16.	Coolant Coefficient of Reactivity (1/°F) α_c	-2.0×10^{-4}
17.	Pressure Coefficient of Reactivity (1/psi) α_p	-1.0×10^{-6}
18.	Initial power level (MWt) P_o	3436.0
19.	Mass of Fuel (lbm) M_F	222739.0
20.	Specific Heat of the Fuel (B/lbm-F) C_{PF}	0.059
21.	Total Heat Transfer Area (ft^2) A	59900.0
22.	Fraction of the Total Power Produced in the Fuel f	0.974

TABLE I (continued)

23.	Overall Heat Transfer Coefficient From Fuel to Coolant (B/hr-ft^2-F) h	200.0
24.	Volume of Coolant in Upper Plenum (ft^3) V_{UP}	1376.0
25.	Volume of Coolant in Lower Plenum (ft^3) V_{LP}	1791.0
26.	Volume of Coolant in Hot Leg Piping (ft^3) V_{HL}	250.0
27.	Volume of Coolant in Cold Leg Piping (ft^3) V_{CL}	500.0
28.	Total Volume of Coolant in Core (ft^3) V	540.0
29.	Total Mass Flow Rate in Core (lbm/hr) $\dot{m}$	$1.5\text{x}10^{+8}$
30.	Hot Leg Temperature at 100% Power (°F) T_{HL}	592.5
31.	Cold Leg Temperature at 100% Power (°F) T_{CL}	542.5
32.	Nominal Reactor Coolant System Pressure (psia) P_{Po}	2250.0
33.	Coolant Density at System Pressure and Average Temperature (lbm/ft^3) ρ_C	45.71
34.	Coolant Specific Heat at System Pressure and Average Temperature (B/lbm-°F) C_{PC}	1.390

TABLE II

LIST AND DESCRIPTION OF THE HIGH ORDER REACTOR CORE MODEL STATE VARIABLES

NUMBER	SYMBOL	DESCRIPTION
1.	$\delta P / P_0$	Fractional Change in Initial Power
2.	δC_1	Precursor 1 Deviation
3.	δC_2	Precursor 2 Deviation
4.	δC_3	Precursor 3 Deviation
5.	δC_4	Precursor 4 Deviation
6.	δC_5	Precursor 5 Deviation
7.	δC_6	Precursor 6 Deviation
8.	δT_f	Fuel Temperature Deviation (°F)
9.	$\delta \Theta_1$	Coolant Node 1 Temperature Deviation (°F)
10.	$\delta \Theta_2$	Coolant Node 2 Temperature Deviation (°F)
11.	$\delta \Theta_{UP}$	Upper Plenum Temperature Deviation (°F)
12.	δT_{HL}	Hot Leg Temperature Deviation (°F)
13.	$\delta \Theta_{LP}$	Lower Plenum Temperature Deviation (°F)
14.	δT_{CL}	Cold Leg Temperature Deviation (°F)

The forcing term in equation (II.14) (which is equation(II.16)) will become a coupling term when the core model is coupled with a steam generator model. In order to verify the validity of the reactor model, a case was run for each of these two disturbances. Only the fractional change in power (state variable 1) and the hot leg temperature (state variable 12) are plotted. These will be the coupling terms for additional models added later. Figure 2.2 shows the response of the fractional power and hot leg temperature to a +10 cent step in reactivity. Figure 2.3 shows the response of the fractional power and hot leg temperature to a +10 F step in the inlet coolant temperature. The response is plausible and is consistent with similar modeling done previously. (Kiser[18], Cherng[6])

II.2 The Steam Generator

The steam generator considered in this work is a vertical, U-tube, recirculation type steam generator (hereafter abbreviated by UTSG). This type of steam generator is used by such vendors as Westinghouse and Combustion Engineering. Figure 2.4 shows a typical UTSG.

The reactor coolant from the hot leg piping enters at the bottom of the UTSG through the inlet nozzle to an inlet mixing plenum. Then the coolant flows through the U-tubes, transferring energy to the secondary fluid outside the tubes. The coolant then enters an outlet mixing plenum before leaving the system through the outlet nozzles into the cold leg piping.

The secondary feedwater to the UTSG enters through a feedwater nozzle just above the U-tubes. It mixes with recirculated water and

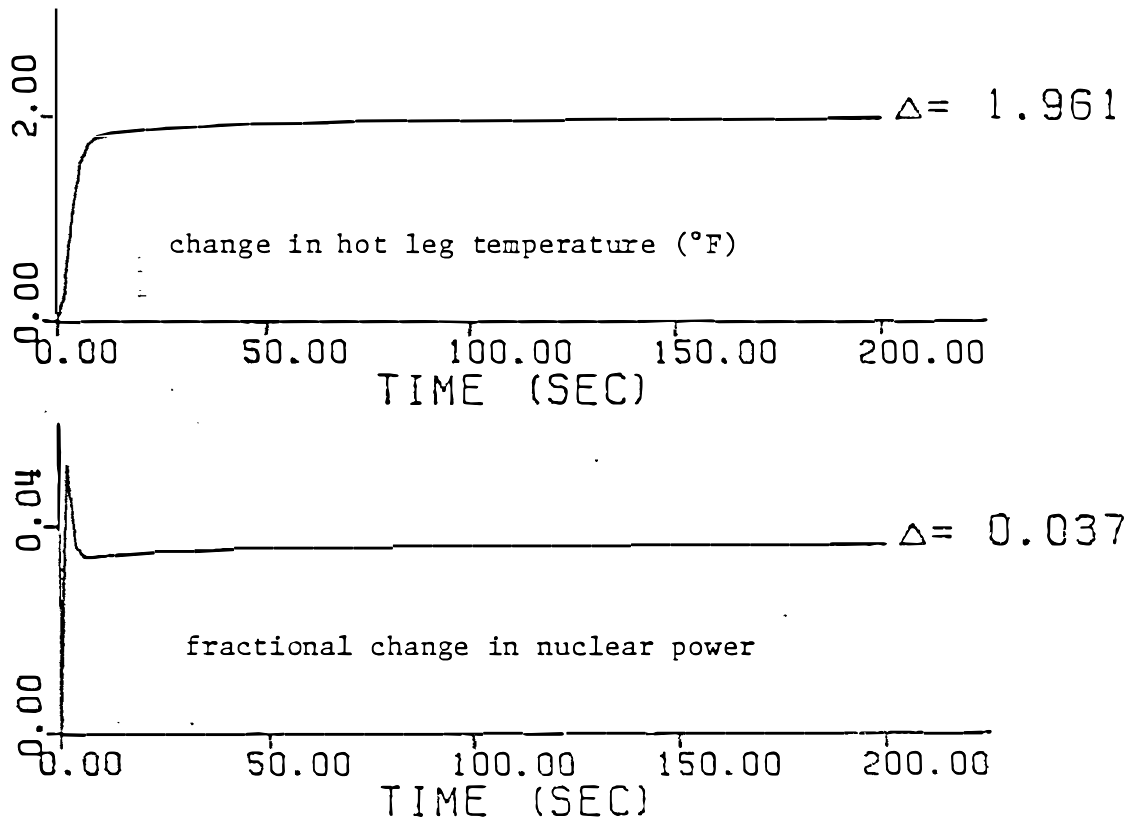

Figure 2.2 Response of the high order core model for a +10 cent step in reactivity.

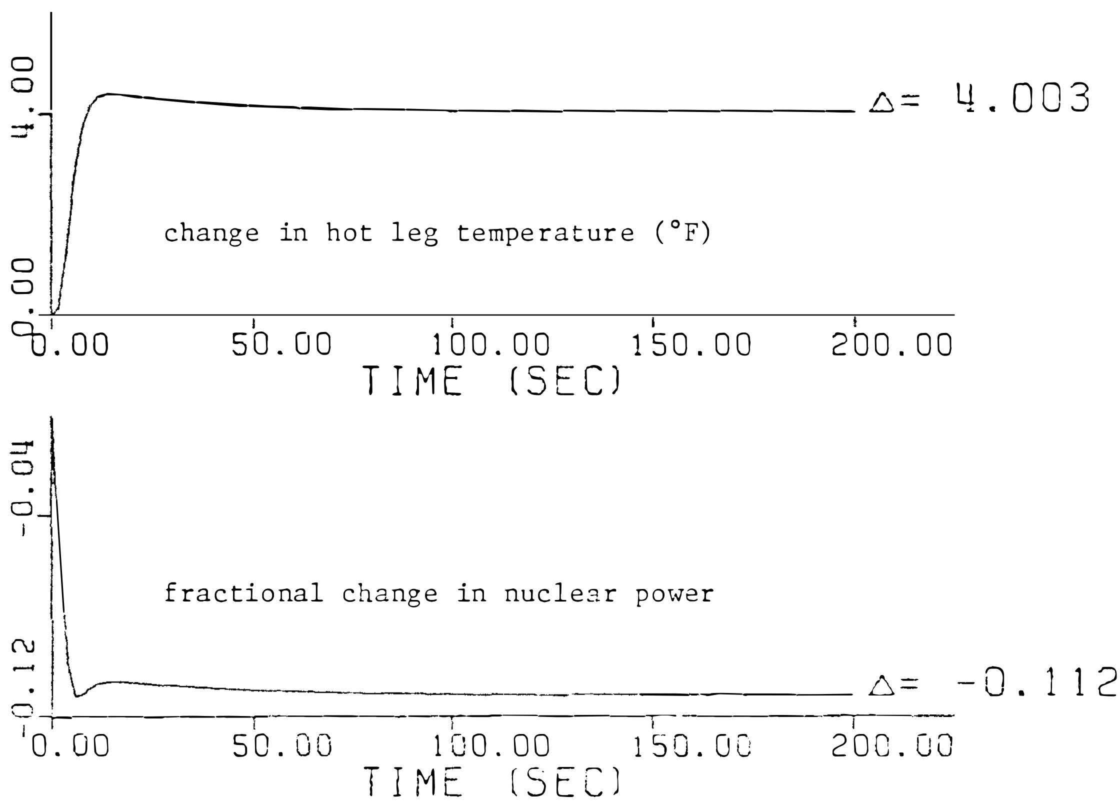

Figure 2.3 Response of the high order core model for a +10°F step in inlet coolant temperature.

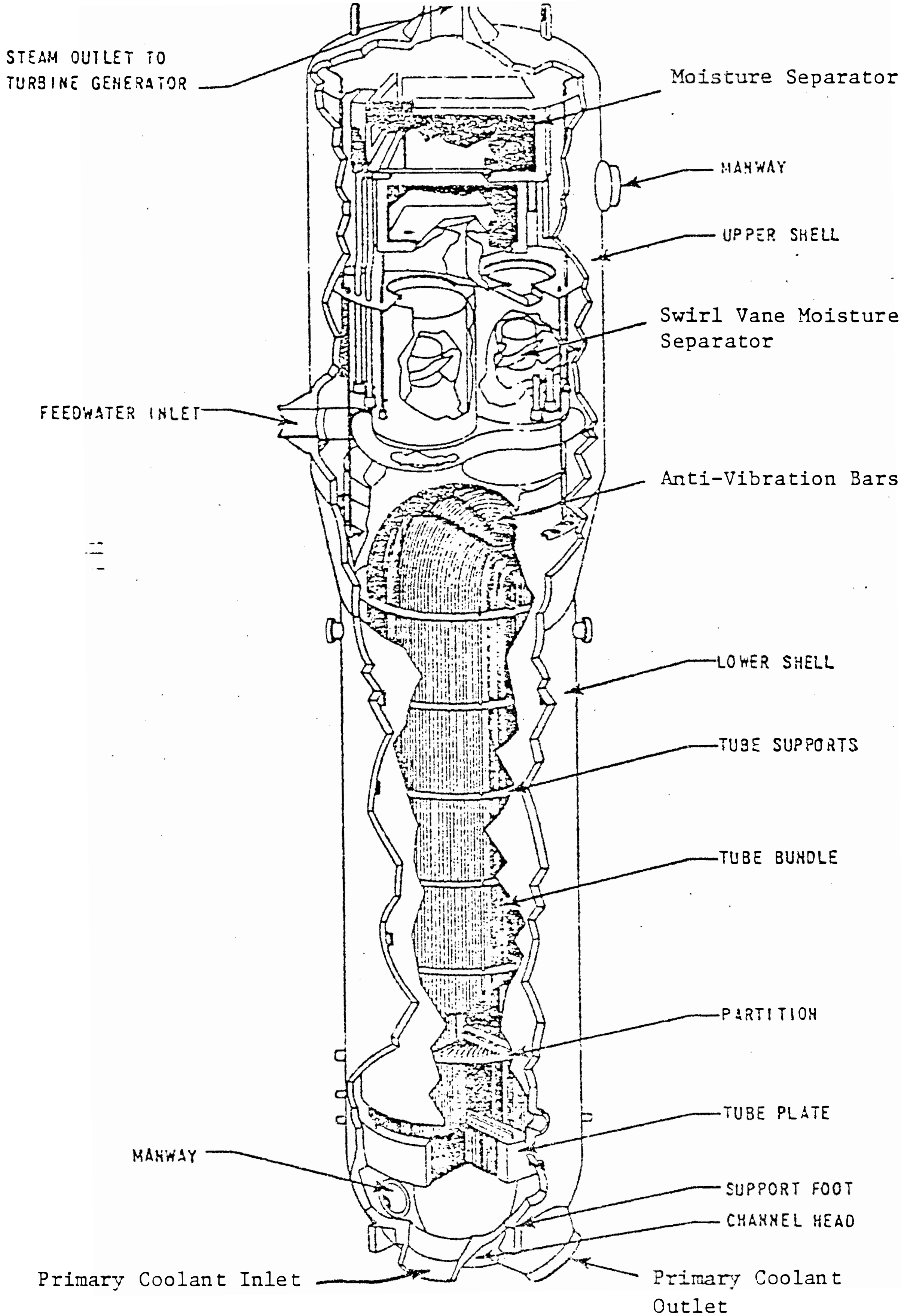

Figure 2.4 A typical U-tube steam generator.

becomes slightly subcooled. Then this subcooled mixture flows downward through the annular region between the tube wrapper and the shell before entering the U-tube region. Heat is transferred to the secondary fluid as it flows upward outside the U-tubes, and a steam-water mixture is formed. This steam-water mixture then passes through steam separators and dryers before leaving the UTSG with a quality of approximately 99.75%. The separated water then returns to mix with the feedwater for another pass through the tube bundle region.

A dynamic model for the UTSG has been developed previously (Ali[2]). For this high order model study, a choice has been made to use the Ali model D. In this model, the following assumptions are made:

1. Only one dimensional flow for both primary and secondary fluids is considered.
2. Constant density and specific heat are assumed for the primary and subcooled secondary fluids.
3. Thermal conductivity of the tube bundle metal is assumed to be constant.
4. Heat transfer coefficients are assumed to be constant.
5. Thermodynamic properties of saturated water and saturated steam are assumed to linear functions of pressure (for small perturbations).
6. The enthalpy and mass quality of the steam-water mixture in the secondary fluid boiling region are taken as linear functions of position along the heat transfer path.
7. No heat transfer takes place between the tube bundle region and the downcomer.

The linearized equation for this model will not be derived or shown in this thesis. (See reference number 2 for details.) Table III gives a list of the resulting state variables for this model. The state variable numbers begin with 15 since the first 14 are assigned to the core and piping. A computer program, written by Ali, is available which generates the system matrix and forcing vectors for this model. The instructions for the use of this program are given in Appendix A. This program is available from The Department of Nuclear Engineering of The University of Tennessee. The essential data for generating a typical UTSG model are given in Table IV. These data again are typical of a Westinghouse PWR plant. It is important when coupling the UTSG model with the reactor core model, to be consistent with the essential data. Therefore to avoid any inconsistency in generating the system matrix, the Ali program has been modified to include the other coupling models.

The forcing terms for this model are listed below.

(II.17) $\left(\frac{\dot{m}}{m}\right)_{P_i} \delta T_{HL}$

(II.18) $\left(\frac{W_{s_o}}{\rho_{dw} A_{dw}}\right) \frac{\delta W_s}{W_{s_o}}$

(II.19) $\left(\frac{W_{s_o}}{\rho_{dw} A_{dw}}\right) \delta T_{FW} + \left(\frac{T_{FW} W_{s_o}}{\rho_{dw} A_{dw}}\right) \frac{\delta W_{FW}}{W_{s_o}}$

(II.20) $-\left(W_{s_o}\right) \frac{\delta W_s}{W_{s_o}}$

TABLE III

LIST AND DESCRIPTION OF THE HIGH ORDER UTSG MODEL STATE VARIABLES

NUMBER	SYMBOL	DESCRIPTION
15.	T_{Pi}	Primary Inlet Temperature (°F)
16.	T_{P1}	First Primary Fluid Lump (°F)
17.	T_{P2}	Second Primary Fluid Lump (°F)
18.	T_{P3}	Third Primary Fluid Lump (°F)
19.	T_{P4}	Fourth Primary Fluid Lump (°F)
20.	T_{Po}	Primary Outlet Plenum Temperature (°F)
21.	T_{M1}	Tube Metal Lump 1 (°F)
22.	T_{M2}	Tube Metal Lump 2 (°F)
23.	T_{M3}	Tube Metal Lump 3 (°F)
24.	T_{M4}	Tube Metal Lump 4 (°F)
25.	L_D	Level of Secondary Fluid in Downcomer (ft)
26.	L_{SUB}	Length of Subcooled Node (ft)
27.	P_S	Steam Pressure (psi)
28.	X_e	Quality of Secondary Fluid Leaving Boiling Lump
29.	T_D	Temperature of Secondary Fluid in Downcomer (°F)

TABLE IV

ESSENTIAL DATA FOR THE UTSG MODEL

1.	number of U-tubes NT	3388
2.	tube outside diameter (inches) TOD	0.875
3.	tube metal thickness (inches) TMT	0.050
4.	upper shell diameter (inches) USHD	178.0
5.	upper shell thickness (inches) USHT	3.50
6.	lower shell diameter (inches) LSHD	135.0
7.	lower shell thickness (inches) LSHT	2.360
8.	overall height (feet) OVHT	67.67
9.	sectional flow area in tube region (ft^2) AFS	60.87
10.	downcomer area (ft^2) AD	32.0
11.	downcomer level (ft) DL	42.17
12.	riser level (ft) RL	9.63
13.	primary water mass flow rate (lbm/hr) WP	$3.939\text{x}10^{+7}$
14.	primary water folume (steam generator) (ft^3) VP	1077.0
15.	specific heat of primary water (B/lbm-°F) CP1	1.390
16.	primary water inlet temperature (°F) TPI	592.5
17.	primary water outlet temperature (°F) TP	542.5
18.	primary loop average pressure (psia) PP	2250
19.	average density of primary water (lbm/ft^3) ROP	45.710
20.	steam flow rate (lbm/hr) WSO	$3.731\text{x}10^{+6}$
21.	steam pressure (psig) PSTG	832.0
22.	saturation temperature at steam pressure (°F) TSAT	521.9

TABLE IV (continued)

23.	feedwater inlet temperature (°F) TFWI	434.3
24.	subcooled secondary water average density (lbm/ft^3) ROS1	52.32
25.	subcooled secondary water specific heat (B/lbm-°F) CP2	1.165
26.	overall heat transfer area of U-tubes (ft^2) HTA	51500.0
27.	primary side film heat transfer coefficient (B/hr) HP	4500.0
28.	tube metal conductance ($B/hr-ft^2$) UM	2160.0
29.	subcooled secondary film heat transfer coefficient ($B/hr-ft^2$-°F) HS1	1972.0
30.	boiling secondary film heat transfer coefficient ($B/hr-ft^2$-°F) HS2	6000.0
31.	conductivity of metal tubing ($B/hr-ft^2$-°F) KM	9.0
32.	metal density (lbm/ft^3) ROM	530.0
33.	metal heat capacity (B/lbm-°F) CM	0.11
34.	enthalpy of saturated water (B/lbm) HF	515.2
35.	latent heat of vaporization (B/lbm) HFG	683.1
36.	enthalpy of saturated steam (B/lbm) HG	1198.3
37.	specific volume of saturated water (ft^3/lbm) VF	0.02098
38.	difference between specific volumes for saturated steam and water (ft^3/lbm) VF	0.52470
39.	specific volume of saturated steam (ft^3/lbm) VG	0.5457
40.	$\frac{\partial T_{sat}}{\partial P_s}$	0.140

TABLE IV (continued)

41.	$\frac{\partial h_f}{\partial P_s}$	0.170
42.	$\frac{\partial h_{fg}}{\partial P_s}$	-.200
43.	$\frac{\partial h_g}{\partial P_s}$	-0.35
44.	$\frac{\partial v_f}{\partial P_s}$	$3.5\text{x}10^{-6}$
45.	$\frac{\partial v_{fg}}{\partial P_s}$	$-7.135\text{x}10^{-4}$
46.	$\frac{\partial v_g}{\partial P_s}$	$-7.1\text{x}10^{-4}$
47.	$\frac{\partial \rho_g}{\partial P_s}$	$2.37\text{x}10^{-3}$
48.	initial quality of steam-water mixture leaving the boiling lump XE	0.200
49.	the number of UTSG per plant NUTSG	4

The four means of disturbing the UTSG system are feedwater flow, feedwater temperature, primary inlet temperature, and steam flow. Feedwater flow will become a coupling term when the UTSG is coupled to a three-element controller model (see Section II.3). Feedwater temperature will become a coupling term when the turbine model is coupled to the UTSG model (see Section II.6). Primary inlet temperature will become a coupling term (hot leg temperature) when the UTSG model is coupled to the reactor core model (see Section II.1). The Ali program for Model D will generate a set of equations of the form

(II.21) $$A \frac{d\bar{x}}{dt} = B\bar{x} + \bar{f}$$

Then equation 2.21 is multiplied through by A^{-1} to yield

(II.22) $$\frac{d\bar{x}}{dt} = (\overline{A^{-1}B})x + A^{-1}\,\bar{f}$$

Thus the forcing terms in equations II.17 through II.20 will actually be vectors. When coupling feedwater flow and feedwater temperature to the UTSG model, a forcing vector must be generated before coupling this to the UTSG model. Further comments will be made on this procedure in Section II.3 and Section II.6.

In this study, the steam flow can be expressed in two ways. The first way is to simply let the steam flow itself be the forcing function. This can be written in equation form as

(II.23) $$\delta W_s = \delta W_s$$

The second way to express the steam flow is to relate the steam flow rate to the steam generator pressure and turbine first stage pressure using the orifice flow equation (Ali[2]). Thus the steam flow will be proportional to the square root of the pressure drop between steam generator and turbine first stage pressure, if it is assumed that any drop in the downstream or turbine pressure will not change the steam flow rate from the steam generator. This assumption is commonly known as the "critical flow" assumption. If this assumption is used, the following equation can be written

$$\delta W_S = \epsilon_o \, \delta P_S + W_{S_o} \frac{\delta\epsilon}{\epsilon_o} \tag{II.24}$$

when

δP_S = change in steam pressure of UTSG

$\delta\epsilon/\epsilon_o$ = fractional change in valve coefficient

ϵ = valve coefficient $\equiv \dfrac{W_S}{P_S}$.

Before coupling the UTSG model to other models, it is necessary to verify the results of an isolated UTSG model. Therefore a case was run for each of the five types of perturbations. The state variables which will be coupled to other models are steam pressure, downcomer level, inlet plenum temperature, and outlet plenum temperature. Figures 2.5 through 2.9 show the responses of these state variables to +10 percent step in feedwater flow, +10°F step in feedwater temperature, +10°F step in primary inlet temperature, +10 percent step in steam flow, and +10 percent step in steam valve coefficient respectively. In Figure 2.5, the change in steam flow is expressed as in equation (II.23) and is always equal to zero. Therefore the response should be unstable for a step in feedwater flow. In Figure 2.6, the change in steam flow again is expressed as in equation (II.23) and is equal to zero. However for a step in feedwater temperature, the response will be stable. In Figure 2.7, the steam flow is expressed

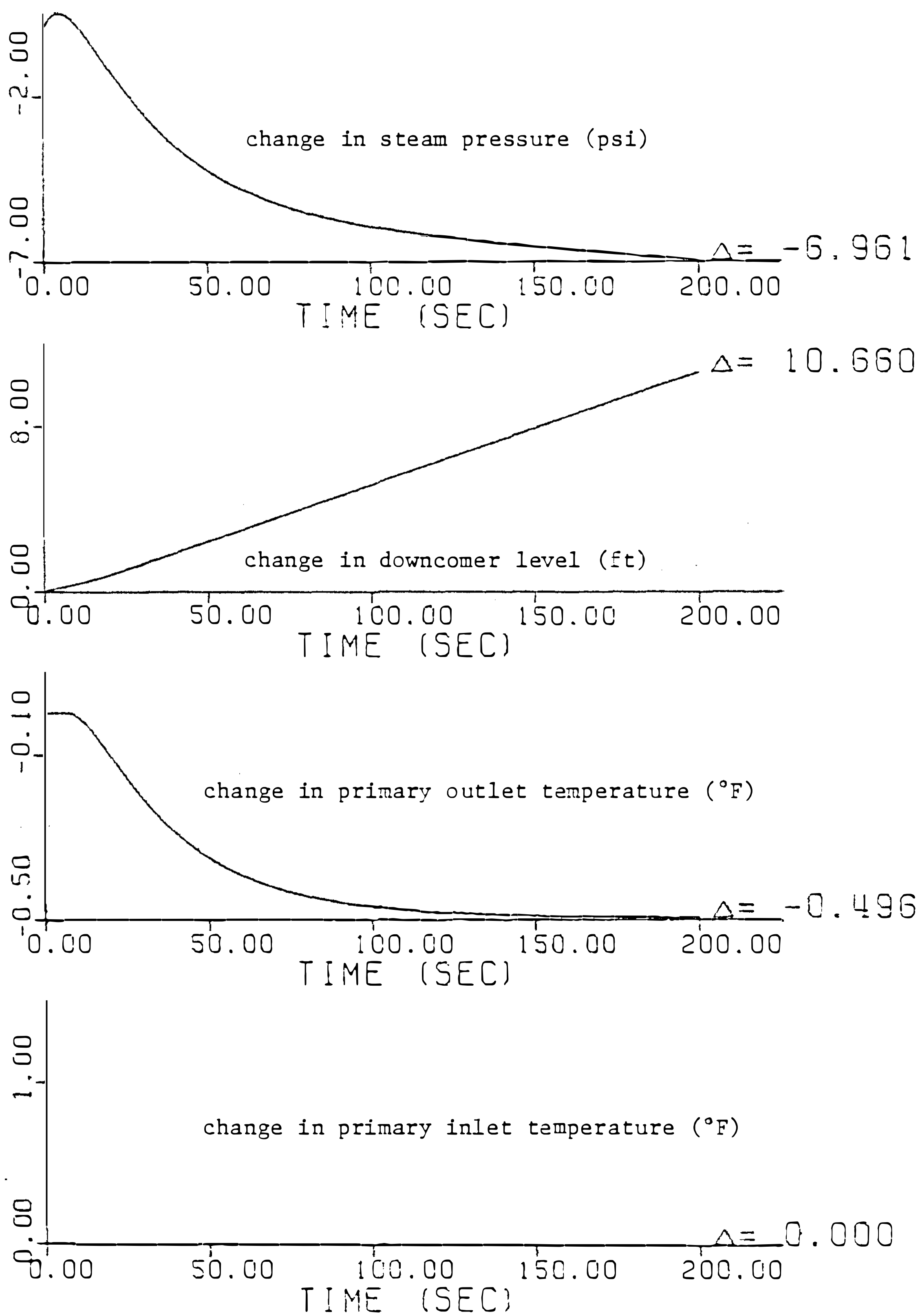

Figure 2.5 Response of the isolated UTSG high order model for a +10 percent step in feedwater flow.

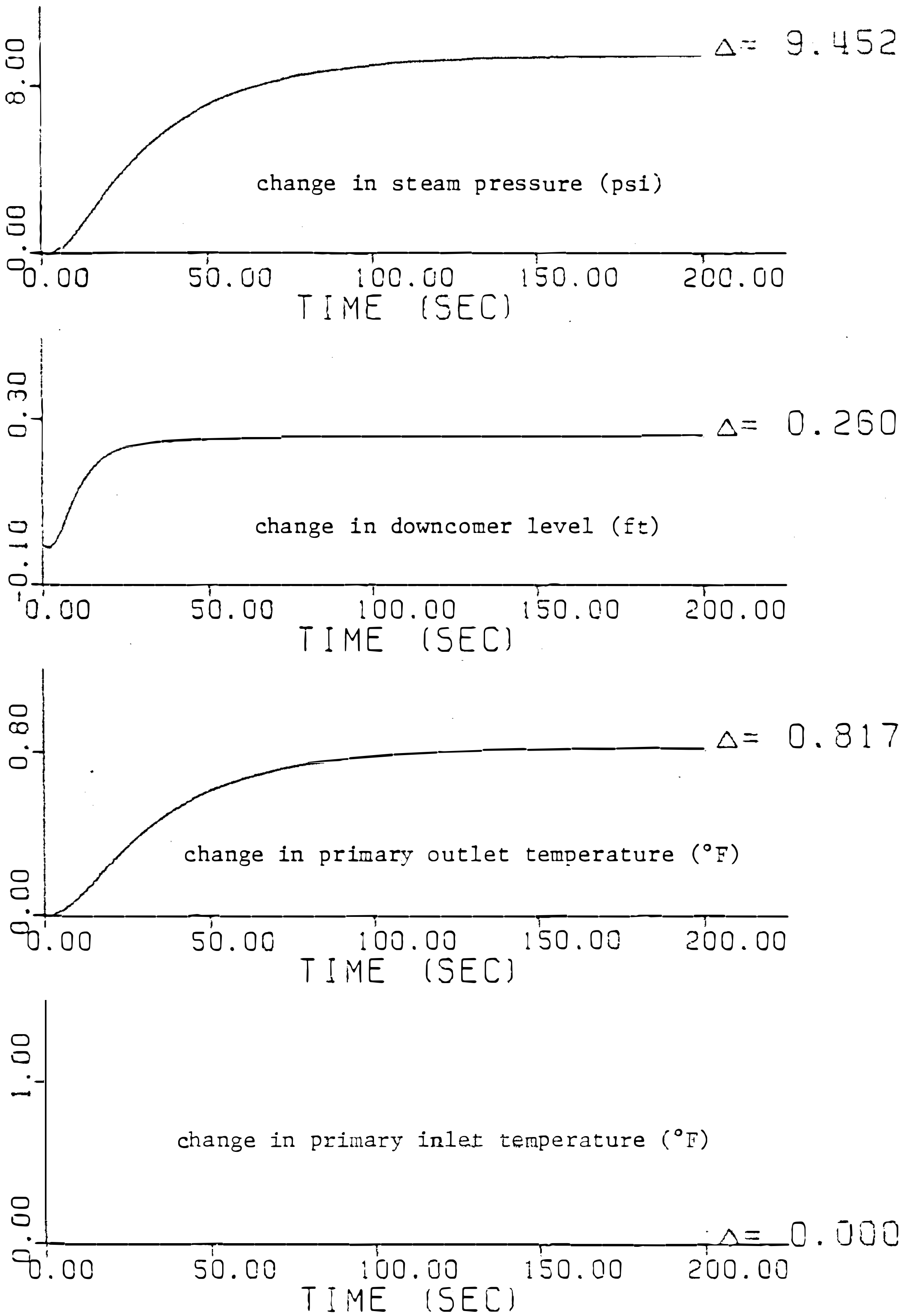

Figure 2.6 Response of the isolated UTSG high order model for a +10°F step in feedwater temperature.

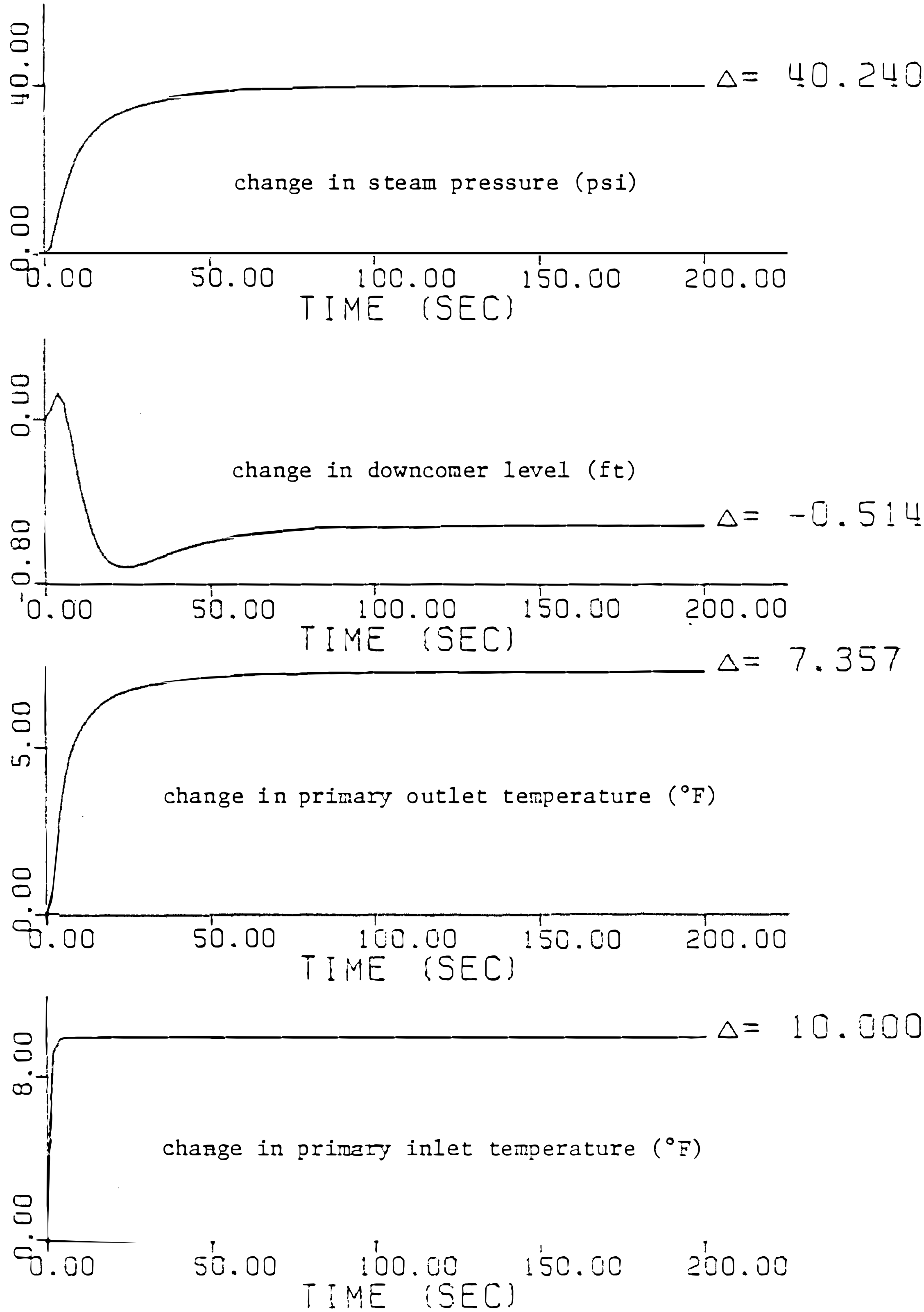

Figure 2.7 Response of isolated UTSG model for a +10°F step in primary inlet temperature.

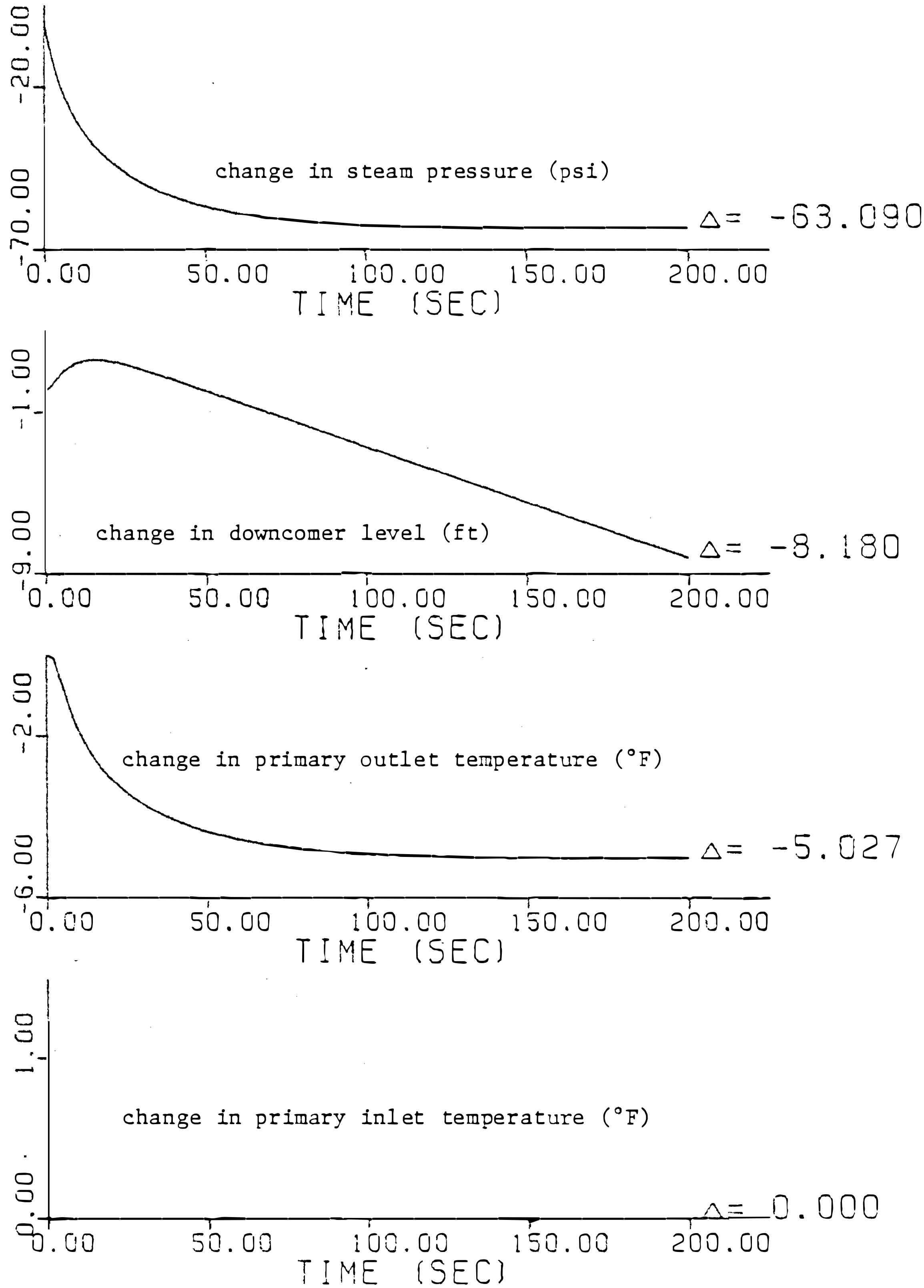

Figure 2.8 Response of isolated UTSG high order model for a +10 percent step in steam flow.

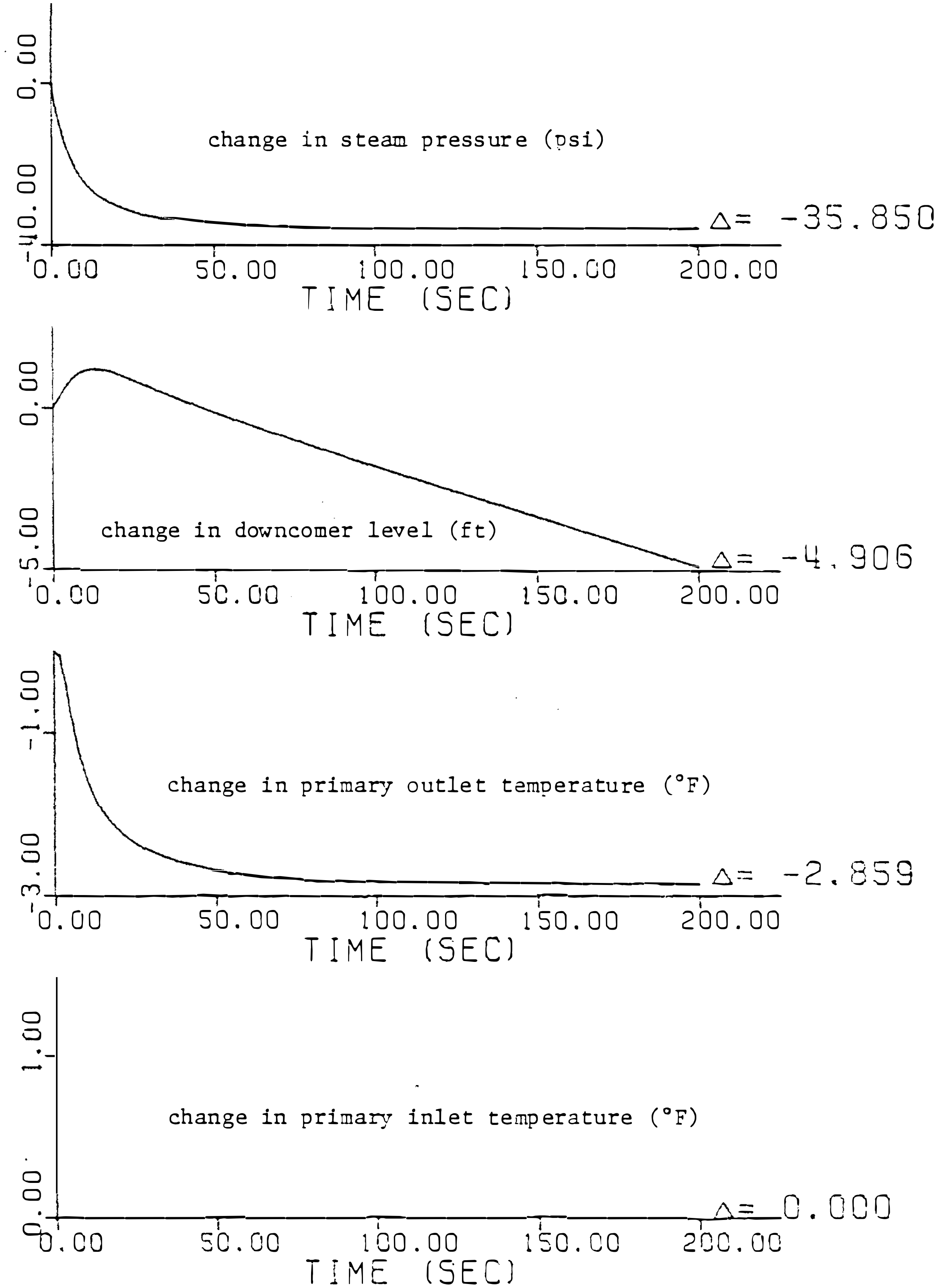

Figure 2.9 Response of the isolated UTSG high order model for a +10 percent step in steam valve coefficient.

as in equation (II.24) where the change in valve coefficient is zero. In addition, the feedwater flow is assumed to have "perfect control." If the feedwater flow had been controlled by a three element controller (see Section II.3), then the downcomer level signal would also be used in the control action. However, in this case, using "perfect control," which means that the feedwater flow is equal to steam flow, the response will be stable, yet a change in the downcomer level will result. In Figure 2.8, the steam flow is expressed as in equation (II.23). The feedwater flow is assumed to have no change (i.e., no control). Therefore the response should be unstable for a step in steam flow. The conditions for Figure 2.9 are the same as for Figure 2.8. Therefore the response should be unstable for a step in steam valve coefficient.

The results of these five cases are consistent with what has been obtained previously in PWR modeling (Ali[2], Cherng[6]). In order to develop a complete PWR high order system model, additional models must be coupled.

II.3 The Three Element Controller

In a recirculation type steam generator, the feedwater is controlled to maintain the downcomer water level in the steam generator as close to a desired level as possible. The controller currently used with a UTSG is called a three-element controller because it uses three signals to determine whether the feedwater flow rate should be adjusted by changing the feedwater valve position. The three signals are steam flow rate, feedwater flow rate, and downcomer water level.

The particular three-element controller and model used in this study is the type designed by Westinghouse Corporation.[38,39] The block diagram of this control system is shown in Figure 2.10. The downcomer level deviation signal is passed through a filter with a time constant τ. This is done to reduce the effect of rapid variations in the water level due to sloshing. Proportional and integral control is then taken on the filtered level signal. The resulting signal is then summed with steam flow and negative feedwater flow and passed through another proportional and integral controller. The final signal is then used as an input to a transfer function which describes the valve position.

Previous work has already been done on the development of a state variable representation of this three-element controller (Cherng[6]). The resulting equations for this model are shown below.

(II.25) $$\frac{d\delta x}{dt} = \frac{1}{\tau}\left[\delta L_D - \delta x\right]$$

(II.26) $$\frac{d\delta y}{dt} = \frac{K_1}{\tau}\left[\delta L_D - \delta x\right] + \frac{1}{\tau_1}\delta x$$

(II.27) $$\frac{d\delta z}{dt} = K_2\left[\frac{1}{\tau_1} - \frac{K_1}{\tau}\right]\delta x + \frac{\delta y}{\tau_2} + \frac{K_1 K_2}{\tau}\delta L_D$$

(II.28) $$\frac{d\delta v}{dt} = \delta W_S - \delta W_{FW}$$

(II.29) $$\frac{d\delta r}{dt} = K\omega_n^2\,\delta z + \frac{K\omega_n^2}{\tau_2}\delta v - 2\zeta\omega_n\,\delta r - \omega_n^2\,\delta W_{FW} + KK_2\,\omega_n^2\left(\delta W_S - \delta W_{FW}\right)$$

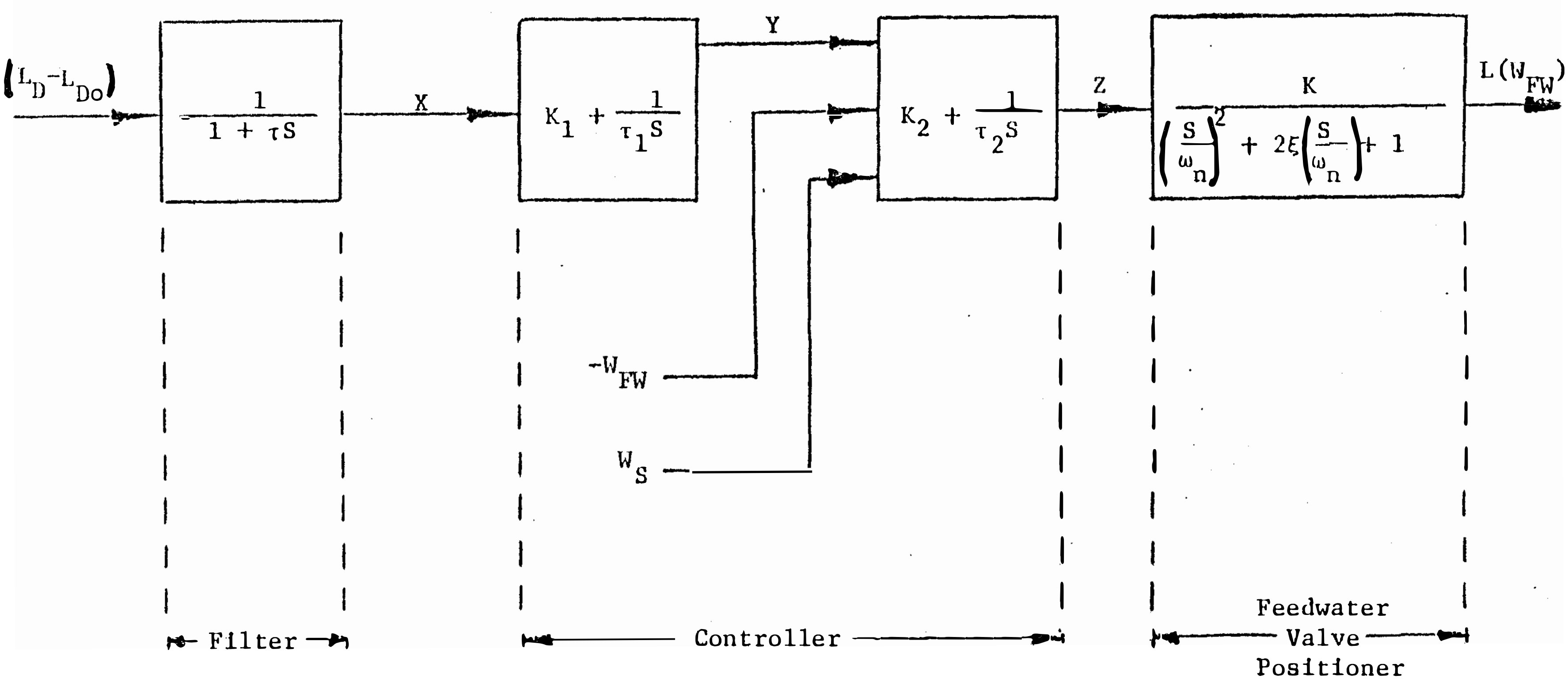

Figure 2.10. Block diagram of three element feedwater flow controller model.

$$\text{(II.30)} \quad \frac{d\,\delta W_{FW}}{dt} = \delta r$$

The resulting state variables for the three-element controller are given in Table V. The state variable numbers are arrived at by coupling the three-element controller model to the UTSG and reactor core model. There are two sets of values used for the parameters in the three-element controller model. One set of parameters are those given in Westinghouse documentation on the three-element controller (Westinghouse[39]). The other set of parameters will be given the name "optimized parameters." These parameters were determined by Cherng to be those values which give the minimum error of the downcomer level during a transient (Cherng [6]). Both sets of parameters are given in Table VI. The calculation of the Westinghouse three-element controller coefficients is given in Appendix B. A computer program is used to generate the system matrix for the three-element controller model in order to assure consistent data when coupling the controller model to the UTSG model. The instructions for this program are given in Appendix A.

The coupled UTSG and three-element controller models can now be disturbed by steam flow, steam valve coefficient, feedwater temperature, and primary inlet temperature. A case is presented in this section for a +10 percent step in valve coefficient. Figure 2.11 shows the response of the coupled UTSG and three-element controller model using the Westinghouse parameters. Figure 2.12 shows the response of the coupled UTSG and three-element controller model using the "optimized parameters." In both figures only the feedwater flow,

TABLE V

LIST AND DESCRIPTION OF THE THREE-ELEMENT CONTROLLER MODEL STATE VARIABLES

NUMBER	SYMBOL	DESCRIPTION
30.	X	filtered level signal
31.	Y	level equivalent flow signal after proportional and integral control
32.	Z	final error signal to valve dynamics after proportional and integral control
33.	r	state variable used to arrive at feedwater flow from the valve dynamics
34.	V	state variable used to arrive at feedwater flow from the valve dynamics
35.	W_{FW}	feedwater flow rate

TABLE VI

PARAMETERS USED TO CALCULATE THE THREE-ELEMENT CONTROLLER MODEL MATRIX COEFFICIENTS

SYMBOL	DESCRIPTION	VALUE WESTINGHOUSE	VALUE OPTIMIZED
1. τ	time constant for level signal filter (sec)	5.0	5.0
2. τ_1	reset constant for level signal (sec)	6.947	199.95
3. τ_2	reset constant for flow signal (sec)	200.0	17.87
4. K_1	proportional gain for level signal	259.10	75.40
5. K_2	proportional gain for flow signal	1.00	30.69
6. K	proportional gain for valve positioner	31.85	31.85
7. ω_n	undamped natural frequency of valve positioner	0.63	0.63
8. ζ	damping ratio of the valve positioner	3.18	3.18

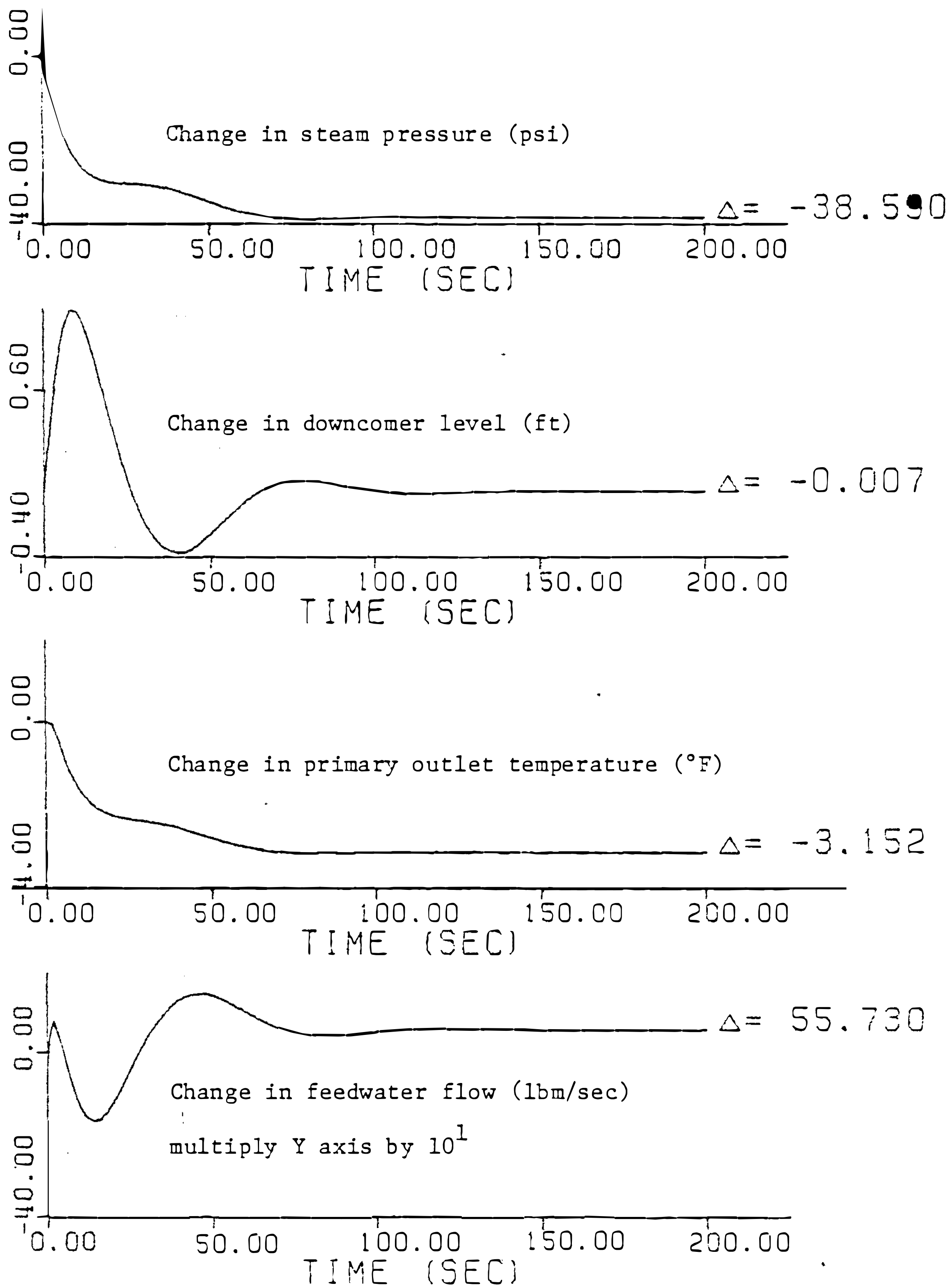

Figure 2.11 Response of the coupled UTSG and three element controller models with Westinghouse parameters for a +10 percent step in steam valve coefficient.

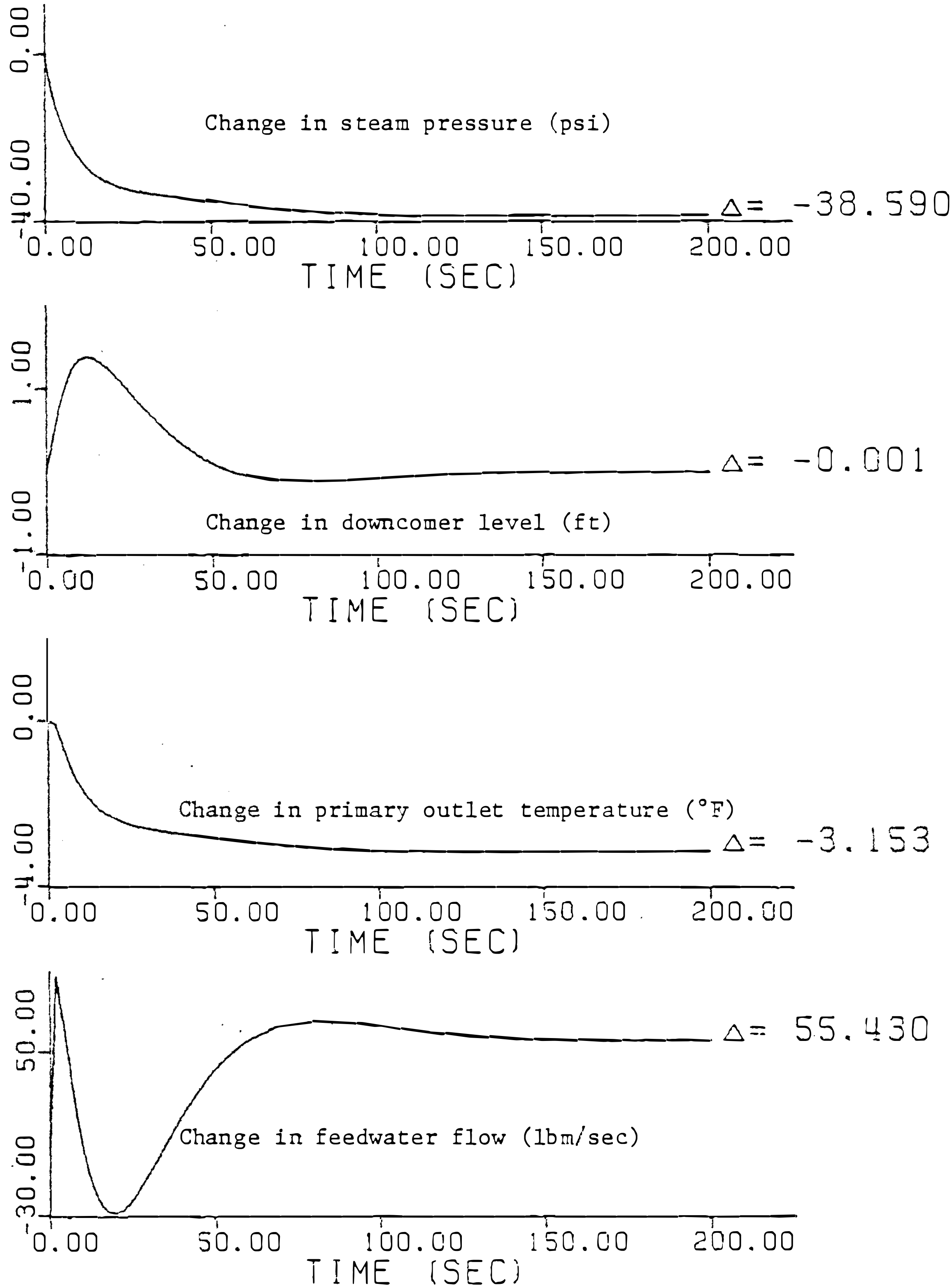

Figure 2.12 Response of the coupled UTSG and three element controller models with optimized controller parameters for a +10 percent step in steam valve coefficient.

steam pressure, downcomer level, and outlet primary temperature are plotted. In Figure 2.11, the downcomer level transient has greater peaks than in Figure 2.12. This demonstrates the fact that the "optimized parameters" do in fact result in a smoother response than the Westinghouse parameters. At this point, the reader should compare the results of Figure 2.12 with those of Figure 2.9. Both are for the same perturbation (+10 percent step in valve coefficient), except that Figure 2.9 is the response of the system using "perfect control" on the feedwater flow while Figure 2.12 uses the three-element controller on the feedwater flow. The main difference in the results of these two figures is the response of the downcomer level. In the case of "perfect control," the downcomer level is not equal to zero at steady state, while in the case of the three-element feedwater control, the downcomer level deviation is approaching zero. For the remainder of this study, the "optimized parameters" will be used in the three-element controller. The results in Figure 2.12 are consistent with previous work (Cherng[6]). Additional models can now be coupled to the system.

II.4 The Reactor Control System

In a PWR system, a change in power level is initiated by changing the steam flow entering the steam turbine. If no control action were taken on the reactor core, the reactor could achieve a new power level without moving the control rods. This is possible because of negative feedback from the coefficients of reactivity in the fuel and reactor coolant. It can be shown that this is true by changing the steam flow for a coupled PWR system model without a control system (this will be done after more discussion of the reactor control system). However, if this were the normal operating procedure in a PWR power plant, the resulting transients of reactor coolant temperature, steam pressure, etc., would be intolerable. Therefore, the need arises for a reactor control system.

In a PWR system, the reactor coolant average temperature is defined to be

$$\text{(II.31)} \qquad T_{avg} = (T_{\substack{hot \\ leg}} + T_{\substack{cold \\ leg}})/2$$

During normal operation of the plant, the hot and cold leg temperatures and thus the average temperature are governed by a "steady state program." A typical steady state program for a Westinghouse PWR[29] is shown in Figure 2.13. The steady state program says that at steady state the average coolant temperature set point is linearly related to power level. It can be shown that the slope of the Tavg curve is the same as the "gain" of the average temperature set point transfer function for a change in power level.

The reactor control system has three inputs which ultimately determine the movement of the control rods. These three inputs will be defined to be the average temperature set point for a change in power level, the lead-lag compensated average temperature, and the temperature equivalent of a power mismatch. These signals are combined and result in a temperature error signal. This error signal then governs the rate and direction of control rod movement. Figure 2.14 shows a block diagram of the reactor control system. Notice that the lead-lag temperature is subtracted while the power mismatch (as

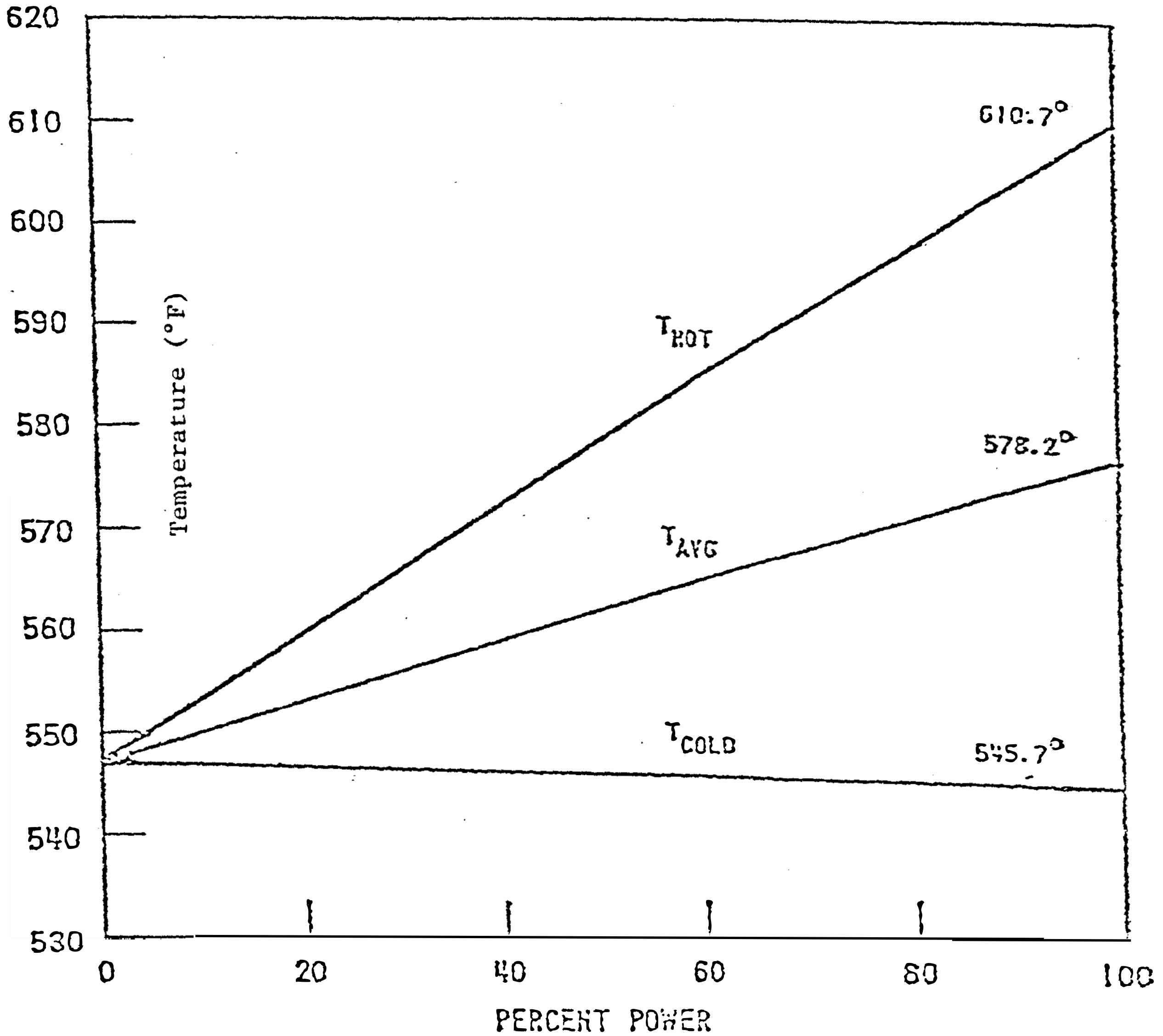

Figure 2.13 Typical steady state program.

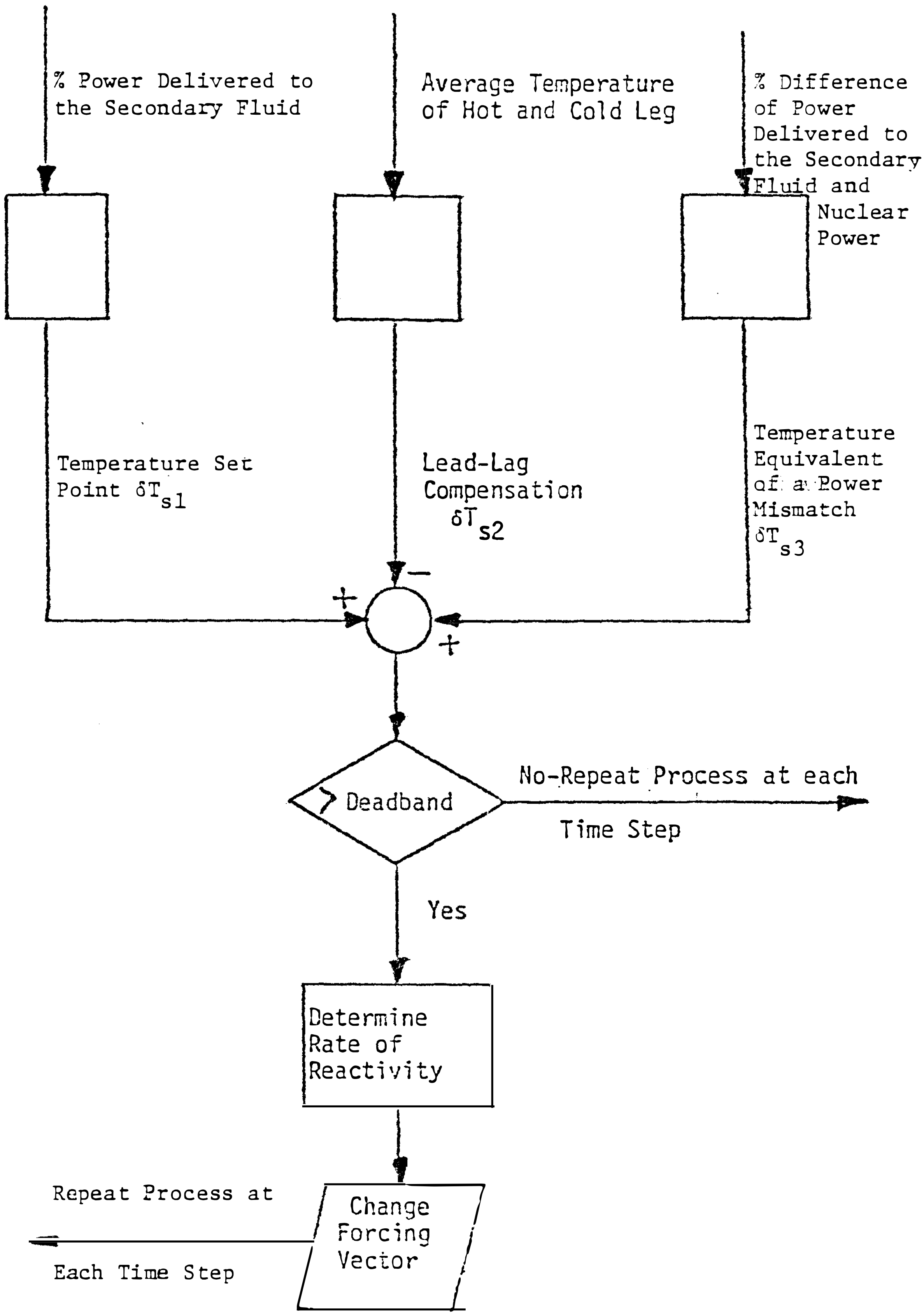

Figure 2.14 Reactor control system logic block diagram

will be defined) and temperature set point are added to arrive at the temperature error signal. The rate and direction of control rod movement are determined by the curve shown in Figure 2.15. Notice that for positive error signals, the reactivity induced is positive and for negative error signals, the reactivity induced is negative. This is consistent with the steady state program since nuclear power increases with positive changes in reactivity.

The reactor control system temperature signals are derived from transfer functions given in Westinghouse documentation (Westinghouse[38]). At this point it is important to mention that the control system does not actually monitor the hot and cold leg temperatures, but it monitors the hot and cold leg temperatures as measured by resistance temperature detectors (hereafter abbreviated RTD). The difference is that the RTD temperature measurements will always lag the actual temperature in time. This is taken into account in the modeling of the reactor control system. The average temperature set point is defined by the transfer function

$$\frac{\delta T_{s1}(s)}{\delta \% P_s(s)} = \frac{K_1}{1 + \tau_{set1} s} \tag{II.32}$$

where

δT_{s1} = deviation in average temperature setpoint

$\delta \% P_s$ = deviation in the percent of full power delivered to the secondary fluid in the UTSG.

The lead-lag average temperature is defined by the transfer function

$$\frac{\delta T_{s2}(s)}{\left[\frac{\delta T_H' + \delta T_C'}{2}\right](s)} = \frac{1 + \tau_{LEAD} s}{(1 + \tau_{LAG1} s)(1 + \tau_{LAG2} s)} \tag{II.33}$$

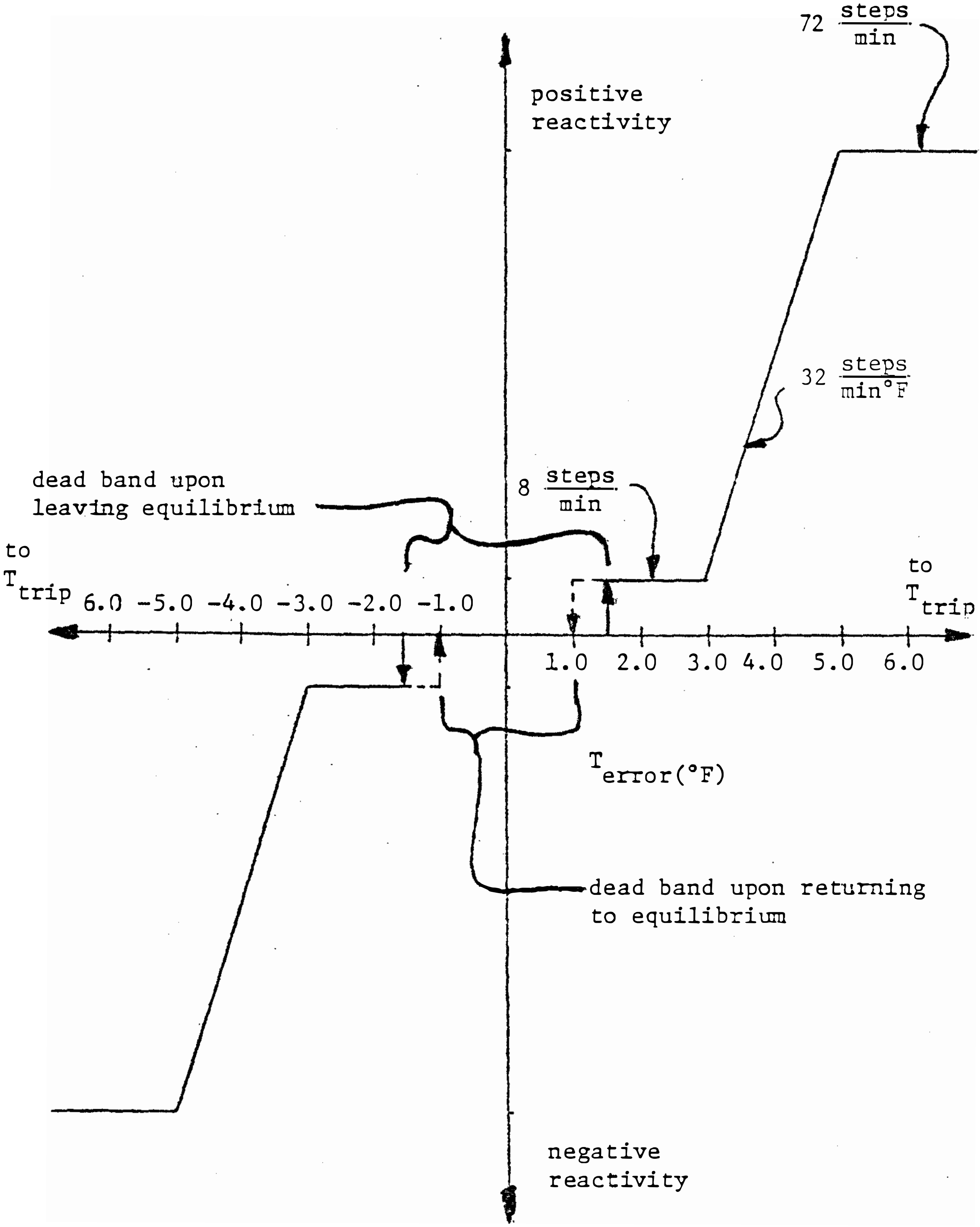

Figure 2.15 Rod speed vs. temperature error signal.

where

δT_{S2} = deviation in lead-lag compensated average temperature

$\delta T_H'$ = deviation in hot leg temperature as measured by the RTD

$\delta T_C'$ = deviation in cold leg temperature as measured by the RTD.

The temperature equivalent of a power mismatch is defined by the transfer function

$$\frac{\delta T_{S3}(s)}{\left[\delta \%P_S - \delta \%P_N\right](s)} = \frac{K_2 K_3}{1 + \tau_{set3} s} \tag{II.34}$$

where

δT_{S3} = deviation in temperature equivalent of a power mismatch

$\delta \%P_S$ = deviaton in the percent of full power delivered to the secondary fluid in the UTSG

power

$\delta \%P_N$ = deviation in the percent of full pwoer delivered by the reactor core.

The hot and cold leg temperatures as measured by the RTDs are given by

$$\frac{\delta T_H'(s)}{\delta T_{HL}(s)} = \frac{1}{1 + \tau s} \tag{II.35}$$

$$\frac{\delta T_C'(s)}{\delta T_{CL}(s)} = \frac{1}{1 + \tau s} \tag{II.36}$$

where

$\delta T_H'$ = deviation in hot leg temperature as measured by the RTD

δT_{HL} = deviation in hot leg temperature

$\delta T_C'$ = deviation in cold leg temperature as measured by the RTD

δT_{CL} = deviation in cold leg temperature.

Equations (II.35) and (II.36), which define the RTD temperatures, assume that the RTD response can be represented by a first order lag.

In order to incorporate the reactor control system into the PWR system model, a state variable model of the reactor control system has been formulated. The derivation of this formulation is given in Appendix C. The resulting state variables are described in Table VII. The state variable numbers were selected to follow the numbers of the variables in the previous models described. The values of the parameters used in the differential equations are given in Table VIII. All the parameters are constant except K_3 and K_2. The value of K_2 is determined by Figure 2.16. The value of K_3 is determined by Figure 2.17. A computer program which generates the matrix and forcing vectors for this model has been written in order to be consistent with the input data. The instructions for the program are given in Appendix A.

It is evident from Figures 2.15, 2.16, and 2.17 that a nonlinear solution to the reactor control system equations may be needed. However, the computer code MATEXP[25], which gives a solution to a set of first order linear differential equations, can be used to solve these equations. This is because MATEXP has a subroutine called DISTRB which can be used to produce time varying forcing functions by updating the forcing functions at each time step in the solution. The DISTRB subroutine will monitor the temperature error signal at each time step. Then, depending on the position of the temperature error signal on the X axis of Figure 2.15, the proper reactivity change is made by changing the forcing term of equation (II.15). The Fortran listing of DISTRB is not shown in this thesis. DISTRB is a part of

TABLE VII

LIST AND DESCRIPTION OF THE HIGH ORDER REACTOR CONTROL SYSTEM MODEL STATE VARIABLES

NUMBER	SYMBOL	DESCRIPTION
36	T_H'	hot leg temperature as measured by an RTD (°F)
37	T_C'	cold leg temperature as measured by an RTD (°F)
38	T_{S1}	average temperature at set point (°F)
39	T_{dummy}	state variable used to arrive at the lead-lag compensated average (°F)
40	T_{S2}	lead-lag compensated average coolant temperature (°F)
41	T_{S3}	temperature equivalent of a power mismatch between power delivered to the secondary fluid and nuclear power (°F)

TABLE VIII

PARAMETERS USED TO CALCULATE THE REACTOR CONTROLLER MODEL MATRIX COEFFICIENTS

1.	W_{max}	the steam flow rate of the system at 100% power (lbm/hr)	3.733x10+6
2.	hg_{max}	the enthalpy of the steam entering turbine at 100% power (Btu/lbm)	1198.30
3.	SET1	the first order lag time constant for the average temperature set point transfer function (sec)	30.0
4.	K_1	the gain of the average temperature set point transfer function (°F/%power) at beginning of core life at the end of core life	 0.208 0.152
5.	LEAD	the lead time constant for the lead-lag compensated average temperature transfer function (sec)	80.0
6.	LAG1	the first lag time constant for the lead-lag compensated average temperature transfer function (sec)	10.0
7.	LAG2	the second lag time constant for the lead-lag compensated average temperature (sec)	5.0
8.	τ	the first order lag time constant for the RTD transfer function (sec)	4.0
9.	SET3	the first order lag time constant for the temperature equivalent of a power mismatch transfer function (sec)	40.0
10.	K_2	the non-linear gain of the power mismatch transfer function (°F/%power)	see Figure 2.16
11.	K_3	the variable gain of the power mismatch transfer function (unitless)	see Figure 2.17

TABLE VIII (continued)

12.	h_f	enthalpy of the saturated liquid (Btu/lbm)	515.24
13.	C_{p2}	specific heat of entering feedwater (Btu/lbm-°F)	1.165
14.	T_{sat}	the saturation temperature (°F)	522.89
15.	T_{FWi}	the temperature of entering feedwater (°F)	434.30
16.	$\frac{\partial h_s}{\partial P_s}$	steam enthalpy gradient with respect to pressure (Btu/lbm-psi)	-0.035
17.	ϵ_o	the initial value of the valve coefficient (lbm/sec-psi)	1.2463
18.	W_{so}	the initial value of the steam flow rate (lbm/hr)	$3.733\text{x}10^{+6}$
19.	h_g	the enthalpy of saturated steam (Btu/lbm)	1198.3

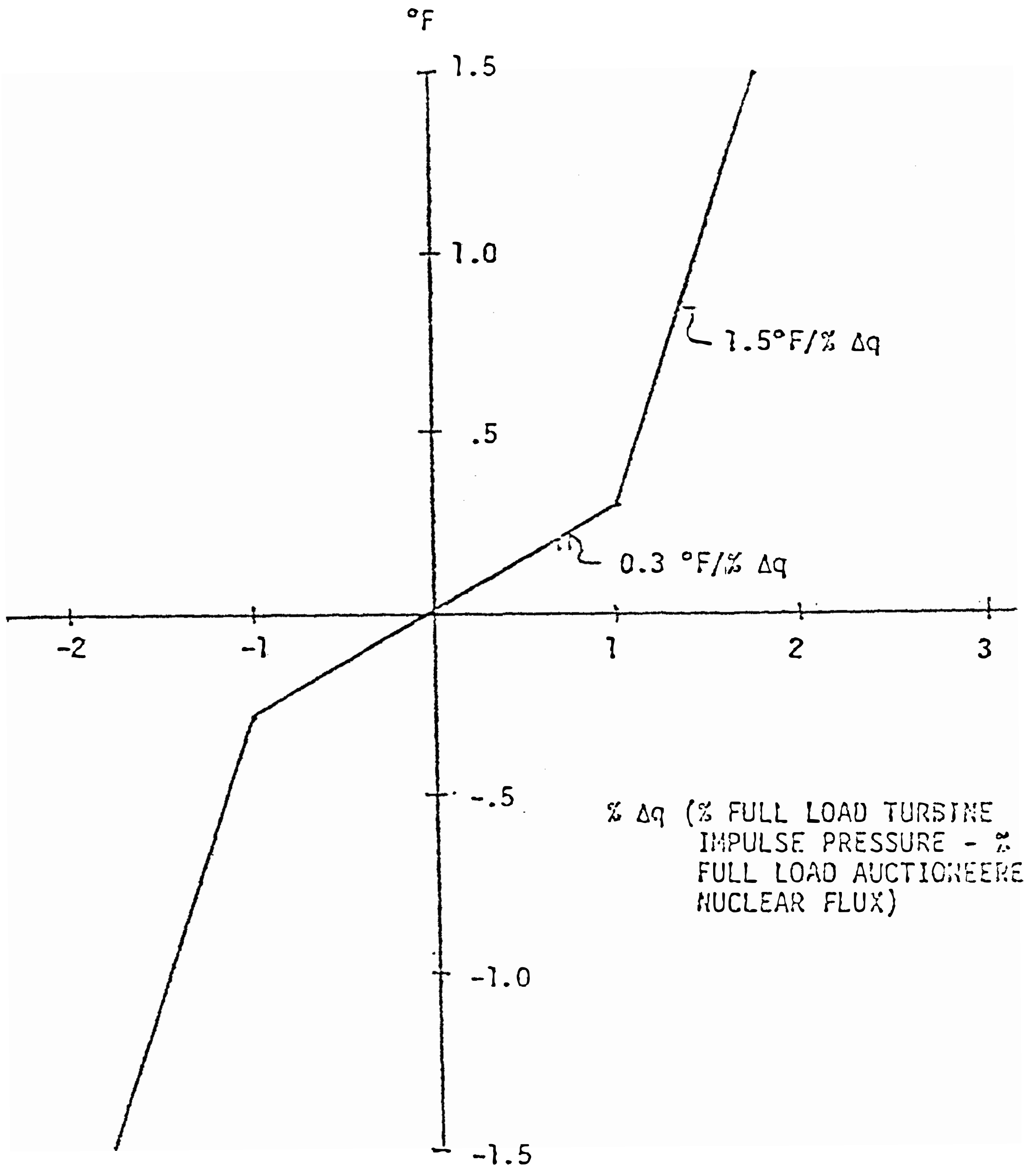

Figure 2.16 Power mismatch channel, nonlinear gain.

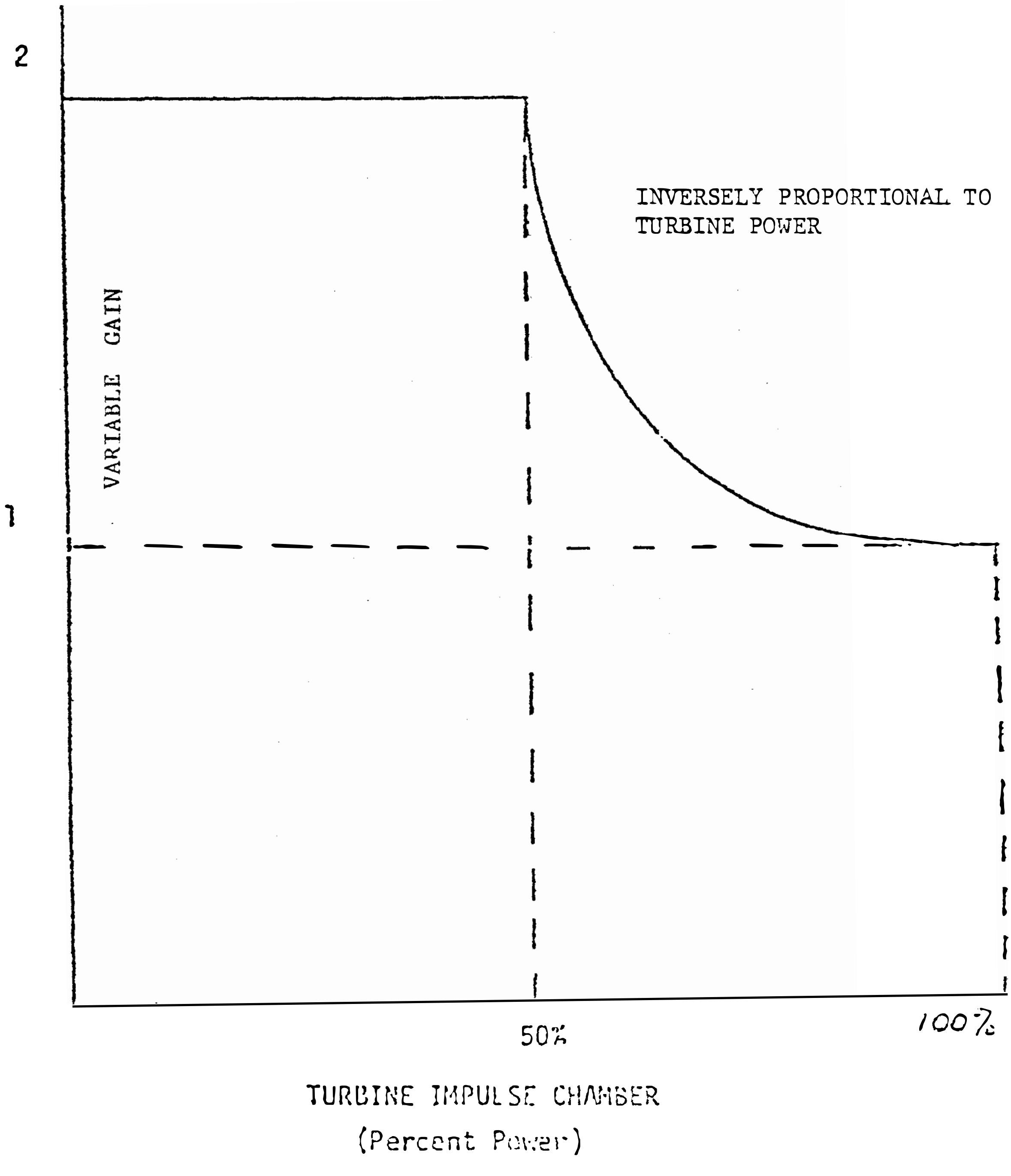

Figure 2.17 Power mismatch variable gain.

the SYSTEM-MATEXP programming package which is available from The Department of Nuclear Engineering of The University of Tennessee. In order to do this, the assumption must be made that the forcing function is constant during the computational time interval(Δt).

The highest rate of the rod speed shown in Figure 2.15 is 72 steps/minute. This means that the rods cannot move more than one time every 0.833 seconds (60/72). A typical computational time interval in this thesis is never more than 0.02 seconds for the overall system model (see Section II.7). It is assumed in this study that the rods are moved continuously rather than in discrete steps. This is done by assuming a constant value of the reactivity induced per step (see a typical value in Table VIII). Therefore, the assumption that the forcing function is constant over the computational time interval does not cause excessive error due to the discrete nature of the rod speed programmer.

Subroutine DISTRB not only can be used to update the forcing functions, but it can also be used to update algebraic variables, which depend on the state variables, but do not have any direct feedback on the system. Such an algebraic variable might be the percent of full power delivered to the secondary fluid ($\%P_s$). This has been defined to be (see Appendix C)

$$\delta\%P_s = \frac{100}{W_{max}(h_g - h_{FW})_{max}}\left[W_s \frac{\partial h_g}{\partial P_s^o}\,\delta P_s + h_g\,\delta W_s - h_{FW}\,\delta W_{FW} - W_{FW}\,C_{P2}\,\delta T_{FW}\right]. \tag{II.37}$$

From equation (II.37) and Figure 2.16 and 2.17, the desired value of K_2 and K_3 can be calculated. If these values are different from the initial values, then the difference can be represented by a difference in the forcing function.

The power mismatch equation from equation (II.34) may be rewritten as

$$\left[1+\tau_{set3}S\right]\delta T_{s3}(s)=K_2K_3\left[\delta\%P_s-\delta\%P_N\right](s). \tag{II.38}$$

Performing an inverse Laplace transform on equation (II.38) gives:

$$\frac{d\,\delta T_{s3}}{dt}=-\frac{1}{\tau_{set3}}\delta T_{s3}+\frac{K_2K_3}{\tau_{set3}}\left[\delta\%P_s-\delta\%P_N\right]. \tag{II.39}$$

By letting $K_3=K_{30}+\delta K_3$ and $K_2=K_{20}+\delta K_2$, equation (II.39) becomes

$$\frac{d\,\delta T_{s3}}{dt}=-\frac{\delta T_{s3}}{\tau_{set3}}+\frac{K_{2_0}K_{3_0}}{\tau_{set3}}\left[\delta\%P_s-\delta\%P_N\right] \tag{II.40}$$
$$+\frac{\left[\delta\%P_s-\delta\%P_N\right]}{\tau_{set3}}\left[K_{2_0}\delta K_3+K_{3_0}\delta K_2+\delta K_2\delta K_3\right].$$

The third term on the right hand side of equation (II.40) will become a forcing function which is updated at each time step by subroutine DISTRB.

This aspect of the reactor control system is included in the computer code package SYSTEM-MATEXP. The instructions for this program are included in Appendix A.

Two parameters used as input data for the program are DBIN and DBOUT (deadband going into equilibrium and deadband going out of equilibrium respectively). These parameters are shown in Figure 2.15 on page 41. At first one would think that the purpose of the deadband would be to avoid over working of the control system due to inherent fluctuations in the instrumentation (noise, etc.). Although to some extent this may be true, there is another benefit associated with the deadband. The effect of a reactivity change on nuclear power is almost instantaneous. Whereas, the effect of a reactivity change on the average coolant temperature is "sluggish" due to large time constants in the average temperature to reactivity change transfer function. For example, let it be assumed that a change in power level has taken place and the control rods have caused a subsequent change in reactivity. After the controls rods have stopped moving, the hot and cold leg temperatures will still be changing for some time. Therefore, the deadband allows the temperature error signal to fluctuate near a desired equilibrium point without changing the control rod reactivity. The advantage of having DBIN and DBOUT as input data is to allow the user to investigate the effect of changing the deadband. Figure E.1 (in Appendix E) shows the effect of making the deadband too small. The system response is oscillating. It is important to note that, because of the presence of the deadband, the average temperature will probably never reach the temperature set point as specified by the steady state program (Figure 2.13, page 38).

Another input parameter in the program is ROWSTP (the assumed average reactivity induced per step change in the control rod position in dollars). This value will always be dependent on the conditions of the plant. A value of 0.225 cents/step has been used throughout this study. The reason for this is because this value caused the model to more closely simulate some available plant data. Figure E.2 (in Appendix E) shows the effect of making ROWSTP too large. The system is again oscillatory.

The program also includes as an input option the ability to specify the temperature error signal in four different ways. This is done with the input parameter NTYPE. The options of NTYPE are:

1. $T_{BAR} = \delta T_{S1} - \delta T_{S2} + \delta T_{S3}$

2. $T_{BAR} = \delta T_{S3}$

3. $T_{BAR} = \delta T_{S1} - \delta T_{S2}$

4. $T_{BAR} = 0$

where T_{BAR} is the temperature error signal. Although NTYPE = 1 or NTYPE = 4 are the only reasonable options, the others are included to investigate the effect of the power mismatch signal.

In this section, three cases will be presented. The first case is the NSSS system model without taking any reactor control system action. The only feedback that the reactor control system equations has on the rest of the system is through the reactivity forcing term (equation 2.15). By making the temperature error signal always equal to zero (NTYPE=4), the reactor control system state variables can be calculated without affecting the rest of the system. Figure 2.18 shows the response of the system to a +10 percent step in steam valve coefficient with no reactor control action and with three element

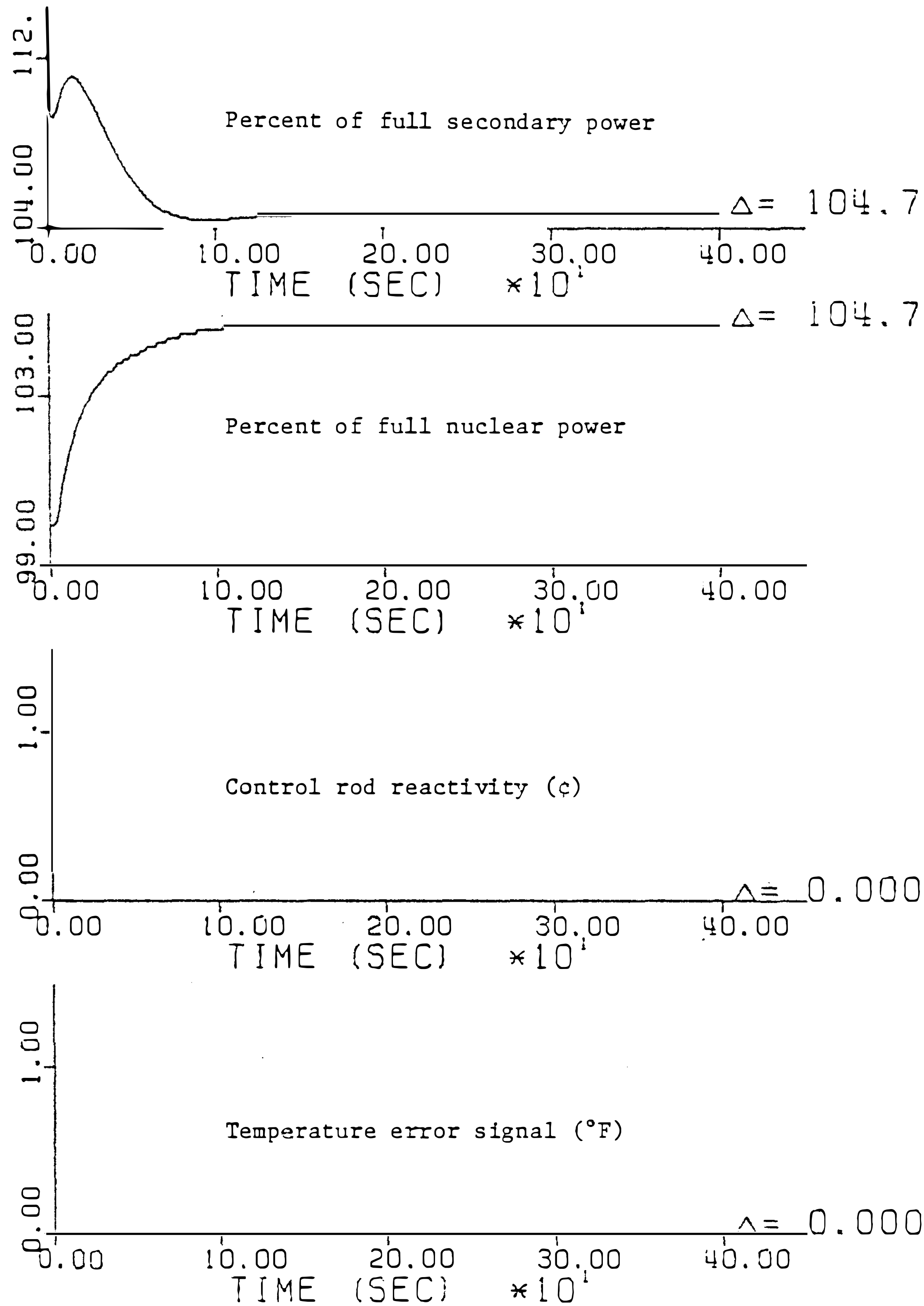

Figure 2.18 Response of coupled UTSG, reactor core, three element controller, and reactor controller models for a +10 percent step in steam valve coefficient with no reactor control action. (NTYPE=4)

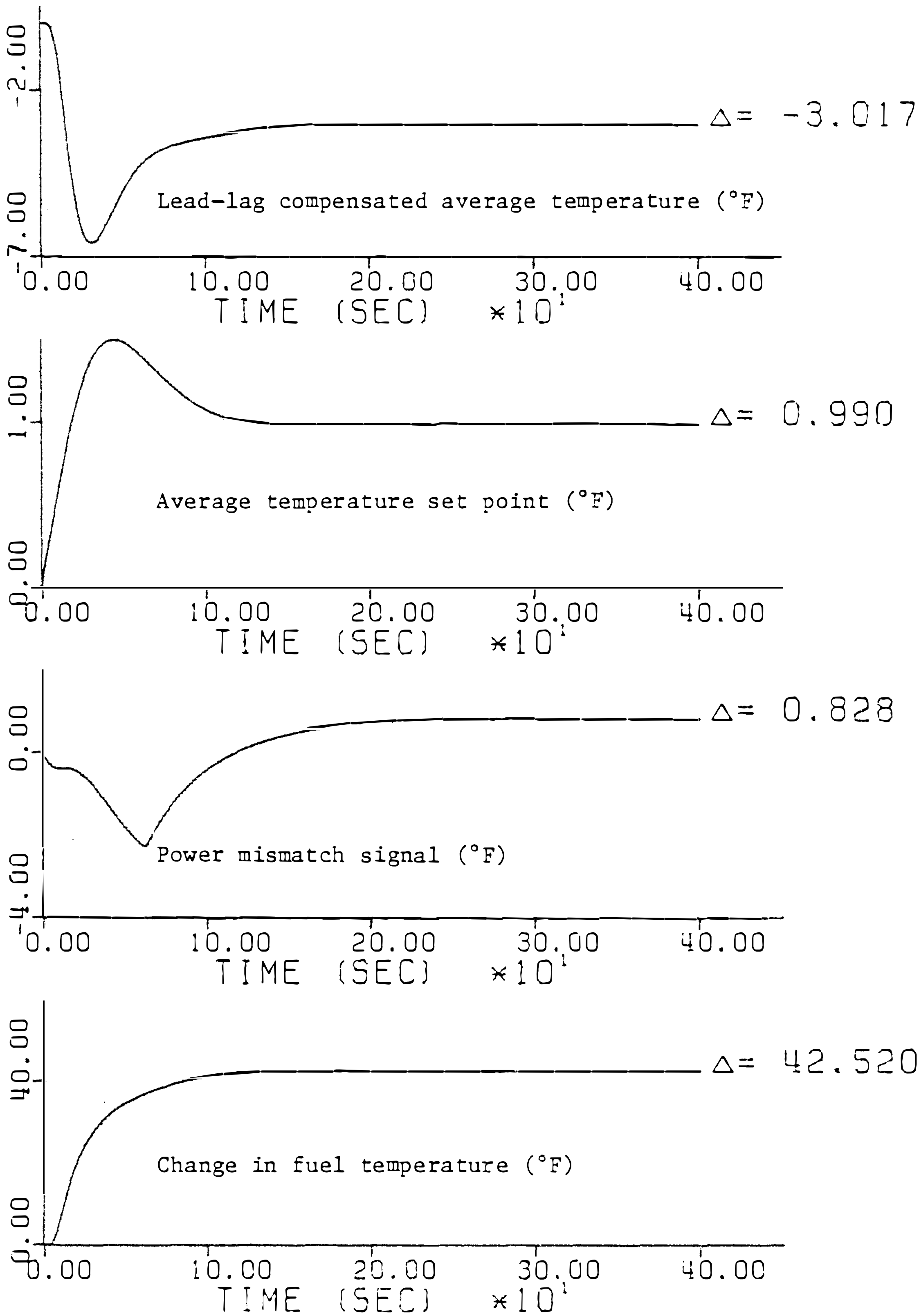

Figure 2.18 (continued)

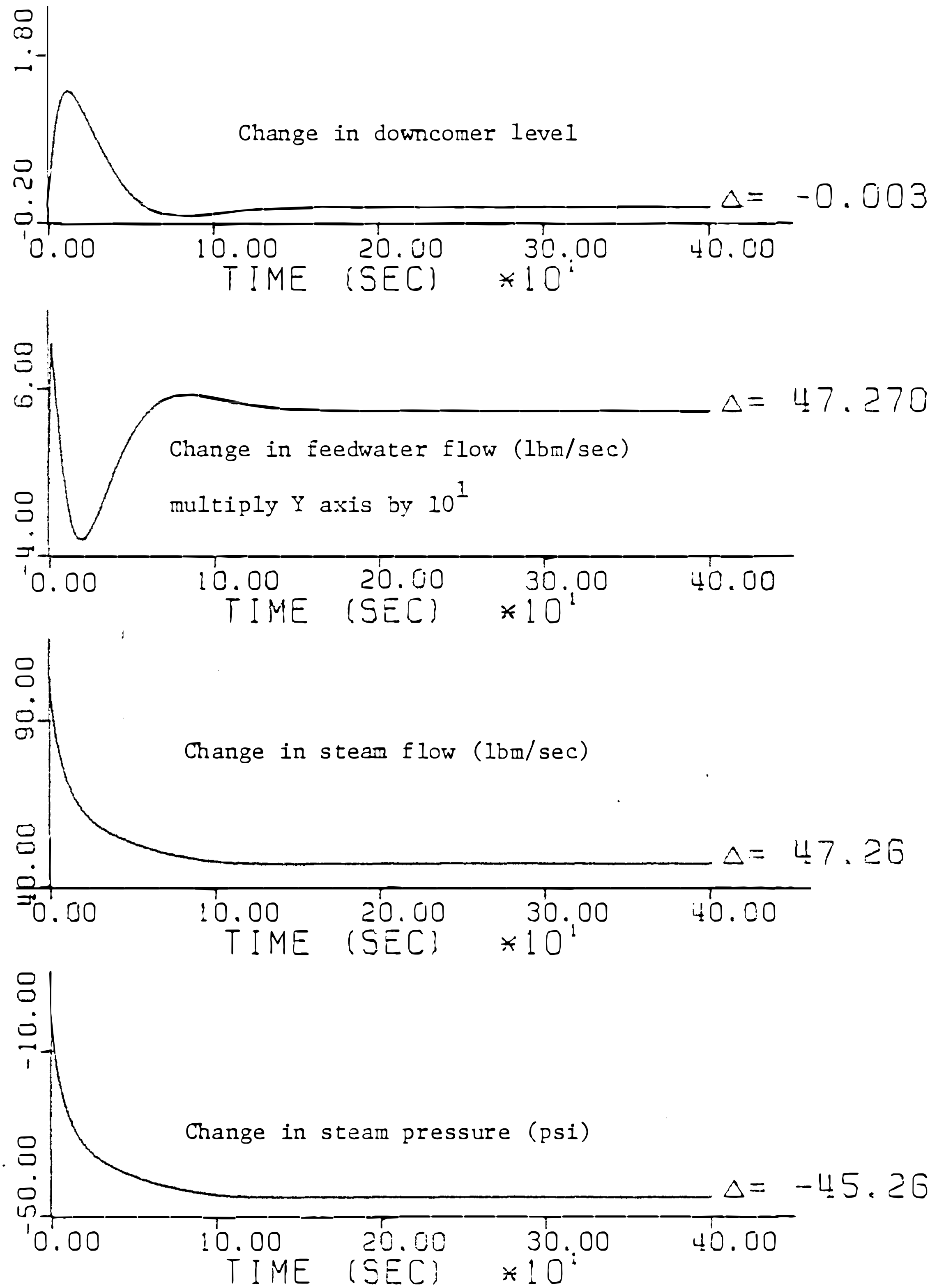

Figure 2.18 (continued)

control of the feedwater flow. The average temperature has decreased rather than increased as desired. The steam pressure deviation is rather large at -45.26 psi.

The second case is the same as the first case except this time the reactor control system action is allowed to take place (NTYPE=1). Figure 2.19 is the response of the system to a +10 percent step in valve coefficient with reactor control action and with three element control of the feedwater flow. In this case the average temperature has gone in the direction required by the steady state program. But there is a difference in the temperature set point and the average temperature at steady state due to the deadband. The steam pressure change is much smaller than in the uncontrolled case.

The third case is shown in Figure 2.20 for a -10 cent step in control rod reactivity beginning after ten seconds of observation time with reactor control system action and with three element control of the feedwater flow. In this case, the steam flow is held constant (equation II.23). Therefore, the power removed is nearly constant, and the average temperature and control rod reactivity should return to zero. But because of the deadband, there is still -2.646 cents of reactivity induced by the control rods at steady state. This amount of reactivity can be accounted for by feedback reactivity induced on the system by fuel and coolant temperature changes (the reactivity induced by primary system pressure changes has not been included). This reactivity can simply be added up in equation form

$$\rho_{TOTAL} = \rho_{\substack{\text{external}\\ \text{control rods}}} + \rho_{\text{fuel}} + \rho_{\text{coolant}} + \rho_{\substack{\text{primary}\\ \text{pressure}}} \quad \text{(II.41)}$$

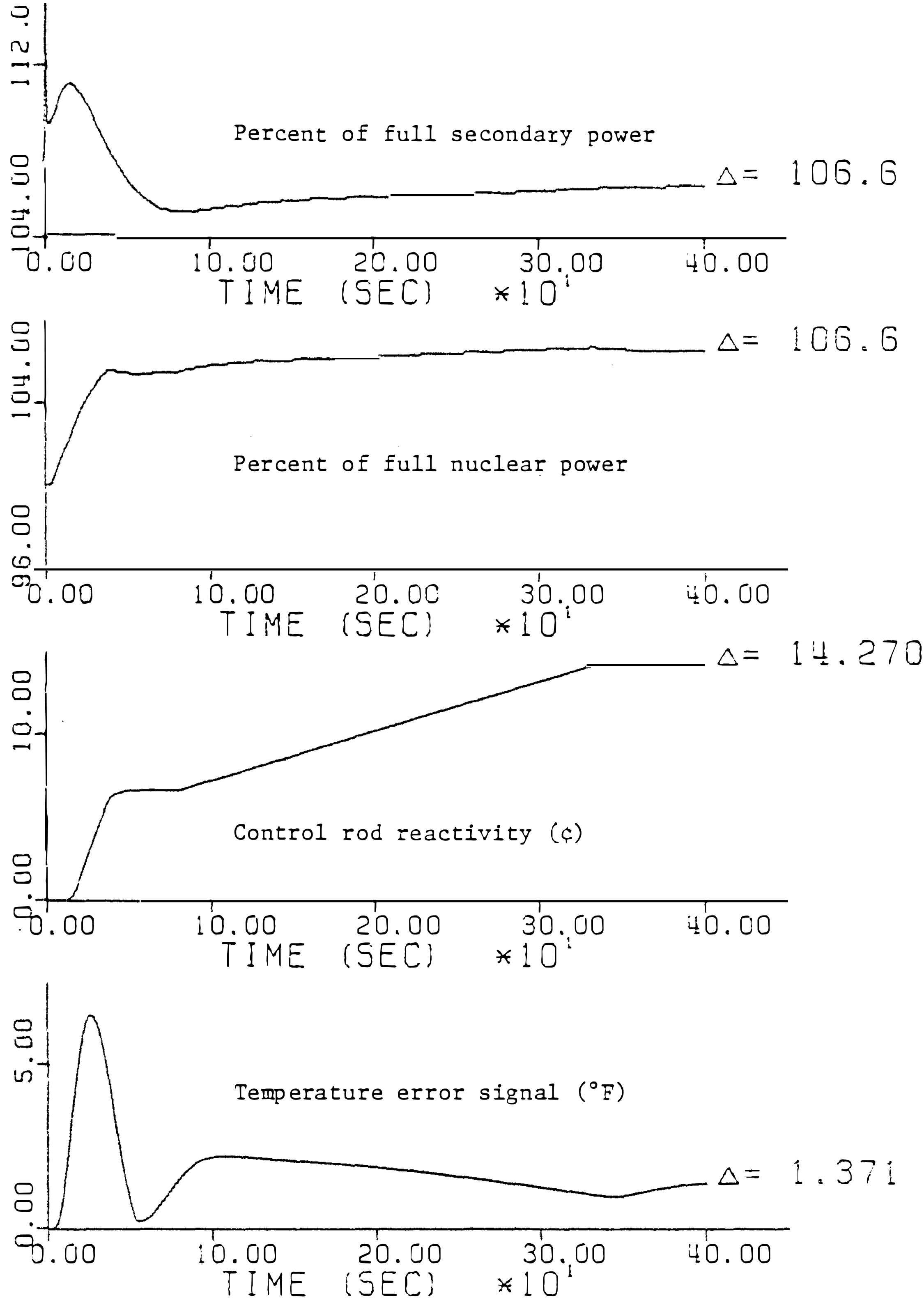

Figure 2.19 Response of coupled UTSG, reactor core, three element controller, and reactor controller for a +1.0 percent step in steam valve coefficient with reactor control action. (NTYPE=1)

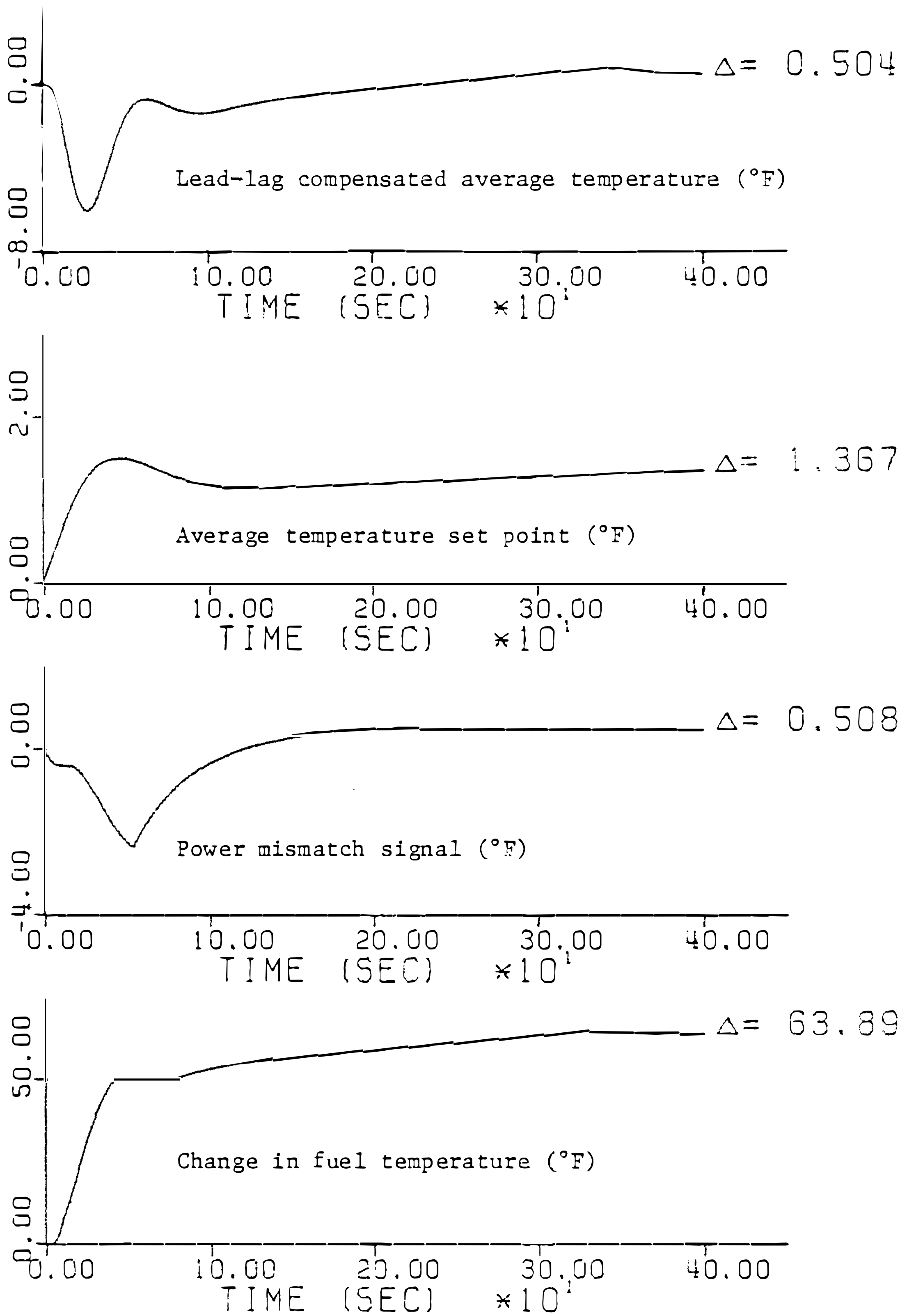

Figure 2.19 (continued)

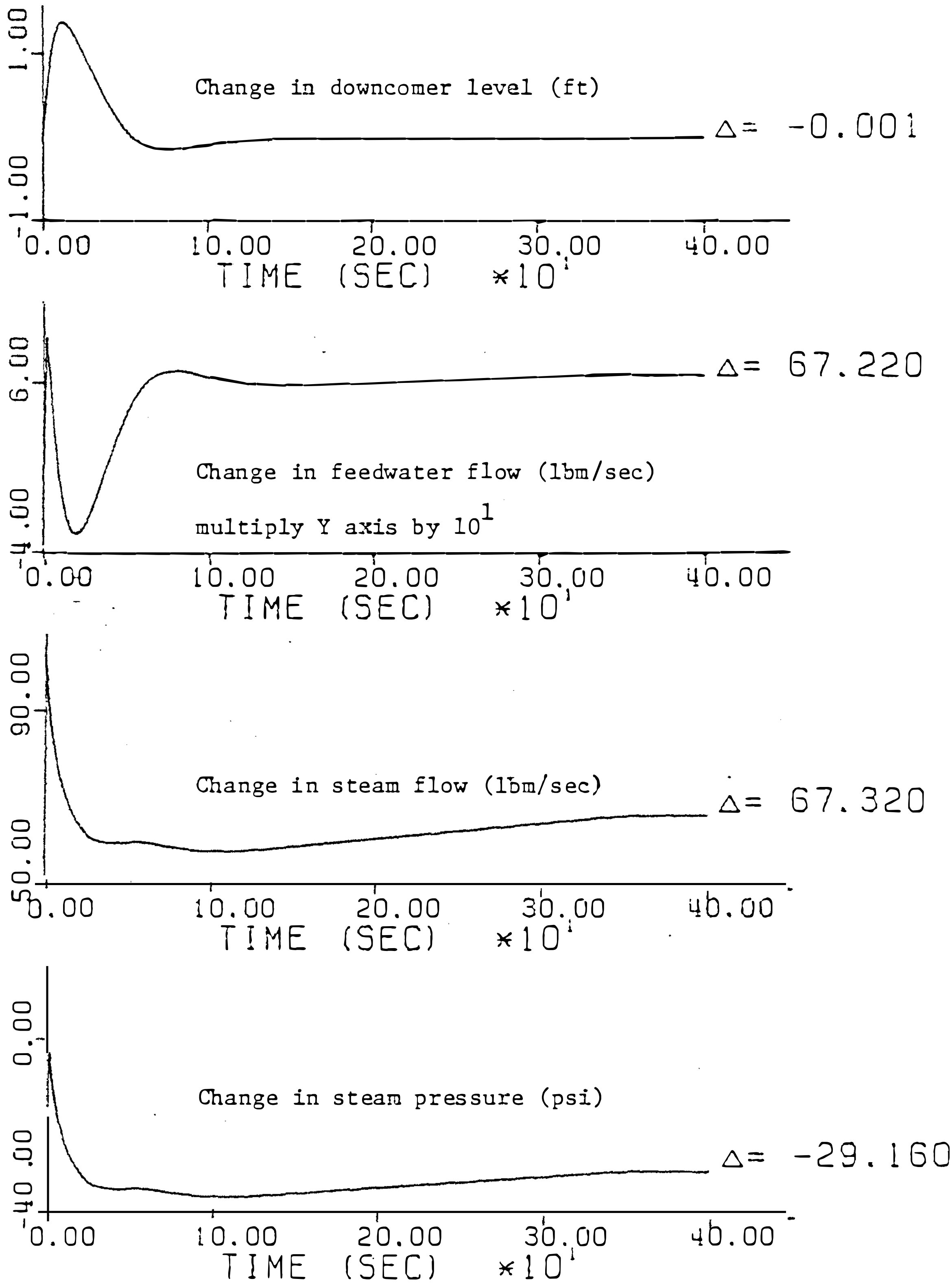

Figure 2.19 (continued)

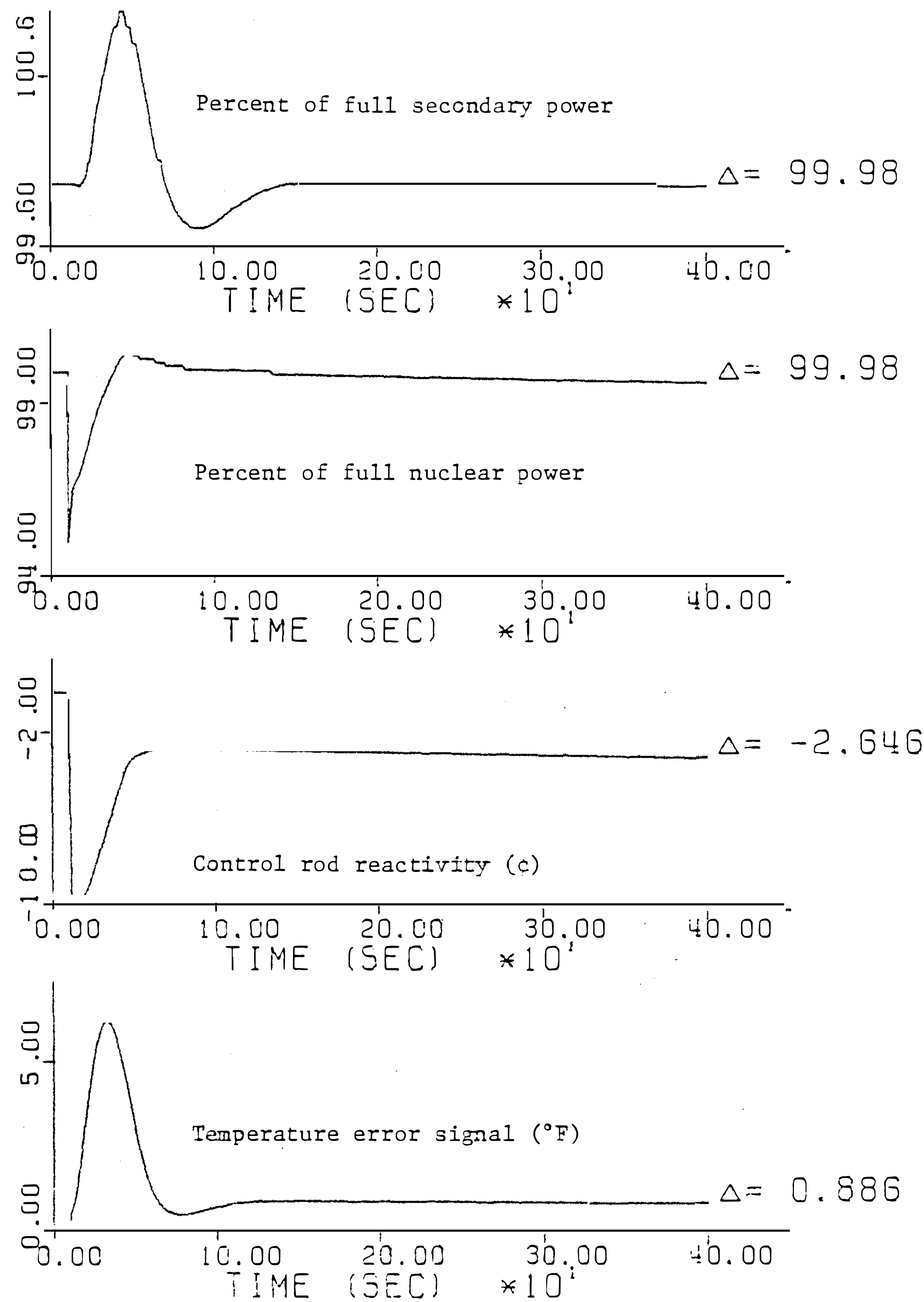

Figure 2.20 Response of coupled UTSG, reactor core, three element controller, and reactor controller models for a -10 cent step in reactivity after 10 seconds of observation time.

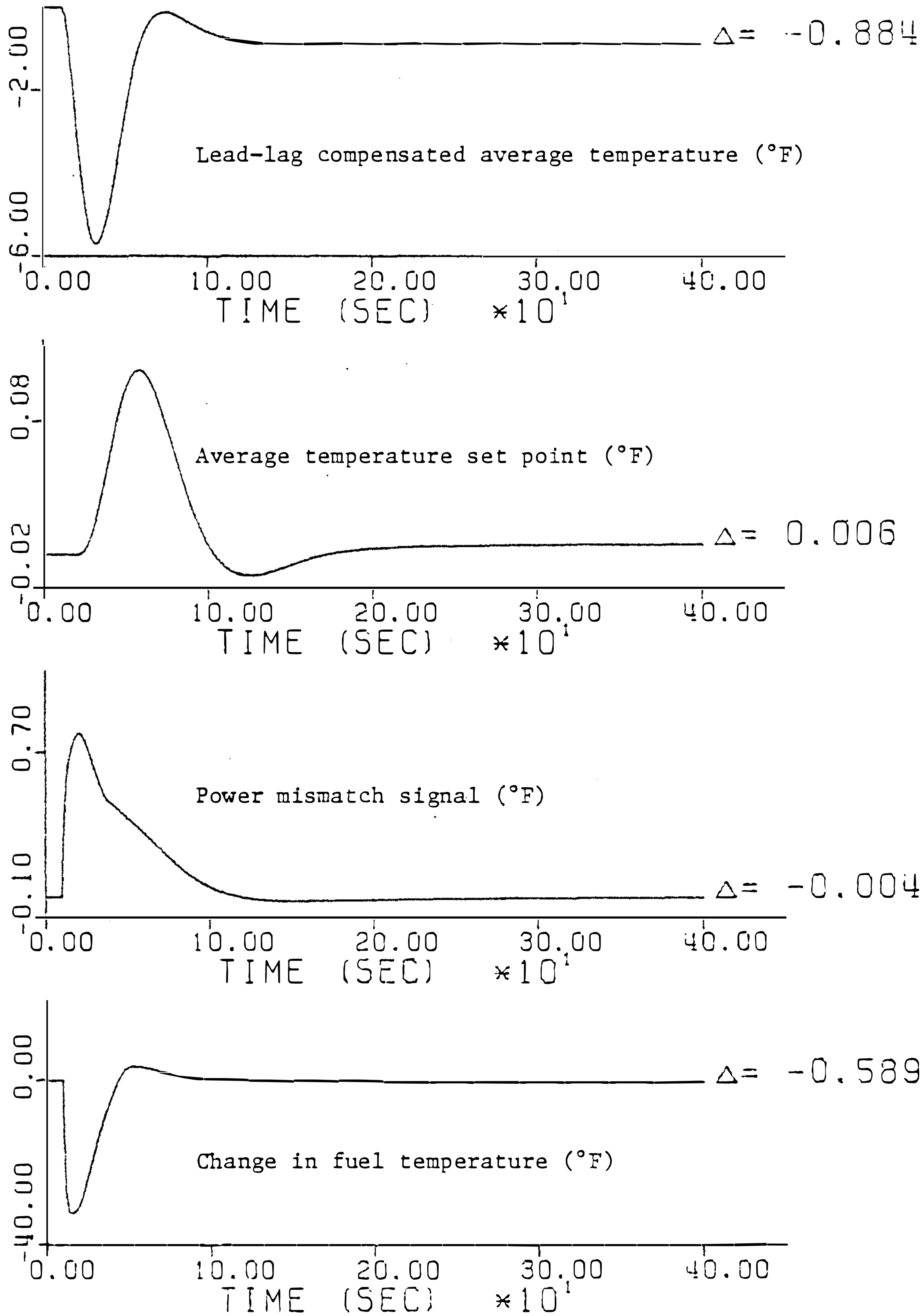

Figure. 2.20 (continued)

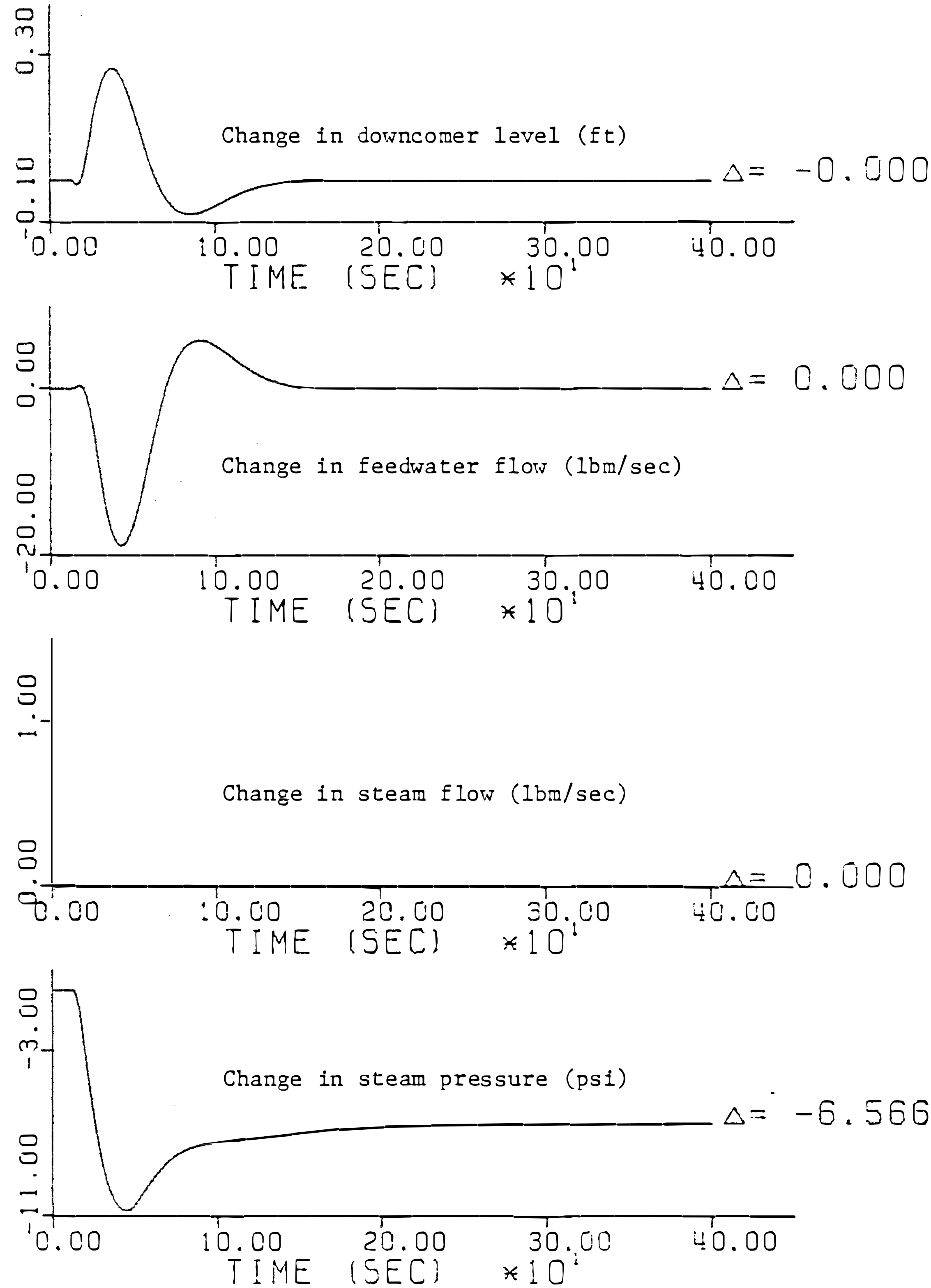

Figure 2.20 (continued)

At steady state, ρ_{TOTAL} should be equal to zero (because $\delta P_N = 0$). Assuming that the reactivity due to primary pressure is small, the following equation can be written

$$(II.42) \quad 0 = \rho_{ext} + \rho_{fuel} + \rho_{coolant} \, .$$

Then by applying the definition of reactivity induced by fuel and coolant due to temperature changes

$$(II.43) \quad \rho_{fuel} = \left(\frac{\alpha_F}{\beta_T}\right) 100 \; \delta T_F = 0.09395$$

$$\rho_{coolant} = \left(\frac{\alpha_c}{\beta_T}\right) \frac{100}{2} (\delta\Theta_1 + \delta\Theta_2) = 2.55146$$

$$\text{Total} = 2.6454 \text{ ¢}$$

$$= - \rho_{ext} \, .$$

This demonstrates that the existence of the deadband in the reactor control system will not allow the average temperature to reach the average temperature setpoint as defined by the steady state program. The reactivity necessary to achieve a new power level will then have to be induced on the system by the difference in the coolant temperature from the average temperature setpoint.

These three cases demonstrate that the reactor control system model can be coupled with existing models by modifying existing computer programs.

II.5 The Pressurizer and Pressurizer Control System

The pressurizer maintains the reactor coolant system pressure at a constant value during steady-state operation of the plant. During a transient, the pressure changes are limited by the pressurizer control system. A typical pressurizer is shown in Figure 2.21. The pressurizer is basically a large tank filled with a two-phase mixture of the primary coolant. Replaceable immersion heaters and a spray nozzle are located in the pressurizer. Relief valves discharge to a pressurizer relief tank.

During steady-state operating conditions, approximately 60 percent of the pressurizer volume is occupied by water and 40 percent by steam. The electric immersion heaters, located in the lower section of the vessel, maintain a constant system operating pressure.

A reduction in plant electrical load causes a temporary increase in average reactor coolant temperature. This in turn causes an increase in the reactor coolant volume because the coolant density decreases. The reactor coolant is connected to the pressurizer by a "surge" line from the hot leg piping to the bottom of the pressurizer tank. Therefore, flow of water into and out of the pressurizer is constantly taking place in the "surge" line. The expansion of the reactor coolant raises the water level in the pressurizer. This increase in water level compresses the steam, and thus raises the pressure. Reactor coolant from the cold leg piping is connected to the top of the pressurizer to spray nozzles. A nominal spray flow rate of about (1) gallon per minute is maintained through the spray nozzle at all times to keep it from plugging. If a positive pressure

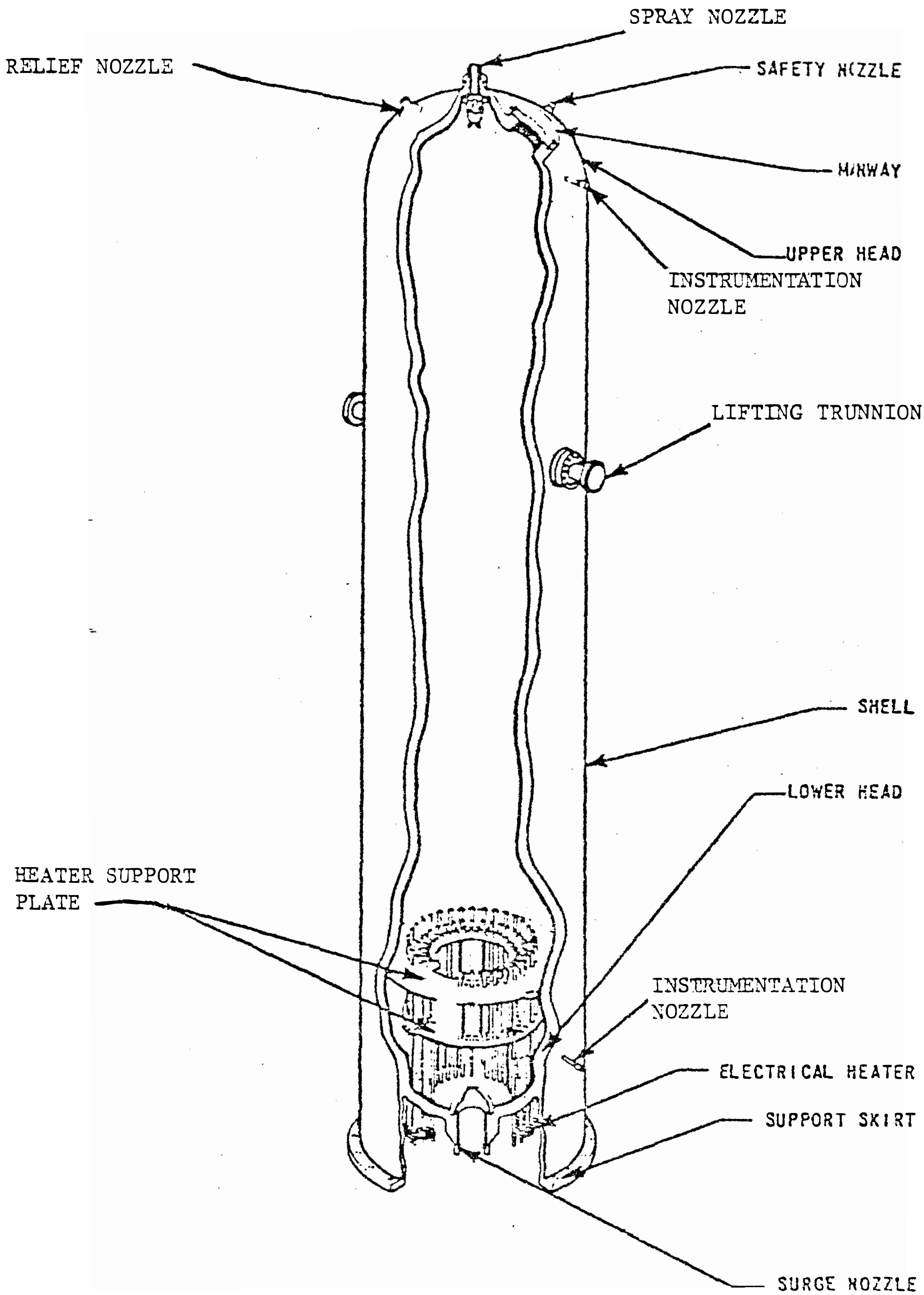

Figure 2.21 Pressurizer

transient is too large to be handled by a reduction of power to the immersion heaters alone, then the spray is increased to condense a portion of the steam. This quenching action reduces pressure and limits the pressure increase. In the event that the pressure increase still cannot be reduced, at some point, the relief valves will open and send steam to the pressurizer relief tank. A further increase in pressure will cause safety valves to open and send more steam to the pressurizer relief tank.

An increase in plant electrical load results in a temporary decrease in average coolant temperature and thus a contraction of coolant volume. Coolant then flows from the pressurizer into the reactor coolant loops, thus reducing the pressurizer level and pressure. Water in the pressurizer flashes to steam to limit the pressure reduction. This reduction in pressure also causes the immersion heaters to increase their output to further limit the pressure reduction.

A dynamic model which represents the pressurizer pressure has been developed previously (Thakkar[37]). The pressurizer water level will not be considered in this study. When water level begins to change, there will be an imbalance of water in-flow and out-flow. This imbalance represents a change in water inventory in the reactor coolant system. A pressurizer level control system regulates this level and maintains it at a desired point. The reactor coolant pressure will have some feedback on the rest of the system through the pressure coefficient of reactivity in the power equation (equation II.1). However, there is no feedback from pressurizer water level on the rest of the system model. Therefore, a pressurizer model which represents only the pressurizer pressure is sufficient for this study.

The derivation of this model will not be presented here (the reader is referred to Thakkar[37] for this information). This deriviation involves a mass balance of water and steam and an energy balance of the whole system. Saturation conditions are assumed throughout the pressurizer and the ideal gas law is used as an equation of state for the steam. The mass flow rate of water in and out of the pressurizer is assumed linearly related to the coolant density gradient with respect to temperature at the design operating pressure. The pressurizer pressure equation is shown below

$$
\begin{aligned}
\text{(II.44)}\quad & \left\{ M_{w_o} \frac{\partial u_w}{\partial P_p} + M_{w_o} P_{p_o} \frac{\partial v_w}{\partial P_p} + \frac{(h_{fg} + P v_w)_o}{A} \right. \\
& \left. + \frac{(h_{fg} + P v_w)_o B}{A(A-B)} \right\} \frac{d\,\delta P_p}{dt} = \left[W_{w_o} \left\{ -C_p \frac{\partial T_w}{\partial P_p} \right. \right. \\
& \left. + P_{p_o} \frac{\partial v_w}{\partial P_p} + v_{w_o} \right\} + W_{sp_o} \left\{ -C_p \frac{\partial T_w}{\partial P_p} + P_{p_o} \frac{\partial v_w}{\partial P_p} \right. \\
& \left. \left. + v_{w_o} \right\} - W_{s_o} \left\{ P_{p_o} \frac{\partial v_w}{\partial P_p} + v_{w_o} \right\} \right] \delta P_p + \delta q \\
& + \left\{ h_{w_i} - h_{w_o} + P_{p_o} v_{w_o} + \frac{B(h_{fg} + P_p v_w)_o}{A-B} \right\} \delta W_w \\
& + \left\{ h_{sp_o} - h_{w_o} + P_{p_o} v_{w_o} + \frac{B(h_{fg} + P_p v_w)_o}{A-B} \right\} \delta W_{sp} \\
& + C_p W_{w_o} \delta T_{w_i} + C_p W_{sp_o} \delta T_{sp}
\end{aligned}
$$

equation (II.44) continued

where

$$A = RT_s \Big/ \left[V_{s_o} - R M_{s_o} \frac{\partial T_s}{\partial P_s}\right]$$

$$B = P_{s_o} \Big/ \left[\rho_w \left(V_{s_o} - R M_{s_o} \frac{\partial T_s}{\partial P_s}\right)\right]$$

where

(II.45) $$\delta W_w = \sum_{i=1}^{n} V_i \beta_i \frac{d\,\delta\Theta_{ci}}{dt}$$

and $\delta\Theta_{ci}$ is the deviation of the ith reactor coolant temperature node.

The design parameters necessary to calculate the coefficients for this model are shown in Table IX. After calculating the coefficients, one finds that there are two important coefficients. The first is the coefficient appearing on the derivative which will be very large. The second is the coefficient of the insurge flow rate. The coefficient

TABLE IX

PARAMETERS NEEDED TO CALCULATE A TYPICAL PRESSURIZER PRESSURE MODEL

1.	P_{Po}	primary system pressure (psia)	2250.0
2.	R	ideal gas constant (ft-lbf/lbm-R)	53.35
3.	T_{sat}	saturation temperature (°F)	652.90
4.	V_{so}	initial steam volume (ft^3)	720.0
5.	ρ_{so}	initial steam density (lbm/ft^3)	6.3727
6.	M_{so}	initial steam mass (lbm)	4588.33
7.	$\frac{\partial T_{sat}}{\partial P_p}$	saturation temperature gradient with respect to pressure (°F/psi)	0.0645
8.	ρ_{wo}	initial water density (lbm/ft^3)	37.0645
9.	V_{wo}	initial water volume (ft^3)	1080.0
10.	M_{wo}	initial water mass (lbm)	40029.65
11.	$\frac{\partial u_w}{\partial P_p}$	internal energy of the liquid gradient with respect to pressure (B/lbm-psi)	0.11
12.	$\frac{\partial v_w}{\partial P_p}$	specific volume gradient with respect to pressure (ft^3/lbm-psi)	5.8×10^{-6}
13.	h_{fg}	latent heat of vaporization (B/lbm)	414.8
14.	v_{wo}	initial specific volume of the water (ft^3/lbm)	0.02698
15.	W_{spo}	initial spray flow rate (gal/min) (ft^3/sec)	1.0 3.85
16.	W_{so}	initial steam relief valve flow rate	0.0
17.	h_{wi}	initial water inlet enthalpy (B/lbm)	672.81
18.	h_{wo}	initial water outlet enthalpy (B/lbm) = enthalpy of saturated liquid	701.1
19.	h_{spo}	initial enthalpy of the liquid entering the spray nozzle (B/lbm)	574.36

TABLE IX (continued)

20.	$C_{P_{HL}}$	specific heat of the hot leg fluid (B/lbm-°F)	1.1386
21.	$C_{P_{CL}}$	specific heat of the cold leg fluid (B/lbm-°F)	1.1226
22.	$C_{P_{sat}}$	specific heat of the saturated liquid (B/lbm-F)	2.115
23.	ρ_{CL}	density of the cold leg piping (lbm/ft^3)	46.62
24.	α_P	pressure coefficient of reactivity (psi)	-1.0×10^{-6}

COOLANT NODE DATA AT 75% POWER

NODE	SYMBOL	TEMPERATURE °F	VOLUME ft^3	DENSITY GRADIENT (lbm/ft^3-°F)
9	Θ_1	562.5	270.0	-0.06916
10	Θ_2	585.0	270.0	-0.07578
11	Θ_{UP}	585.0	1376.0	-0.7578
12	T_{HL}	585.0	250.0	-0.7578
13	Θ_{LP}	540.0	1791.0	-0.06115
14	T_{CL}	540.0	500.0	-0.06115
15	T_{Pi}	585.1	170.3	-0.7578
16	T_{P1}	581.3	48.22	-0.7469
17	T_{P2}	556.6	320.0	-0.06799
18	T_{P3}	556.6	320.0	-0.06799
19	T_{P4}	541.6	48.22	-0.06115

TABLE IX (continued)

20	T_{Po}	540.1	170.3	-0.06115
pressurizer temperature		652.9	1080.0	-0.12388

NOTE

The volumes and temperatures for nodes 15 through 20 were calculated from a steady state calculation of the UTSG by SYSTEM.

NOTE

State variables 12, 14, and 15 through 20 must have their volumes multiplied by the number of UTSG's.

NOTE

The pressurizer temperature node is assumed to change at the same rate as the hot leg temperature.

on the pressure term will be very small after dividing through by the derivative coefficient (typically 10^{-6}) and could be set equal to zero if desired. The insurge flow rate depends on all the reactor coolant state variables. All the equations for the reactor coolant state variables have been calculated previously. All that is necessary is to calculate the two "important" coefficients and have the computer generate the remaining coefficients. A convenient place to do this is immediately after the system matrix has been read in by MATEXP. Subroutine PRESS has been added to MATEXP to calculate the pressurizer coefficients. The only other input necessary to calculate the coefficients is to look up the density gradients in a steam table and change them when a new initial power level is desired. The FORTRAN listing for this subroutine is shown in Figure 2.22. The instructions for the use of this subroutine are included in Appendix A.

All the other terms in the pressurizer equation are forcing terms and are not considered in this study except the heater power forcing term. This term will be coupled to a pressurizer pressure control system model. The coefficient on this term is unity and needs no calculation.

Figure 2.23 shows the response of the coupled pressurizer pressure model for a +10 cent step in reactivity that begins after ten seconds of observation time. The final value at steady state is 8.682 psi. The shape of the response and its final value are consistent with previous work (Thakkar[37]). Therefore, a pressurizer pressure control system model can now be coupled.

```
SUBROUTINE PRESS
      DIMENSION A(70,70),C(70,70),HP(70,70),QPT(70,70),
     1X(70),Y(70),Z(70),XIC(70),TQP(70)
      DIMENSION NSPTV(24)
DIMENSION COFX(70)
DIMENSION V(20),B(20)
     0COMMON C,HP,A,QPT,X,Z,Y,ITMAX,KK,LL,MM,
     1JJFLAG,XIC,NI,TIME,TMAX,TZERO,NE,TQP,T,
     2I1Z,ICONTR,PLTINC,MATYES,ICSS,JFLAG,PLT
      COMMON KIT,ZRP,NR,MF,M12,MF1,AMP,NSA,NII,XP,YP
      COMMON NPLOT,NSPTV
      COMMON ITYPE,JTYPE,NTYPE,NSET3,NSET2,NSET1,NROW1,NP
     #NREAC,NTBAR,NDQ,NSTM,NK3,NK2,NPT,NPN,ROWSTP,BETAT,G
     #DBIN,RK1,RK2,RK3,WMAX,WSO,HG,HGMAX,DHG,COFX,HFW,CP2
V(9)=270.0
V(10)=V(9)
V(11)=1376.
V(12)=250.*3.0
V(13)=1791.
V(14)=500.*3.0
V(15)=170.3*3.0
V(16)=48.22*3.0
V(17)=320.*3.0
V(18)=V(17)
V(19)=V(16)
V(20)=170.3*3.0
B(9)=-0.06916
B(10)=-.07578
B(11)=B(10)
B(12)=B(11)
B(13)=-.06115
B(14)=B(13)
B(15)=-.07578
B(16)=-.07469
B(17)=-.06799
B(18)=-.06799
B(19)=-.06115
B(20)=-.06115
DO 10 I=1,NE-1
DO 10 J=1,20
IF((V(J).AND.B(J)).EQ.0.0)GO TO 10
A(42,I)=A(42,I) - 1.0412050E-2*B(J)*V(J)*A(J,I)
  10    CONTINUE
C  ADD THE PRESSURIZER WATER VOLUME
DO 20 I=1,NE-1
A(42,I)=A(42,I) -1.3547E-3*(-0.12388*1080.0)*A(12,I)
  20    CONTINUE
RETURN
END
```

Figure 2.22 Fortran listing of subroutine PRESS.

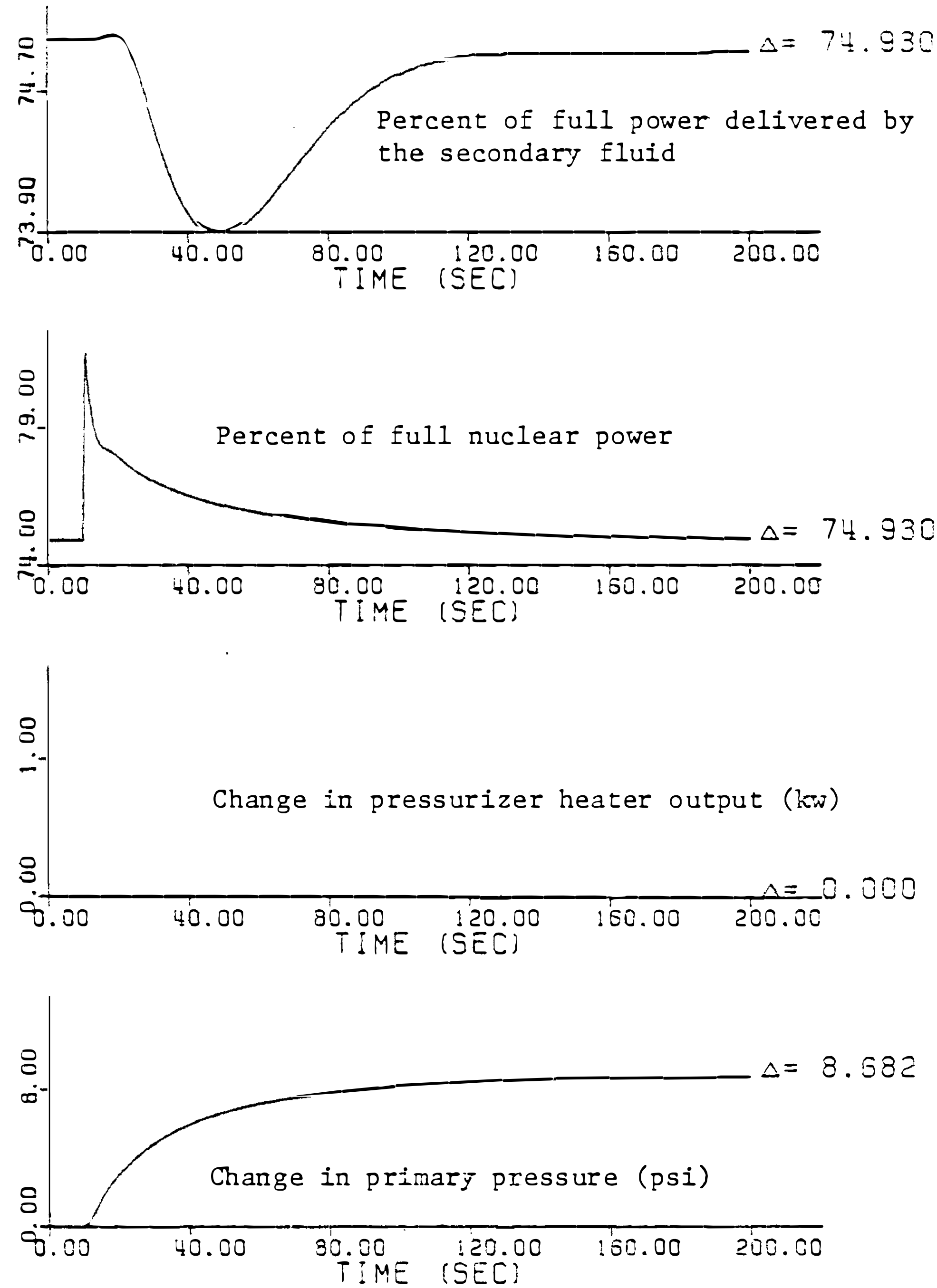

Figure 2.23 Response of coupled pressurizer pressure model for +10 cent step in reactivity after ten seconds of observation time.

The pressurizer pressure control system model is taken from Westinghouse[38] documentation. A block diagram of the control system is shown in Figure 2.24. From Figure 2.24, it can be seen that at ± 15 psi around the design pressure, only the immersion heaters have any control action. If the model that is to be used in this study is to consider only small changes in the primary pressure (less than 15 psi), then the control system can be represented by a linear model.

Figure 2.25 shows a block diagram of the transfer function which describes the heater output governed by the pressurizer pressure control system. A state variable representation has previously been derived for this control system (Strange[35]). The resulting equations are shown below.

$$\frac{d\,\delta P_p}{dt} = C_1\,\delta P_p + C_2\,\delta W_w + C_3\left[AK\,\delta P_p + \delta D + AK\frac{d\,\delta P_p}{dt}\right] \tag{II.46}$$

$$\frac{d\,\delta D}{dt} = AK\,\delta P_p \tag{II.47}$$

where C_1, C_2, and C_3 are constants which have been calculated previously for the pressurizer pressure model. The essential parameters necessary to calculate the parameters for this model are given in Table X. The heater output from this derivation is defined by the following equation

$$\delta q = A\left[\delta P_p + \frac{1}{\tau_1}\,\delta D + \tau_2\,\frac{d\,\delta P_p}{dt}\right]. \tag{II.48}$$

When this model is coupled with the rest of the system, the heater output can be calculated by subroutine DISTRB in MATEXP at each time

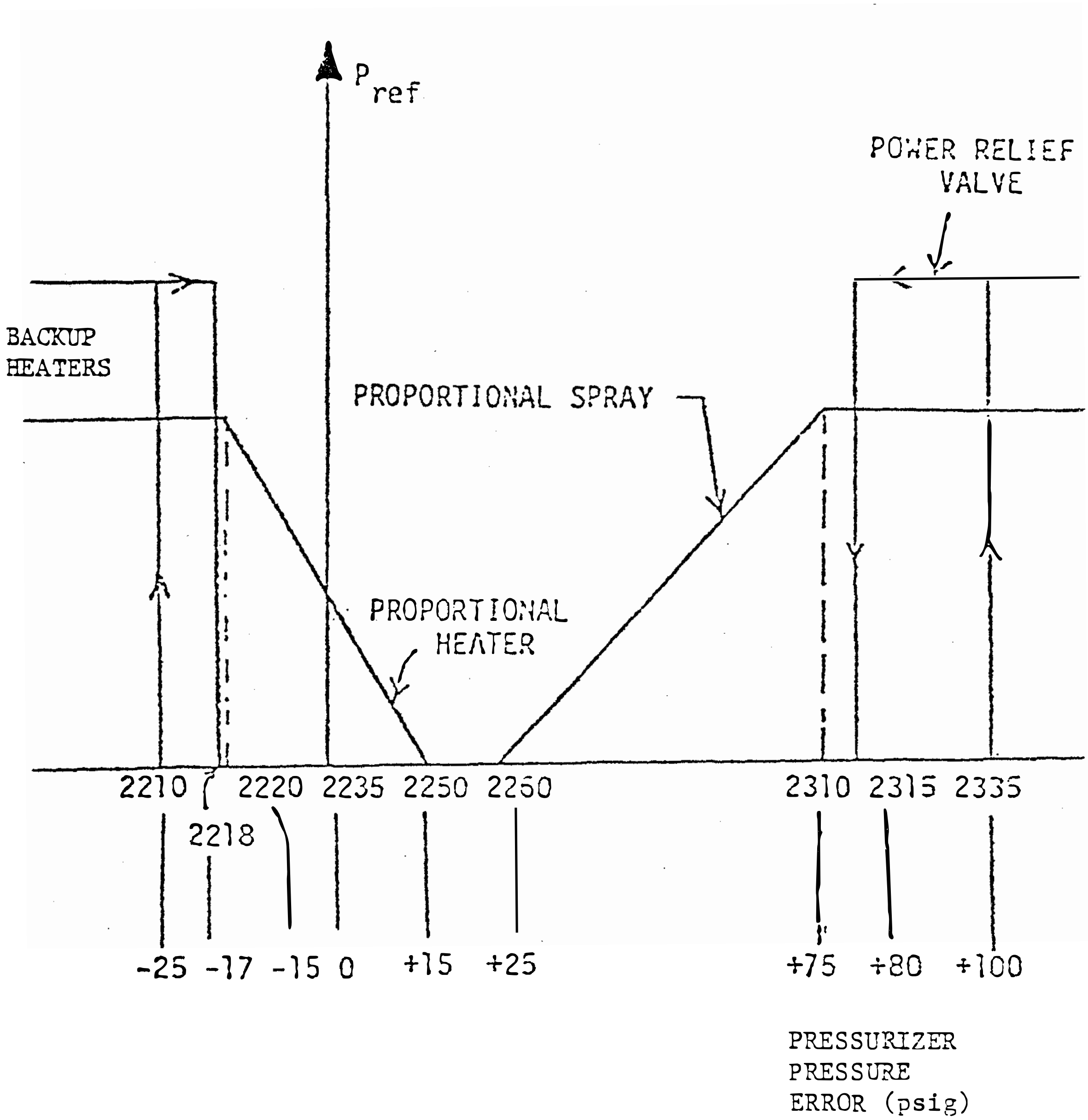

Figure 2.24 Pressurizer pressure control schematic.

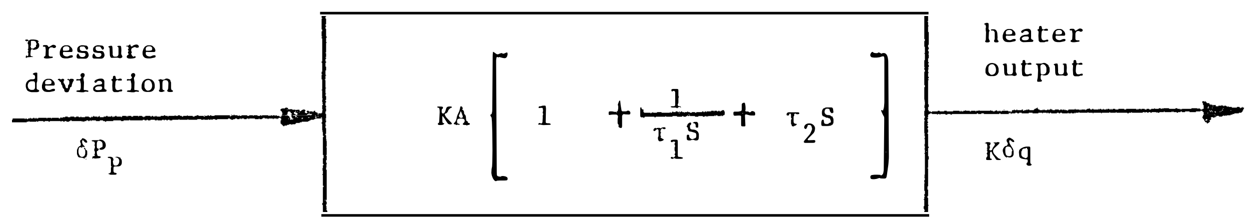

Figure 2.25 Block diagram of the transfer function which describes the heater output of the pressurizer pressure control system.

TABLE X

PARAMETERS NEEDED TO CALCULATE THE
PRESSURIZER PRESSURE CONTROL SYSTEM MODEL

1.	K	unitless gain for PID controller transfer function	5.0
2.	A	gain for PID controller transfer function for heater input (kw/psi)	-60.0
3.	τ_1	time constant for integral control (sec)	900.0
4.	τ_2	time constant for differential control (sec)	1.0
5.	q_{max}	the maximum heater output (kw)	1800.0

step in the solution and the results plotted. Figure 2.26 shows the response of the coupled system including the pressurizer pressure control system model for a +10 cent step in reactivity that begins after ten seconds of observation time. The results are plausible and the pressure deviation has been reduced. Additional results of the overall system which includes pressurizer models are shown in Section II.8.

II.6 The Turbine and Feedwater Heaters

In order to develop a complete model of the mechanical and heat transfer processes in a PWR system, it will be necessary to consider the turbine and feedwater heater systems. The turbine generator and related systems in general do not differ greatly between nuclear plants or between fossil fueled power plants. Therefore the model developed in this section could probably be modified and coupled with many types of systems.

A typical flow diagram and heat balance of a Westinghouse PWR turbo-generator system is shown in Figure 2.27. This figure was obtained from the SEQUOYAH-FSAR[29].

During operation of the plant, four steam generators deliver saturated steam through steam lines to the main turbine. These lines are crosstied near the turbine to ensure that the pressure difference between any of the steam generators does not exceed 10 psi thus maintaining system balance and ensuring uniform heat removal from the reactor coolant system.

As the steam leaves the UTSGs, it passes through throttle and governing valves before entering the main turbine at the high pressure

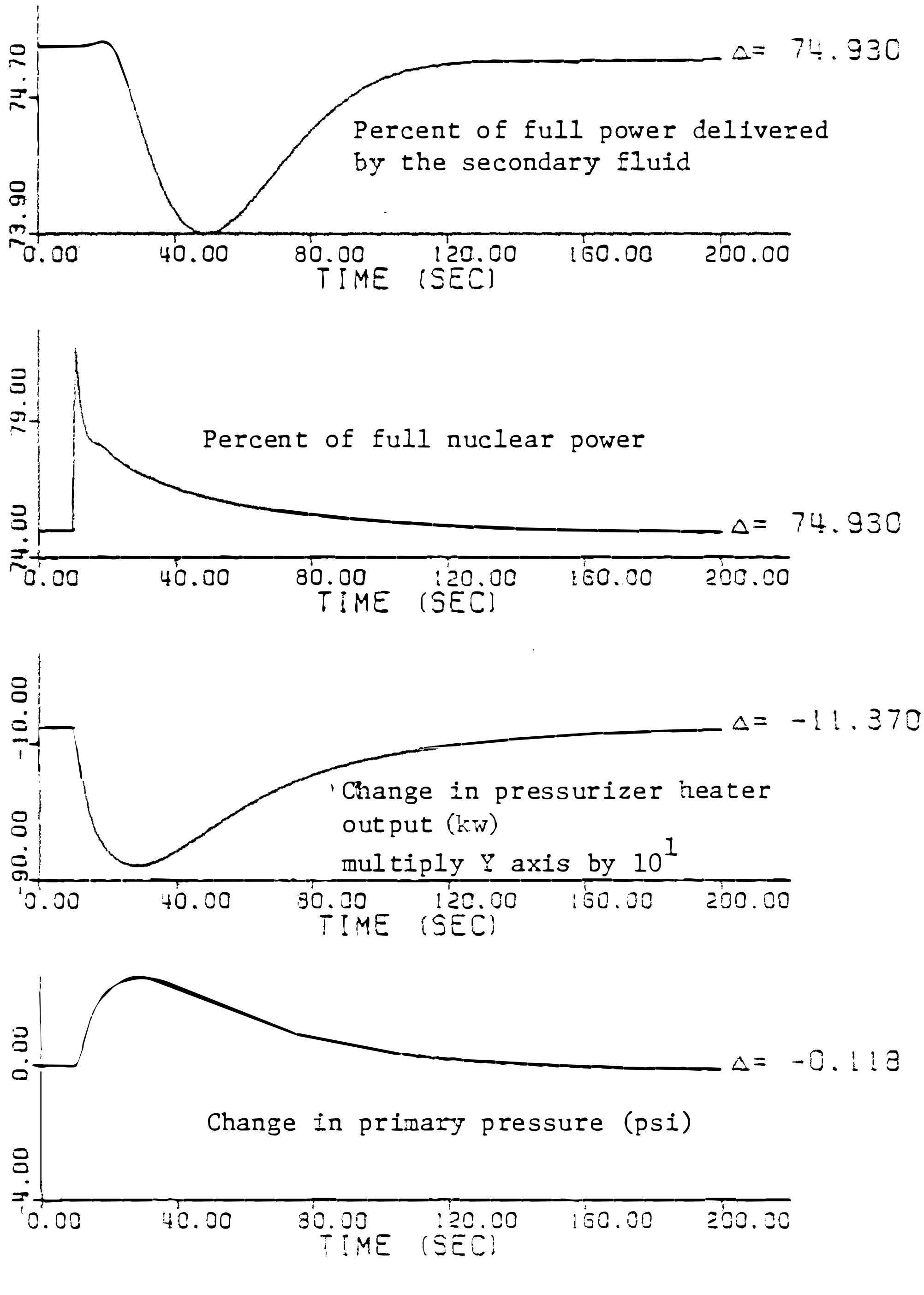

Figure 2.26 Response of coupled pressurizer pressure control model for a +10 cent step in reactivity after ten seconds of observation time.

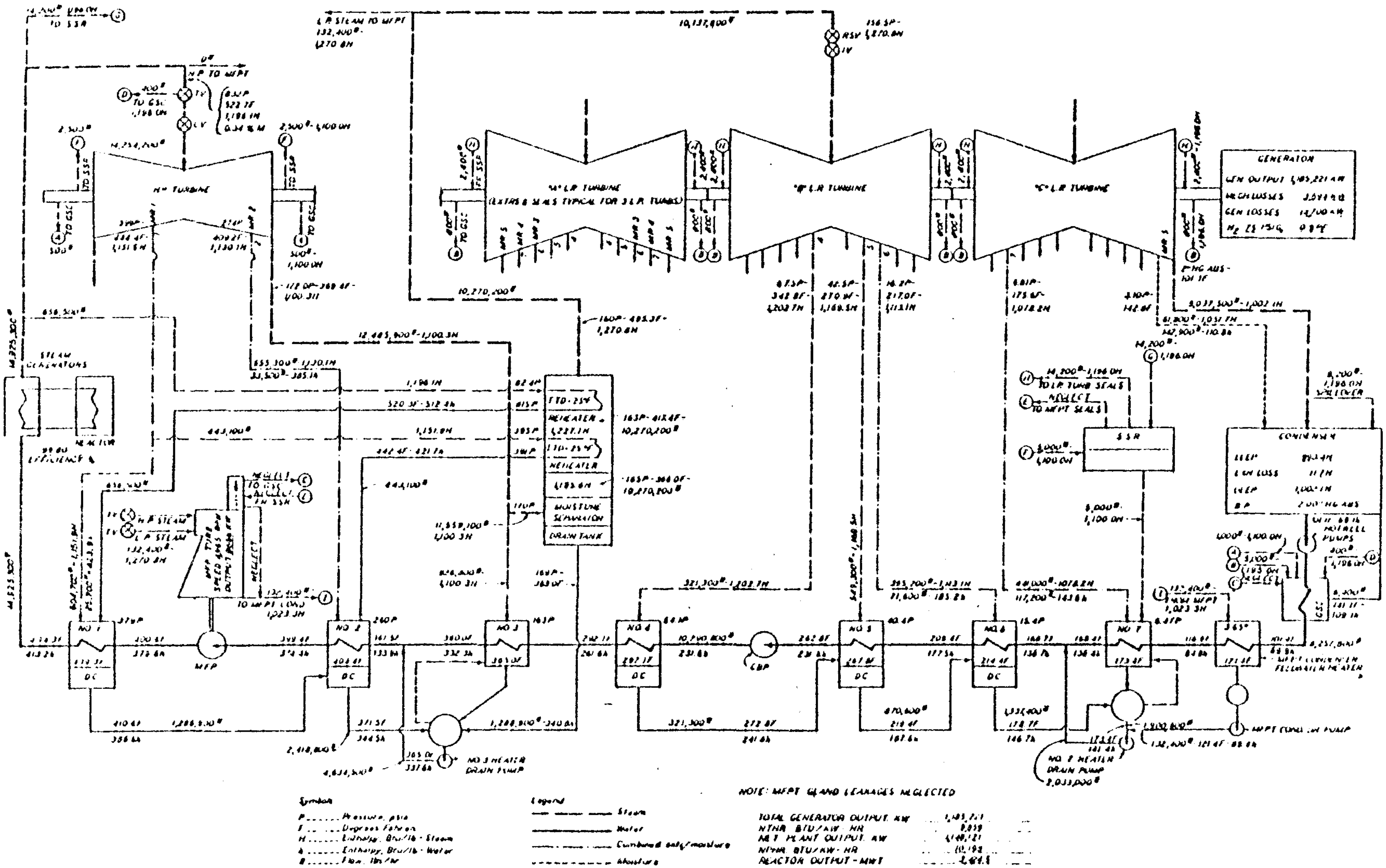

Figure 2.27 Typical flow diagram and heat balance of a Westinghouse PWR turbo-generator system.

stage. A portion of the steam in the high pressrue turbine is extracted to the high pressure feedwater heaters; the remainder is exhausted to moisture separator reheaters and low pressure feedwater heaters. In the moisture separator reheaters, moisture is mechanically separated from the turbine steam and the steam is then superheated before entering three low pressure turbines. The steam is superheated in the moisture separator reheaters by receiving energy from a main steam line which has bypassed the high pressure turbine. Then, while the steam is in the low pressure turbines, part of it is extracted to low pressure feedwater heaters, and the remainder is exhausted to the condenser.

The feedwater heating system is of the closed type with deaeration accomplished in the condenser hotwell. The condensate pumps take the condensate through five stages of low-pressure feedwater heaters to the main feedwater pumps. The water discharge from the feedwater pumps flows through high-pressure heaters and into the steam generators.

A dynamic model for a turbine and feedwater heater system has been developed by IBM[11] and modified by Shankkar[32]. In this development, some additional modifications will be made to this model. Primarily, the model will be adjusted to be used on a PWR system by making some assumptions, and the model will be linearized so that it can be analyzed on existing computer codes and coupled with the present PWR model. The derivation of the model is given in Appendix D. The resulting model is an 11th order state variable representation. At this point, the model has no control action taken on the bypass steam valving and the main steam valving. A block diagram of the model is shown in Figure 2.28. The reader should compare the block diagram with the actual flow diagram. The symbols of the state variables are shown in Figure 2.28. The values of all the necessary data which are needed to calculate the coefficients for this model are given in Table XI. The resulting state variables for this model are described in Table XII. The numbers of the state variables are arrived at by coupling this model to the existing PWR model. Note that some of the state variables have unitless dimensions in order to make the solution to the equations more easily obtainable.

This dynamic model has four possible forcing terms. These are

1. The inlet steam flow rate to the nozzle chest
2. The bypass steam flow rate to the moisture separator reheaters
3. The inlet steam pressure to the nozzle chest and moisture separator
4. The outlet feedwater flow rate to the steam generators.

The forcing terms as they appear in the model are shown in Table XIII. When this model is coupled with the existing PWR model, the only remaining forcing term will be steam flow. Again the steam flow is represented in two ways as given by equations (II.23) and (II.24).

It is important to realize that the final power delivered by the turbine to the electrical generator is not a state variable. This is plausible since the electrical power should have no feedback effect on the turbine except possibly through a control system. But, the power produced by the turbine is a linear combination of the state variables in this model, and can be calculated during a disturbance. This is easily accomplished, as with any algebraic variable, with the use of

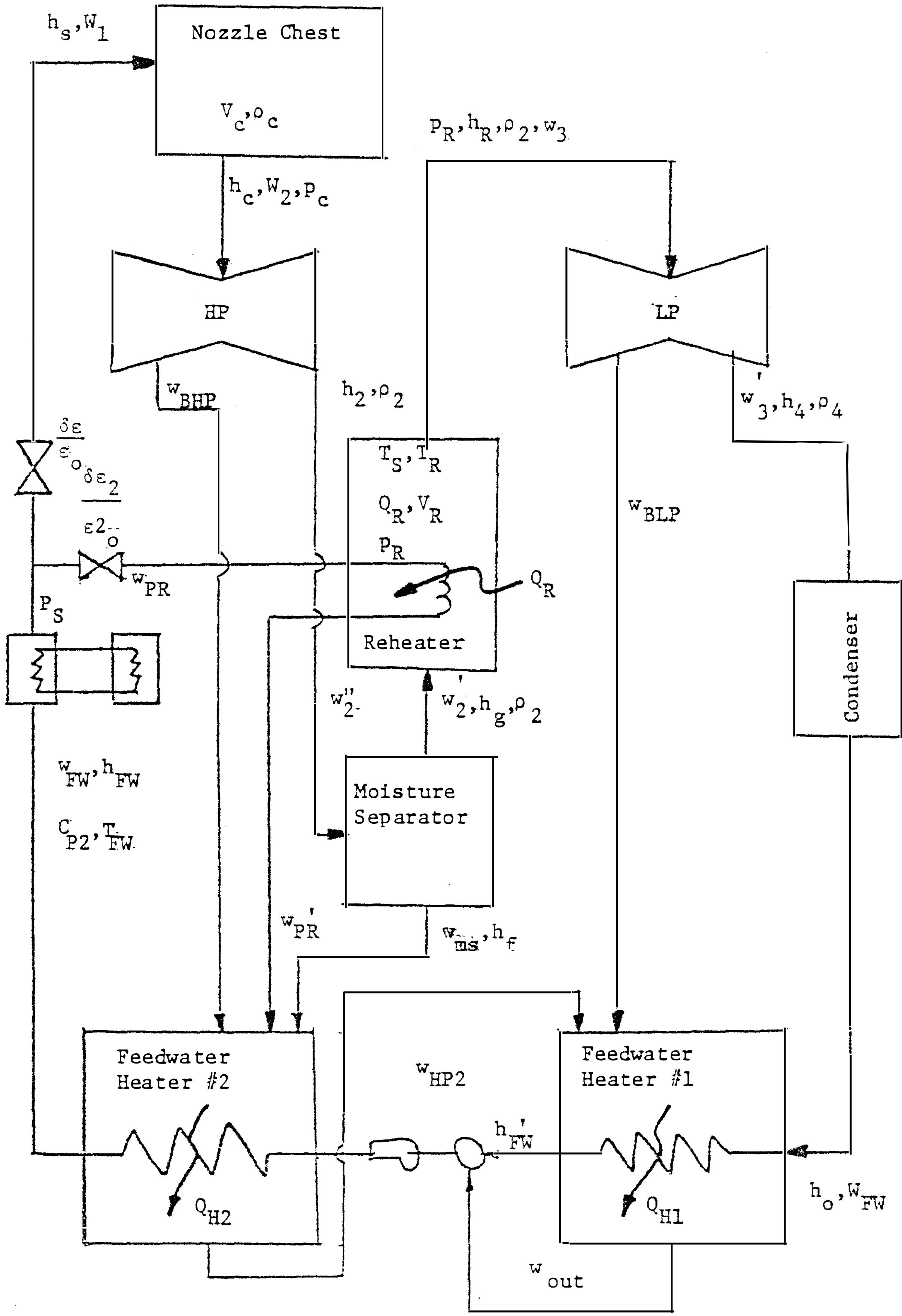

Figure 2.28 Turbine-feedwater heater model block diagram.

TABLE XI

PARAMETERS NEEDED TO CALCULATE THE TURBINE-FEEDWATER HEATER MODEL MATRIX COEFFICIENTS

1. W_1, W_2	flow rate of steam in and out of the nozzle chest (lbm/sec)	3959.5**
2. W_2', W_3	flow rate of steam in and out of the reheater shell side (lbm/sec)	2852.8 **
3. W_{PR}, W_{PR}'	flow rate of steam in and out of the reheater tube side (lbm/sec)	182.36**
4. W_{MS}	the flow rate of the drain from the moisture separator (lbm/sec)	358.03**
5. W_S, W_{FW}	the flow rate of the main steam and feedwater at initial conditions from all UTSG's (lbm/sec)	4145.9**
6. W_2''	flow of steam leaving HP turbine to the moisture separator (lbm/sec)	3210.86**
7. W_3'	flow of steam leaving the LP turbine to the condenser (lbm/sec)	2232.6**
8. W_{HP2}	flow of fluid from feedwater heater 2 to feedwater heater 1 (lbm/sec)	1217.8**
9. K_{BHP}	fraction of steam entering the HP turbine that is extracted to feedwater heater 2	0.1634**
10. K_{BLP}	fraction of steam entering the LP turbine that is extracted to feedwater heater 1	0.2174**
11. τ_{H1}	time constant for feedwater heater 1 heat transfer (sec)	100.0*
12. τ_{H2}	time constant for feedwater heater 2 heat transfer (sec)	40.0*

TABLE XI (continued)

13.	τ_{HP2}	time constant for feedwater heater 2 shell side (sec)	10.0*
14.	τ_{W3}	time constant for flow in LP turbine (sec)	10.0*
15.	τ_{R2}	time constant for heat transfer in reheater (sec)	4.0*
16.	τ_{R1}	time constant for flow in reheater (sec)	3.00*
17.	τ_{W2}	time constant for flow in HP turbine (sec)	2.0*
18.	h_4'	enthalpy of isentropic endpoint of LP turbine expansion (B/lbm)	958.4**
19.	h_R	enthalpy of steam leaving reheater (B/lbm)	1270.8**
20.	h_2	enthalpy of steam leaving HP turbine to moisture separator (B/lbm)	1100.3**
21.	h_s, h_c	enthalpy of steam entering and leaving the nozzle chest (B/lbm)	1196.1**
22.	h_f	enthalpy of saturated water in the moisture separator (B/lbm)	338.75**
23.	h_{fg}	latent heat of vaporization in the moisture separator (B/lbm)	857.7**
24.	h_2'	enthalpy of steam at the isentropic end point of the nozzle chest pressure (B/lbm)	1084.7****
25.	h_4	enthalpy of steam entering condenser from LP turbine (B/lbm)	1002.1**
26.	ρ_2	density of steam leaving HP turbine to the moisture separator (lbm/ft^3)	1.8281****

TABLE XI (continued)

27.	ρ_c	density of steam leaving the nozzle chest (lbm/ft^3)	2.1263****
28.	ρ_R	density of steam leaving the reheater (lbm/ft^3)	0.3566****
29.	ρ_z'	density of the steam at the isentropic endpoint of the nozzle chest pressure (lbm/ft^3)	0.6181****
30.	P_3	pressure of steam leaving the reheater (psf)	1.0868**
31.	P_R	pressure of steam entering the reheater (psf)	1.1111**
32.	P_c	pressure of the steam leaving the nozzle chest (psf)	5.488***
33.	P_{R1}	pressure used in empirical relationship for isentropic endpoint of HP turbine expansion (psf)	1.1111**
34.	$\frac{\partial h_g}{\partial P_s}$	gradient of steam enthalpy to steam pressure in the main steam line (B/lbm-psi)	-0.035****
35.	$\frac{\partial T_{sat}}{\partial P_s}$	gradient of saturation temperature to steam pressure in the main steam line (°F/psi)	0.14****
36.	C_{PZ}	specific heat of the feedwater (B/lbm-°F)	1.14****
37.	C_V	specific heat at constant volume of the steam in the reheater shell side (B/lbm-°F)	0.41****
38.	V_R	volume of the reheater shell side (ft^3)	20000.0***
39.	V_C	volume of the nozzle chest (ft^3)	200.0***

TABLE XI (continued)

40.	H_{FW}	assumed constant enthalpy of shell side in heater 2 (B/lbm)	475.0*
41.	H_R	assumed specific heat of steam in reheater (B/lbm-°F)	21.6*
42.	Q_R	initial heat transfer in reheater (MW)	226.43**
43.	$(T_S - T_R)$	initial temperature difference for heat transfer in the reheater (°F)	54.48**
44.	ϵ_2	valve coefficient of bypass steam (lbm/sec-psi)	0.21918**
45.	ϵ	valve coefficient of main steam (lbm/sec-psi)	1.2458**
46.	A_{K2}	area used in empirical relationship for steam flow out of the nozzle chest (ft^2)	207.82*
47.	K_3	area used in empirical relationship for steam flow out of the reheater shell side (ft^2)	798.7*
48.	k_1	constant used in Callender's relationship	7.415
49.	k_2	constant used in Callender's relationship	149670.0*
50.	R	constant used in ideal gas law (ft-lbf/lbm-°R)	85.78****
51.	γ	gradient of internal energy with respect to enthalpy in the reheater	1.2927****
52.	η_{LP}	efficiency of LP turbine	0.86*
53.	η_{HP}	efficiency of HP turbine	0.86*
54.	J	conversion factor (ft-lbf/B)	778.169****

TABLE XI (continued)

55.	Ω	initial speed of the rotor (Hz)	60.0***
56.	g_c	gravitational constant ($lbm\text{-}ft/lbf\text{-}sec^2$)	32.2***

* Values obtained from IBM[11]

** Values obtained from Figure 10.1-3 SEQUOYAH-PSAR[29]

*** These values were assumed

**** Values obtained from steam tables

TABLE XII

LIST AND DESCRIPTION OF THE TURBINE-FEEDWATER MODEL STATE VARIABLES

NUMBER	SYMBOL	DESCRIPTION
44	$\delta\rho_c$	density of steam in the nozzle chest (lbm/ft^3)
45	$\frac{\delta h_c}{h_{co}}$	fractional change in the enthalpy of nozzle chest steam
46	$\frac{\delta W_2''}{W_{2o}''}$	fractional change in the flow rate of steam entering the moisture separator
47	$\delta\rho_R$	density of steam in the reheater shell side (lbm/ft^3)
48	$\frac{\delta h_R}{h_{Ro}}$	fractional change in enthalpy of reheater shell side
49	$\frac{\delta W_{PR}'}{W_{PRo}'}$	fractional change in flow rate of steam leaving the reheater tube side
50	δQ_R	heat transfer in the reheater shell to tube (Mw-hr/sec)
51	$\frac{\delta W_3'}{W_{3o}'}$	fractional change in flow rate of steam leaving LP turbine to the condenser
52	$\delta h_{FW}'$	change in the enthalpy of feedwater in heater 1 (B/lbm)

TABLE XII (continued)

NUMBER	SYMBOL	DESCRIPTION
53	δT_{FW}	change in feedwater temperature leaving heater 2 (°F)
54	$\frac{\delta W_{HP2}}{W_{HP2_0}}$	fractional change in flow rate of fluid leaving heater 2 to heater 1

TABLE XIII

LIST OF THE FORCING TERMS AS THEY APPEAR IN THE ISOLATED TURBINE-FEEDWATER HEATER MODEL

1) Steam Flow

$$f(44) = \frac{1}{V_c} \delta W_1$$

$$f(45) = \frac{1}{\frac{1-K_1}{g_c}} \left[\frac{h_s}{h_c \rho_c V_c} + \frac{P_c}{h_c \rho_c {}^2 V_c J} - \frac{1}{V_c \rho_c} \right] \delta W_1$$

2) Steam Pressure

$$f(45) = \frac{1}{\frac{1-K_1}{g_c}} \left[\frac{W_1}{\rho_c V_c h_c} \quad \frac{\delta h_s}{\delta P_s} \right] \delta P_s$$

$$f(50) = \frac{H_R}{2T_{R2}} (W_{PR} + W_{PR}') \frac{\delta T_s}{\delta P_s} \delta P_s$$

3) Secondary (Bypass) Steam Flow

$$f(49) = \frac{1}{W_{PR}' T_{R1}} \delta W_{PR}$$

$$f(50) = \frac{H_R}{2T_{R2}} (T_S - T_R) \delta W_{PR}$$

TABLE XIII (continued)

4) Feedwater Flow

$$f(52) = \frac{-H_{FW}}{T_{H1} W_{FW}^{2}} (K_{BLP} W_3 + W_{HP2}) \delta W_{FW} - \frac{h_{FW}'}{W_{FW}} \frac{d\delta W_{FW}}{dt}$$

$$f(53) = \frac{-H_{FW}}{W_{FW}^{2}} (K_{BHP} W_2 + W_{MS} + W_{PR}') \delta W_{FW} - \frac{h_{FW}}{W_{FW}} \frac{d\delta W_{FW}}{dt}$$

Note: The steam flows W_1 and W_{PR} can be expressed by equation (II.23) or equation (II.24).

subroutine DISTRB. The derivation of the algebraic equation describing the power produced by the turbine is also given in Appendix D.

In this section, only one case will be presented. Figure 2.29 shows the time response of the turbine-feedwater heater model for a +10% step in the valve coefficient. The feedback on the PWR model will be from the feedwater temperature which has changed by 3.14 F.

The power produced by the turbine will not be shown here (see Section II.7 and II.8 for typical values for this result). The turbine power result would not be conclusive until the turbine-feedwater heater model is coupled to the rest of the system model. These results are plausible. However, improvements on the accuracy of the results could only be made by improving the accuracy of the input data. Additional results of the isolated turbine-feedwater heater model for all the other types of perturbations are shown in Figures E.3 through E.5 of Appendix E.

II.7 The Main Steam and Bypass Steam Control Systems

In order to complete the PWR system model, the mechanical shaft power must be coupled to the electrical power grid system. Before discussing the derivation of the model equations, it will first be necessary to understand some terms used to describe an electrical power system.

The turbine shaft is directly coupled to an electric power generator. The generator will output electrical power which will be designated $\bar{S}$. This electrical power is of a complex form, that is, it is made up of two components called real and reactive power. In

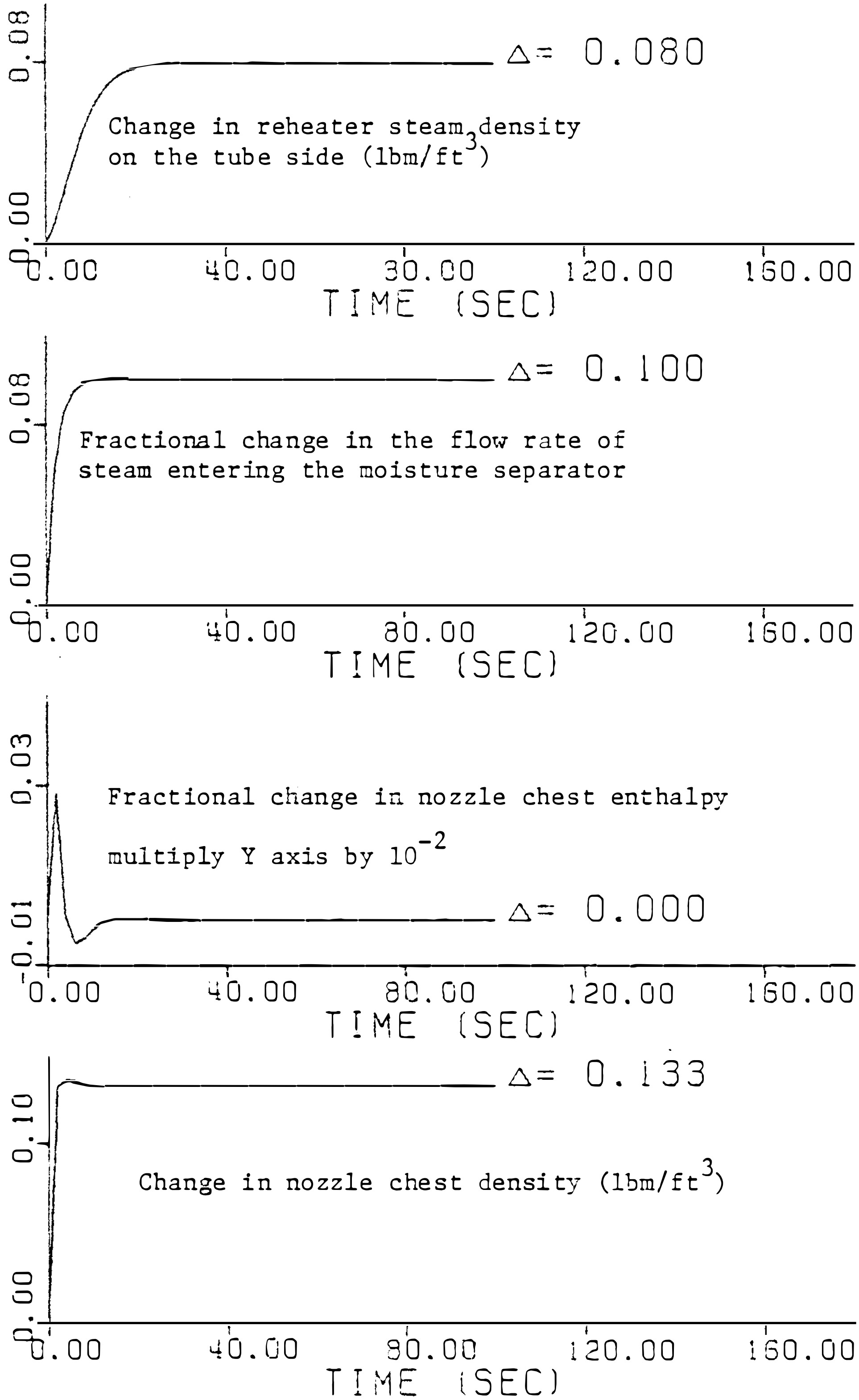

Figure 2.29 Response of the isolated turbine-feedwater heater model for a +10 percent step in steam valve coefficient.

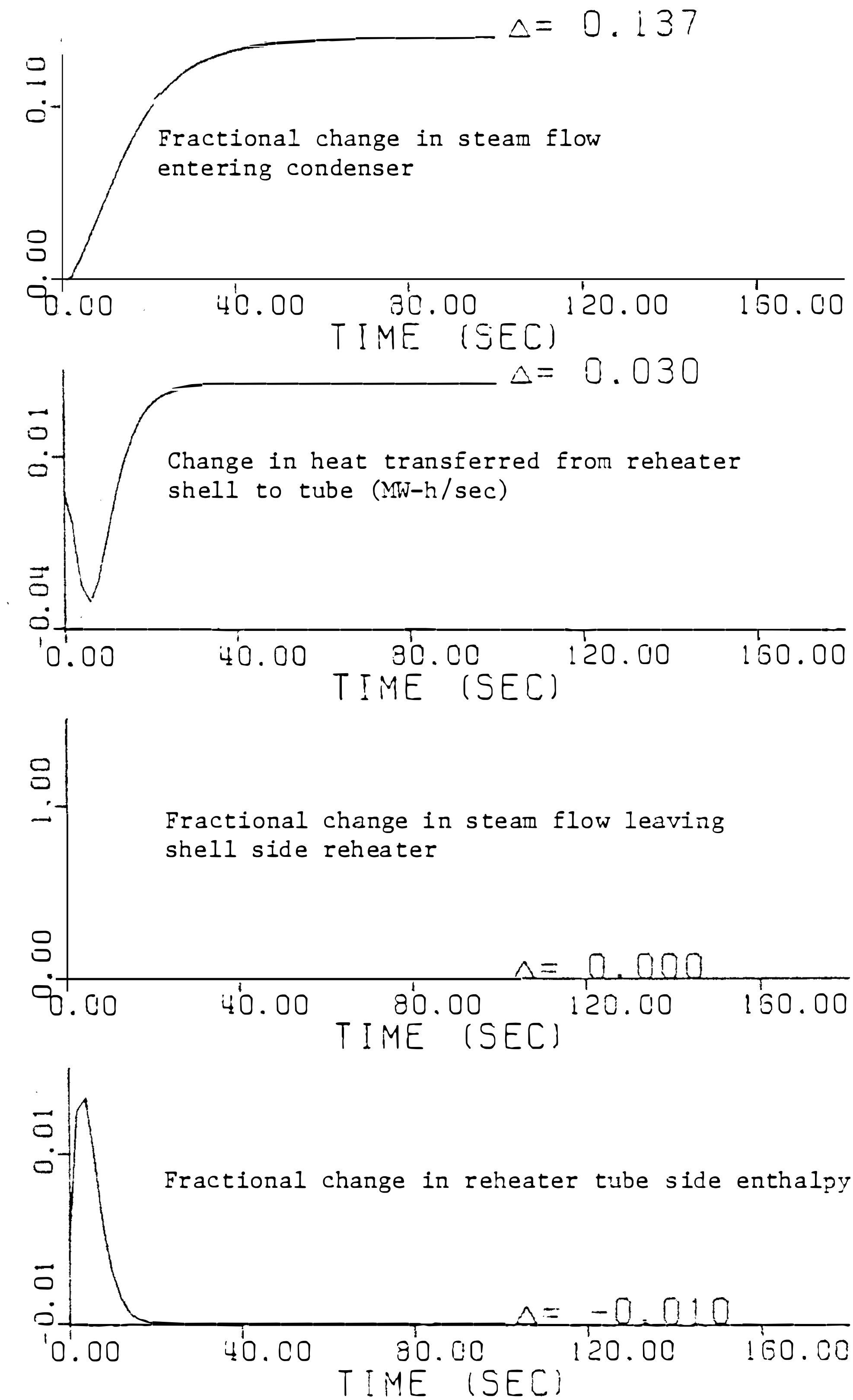

Figure 2.29 (continued)

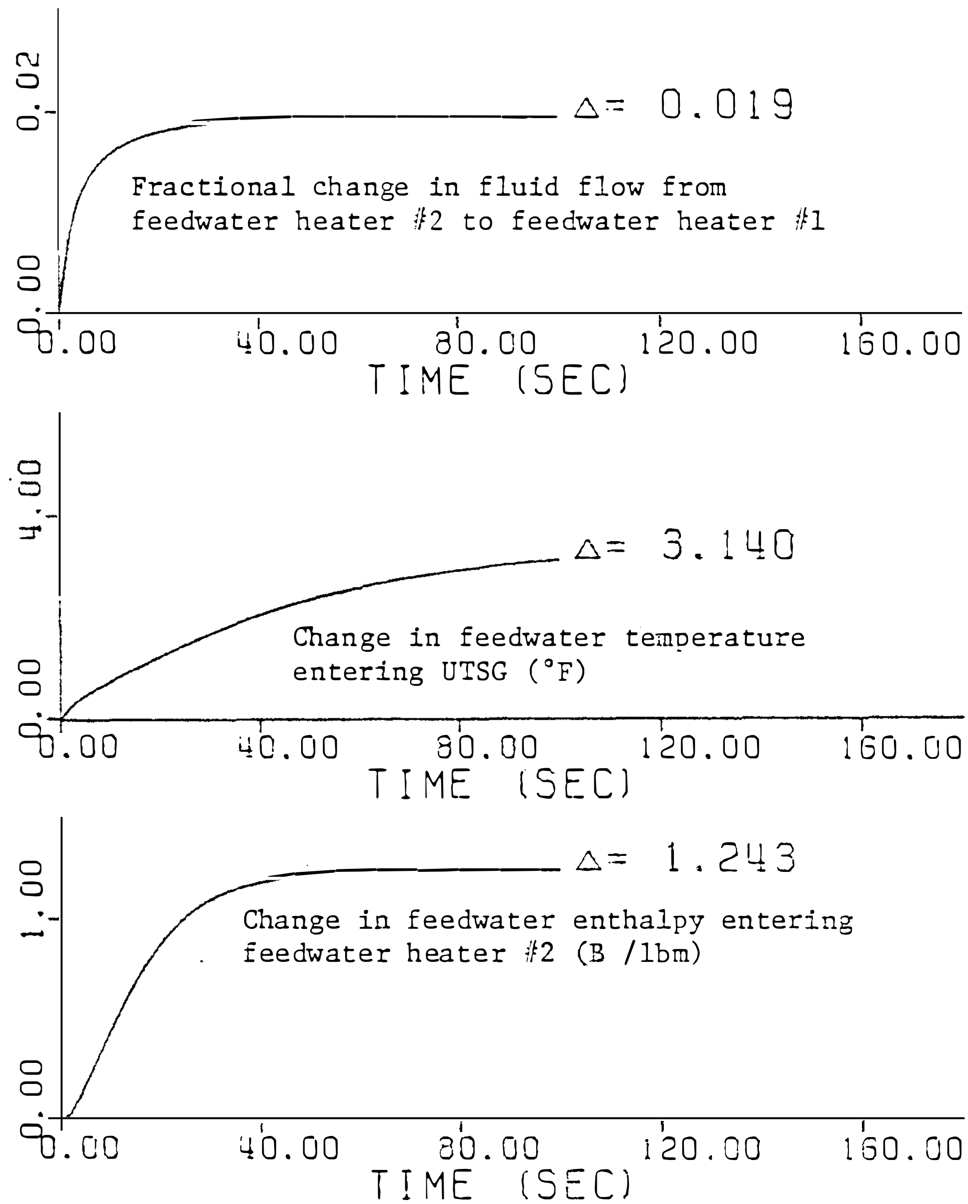

Figure 2.29 (continued)

equation form this is written as

(II.49) $\bar{S} = P + jQ$

P is the real power with typical units of megawatts (Mw), Q is the reactive power with typical units of megavars (Mvar), and $\bar{S}$ is the complex power with typical units of MVA. The complex power can also be written as $\bar{S} = \overline{VI}^*$ where $\bar{V}$ is the generator terminal voltage and $\bar{I}^*$ is the complex conjugate of the current, $\bar{I}$, injected into the electrical system grid by the generator. Since the voltage, $\bar{V}$, and the current, $\bar{I}$, are divided into real and imaginary parts, this explains why it is necessary for the power, $\bar{S}$, to be expressed in a complex form. If it is assumed that no real power losses take place in the generator itself (a typical generator has a 5 percent to 10 percent loss of real power), then the magnitude of P is identically equal to the turbine shaft power Pm. The magnitude of Q, and the angle between P and Q, which will be designated as Θ, is determined by the operating conditions of the generator relative to the electrical grid. The magnitude of the complex power is written in equation form as

(II.50) $|S| = [S^2 + Q^2]^{0.5} = |V||I|$

It is customary to express the electrical units on a per unit basis (pu). In this study, the base power will always be 1000 MVA. Therefore if the generator is producing 500 Mw of real power, this is equivalent to saying that it is producing 0.5 puMw of real power.

The turbo-generator shaft rotates at a frequency F, which in the United States has a normal value of 60 Hz at steady state conditions. Note that at steady state, all the generators in a power grid operate at the same frequency. The electrical power is proportional to the operating frequency of the generator. This can be written as

$$P = F\tau \tag{II.51}$$

where τ is the torque applied on the generator. When a change in power takes place, a torque change is made on the generator. Because the mechanical shaft power has not been changed yet, this will result in a change in frequency of the generator rotation in order to satisfy the power demand. This change in frequency can be denoted by δF and can be written as

$$\delta F = \frac{d\delta\beta}{dt} \tag{II.52}$$

where $\delta\beta$ is the incremental change of the generator rotor angular position. Therefore the generator is said to "swing" when a change in frequency takes place. Excessive swings can cause stability problems for the generator.

In order to minimize the swing of the machine, the generator must be controlled. A block diagram of a generator control system is shown in Figure 2.30. There are two basic control schemes. The megawatt frequency or Pf controller senses the frequency deviation and tie line power (real electrical power from other generating units in the power grid) and determines the steam valve change. This in turn will result in a change of real power delivered to the power grid. The megavar voltage, or QV, controller senses the generator terminal voltage deviation and transforms this to a reactive power demand signal. This in turn will result in a change in the generator rotor field current,

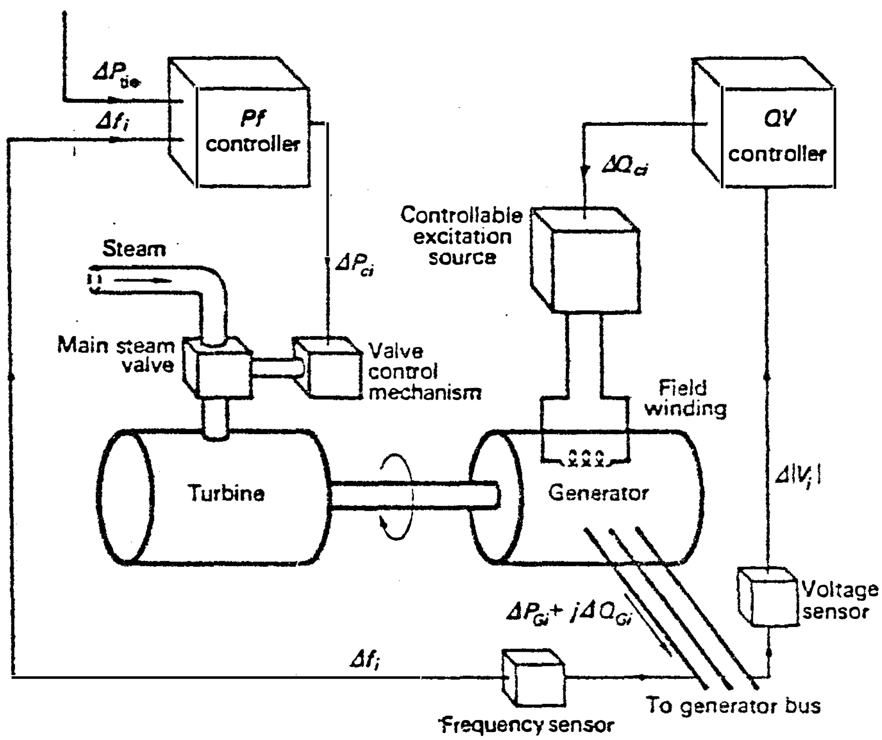

Figure 2.30 Block diagram of a generator control system.

which will ultimately change the reactive power delivered (or absorbed as the case may be). "In general the QV loop is much faster than the Pf loop, due to the mechanical inertia constants in the latter. If it is assumed that the transients in the QV loop are essentially over before the Pf loop reacts, then the coupling between loops can be neglected"[9].

One additional assumption must be made in order to develop a model for the generator control system. It must be assumed that the time difference between the time when a generator receives an increase in turbine shaft power and when it actually delivers the equivalent electrical power is small. This is a valid assumption since the generator electrical processes are much quicker than the turbine mechanical processes. This will eliminate the need to model the generator itself in this study. However, in a study of an electrical power system grid, this assumption may not be valid.

A mathematical model has been developed to describe the Pf controller for small deviations around a nominal steady state (Elgerd[9], Reddoch[27]). The derivation of this model is presented in Appendix F. A block diagram of the model is shown in Figure 2.31.

In order to demonstrate how this model will work, some representation must be made for the mechanical shaft power in order to close the control loop. Ultimately this will be done using the previously developed PWR system model (see Section 2.8). But by representing this mechanical power by a very simple model, it will be easier to understand how the Pf controller model works. "In the crudest model representation we can characterize a non-reheat turbine generator with

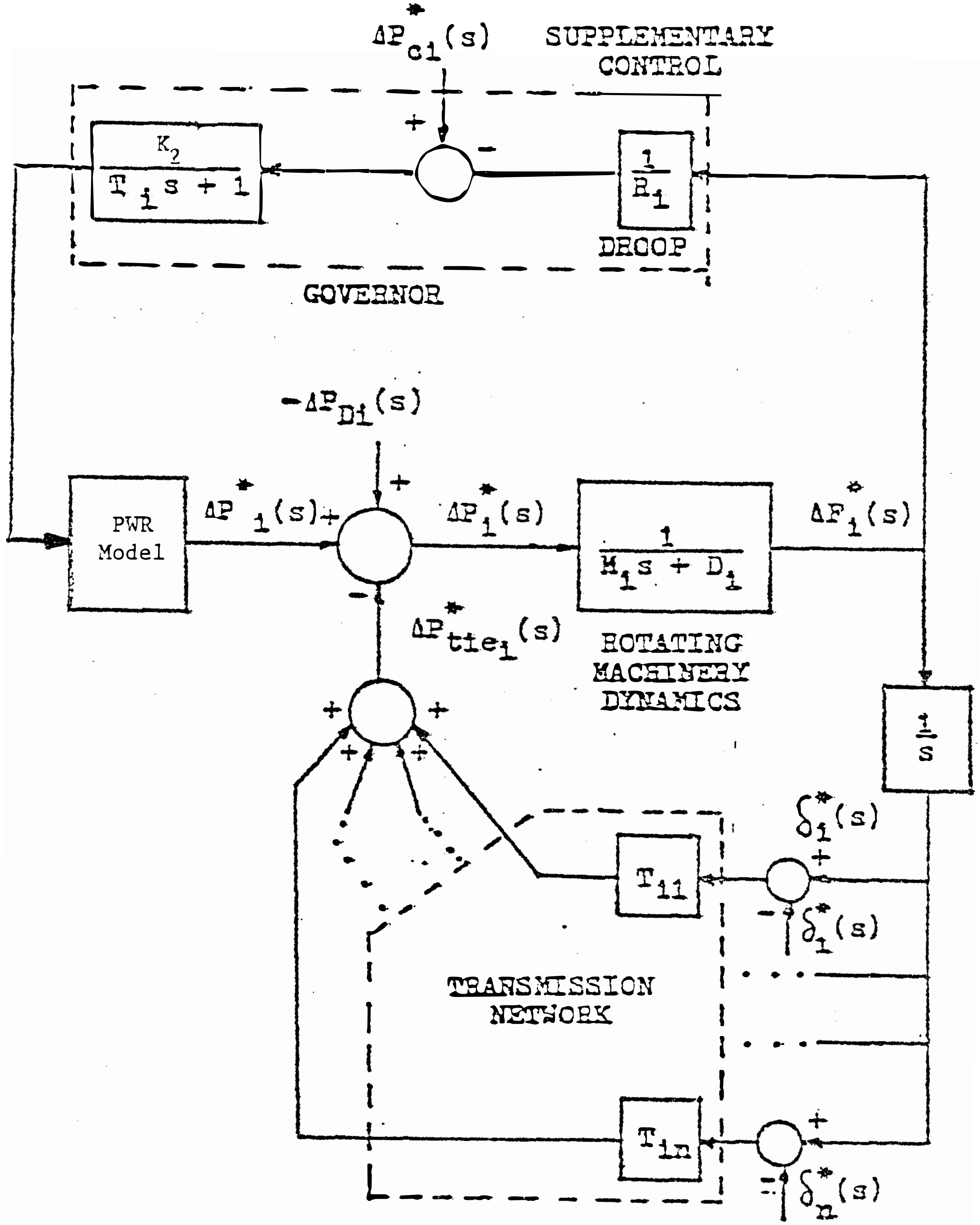

Figure 2.31 Incremental model of the ith control area.

a single gain factor K_T and a single time constant τ_T, and thus write

(II.53) $$\frac{\delta P_m}{\delta \epsilon/\epsilon_o} = \frac{K_T}{1+\tau_T S} .$$

Typically, the time constant τ_T lies in the range of 0.2 to 2 seconds"[9]. In this study, we will use a value of 2 seconds for τ_T and a value of 0.7870 puMw for the gain factor K_T. Therefore we now have a completely closed model for the Pf controller. A state variable representation of this model is shown below

(II.54) $$\frac{d\,\frac{\delta\epsilon}{\epsilon_o}}{dt} = \frac{\delta\epsilon/\epsilon_o}{\tau_G} - \frac{K_2}{\tau_G}\delta P_c - \frac{K_2}{\tau_G R}\delta F$$

(II.55) $$\frac{d\,\delta P_c}{dt} = \delta P_{TIE} + \left(D + \frac{1}{R}\right)\delta F$$

(II.56) $$\frac{d\,\delta F}{dt} = -\frac{D}{M}\delta F + \frac{1}{M}\left[\delta P_m - \delta P_D - \delta P_{TIE}\right]$$

(II.57) $$\frac{d\,\delta P_m}{dt} = -\frac{\delta P_m}{\tau_T} + \frac{K_T}{\tau_T}\,\delta\epsilon/\epsilon_o$$

Equations (II.54) through (II.56) will become the permanent state variable equations in the overall system model (see Section II.8). However, equation (II.57) will not be used in the overall system model, but will be replaced with the complete PWR and balance of plant model.

In order to complete the control systems on the turbine-feedwater heater model, the bypass steam valve position must be controlled. The purpose of this control system is to maintain the steam reheater shell side temperature as constant as possible. In a typical turbine system, the bypass steam flow is approximately 5 percent of the total steam flow at 100 percent power. For small changes in power level, the change of the bypass steam flow will be very small compared to the total steam flow change. Any change in the bypass steam flow to the reheaters will ultimately change the low pressure turbine shaft power. The turbine model used in this study predicts that the low pressure turbine shaft power deviation will be approximately one third of the high pressure turbine shaft power (see page 182). In addition, if it is assumed that the reheater enthalpy is approximately proportional to the reheater temperature, then the model predicts only a 1 percent change in reheater temperature for a 10 percent step in the main steam valve coefficient (see Figure 2.29). This means that small changes in the bypass steam flow to the reheaters will result in very small changes in the total turbine shaft power. Therefore, the assumption will be made that the bypass steam flow control does not need to be included in the PWR model. This means that the bypass steam valve coefficient is assumed constant. However the bypass steam flow is assumed to change only proportional to steam pressure.

The value of the parameters used in the Pf controller model are given in Table XIV. These values are typical of a 1200 MWe machine. The value of the gain factor K_T was found by running a case of the overall system model without a Pf controller model but with the reactor controller for a 10 percent step in valve coefficient (see page 182). The result of this case gave a value of 78.70 Mw for the shaft power. This value of K_T will be retained and used again in Section II.8.

TABLE XIV

PARAMETERS NEEDED TO CALCULATE THE Pf CONTROLLER MODEL MATRIX COEFFICIENTS

1. τ_G	governor time constant (sec)	0.2
2. K_2	governor gain (1/puMw)	
	high order model	1.2706
	low order model	1.2136
3. R	frequency "droop" gain (Hz/puMw)	3.0
4. M	mechanical inertia constant (puMw-sec/Hz)	0.08333
5. D	damping factor (puMw/Hz)	0.008333
6. τ_T	time constant of simplified prime mover (sec)	0.5
7. K_T	gain constant of simplified prime mover ($=1/K_2$) (puMw)	
	high order model	0.7870
	low order model	0.8240

Two cases will be presented here. The first case is for a +0.1 puMW step in the power demand signal (+100 MW). The second case is for a +0.1 puMW step in the tie line power signal. These cases are shown in Figures 2.32 and 2.33 respectively.

The difference between the two responses is that in Figure 2.33, the frequency deviation, δF, does not return to zero, and the control power error signal, δP_c, has returned to zero. This is because the tie line flow is used as a power control signal as well as a power demand signal. If this model were coupled to a power grid model, the tie line flow would have to change as a result of changing the electrical power produced by the machine, rather than forcing it to be constant as is done in this simulation. Note that the oscillatory motion shown in Figures 2.32 and 2.33 is due to the simple representation of the turbine mechanical shaft power. When the simple representation given by equation (II.53) is replaced by the more complex PWR model, this oscillatory motion will not be as pronounced. This will be shown to be true in Section II.8.

II.8 The Overall High Order System Model

At this point, it is now possible to couple all the individual model components previously presented into one overall system model. This model will be called the high order PWR system model. The model is described by 57 state variables. The description of these state variables and their numerical order in the model have been shown previously (see the List of Tables).

The parameters needed to calculate the system matrix coefficients and forcing vector coefficients have also been previously presented.

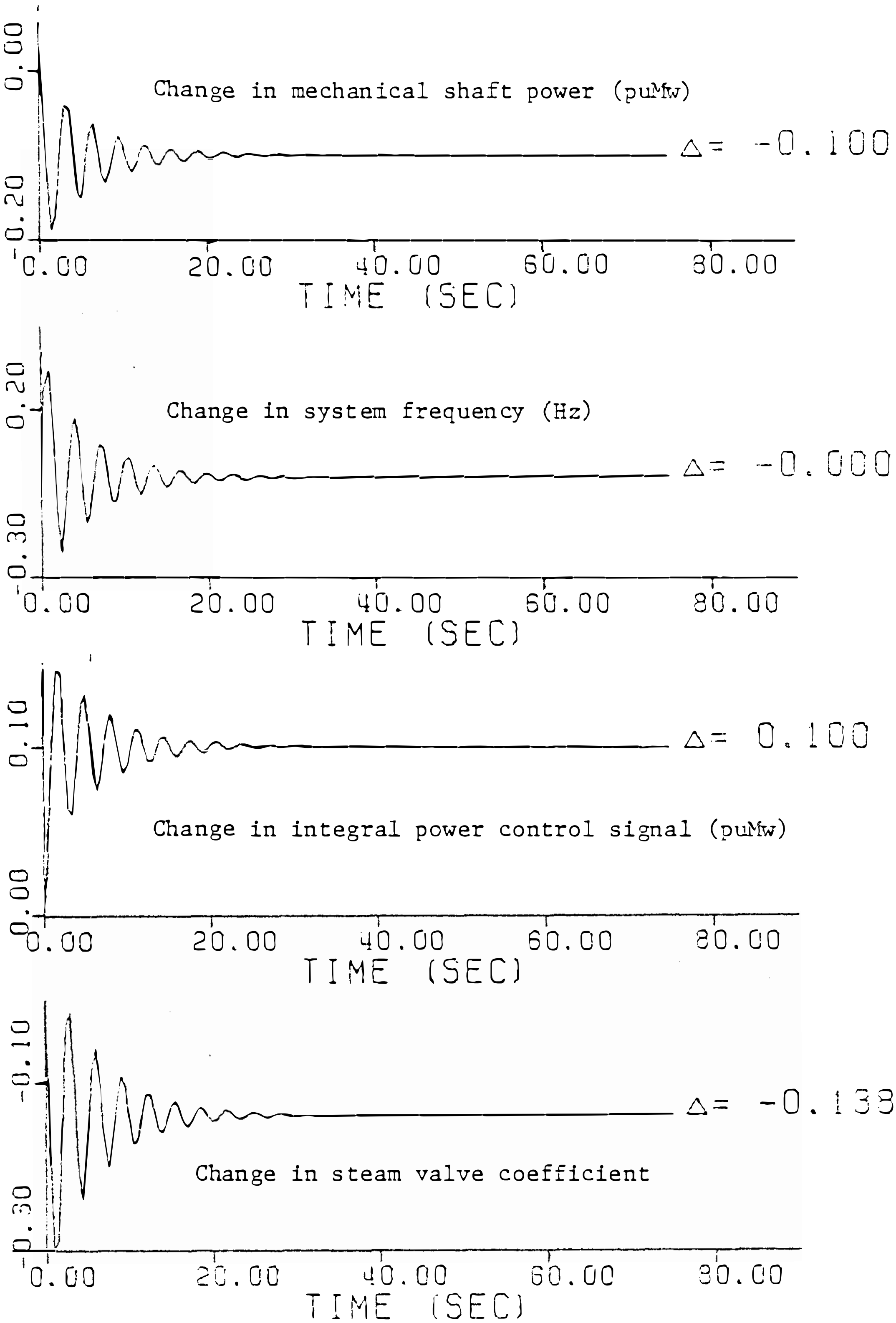

Figure 2.32 Response of the Pf controller model for a -0.1 puMw step in power demand.

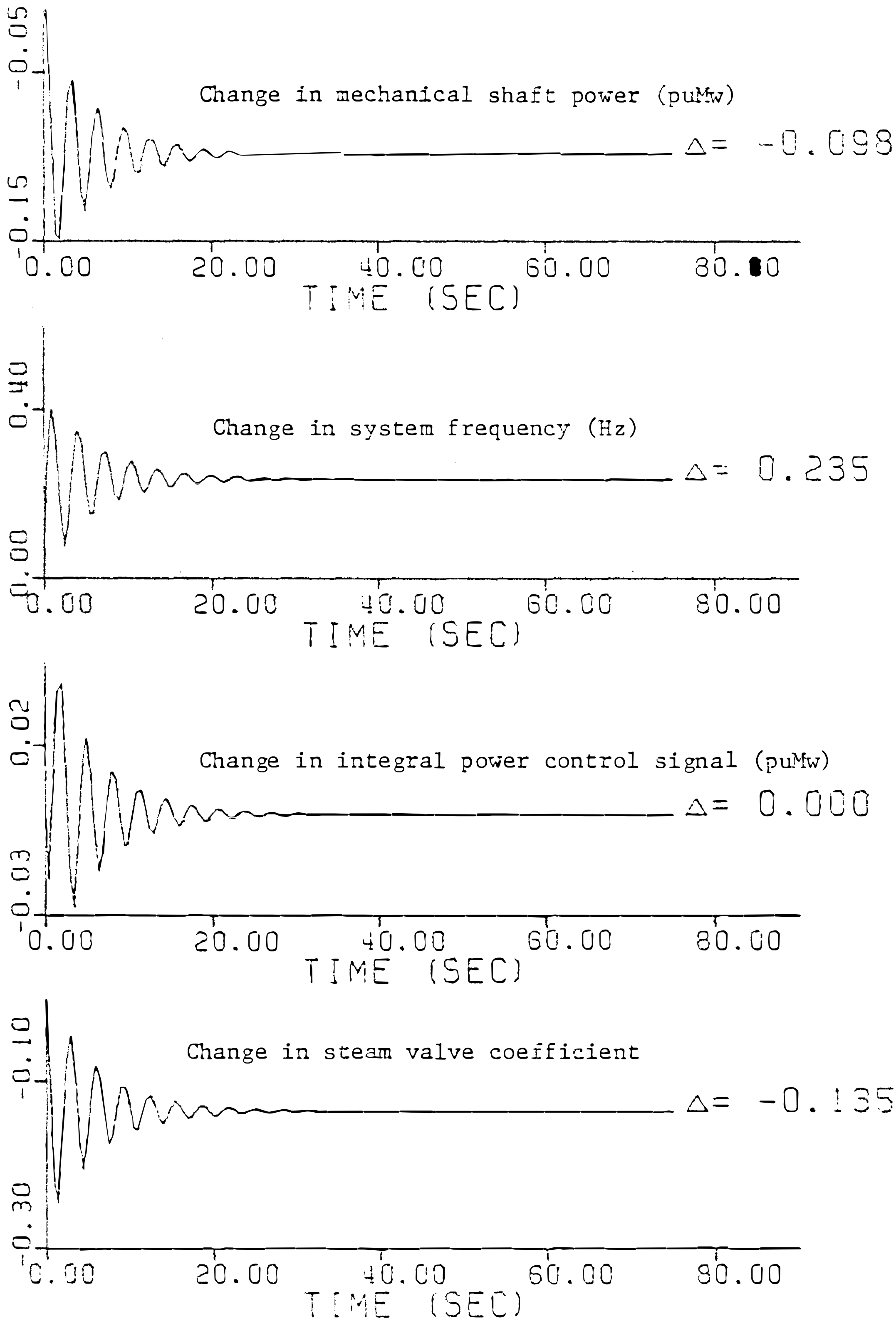

Figure 2.33 Response of the Pf controller model to a -0.1 puMw step in tie line power flow.

These parameters are typical of a 1200 Mwe Westinghouse plant at 100 percent power. The coefficients for state variables 1 through 41 are calculated by the computer program described in Appendix A. The pressurizer pressure control system is represented by state variables 42 and 43. All the coefficients for the pressurizer pressure control system except coefficients (1,42), (42,42), (42,43), and (43,42) are also evaluated by the computer. All the coefficients for state variables 44 through 58, which represent the turbine, feedwater heaters, and Pf controller models are calculated by "hand." The parameter data for the turbine-feedwater heater model are limited to the data available from the heat balance of the turbo-generator system presented in the SEQUOYAH-FSAR[29]. Table XV is a list of the resulting numerical values of the system matrix coefficients.

The high order PWR system model can be disturbed by a reactivity change in the control rods, a power demand signal, or a tie line power signal. If the reactor control system is implemented (NTYPE=1), then the control rod reactivity is changed automatically. Therefore, in this study, only the power demand signal and tie line power flow signal will be considered. The forcing terms for the overall model and their numerical values are shown below

(II.58) $$f(1) = \frac{\beta_T}{\Lambda} \delta\rho_{ext}$$

(II.59) $$f(56) = \delta P_{TIE}$$

(II.60) $$f(57) = -\frac{1}{M}\left[\delta P_D + \delta P_{TIE}\right].$$

TABLE XV

LIST OF THE NUMERICAL VALUES OF THE
HIGH ORDER OVERALL PWR SYSTEM MODEL
MATRIX COEFFICIENTS

ROW	COL	COEFFICIENT	ROW	COL	COEFFICIENT
1	1	-3.8536E+02	1	2	1.2500E-02
1	3	3.0800E-02	1	4	1.1400E-01
1	5	3.0700E-01	1	6	1.1900E+00
1	7	3.1900E+00	1	8	-6.1452E-01
1	9	-5.5866E+00	1	10	-5.5866E+00
1	42	-5.5866E-02	2	1	1.1676E+01
2	2	-1.2500E-02	3	1	7.8994E+01
3	3	-3.0800E-02	4	1	7.3128E+01
4	4	-1.1400E-01	5	1	1.5235E+02
5	5	-3.0700E-01	6	1	5.1676E+01
6	6	-1.1900E+00	7	1	1.7542E+01
7	7	-3.1900E+00	8	1	2.4137E+02
8	8	-2.5322E-01	8	9	2.5322E-01
9	1	2.6186E+00	9	8	1.0292E-01
9	9	-3.6492E+00	9	13	3.5462E+00
10	1	2.6186E+00	10	8	1.0292E-01
10	9	3.4433E+00	10	10	-3.5462E+00
11	10	6.9585E-01	11	11	-6.9585E-01
12	11	9.5749E-01	12	12	-9.5749E-01

TABLE XV (continued)

ROW	COL	COEFFICIENT	ROW	COL	COEFFICIENT
13	13	-5.3461E-01	13	14	5.3461E-01
14	14	-4.7874E-01	14	20	4.7874E-01
15	12	1.4059E+00	15	15	-1.4059E+00
16	15	4.5264E+00	16	16	-5.1762E+00
16	21	6.4982E-01	16	26	-4.9921E+00
17	16	7.5905E-01	17	17	-1.4089E+00
17	21	4.3606E-02	17	22	5.9878E-01
17	23	-5.1036E-02	17	24	4.3606E-02
17	25	-6.0946E-02	17	26	1.6602E+00
17	27	-1.8505E-02	17	28	-5.4153E-01
17	29	1.6939E-01	17	35	2.0572E-04
17	53	-3.8829E-03	17	55	2.1853E+00
18	17	7.5905E-01	18	18	-1.4089E+00
18	23	6.4982E-01	18	26	5.0472E-01
19	18	4.5264E+00	19	19	-5.1762E+00
19	21	-1.8824E-02	19	22	2.2032E-02
19	23	2.2032E-02	19	24	6.3099E-01
19	25	2.6310E-02	19	26	-2.4626E+00
19	27	7.9884E-03	19	28	2.3377E-01
19	29	-7.3127E-02	19	35	-8.8808E-05
19	53	1.7400E-03	19	55	-9.4360E-01
20	19	1.4059E+00	20	20	-1.4059E+00
21	16	2.4295E+00	21	21	-3.9737E+00

TABLE XV (continued)

ROW	COL	COEFFICIENT	ROW	COL	COEFFICIENT
21	22	-8.4332E-02	21	23	-8.4332E-02
21	24	7.2055E-02	21	25	-1.0071E-01
21	26	1.3969E+00	21	27	8.2554E-02
21	28	-8.9481E-01	21	29	1.0880E+00
21	35	3.3993E-04	21	53	-6.5721E-03
21	55	3.6122E+00	22	17	2.4295E+00
22	21	1.2083E-02	22	22	-5.4018E+00
22	23	-1.4142E-02	22	24	1.2083E-02
22	25	-1.6888E-02	22	26	2.3426E-01
22	27	4.0901E-01	22	28	-1.5005E-01
22	29	4.6939E-02	22	35	5.7004E-05
22	53	-1.0982E-03	22	55	6.0560E-01
23	18	2.4295E+00	23	21	-2.7610E-03
23	22	3.2314E-03	23	23	-5.3845E+00
23	24	-2.7610E-03	23	25	3.8589E-03
23	26	-5.3528E-02	23	27	4.1531E-01
23	28	3.4288E-02	23	29	-1.0725E-02
23	35	-1.3026E-05	23	53	2.3651E-04
23	55	-1.3840E-01	24	19	2.4295E+00
24	21	-1.6465E-02	24	22	1.9270E-02
24	23	1.9270E-02	24	24	-4.0622E+00
24	25	2.3012E-02	24	26	-3.1920E-01
24	27	1.2012E-01	24	28	2.0446E-01
24	29	7.4413E-01	24	35	-7.7676E-05

TABLE XV (continued)

ROW	COL	COEFFICIENT	ROW	COL	COEFFICIENT
24	53	1.4154E-03	24	55	-8.2530E-01
25	21	4.9508E-04	25	22	2.2947E-02
25	23	2.2947E-02	25	24	4.9508E-04
25	25	-4.7793E-02	25	26	5.2058E-03
25	27	-4.8774E-03	25	28	-1.5008E+01
25	29	1.9232E-03	25	35	5.6588E-04
25	53	-4.7303E-05	25	55	9.7900E-01
26	21	-4.0620E-02	26	22	4.7541E-02
26	23	4.7541E-02	26	24	-4.0620E-02
26	25	5.6772E-02	26	26	-7.8751E-01
26	27	1.7238E-02	26	28	5.0444E-01
26	29	-1.5780E-01	26	35	-1.9163E-04
26	53	3.8820E-03	26	55	-2.0363E+00
27	21	2.5758E-02	27	22	1.1939E+00
27	23	1.1939E+00	27	24	2.5758E-02
27	25	-2.0191E-02	27	26	-1.5537E+00
27	27	-4.1018E-01	27	28	4.7154E+00
27	29	1.0006E-01	27	35	2.1845E-03
27	53	-2.4611E-03	27	55	-5.7020E+01
28	21	-1.1189E-03	28	22	2.2115E-03
28	23	2.2115E-03	28	24	-1.1189E-03
28	25	6.6482E-04	28	26	-2.2531E-02
28	27	2.5317E-04	28	28	-2.7242E-01

TABLE XV (continued)

ROW	COL	COEFFICIENT	ROW	COL	COEFFICIENT
28	29	-4.3464E-03	28	35	-5.5847E-06
28	53	1.0687E-04	28	55	-4.7400E-02
29	21	2.0801E-04	29	22	9.6412E-03
29	23	9.6412E-03	29	24	2.0801E-04
29	25	2.6274E-03	29	26	-1.4612E-02
29	27	5.9822E-03	29	28	-5.5759E+00
29	29	-7.2594E-02	29	35	-1.0184E-03
29	53	1.4661E-02	29	55	4.1120E-01
30	25	-2.0000E-01	30	30	-2.0000E-01
31	25	-1.5080E+01	31	30	-1.5075E+01
32	25	-4.6281E+02	32	30	-4.6265E+02
32	31	5.5960E-02	33	27	1.2458E+00
33	35	-1.0000E+00	33	55	9.8949E+02
34	27	4.8331E+02	34	32	1.2641E+01
34	33	7.0740E-01	34	34	-4.0068E+00
34	35	-3.8836E+02	34	55	3.8405E+05
35	34	1.0000E+00	36	14	2.5000E-01
36	36	-2.5000E-01	37	12	2.5000E-01
37	37	-2.5000E-01	38	27	1.2386E-03
38	35	-3.5038E-04	38	38	-3.3333E-02
38	53	-1.0283E-03	38	55	1.0086E+00
39	12	2.0000E-01	39	14	2.0000E-01
39	36	-1.9000E-01	39	37	-1.9000E-01
39	39	-3.0000E-01	39	40	-2.0000E-02

TABLE XV (continued)

ROW	COL	COEFFICIENT	ROW	COL	COEFFICIENT
40	39	1.0000E+00	41	1	-7.4964E-01
41	27	8.7911E-04	41	35	-3.7901E-04
41	41	-2.5000E-02	41	53	-1.1124E-03
41	55	1.0912E+00	42	42	-5.1520E-02
42	43	1.7159E-04	43	42	-3.3333E-01
44	27	2.4920E-02	44	44	-1.6293E+01
44	45	-3.6720E+01	44	47	1.9290E+00
44	48	5.8749E+00	44	55	2.0730E+01
45	27	1.4870E-02	45	44	-9.9553E+00
45	45	-3.1153E+01	45	47	1.1785E+00
45	48	3.5892E+00	45	55	1.2667E+01
46	44	3.9300E-01	46	45	8.8583E-01
46	46	-5.0000E-01	46	47	-4.6530E-02
46	48	-1.4176E-01	47	46	1.9532E-01
47	47	-2.7134E-01	47	48	-2.1010E-01
48	46	6.1613E-01	48	47	-1.0747E+00
48	48	-1.2767E+00	48	50	3.7648E-01
49	27	4.0064E-04	49	49	-3.3333E-01
50	27	8.3500E-05	50	48	-1.0102E+00
50	49	7.8624E-03	50	50	-2.5000E-01
51	47	1.9020E-01	51	48	1.4590E-01
51	51	-1.0000E-01	52	35	-2.1678E-03
52	47	1.3517E+00	52	48	1.0365E+00

TABLE XV (continued)

ROW	COL	COEFFICIENT	ROW	COL	COEFFICIENT
52	52	-1.0000E-01	52	54	1.3953E+00
53	35	-1.2707E-03	53	44	1.3378E+00
53	45	3.0144E+00	53	46	-1.1006E+00
53	47	-1.5838E-01	53	48	-3.7430E-01
53	49	4.5818E-01	53	52	2.1930E-02
53	53	-2.5000E-02	54	44	4.3722E-02
54	45	9.8510E-02	54	46	-3.5970E-02
54	47	-5.1760E-03	54	48	-1.2240E-02
54	49	1.4970E-02	54	54	-1.0000E-01
55	55	-5.0000E+00	55	56	-7.0050E+00
55	57	-2.3350E+00	56	57	3.4167E-01
57	57	-1.0000E-01			

One additional forcing term will be generated by the reactor control system in state variable equation number 41. This will happen when subroutine DISTRB is called upon to include the nonlinear affects of the reactor control system.

When calculating the system matrix coefficients, it is very easy to make a mistake on the coupling terms for the individual component models. One method of eliminating these mistakes is to show the signs of the matrix coefficients and forcing vector coefficients on a chart (Machado[23]). Figure 2.34 shows a chart of the system coefficients. The positive coefficients are represented by a * and the negative coefficients are represented by a -.

Because the coefficients for state variable 44 through 57 are calculated by hand, the coupling coefficients for the turbine, feed-water heaters, and Pf controller models must be calculated systematically. Since state variable 53 is the change in feedwater temperature, matrix elements (i,53), i=17, 19, 21 through 29, 38, and 41 are the same as the forcing vector coefficients for a 1°F step in feedwater temperature on the isolated core, UTSG, three element controller, and reactor controller models (hereafter referred to as the isolated PWR model). Likewise, since state variable 55 is the change in valve coefficient, matrix elements (i,55) i=17, 19, 21 through 29, 33, 34, 38, and 41 are the same as the forcing vector coefficients for a 0.95511 (fraction of main steam flow that enters the turbine nozzle chest) step in the valve coefficient on the isolated PWR model. Matrix elements (44,27), (45,27), (49,27), and (50,27) are the same as the forcing vector coefficients for a 1 psi step in steam pressure on the isolated turbine-feedwater heater model.

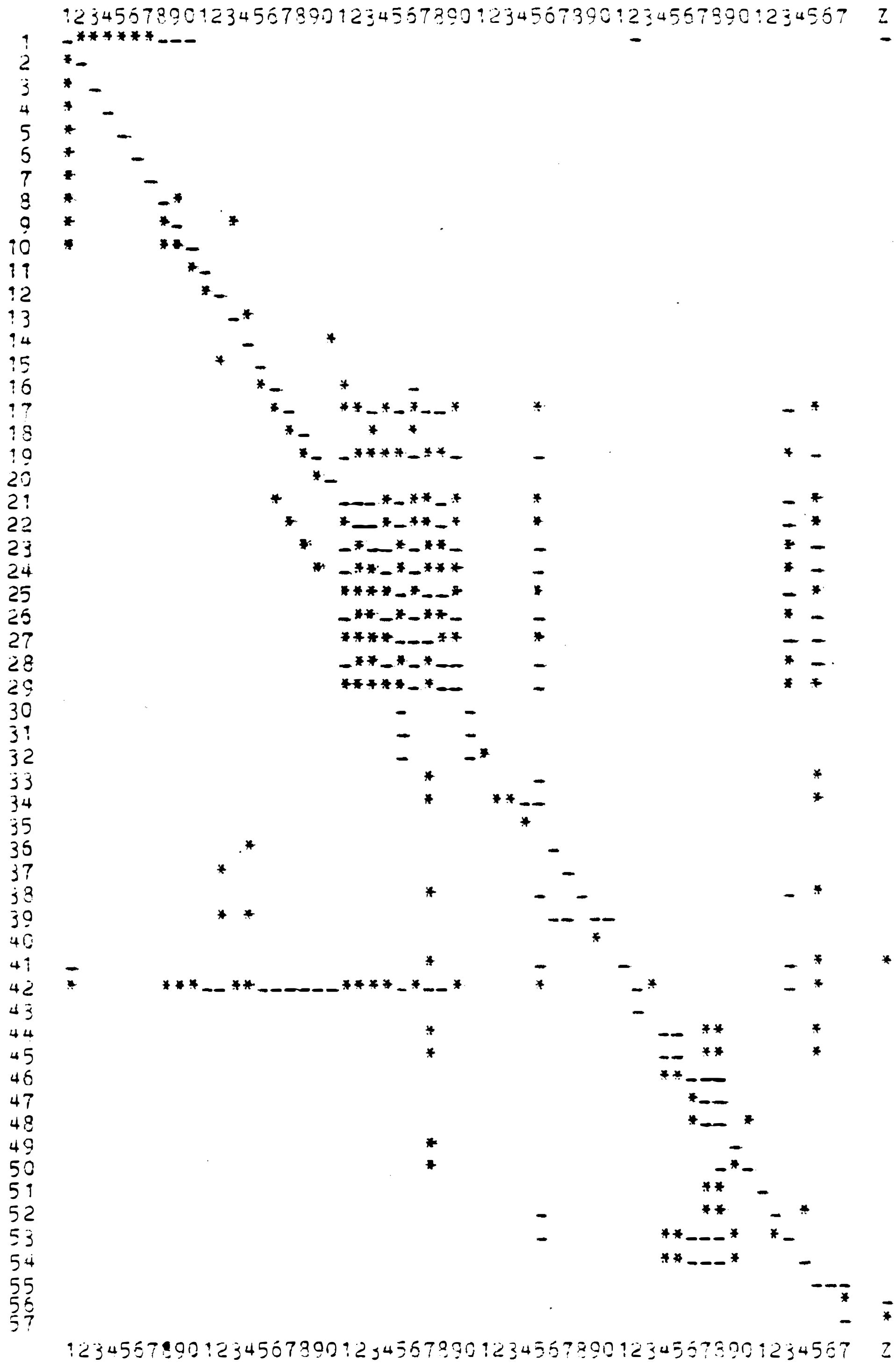

Figure 2.34 Chart of the overall high order PWR model system matrix coefficients.

Matrix elements (52,35) and (53,35) are the same as the forcing vector coefficients for a 1 lbm/sec step in the feedwater flow on the isolated turbine-feedwater heater model. Matrix elements (44,55) and (45,55) are the same as the forcing vector coefficients for a unit step in the valve coefficient for the isolated turbine-feedwater heater model. Similar relations exist for all the coupling terms for the individual component models. Figure 2.34 will help in determining the location and sign of any coefficient in the system model.

In this section, only one case will be presented. Figure 2.35 shows the time response of the high order overall PWR system model for a -0.05 puMw step (-50 Mw step) in the power demand signal.

From Figure 2.35, it is easily seen that the turbine shaft power transient occurs very quickly. This is because the valve coefficient transient is very fast. But later on the valve coefficient starts to "back off" as the steam pressure begins to have its effect on the total steam flow. The reactor control system causes the control rods to move to a final value of -7.56 cents. The nonlinearities of the control system are apparent from the plot of the temperature error signal. The energy balance between nuclear and secondary power is also plotted to show that this balance is achieved. The steam flow and feedwater flow can also be compared to show that the mass balance is satisfied in the UTSG. The average temperature of the hot and cold leg can also be found from Figure 2.35. It is apparent that the average temperature approaches the steady state program value but does not reach it because of the deadband in the reactor control system. The feedwater temperature experiences a small transient and will ultimately have a small effect on the UTSG steam pressure. The system

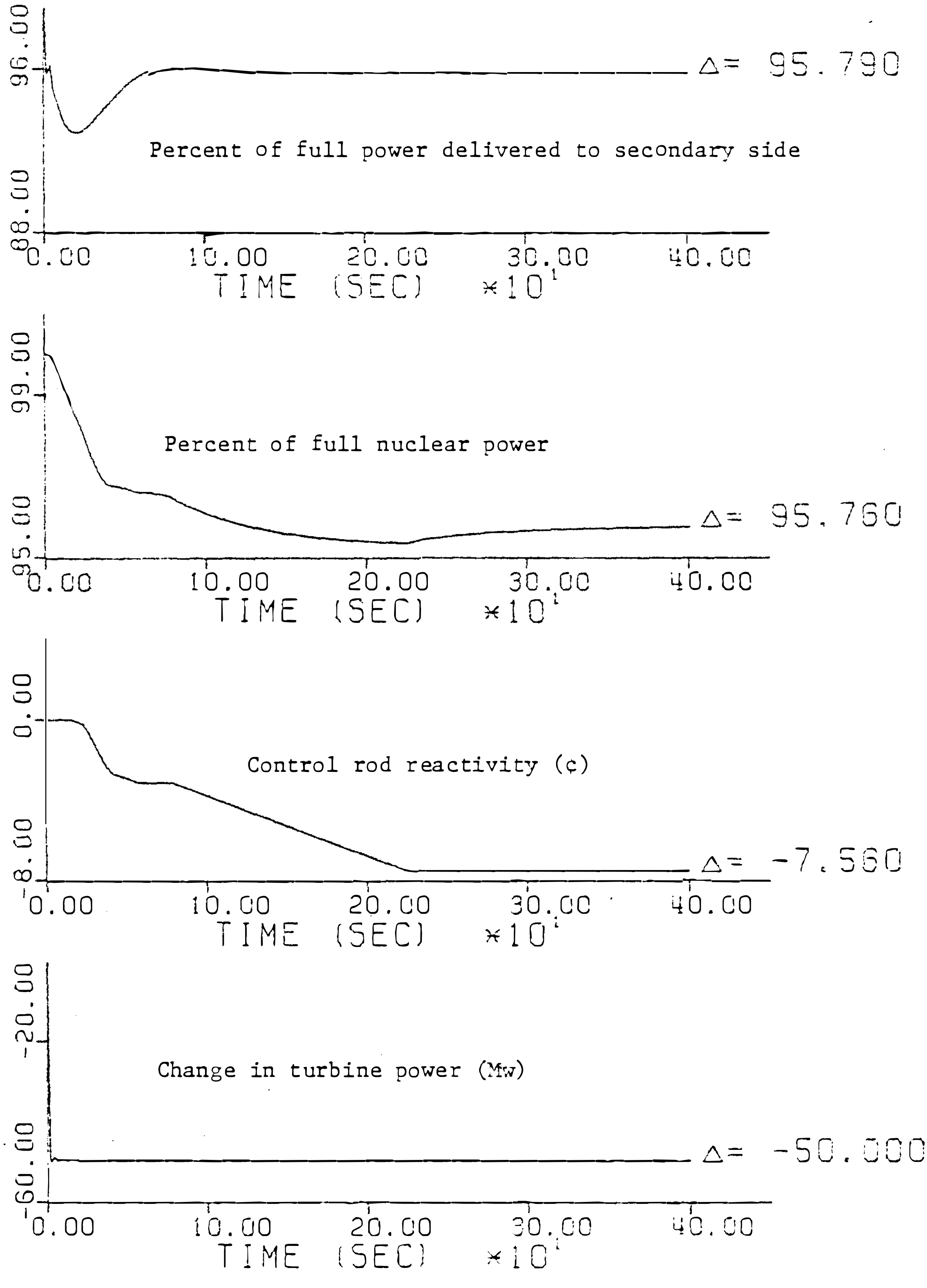

Figure 2.35 Response of the overall high order PWR system model for a -0.05 puMw (-50 Mw) step in power demand.

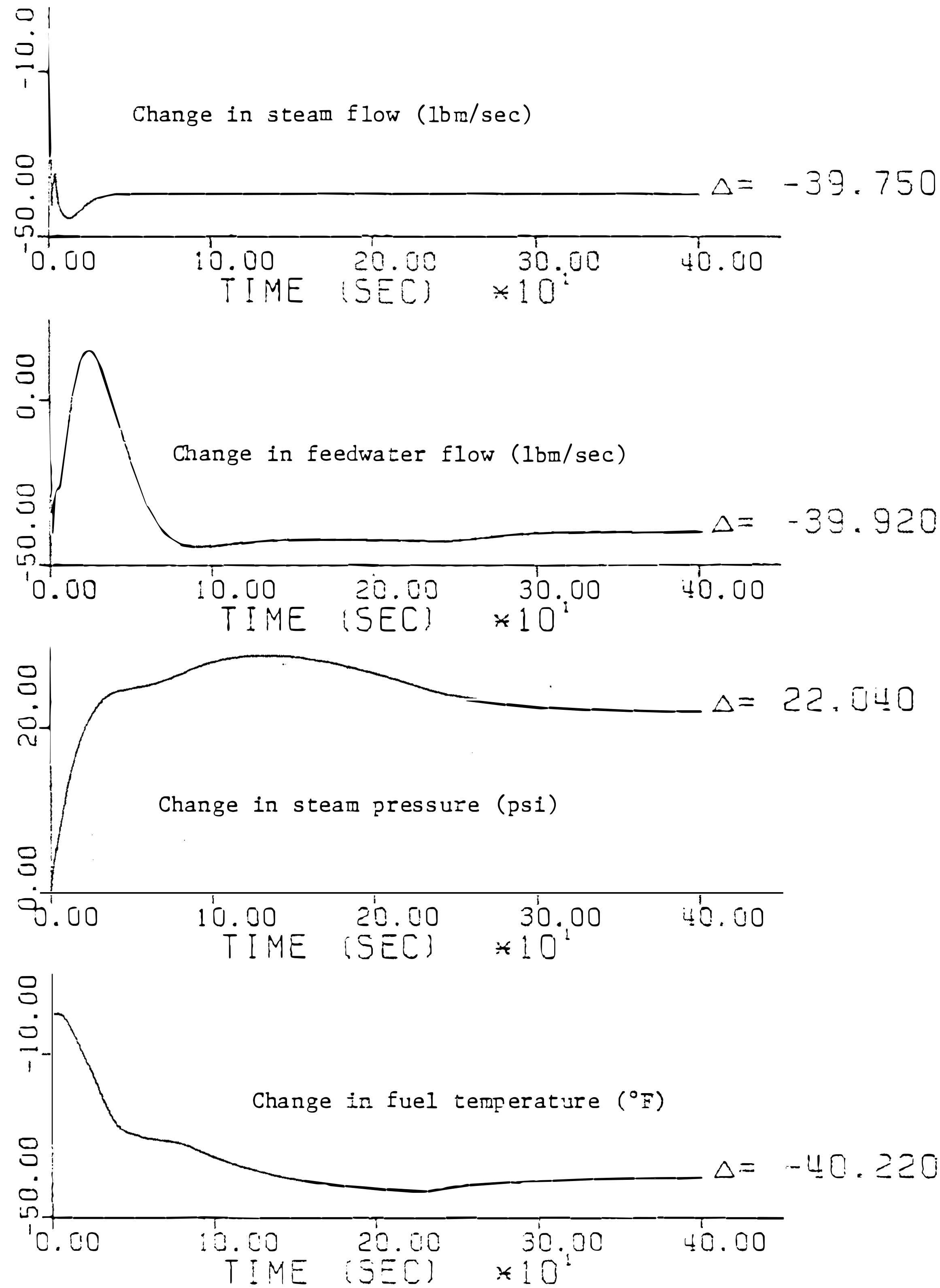

Figure 2.35 (continued)

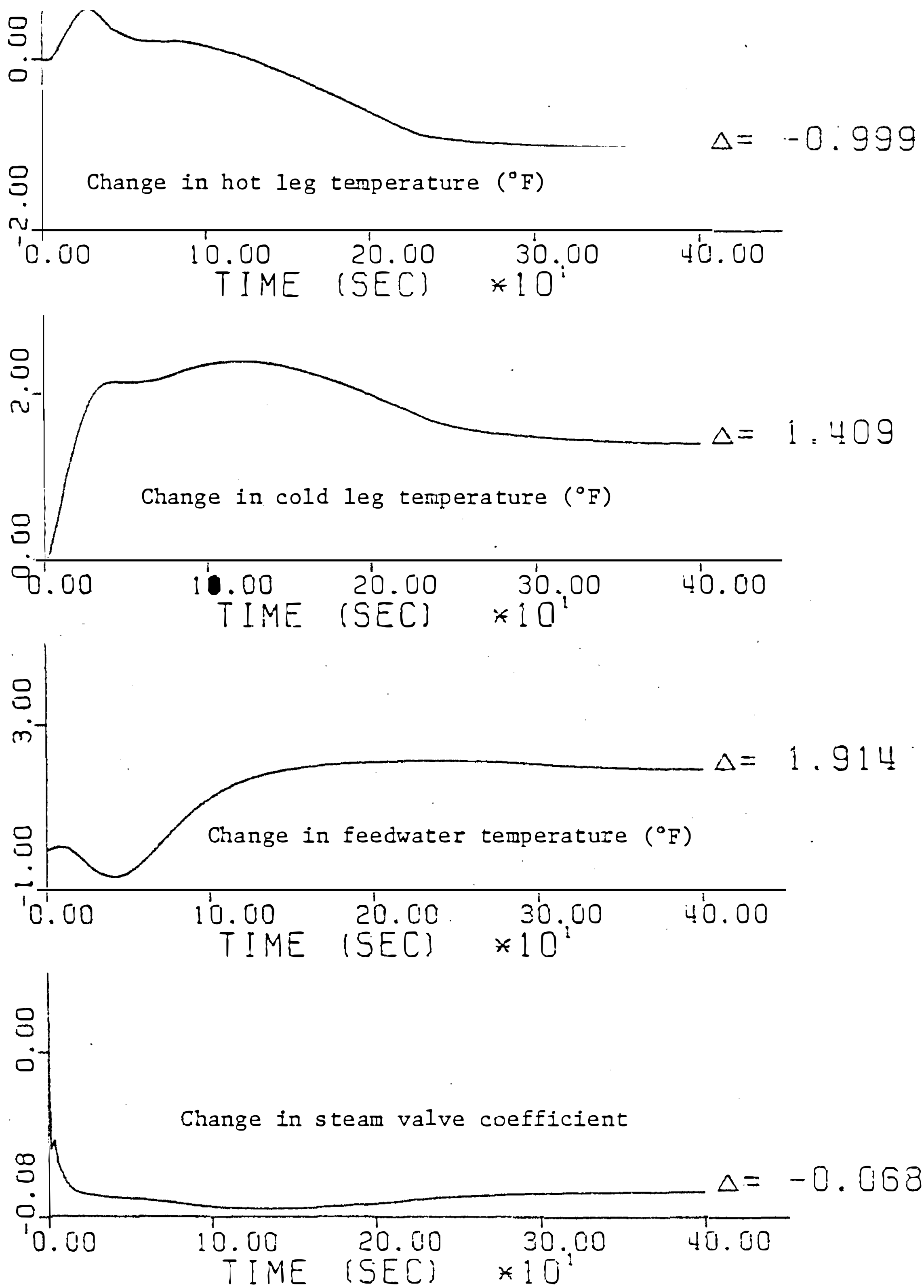

Figure 2.35 (continued)

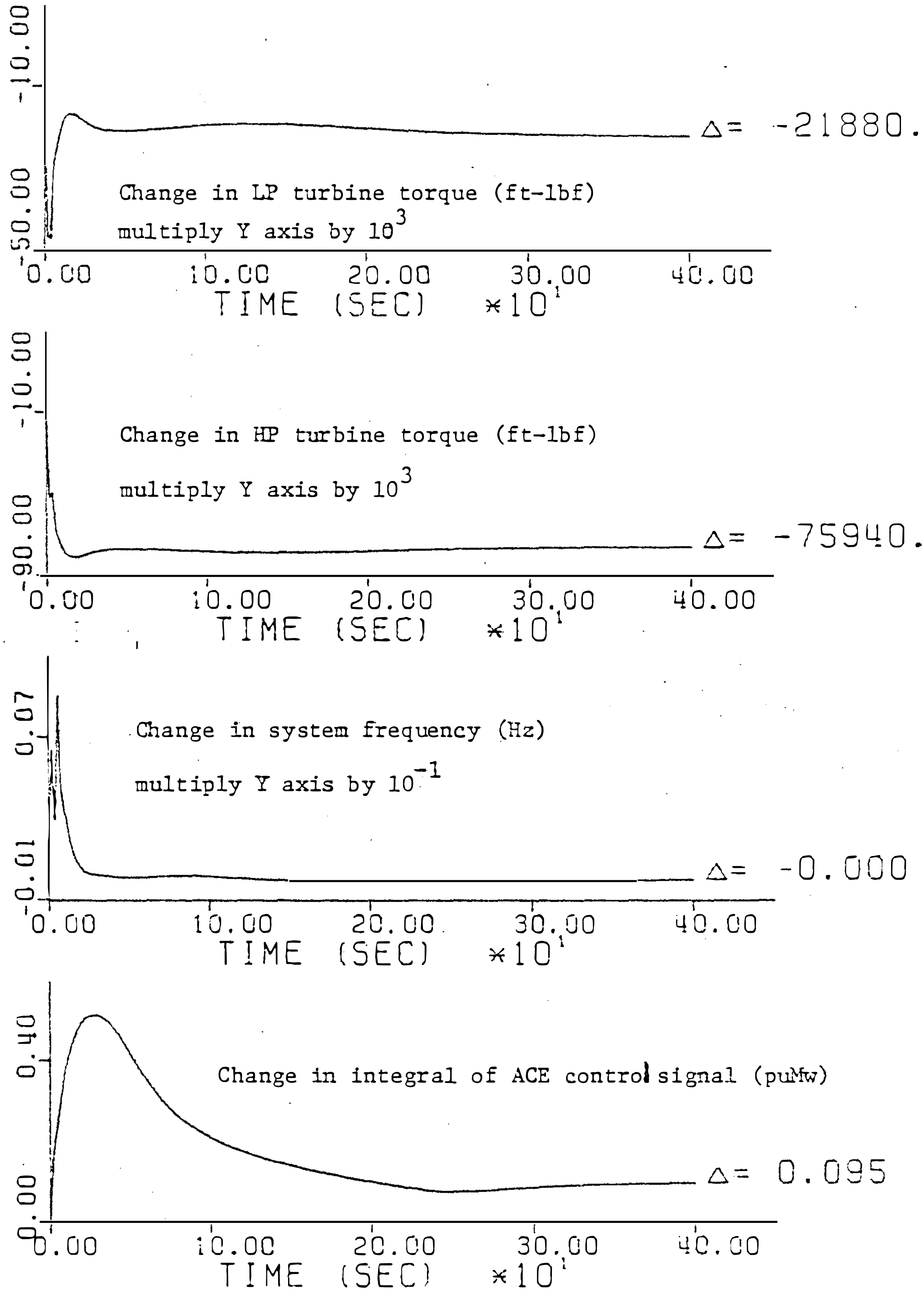

Figure 2.35 (continued)

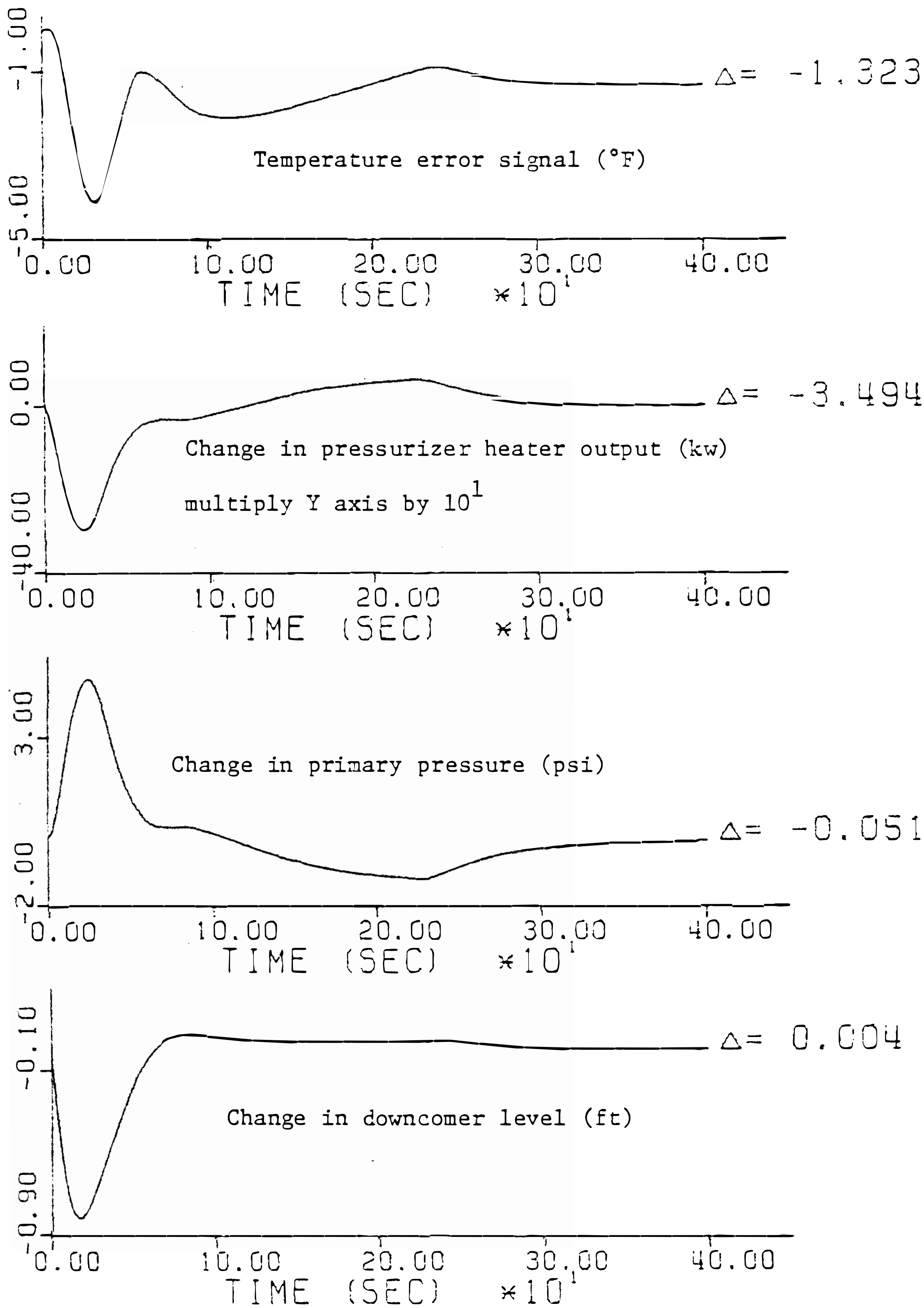

Figure 2.35 (continued)

frequency, primary pressure, and downcomer level deviations have been eliminated by the Pf, pressurizer pressure, and three element feed-water control systems respectively. The turbine shaft power is shown subdivided into the high pressure and low pressure turbine torque. This figure will be compared to a similar low order model response in Chapter IV.

Figure E.6 shows a similar time response of both the high and low order overall PWR system model for a -0.05 puMw step in the tie line power flow.

Thus a complete high order PWR system is now described by 57 state variables. Subroutine DISTRB must be used to simulate the nonlinear reactor control system. The input to the model is the power demand, and tie line power flow signals. The output of turbine mechanical shaft power is calculated at each time step from turbine model state variables. Other state variables of interest can also be obtserved.

II.9 Additional Considerations for Coupling the Overall PWR System Model to an Electrical Grid System Model

It may be desirable to couple the overall PWR system model to an electrical grid system model. In this case, the electrical system frequency deviation, δF, and the change in the tie line power flow, δP_{TIE}, previously used as forcing terms would become coupling terms. However some additional considerations must be dealt with.

An obvious restriction will be the maximum nuclear power. In this study, the percent of full nuclear power, $\%P_N$ (defined by equation (II.34) and (C.15)), should not exceed 100.

Many of the components in a PWR nuclear plant are powered by the electrical system grid itself. Such components include the reactor coolant pumps. If the power supply to these components experiences an undervoltage or an underfrequency, it would cause the plant to trip and thus be isolated from the electrical grid system. For a typical PWR nuclear plant, an underfrequency of 56 Hz from the nominal 60 Hz or an undervoltage of 70 percent of the rated voltage will cause the plant to trip. However, if the undervoltage is obtained at a slow rate, then a time lag of 20 to 25 seconds can be experienced at 70 percent of the rated voltage before the plant will trip.

In this thesis the overall PWR system model was not coupled to an electrical grid system model. Therefore, the nonlinear effects of underfrequency, undervoltage, and maximum nuclear power were not considered.

If an electrical grid system model is coupled to the overall PWR system model, and the power supply to the PWR system components experiences an underfrequency or undervoltage which exceeds the requirements, then the turbine mechanical shaft power output of the PWR plant must be set equal to zero. That is, the PWR plant can no longer supply power to the electrical grid system if the electrical supply to the PWR system components is in this condition.

CHAPTER III

THE LOW ORDER MODEL

III.1 Introduction

In Chapter II a high order PWR system model was presented which used 57 state variables to describe the system. It may be desirable to reduce the number of state variables which are needed to describe the system and thus reduce the complexity of the model. For example, if the only output desired of the system were the power delivered by the turbine for a power demand input, then a reduction in the order of the system might be desirable.

In this study, three major methods were pursued in reducing the order of the model. The first method used will be called the physical method. The equations used to describe the system are lumped parameter first order differential equations. If certain sets of these equations for the plant components could be combined into one equation, this would reduce the total number of equations needed to describe the overall system. In order to combine the equations, physical intuition must be used. For example, six delayed neutron groups might be combined into one delayed neutron group to describe the reactor kinetics in a simpler form.

The second method used is to take the set of linear equations in its state variable form and numerically reduce the order of the model. This could be performed on the high order model of Chapter II, or the physically reduced model which is also in a state variable formulation. This method has been pursued previously and was originally seen as a possible candidate for this study (Akin[1]).

The third method considered will be called purely empirical model reduction. This method would use available performance data from an operating plant and find the minimum number of coefficients needed to describe the input-output characteristics of the system (Kerlin[17], Zwingelstein[17], Upadhyaya[17]. However, this method is limited to available plant data. For example, if the desired input-output characteristics were the turbine shaft power produced for a power demand signal, that data must be available in order to use the purely empirical method. Another possibility would be to generate simulated data (for example, the results of the 57th order model of Chapter II), and use these results as if they were real plant data. This method was not used in this study. However, if the necessary data were available, a purely empirical model reduction method would be an excellent candidate for further study.

In this chapter, the high order model of Chapter II will be reduced by physical methods. Then a numerical method of model reduction will be applied to the physically reduced low order model.

III.2 Model Reduction by Physical Methods

The intent of this section is to show how the detailed high order PWR model presented in Chapter II can be reduced in a physical manner. All the models which have been presented previously will be reduced except the turbine-feedwater heater, and Pf controller models. These models will not be reduced because they are already in a simplified form.

The high order reactor core model is described by fourteen equations. Incorporated in this model are equations which use six groups of delayed neutron precursors. These six groups of delayed neutrons can be reduced to one group of delayed neutrons. In order to do this, the delayed neutron decay constant must be defined to be:[41]

$$\text{(III.1)} \quad \lambda = \beta_T \Big/ \left[\sum_{i=1}^{6} \beta_i / \lambda_i \right].$$

The number of equations which describe the core neutronics and heat transfer can then be reduced by five. These resulting equations are

$$\text{(III.2)} \quad \frac{d\frac{\delta P}{P_0}}{dt} = -\frac{\beta_T}{\Lambda}\frac{\delta P}{P_0} + \lambda\,\delta C + \frac{\alpha_F}{\Lambda}\,\delta T_F + \frac{\alpha_c}{2\Lambda}\left(\delta\Theta_1 + \delta\Theta_2\right) + \frac{\beta_T}{\Lambda}\,\delta\rho_{ext}$$

$$\text{(III.3)} \quad \frac{d\,\delta C}{dt} = \frac{\beta_T}{\Lambda}\frac{\delta P}{P_0} - \lambda\,\delta C$$

$$\text{(III.4)} \quad \frac{d\,\delta T_F}{dt} = \frac{f P_0}{(mc_p)_F}\frac{\delta P}{P_0} + \frac{hA}{(mc_p)_F}\left(\delta\Theta_1 - \delta T_F\right)$$

$$\text{(III.5)} \quad \frac{d\,\delta\Theta_1}{dt} = \frac{(1-f)P_0}{(mc_p)_c}\frac{\delta P}{P_0} + \frac{hA}{(mc_p)_c}\left(\delta T_F - \delta\Theta_1\right) + \left(\frac{\dot{M}}{M}\right)_c\left(\delta T_{CL} - \delta\Theta_1\right)$$

$$\text{(III.6)} \quad \frac{d\,\delta\Theta_2}{dt} = \frac{(1-f)P_0}{(mc_p)_c}\frac{\delta P}{P_0} + \frac{hA}{(mc_p)_c}\left(\delta T_F - \delta\Theta_1\right) + \left(\frac{\dot{m}}{m}\right)_c\left(\delta\Theta_1 - \delta\Theta_2\right).$$

The next simplification that can be made on the high order core model is to assume that the upper plenum, hot leg, and UTSG inlet plenum volumes can be combined into one volume. This will allow the hot leg temperature to be represented by a single time constant. The same assumption can be made on the UTSG outlet plenum, cold leg, and core lower plenum. These time constants will be defined to be the hot and cold leg time constants respectively. The hot leg time constant can be written as

$$\tau_{HL} = \frac{\rho_{ave}}{\dot{m}} \left[\frac{V_{UP}}{NUTSG} + V_{HL} + V_{Pi} \right]. \tag{III.7}$$

The cold leg time constant can be written similarly as

$$\tau_{CL} = \frac{\rho_{ave}}{\dot{m}} \left[V_{Po} + V_{CL} + \frac{V_{LP}}{NUTSG} \right]. \tag{III.8}$$

The variables of equations (III.7) and (III.8) have been defined previously in Chapter II. Thus the equations of the hot and cold leg piping are

$$\frac{d\delta T_{HL}}{dt} = \frac{1}{\tau_{HL}} \left[\delta\Theta_2 - \delta T_{HL} \right] \tag{III.9}$$

$$\frac{d\delta T_{CL}}{dt} = \frac{1}{\tau_{CL}} \left[\delta T_P - \delta T_{CL} \right] \tag{III.10}$$

where δT_p is the average temperature of the primary fluid in the UTSG.

The 15th order UTSG model as described in Chapter II was Ali's model D[2]. In addition to model D, Ali also developed a model A. This model consists of a primary fluid lump, a heat conducting tube metal lump, and a secondary fluid lump. The equations will not be derived here (the reader should refer to reference 2 for this information). The derivation involves an energy balance on the subcooled primary fluid lump which results in the primary fluid temperature as a state variable. An energy balance is also made on the tube metal which results in the tube metal temperature as a state variable. The governing equation for the secondary fluid lump is obtained by applying mass balances for the water and steam components, a volume balance on all the secondary fluid in the whole steam generator, and also an energy balance on the secondary fluid. Saturation conditions are assumed to exist throughout the secondary fluid lump. The resulting equation will have the steam pressure as a state variable. The weakness of this model is that it will not describe the downcomer water level. This may be important for some applications of the overall system model. However, for applications where the primary concern of the overall system model is to describe the turbine shaft power as accurately as possible, the downcomer level will not need to be described.

In Chapter II, a three element controller model was shown coupled to the high order UTSG model. This model, which is described by six equations, can be eliminated if the feedwater flow is assumed to be controlled perfectly. Perfect feedwater flow control, as defined in

Chapter II, means that at every instant, the feedwater flow is assumed equal to the steam flow. A detailed study has been done previously on the effect of this assumption (Cherng[6]). For the application of this model, this assumption is valid. In addition, the steam flow will be expressed as in equation (II.24). The 20 equations of the combined high order UTSG and three element controller model will then be reduced to three equations. The resulting equations are:

$$\frac{d\,\delta T_p}{dt} = -\left[\frac{1}{\tau_p} + \frac{U_{pm} S_{pm}}{m_p C_{p1}}\right]\delta T_p + \left[\frac{U_{pm} S_{pm}}{M_p C_{p1}}\right]\delta T_m + \left[\frac{1}{\tau_p}\right]\delta T_{HL} \tag{III.11}$$

$$\frac{d\,\delta T_m}{dt} = \left[\frac{U_{pm} S_{pm}}{M_m C_m}\right]\delta T_p - \left[\frac{U_{pm} S_{pm} + U_{ms} S_{ms}}{M_m C_m}\right]\delta T_m + \left[\frac{U_{ms} S_{ms}}{M_m C_m}\right]\frac{\partial T_{sat}}{\partial P_s}\,\delta P_s \tag{III.12}$$

$$\frac{d\,\delta P_s}{dt} = \frac{1}{K}\left\{ U_{ms} S_{ms}\,\delta T_m - \left[U_{ms} S_{ms}\frac{\partial T_{sat}}{\partial P_s} + W_s\frac{\partial h_g}{\partial P_s} + \epsilon_o\,(h_g - h_{FW})\right]\delta P_s + W_s C_{p2}\,\delta T_{FW} - W_s\,(h_g - h_{FW})\,\frac{\delta\epsilon}{\epsilon_o}\right\} \tag{III.13}$$

where $K = M_{sw}\dfrac{\partial h_f}{\partial P_s} + M_{ss}\dfrac{\partial h_g}{\partial P_s} - M_{ss}\dfrac{\partial h_{fg}}{\partial V_{fg}}\dfrac{\partial V_{fg}}{\partial P_s}$

and $\tau_p = \dfrac{M_p}{W_p}$.

The pressurizer pressure control system was described previously in Chapter II by two equations. The only feedback this model has on the rest of the system is through the pressure coefficient of reactivity. Because this coefficient is so small, (typically on the order of 1×10^{-6}/psi) this model which is described by two equations, can simply be eliminated by assuming this coefficient to be equal to zero.

The reactor control system model was previously described by six state variables. In addition, subroutine DISTRB in MATEXP had to be used to simulate the different rates of control rod motion and the non-linearities of the reactor control system. Two state variables in this model, the outputs of RTDs that measure hot and cold leg temperatures will be ignored. This will not result in any large error in the operation of the reduced reactor control system model. The remaining four equations in the complete model are used to describe a temperature error signal. This temperature error signal is then sent to DISTRB to change the forcing term for reactivity induced by control rods. The purpose of the reactor control system is to force the average reactor coolant temperature to follow the steady state program (see page 38) as closely as possible. This is equivalent to saying that the reactor control system reduces the temperature error signal to a minimum.

A simplification can be made on the reactor control system model by assuming that integral control action is taken on the difference between the average temperature set point for a change in power level and the actual average reactor coolant temperature. The result of integral control is that the error signal used for the control action will be driven to zero. In this case, the error signal is the difference in the temperature set point and the average temperature. In equation form this can be written as

$$\text{(III.14)} \quad \frac{d\delta\rho_{ext}}{dt} = K\left[\delta T_{set} - \delta T_{ave}\right]$$

where $\delta\rho_{ext}$ is the reactivity induced by the control rods. The average temperature set point is defined by the steady state program. In perturbation form this can be written as

$$\text{(III.15)} \quad \delta T_{set} = K_1\, \delta\% P_s$$

where $\delta\% P_s$ is the change in percent of full power delivered to the secondary fluid as defined by equation (II.37), and K_1 is equal to the gain of the average temperature set point transfer function as defined by equation (II.32). K_1 is also equal to the slope of the average temperature line of the steady state program (see page 38). At steady state conditions, $\frac{d\delta\rho_{ext}}{dt}$ is equal to zero. This means that at steady state, $\delta T_{set} = \delta T_{ave}$. Thus, if integral control action is used, as given by equation (III.14), the criterion for the reactor control system will be satisfied. The remaining task is to define a K that will simulate as closely as possible the more detailed reactor control system.

K can be broken down into two factors so that K=K' x K". It is desirable for the units of K to be (dollars/°F-sec). Since the control rods move in discrete steps, the units of K' can be set equal to (dollars/step). The magnitude of K' will be identically equal to the value of ROWSTP as defined in Section II.4. Therefore, K" must be set equal to an "average" control rod rate of movement with units of (steps/sec-°F). The value of K" will be assumed equal to 0.1 (steps/sec-°F). The effect of this assumption can be seen in Figure 3.1. This figure is a duplicate of Figure 2.15 on page 41 except the slope of the dashed line is equal to K".

The turbine-feedwater heater and Pf controller models will not be reduced. Therefore, the high order model described by 57 state variables in Chapter II has been reduced to 25 state variables by physical methods. Table XVI is a description of the state variables in their numerical order in the model. All the input parameters necessary to calculate the system coefficients will be the same as for the high order model except the following

1. λ = Delayed neutron decay constant = $\beta_T \Big/ \left[\sum_{i=1}^{6} \beta_i / \lambda_i \right]$

2. U_{pm} = steam generator overall heat transfer coefficient from primary fluid to metal =

$$\left[\frac{1}{HP} + \left(\frac{TOD - 2TMT}{24\,KM} \right) \ln \left(\frac{TOD - TMT}{TOD - 2TMT} \right) \right]^{-1.0}$$

3. U_{ms} = steam generator overall heat transfer coefficient from metal to secondary fluid =

$$\left[\frac{1}{HS2} + \left(\frac{TOD}{24\,KM} \right) \ln \left(\frac{TOD}{TOD - TMT} \right) \right]^{-1.0}$$

4. K = reactor control system gain = K' K"

5. K_2 = Pf controller gain = $\dfrac{\delta b / b_0}{\delta P_m}$ at steady state

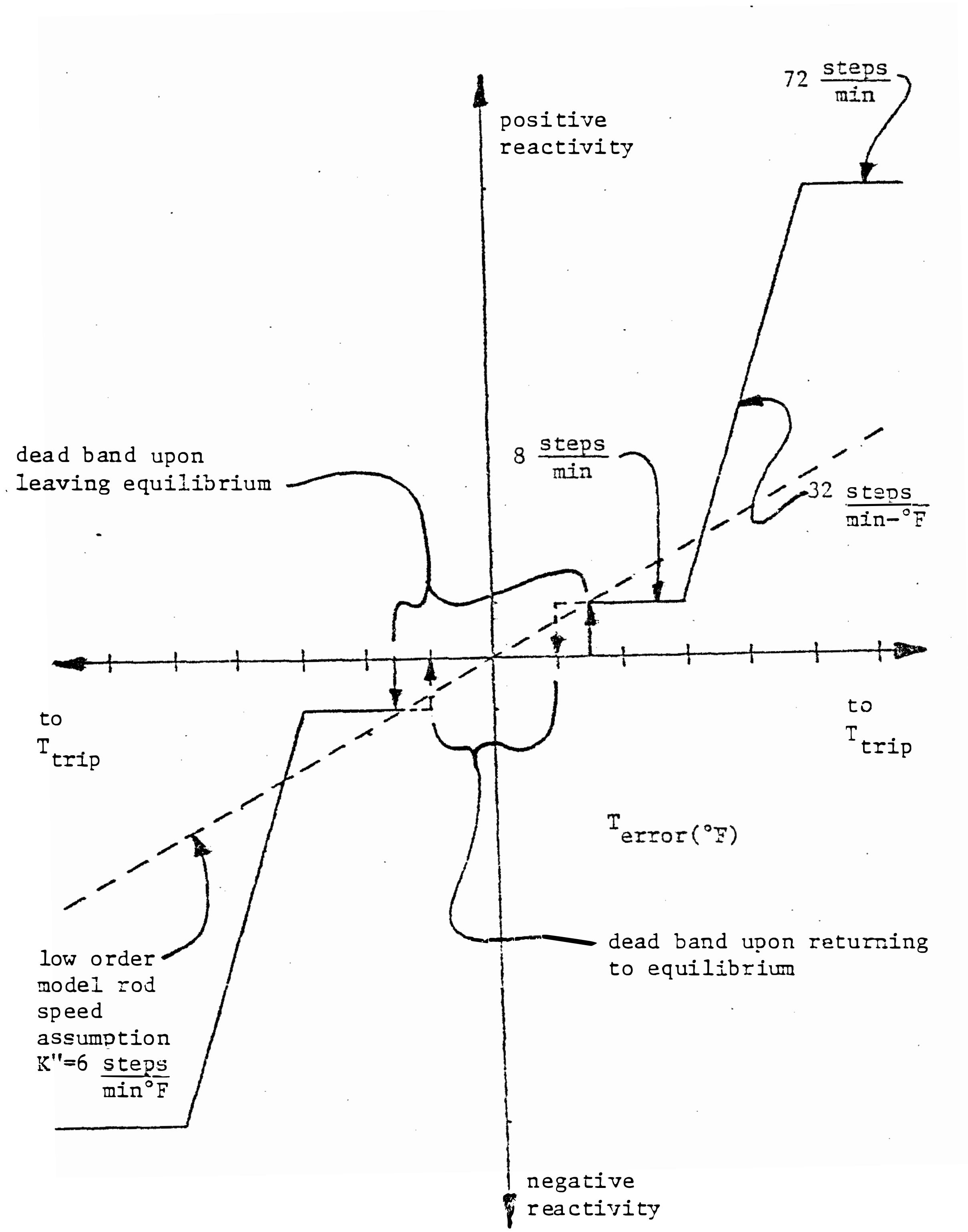

Figure 3.1 Rod speed vs. temperature error signal. The low order model representation is shown by the dashed line.

TABLE XVI

LIST AND DESCRIPTION OF THE LOW ORDER OVERALL PWR SYSTEM MODEL STATE VARIABLES

1.	$\delta P/P_o$	Fractional change in nuclear power
2.	δC	Fractional change in delayed neutron precursor group
3.	δT_F	Change in average fuel temperature of the core (°F)
4.	$\delta\theta_1$	Change in coolant node 1 of the reactor core (°F)
5.	$\delta\theta_2$	Change in coolant node 2 of the reactor core (°F)
6.	$\delta\theta_{HL}$	Change in hot leg temperature (°F)
7.	$\delta\theta_{CL}$	Change in cold leg temperature (°F)
8.	$\delta\theta_P$	Change in the average primary fluid temperature in the UTSG (°F)
9.	δT_M	Change in the average tube temperature in the UTSG (°F)
10.	δP_S	Change in the average steam pressure of the UTSG (psi)
11.	$\delta\rho_{ext}$	The reactivity induced by control rods (dollars)
12.	$\delta\rho_c$	Change in the density of the steam in the nozzle chest (lbm/ft^3)
13.	$\frac{\delta h_c}{h_{co}}$	Fractional change in the enthalpy of the nozzle chest
14.	$\frac{\delta W''_2}{W''_{2_o}}$	Fractional change in the flow rate of steam entering the moisture separator
15.	$\delta\rho_R$	Density of steam in the reheater tube side (lbm/ft^3)
16.	$\frac{\delta h_R}{h_{R_o}}$	Fractional change in enthalpy of reheater tube side

TABLE XVI (continued)

17.	$\frac{\delta W'_{PR}}{\omega'_{PRo}}$	Fractional change in flow rate of steam leaving the reheater shell side
18.	δQ_R	Heat transfer in the reheater shell to tube (Mw-hr/sec)
19.	$\frac{\delta W'_3}{W'_{20}}$	Fractional change in flow rate of steam leaving LP turbine to the condenser
20.	$\delta h'_{FW}$	Change in the enthalpy of feedwater in heater 1 (B/1bm)
21.	δT_{FW}	Change in feedwater temperature leaving heater 2 (°F)
22.	$\frac{\delta W_{HP2}}{W_{HP2}}$	Fractional change in flow rate of fluid leaving heater 2 to heater 1
23.	$\frac{\delta \varepsilon}{\varepsilon_o}$	Fractional change in the main steam valve coefficient
24.	$-\delta P_c$	Change in the integral of the ACE control signal (puMw)
25.	δF	Change in the system frequency (Hz)

6. SPM = Total heat transfer area of primary side to tubes

$$= HTA \left[\frac{TOD - 2TMT}{TOD}\right]$$

7. SMS = Total heat transfer area of metal tubes to secondary fluid

$$= HTA$$

8. M_m = mass of metal tubes

$$= HTA \left[\frac{TOD^2 - (TOD - 2TMT)^2}{48\ TOD}\right] ROM$$

9. M_p = mass of water inside tubes

$$= \left[\frac{TOD}{12} - \frac{2TMT}{12}\right]^2 \left[\frac{3\ HTA}{TOD}\right] ROP$$

10. M_{sw} = mass of secondary liquid = (VSW)(ROS1)

11. M_{ss} = mass of secondary steam = VSS/VG

These values can be calculated from the input data for the high order model. The gain of the Pf controller must be reevaluated as in the high order model (see Section II.7). This gain is determined by running a case of the system model without the Pf controller for a 10 percent step in main steam valve coefficient. The value of K_2 will be defined to be $\frac{\delta G/G_0}{\delta P_m}$ at steady state conditions. For the high order model, this gain turned out to be 1.2706 for a 100 percent power model. For the 100 percent power low order model, this gain was found to be 1.2136.

A computer program has been written to calculate the system coefficients for the isolated low order PWR model (Machado[23]). The turbine-feedwater heater and Pf controller model coefficients, as in Chapter II, are calculated by "hand." The input data is formed exactly as the program described in Appendix A for the high order model. This will assure consistent design data is used when comparing the results with the high order model. The resulting numerical values for the system matrix coefficients for a typical 1200 Mwe plant at 100% power are shown in Table XVII.

The forcing terms for the low order model are shown below

(III.16) $$f(24) = \delta P_{TIE}$$

(II.17) $$f(25) = -\frac{1}{M}\left[\delta P_{TIE} + \delta P_D\right].$$

Therefore, the tie line power flow and power demand signal are two methods of disturbing the low order PWR model. Only one case will be presented in this section. Figure 3.2 shows the time response of the overall low order PWR system model to a +0.05 puMw (+50Mw) step in the power demand signal. Figure 2.35 (page 118) and Figure 3.2 will be compared in Chapter IV.

III.3 Model Reduction by Numerical Methods

In Section III.2 the high order PWR model was reduced to a 25th order model by physical methods. Several methods were considered in reducing the PWR model by numerical methods (Genesio[10], Shieh[33], Bosley [5,21], Wei[33], Milanese[10], Lal[20], Mitra[20], Jain[20], Krishnamurthi[19], Seshadri[19], Bille[4], Sinha[34,4], Arumugam[3], Ramamoorty[3], Bereznai[34], Lees[21,22,5], Davison[8], Gibilaro[22], Kropholler[5], Neale[5]). The majority of these methods involved placing the responses of the state variables in a transfer function form (Laplace domain) before reducing the order of the model. In

TABLE XVII

LIST OF THE NUMERICAL VALUES OF THE LOW ORDER OVERALL PWR SYSTEM MODEL MATRIX COEFFICIENTS

ROW	COL	COEFFICIENT	ROW	COL	COEFFICIENT
1	1	-3.8536E+02	1	2	8.2246E-02
1	3	-6.1452E-01	1	4	-5.5866E+00
1	5	-5.5866E+00	1	11	3.8536E+02
2	1	3.8536E+02	2	2	-8.2246E-02
3	1	2.4137E+02	3	3	-2.5322E-01
3	4	2.5322E-01	4	1	2.6186E+00
4	3	1.0292E-01	4	4	-3.6492E+00
4	7	3.5462E+00	5	1	2.6186E+00
5	3	1.0292E-01	5	4	3.4433E+00
5	5	-3.5462E+00	6	5	3.1321E-01
6	6	-3.1321E-01	7	7	-2.1411E-01
7	8	2.1411E-01	8	6	3.2502E-01
8	8	-1.6055E+00	8	9	1.2805E+00
9	8	4.7874E+00	9	9	-7.7818E+00
9	10	4.1922E-01	10	9	5.5986E+00
10	10	-9.3331E-01	10	21	1.9140E-01
10	23	-1.2338E+02	11	6	-1.1250E-04
11	7	-1.1250E-04	11	10	5.3816E-06
11	21	-8.0130E-06	11	23	4.4699E-03

TABLE XVII (continued)

ROW	COL	COEFFICIENT	ROW	COL	COEFFICIENT
12	10	2.4920E-02	12	12	-1.6293E+01
12	13	-3.6720E+01	12	15	1.9290E+00
12	16	5.8749E+00	12	23	2.0730E+01
13	10	1.4870E-02	13	12	-9.9553E+00
13	13	-3.1153E+01	13	15	1.1785E+00
13	16	3.5892E+00	13	23	1.2667E+01
14	12	3.9300E-01	14	13	8.8583E-01
14	14	-5.0000E-01	14	15	-4.6530E-02
14	16	-1.4176E-01	15	14	1.9532E-01
15	15	-2.7134E-01	15	16	-2.1010E-01
16	14	6.1613E-01	16	15	-1.0747E+00
16	16	-1.2767E+00	16	18	3.7648E-01
17	10	4.0064E-04	17	17	-3.3333E-01
18	10	8.3500E-05	18	16	-1.0102E+00
18	17	7.8624E-03	18	18	-2.5000E-01
19	15	1.9020E-01	19	16	1.4590E-01
19	19	-1.0000E-01	20	10	-2.7006E-03
20	15	1.3517E+00	20	16	1.0365E+00
20	20	-1.0000E-01	20	22	1.3953E+00
20	23	-2.1460E+00	21	10	-1.5830E-03
21	12	1.3378E+00	21	13	3.0144E+00
21	14	-1.1006E+00	21	15	-1.5838E-01
21	16	-3.7430E-01	21	17	4.5818E-01

TABLE XVII (continued)

ROW	COL	COEFFICIENT	ROW	COL	COEFFICIENT
21	20	2.1930E-02	21	21	-2.5000E-02
21	23	-1.2579E+00	22	12	4.3722E-02
22	13	9.8510E-02	22	14	-3.5970E-02
22	15	-5.1760E-03	22	16	-1.2240E-02
22	17	1.4970E-02	22	22	-1.0000E-01
23	23	-5.0000E+00	23	24	-6.0745E+00
23	25	-2.0248E+00	24	25	3.4167E-01
25	25	-1.0000E-01			

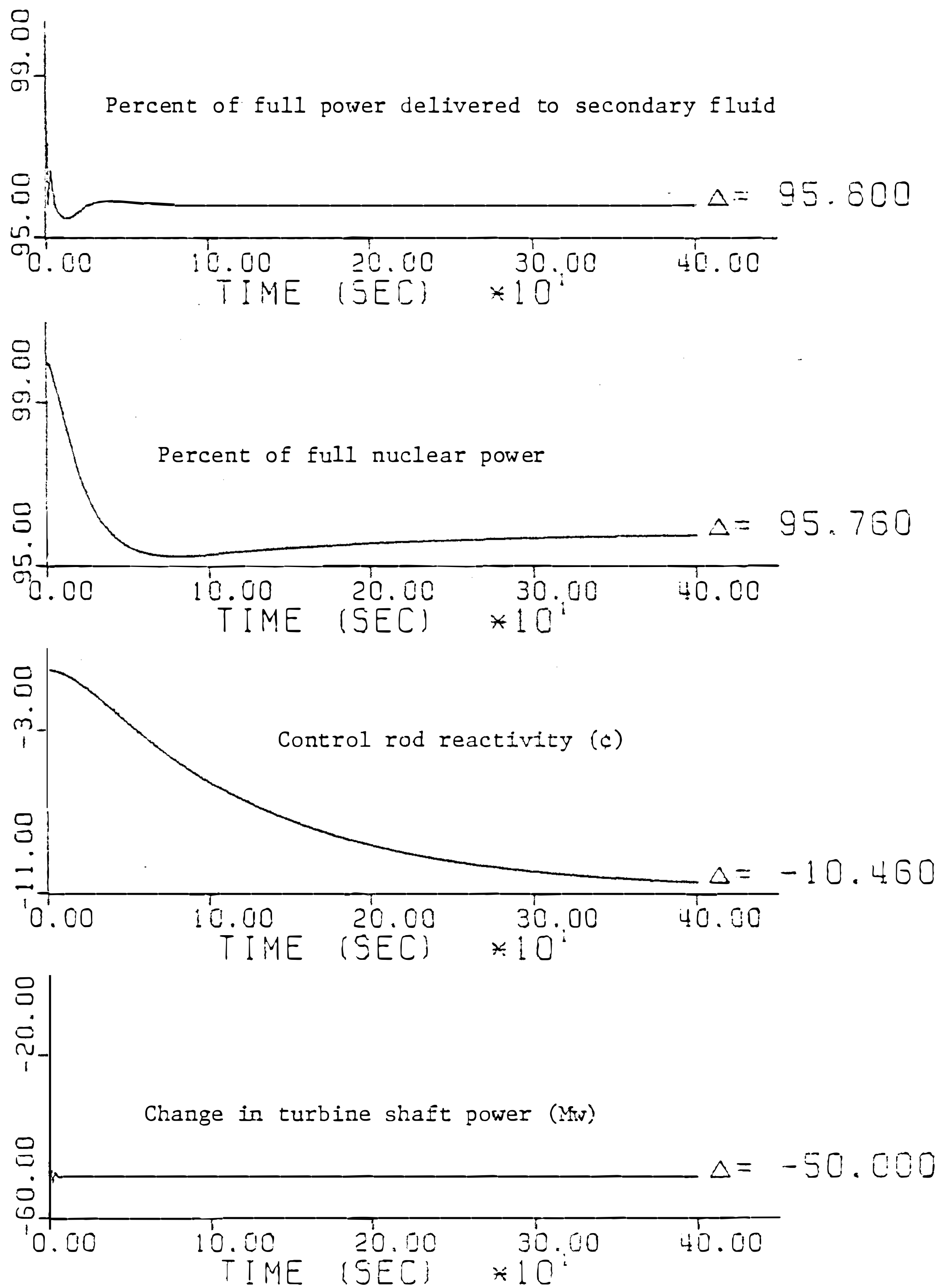

Figure 3.2 Response of the overall low order PWR system model for a -0.05 puMw (-50 Mw) step in the power demand signal.

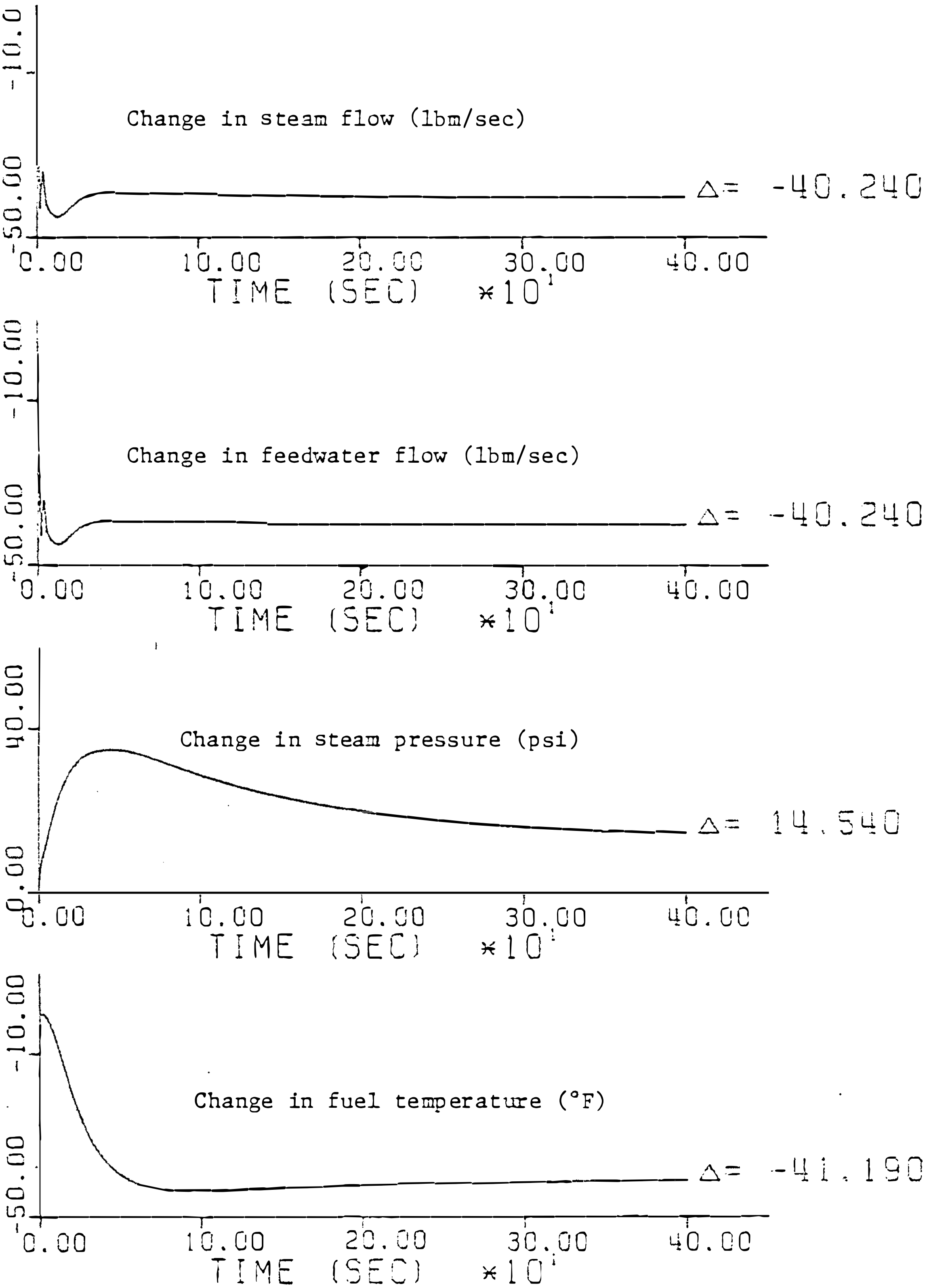

Figure 3.2 (continued)

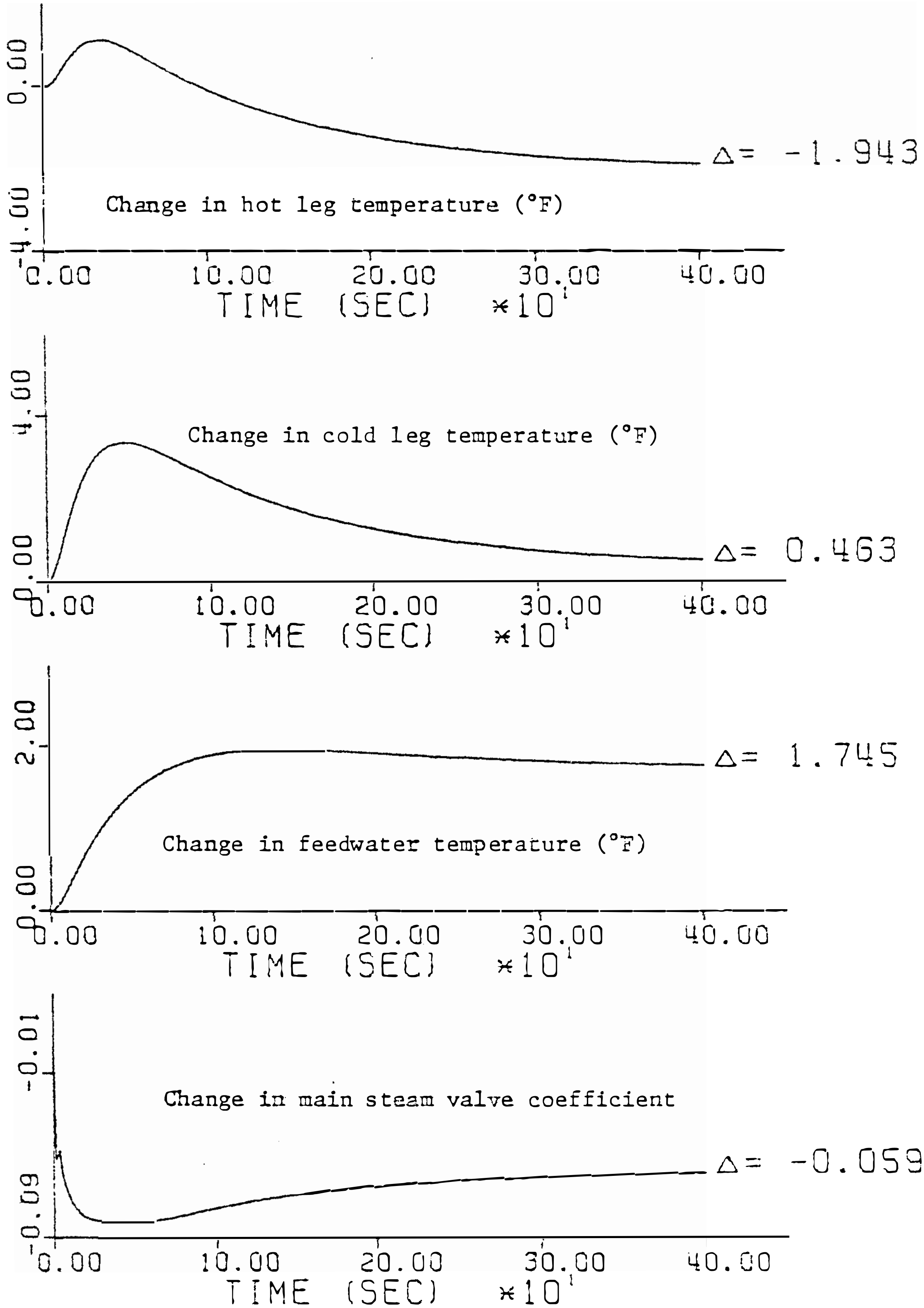

Figure 3.2 (continued)

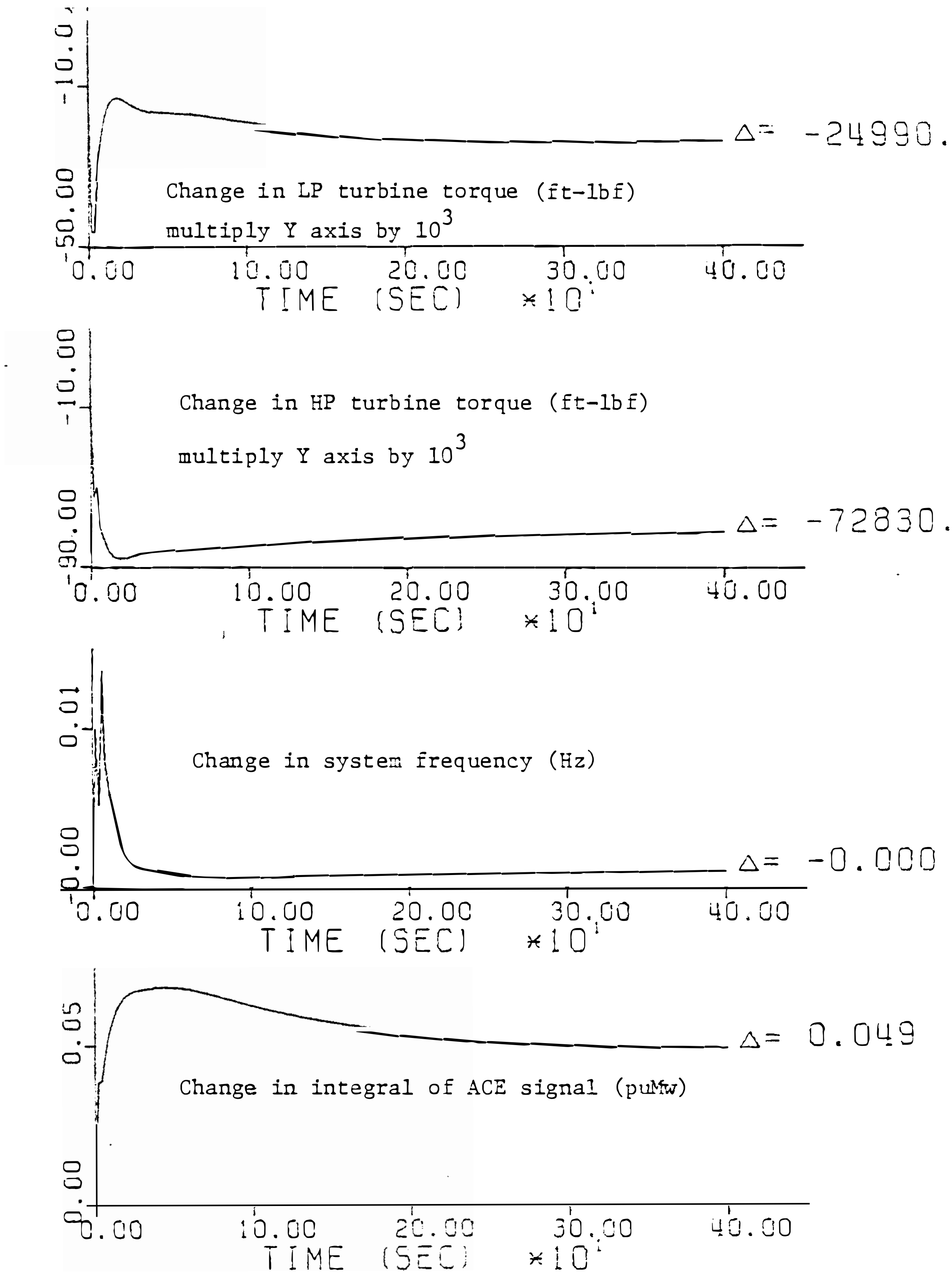

Figure 3.2 (continued)

this section, a numerical method for reducing the model will be presented which will be called the pole-zero deletion method. Then, the pole-zero deletion method will be applied to the 25th order PWR model.

III.4 Model Reduction by the Pole-Zero Deletion Method

If a system model is represented in state variable form, as in equation (II.21), then a Laplace transformation of the state variables can be applied and the resulting equation will be of the form

$$[sI - A]\,\bar{X}(s) = \bar{f}\,g(s). \qquad \text{(III.18)}$$

One method of solution to this linear algebraic equation is to use Cramer's rule. The form of the ith row of the solution vector by using Cramer's rule is

$$\frac{X_i(s)}{g(s)} = \frac{B}{C} \qquad \text{(III.19)}$$

where $C=|sI - A|$ and B is equal to C except the ith column of the matrix $(sI - A)$ has been replaced by the vector of forcing coefficients, $\bar{f}$, before calculating the determinant. The determinants, B and C, can be expanded and written in polynomial form. If the solution to the resulting polynomials were found, then equation (III.19) could be written as

$$\frac{X_i(s)}{g(s)} = K \frac{\prod_{k=1}^{m}(s - Z_k)}{\prod_{\ell=1}^{n}(s - P_\ell)} \qquad \text{(III.20)}$$

where the Z_k's are the zeroes and the P_ℓ's are the poles; m is the total number of zeroes, and n is the total number of poles. K will be called the gain of the transfer functions.

The poles are equal to the eigenvalues of the system matrix A.[16] The problem is to find the zeroes of a desired transfer function. A method has been developed (Davison[8], Bosley[5]) to find the zeroes of a state variable model. The zeroes of the <u>ith</u> row of the solution vector are the eigenvalues of the matrix formed by replacing the <u>ith</u> column of (sI - A) with the forcing vector. The form of this matrix is shown in the following equation

(III.21)

$$B = \det \begin{bmatrix} s-a_{11} & -a_{12} & -a_{13} \cdots & f_1 & \cdots & -a_{1n} \\ -a_{21} & s-a_{22} & -a_{23} \cdots & f_2 & \cdots & -a_{2n} \\ -a_{31} & -a_{32} & s-a_{33} \cdots & f_3 & \cdots & -a_{3n} \\ \vdots & \vdots & \vdots & \vdots & & \vdots \\ \cdot & \cdot & \cdot & f_i & \cdots & a_{in} \\ \vdots & \vdots & \vdots & \vdots & & \vdots \\ -a_{n1} & -a_{n2} & \cdot & f_n & & s-a_{nn} \end{bmatrix}$$

From equation (III.21) it is easily seen that the matrix element of the ith row and ith column is equal to f_i and does not have an s present. A standard eigenvalue routine (Cope[7], Dunphey[7]) will take the original matrix A and perform the operation (sI - A) before finding the eigenvalues. Therefore, the matrix element of the ith row and ith column will be automatically set equal to $(s - f_i)$. This means that the standard eigenvalue routine would result in some "undesired solutions" to the determinant B. If the forcing vector is arbitrarily multiplied by a "large" constant, which will be called HCRIT, the matrix elements of the ith column will become "large." Then if the eigenvalues of this matrix are found, there will be some numbers that are large relative to the other eigenvalues. These large undesired solutions can then be disregarded and the remaining eigenvalues will be the zeroes. There is no guarantee that the correct eigenvalues have been obtained for the zeroes. Therefore, the results of this method must be compared to other methods of solution in order to be assured of the correct zeroes.

The gain of the transfer function can be found by applying the final value theorem[16] to equation (III.20). If it is assumed that the forcing vector is applied as a unit step input, then s(s) = 1/s. The result will be

$$X(t=\infty) = \lim_{s \to 0} s\,X_i(s) = (-1)^{m-n} K \frac{\prod_{k=1}^{m} z_k}{\prod_{l=1}^{n} p_l}, \tag{III.22}$$

and therefore the gain can be written as

$$K = X(t=\infty)\,(-1)^{n-m}\,\frac{\prod_{l=1}^{n} P_l}{\prod_{k=1}^{m} Z_k} \,. \tag{III.23}$$

The final value of the state vector can be found by setting the derivative vector of equation (III.22) equal to zero and solving for x. In equation form this can be written as

$$\bar{X}(t=\infty) = -A^{-1}\,\bar{f} \tag{III.24}$$

Then equation (III.24) is substituted into equation (III.23) to get the gain of the transfer function.

Every quantity in equation (III.20) can now be obtained. A computer code called REDUCE has been written that uses this method. The instructions for the use of this code are given in Appendix G.

After the response is written as in equation (III.20), m and n can be reduced by deleting poles and zeroes that are "close" to the same value. Two problems arise in doing this. First, the poles and zeroes have real and imaginary parts. And second, the poles and zeroes are found by an eigenvalue routine on a digital computer. Thus, the resulting numerical values of the poles and zeroes may not be found exactly due to the limited number of digits allowed by the machine. Thus, this method is highly dependent on the type of computer used. The computer used in this study was the DEC System 10 at The University of Tennessee. The REDUCE code is executed in double precision arithmetic. Therefore, approximately 16 digits of accuracy can be expected.

The following algorithm was used to delete poles and zeroes.

1. Determine the mantissa and exponent of the real part of all the poles and zeroes. The mantissas will have a value between 1.0 and 10.0.
2. Check to see if any pole-zero pair combination has a real part less than an input parameter LCRIT. This is because occasionally a pole or zero may be found which is close to zero. If a pole is only slightly positive, the response would be unstable. Therefore, if a pole-zero pair of a "small" value is found, it will be deleted. In this study a typical value used for LCRIT is 1.0×10^{-10}.
3. Determine whether any pole-zero pair has the same exponent. Compare all pole-zero pair combinations not previously deleted. Store these pole-zero pairs as possible candidates for deletion and continue to step 4.
4. Determine whether the absolute value of the difference between the mantissas of this pole-zero pair is less than an input parameter EPIL. If not, keep comparing all pole-zero pairs with the same exponent against each other until all combinations of pole-zero pairs, which have been stored from step 3, have been compared. If so, go to step 5.
5. If step 3 and step 4 pass, or if step 2 alone passes, then delete that pole-zero pair.
6. Repeat step 2 through 5 until no more pole-zero pairs can be deleted.

Steps 3 and 4 are carried out at the option of the user of REDUCE. Step 2 is always carried out.

The arbitrarily large number which has been called HCRIT is not easily found. It can have a value typically in the range of 10^{15} to 10^{50}. The number of zeroes, m, appears to be a function of the number of elements appearing in the ith row for the x_i response. That is $m \quad n$ - (number of non-zero terms in the ith row). If any eigenvalue appears that is greater than $(\mathrm{HCRIT})^{n-m}$, then it should be thrown away.

Another problem associated with calculating the gain K is that it may not work if there is not an element appearing on all the diagonal positions. If it is impossible to rearrange the rows of the matrix to achieve this condition before using the REDUCE program, then it may still be possible to find the steady state value of the state variable desired. This is because the vector can be evaluated without calculating the inverse matrix. This is done by placing the matrix A in upper triangular form and back substituting to find the solution. If a zero diagonal is still present, the solution of that row cannot be found. However, not all the remaining back calculations will depend on this solution and some, if not all, of the remaining solutions might be found.

After the pole-zero pairs have been deleted, then the gain constant K must be reevaluated for the reduced representation. This is to assure that the steady state behavior for the reduced representation will be equal to the full representation.

The computer program REDUCE will then calculate the frequency response for both the full and reduced representation. REDUCE will also calculate the time response for a step input for both the full and reduced representation. The process can then be repeated as many times as desired.

The pole-zero deletion method can now be applied to the 25th order PWR model presented in Section III.2. The first observation of this model is that the system does not have diagonal elements on rows 11 and 24. It is not coincidental that these rows correspond to the integral control action taken by the reactor and Pf controllers respectively. In order to set the system matrix in a form that can be used by the REDUCE program, the following steps were taken.

1. Ignore equation 25 so that the electrical system frequency, δF, will be a forcing function.
2. Ignore the integral control action of the ACE signal so that equation 24 will also be eliminated. Now the only forcing function appears in equation 23 and the system is now 23rd order rather than 25th.
3. Change state variable 1 which is $\frac{\delta P}{P_o}$ to $-\frac{\delta P}{P_o}$. This will cause the following matrix elements to change sign: (1,2), (1,3), (1,4), (1,5), (1,11), (2,1), (3,1), (4,1), (5,1). This is to assure that negative diagonal elements will appear everywhere after step 5 is taken.
4. Change state variable 5 which is $\delta\theta_2$ to $-\delta\theta_2$. This will cause the following matrix elements to change sign: (5,1), (5,3), (5,4), (1,5), (6,5). This is to assure that negative diagonal elements will appear after step 5 is taken.
5. Interchange the matrix rows in the following manner

Existing Row	Modified Row
1	11
11	6
6	5
5	1

This is done to assure that a diagonal element will appear on every row of the matrix.

Now the matrix is in a form that can be used by REDUCE. Table XVIII is a list of the 23rd order system matrix used by REDUCE. As an example of the use of this method, the transfer function of fractional change in nuclear power for a change in electrical system frequency can be found. In equation form this will be

$$G(s) = \frac{\frac{\delta P}{P_o}(s)}{\delta F(s)} \quad \text{(III.24)}$$

Then this transfer function will be reduced by deleting poles and zeroes. The REDUCE program deleted poles and zeroes 17 times with increasing values of the input parameter EPIL until 17 pole-zero pairs were deleted. A value of HCRIT for this case was chosen to be 5×10^{20} by trial and error. In order to assure that this value of HCRIT is correct, the results of REDUCE must be compared to results from similar computer programs such as MATEXP[25] or SFR3[30]. A listing of the input data used for this case is included in Appendix G. A listing of the resulting poles and zeroes for the 23rd order transfer function of fractional change in nuclear power vs. change in electrical system frequency is shown in Table XIX. The gain factor K

TABLE XVIII

LIST OF THE NUMERICAL VALUES OF THE 23rd ORDER MODEL MATRIX COEFFICIENTS USED IN THE EXAMPLE CASE OF THE REDUCE COMPUTER CODE

ROW	COL	COEFFICIENT	ROW	COL	COEFFICIENT
1	1	-2.6190E+00	1	3	1.0290E-01
1	4	3.4430E+00	1	5	3.5460E+00
2	1	-3.8540E+02	2	2	-8.2250E-02
3	1	-2.4140E+02	3	3	-2.5320E-01
3	4	2.5320E-01	4	1	-2.6190E+00
4	3	1.0290E-01	4	4	-3.6490E+00
4	7	3.5460E+00	5	5	-3.1320E-01
5	6	-3.1320E-01	6	6	-1.1250E-04
6	7	-1.1250E-04	6	10	5.3820E-06
6	21	-8.0130E-06	6	23	4.4700E-03
7	7	-2.1410E-01	7	8	2.1410E-01
8	6	3.2500E-01	8	8	-1.6050E+00
8	9	1.2800E+00	9	8	4.7870E+00
9	9	-7.7820E+00	9	10	4.1920E-01
10	9	5.5990E+00	10	10	-9.3330E-01
10	21	1.9140E-01	10	23	-1.2340E+02
11	1	-3.8540E+02	11	2	-8.2250E-02
11	3	6.1450E-01	11	4	5.5870E+00
11	5	-5.5870E+00	11	11	-3.8540E+02

TABLE XVIII (continued)

ROW	COL	COEFFICIENT	ROW	COL	COEFFICIENT
12	10	2.4920E-02	12	12	-1.6290E+01
12	13	-3.6720E+01	12	15	1.9290E+00
12	16	5.8750E+00	12	23	2.0730E+01
13	10	1.4870E-02	13	12	-9.9550E+00
13	13	-3.1150E+01	13	15	1.1780E+00
13	16	3.5890E+00	13	23	1.2670E+01
14	12	3.9300E-01	14	13	8.8580E-01
14	14	-5.0000E-01	14	15	-4.6530E-02
14	16	-1.4180E-01	15	14	1.9530E-01
15	15	-2.7130E-01	15	16	-2.1010E-01
16	14	6.1610E-01	16	15	-1.0750E+00
16	16	-1.2770E+00	16	18	3.7650E-01
17	10	4.0060E-04	17	17	-3.3330E-01
18	10	8.3500E-05	18	16	-1.0100E+00
18	17	7.8620E-03	18	18	-2.5000E-01
19	15	1.9020E-01	19	16	1.4590E-01
19	19	-1.0000E-01	20	10	-2.7010E-03
20	15	1.3520E+00	20	16	1.0370E+00
20	20	-1.0000E-01	20	22	1.3950E+00
20	23	-2.1460E+00	21	10	-1.5830E-03
21	12	1.3380E+00	21	13	3.0140E+00
21	14	-1.1010E+00	21	15	-1.5840E-01
21	16	-3.7430E-01	21	17	4.5820E-01

TABLE XVIII (continued)

ROW	COL	COEFFICIENT	ROW	COL	COEFFICIENT
21	20	2.1930E-02	21	21	-2.5000E-02
21	23	-1.2580E+00	22	12	4.3720E-02
22	13	9.8510E-02	22	14	-3.5970E-02
22	15	-5.1760E-03	22	16	-1.2240E-02
22	17	1.4970E-02	22	22	-1.0000E-01
23	23	-5.0000E+00			

TABLE XIX

LIST OF THE NUMERICAL VALUES OF THE POLES AND ZEROES FOR THE COMPLETE 23rd ORDER TRANSFER FUNCTION OF FRACTIONAL CHANGE IN NUCLEAR POWER vs ELECTRICAL SYSTEM FREQUENCY

	REAL PART	IMAGINARY PART
A. Poles		
1	-0.3854000015258789D+03	0.0000000000000000D+00
2	-0.8161078603294609D+00	-0.6027362789131288D+01
3	-0.8161078603294609D+00	0.6027362789131288D+01
4	-0.8224999997764829D-01	0.0000000000000000D+00
5	-0.4888984254503823D+01	0.0000000000000000D+00
6	-0.4423026730892135D+02	0.0000000000000000D+00
7	-0.3199164280163355D+01	0.0000000000000000D+00
8	-0.8914372053456591D+01	0.0000000000000000D+00
9	-0.1127285384528623D+01	0.0000000000000000D+00
10	-0.1203821975861004D+01	0.0000000000000000D+00
11	-0.4314690614323917D+00	-0.2281844295007351D-02
12	-0.4314690614323917D+00	0.2881844295007351D-02
13	-0.3132000006735325D+00	0.0000000000000000D+00
14	-0.3194229013039059D+00	0.0000000000000000D+00
15	-0.3329678090048982D+00	0.0000000000000000D+00
16	-0.2003087512600324D+00	0.0000000000000000D+00
17	-0.2150423998650362D+00	0.0000000000000000D+00
18	-0.1000127856222936D+00	-0.4030307367457476D-02
19	-0.1000127856222936D+00	0.4030307367457476D-02
20	-0.2532307050510290D-01	0.0000000000000000D+00
21	-0.1729322606608031D-03	0.0000000000000000D+00
22	-0.9999999962747097D-01	0.0000000000000000D+00
23	-0.5000000000000000D+01	0.0000000000000000D+00
B. Zeroes		
1	-0.4430374867690154D+02	0.0000000000000000D+00
2	-0.3852059669454494D+03	0.0000000000000000D+00
3	-0.8712219028563915D+01	0.0000000000000000D+00
4	0.6594037552966448D+02	0.0000000000000000D+00
5	-0.6922348150124941D+01	-0.1818512956169113D+01
6	-0.6922348150124941D+01	0.1818512956169113D+01
7	-0.3209123523440376D+01	0.0000000000000000D+00

TABLE XIX (continued)

	REAL PART	IMAGINARY PART
8	-0.3656658346498506D+01	0.0000000000000000D+00
9	0.1538612815401276D+01	-0.2856448344664414D+01
10	0.1538612815401276D+01	0.2856448344664414D+01
11	-0.1075726161143901D+01	-0.5097785431205009D+00
12	-0.1075726161143901D+01	0.5097785431205009D+00
13	0.4068989483444778D+01	0.0000000000000000D+00
14	-0.1316823892945096D+00	0.0000000000000000D+00
15	-0.1443983273816879D+00	0.0000000000000000D+00
16	-0.4422183469784892D-01	0.0000000000000000D+00
17	-0.3492260545793666D+00	0.0000000000000000D+00
18	-0.3338528652401436D+00	0.0000000000000000D+00
19	-0.1011449306052564D+00	0.0000000000000000D+00
20	-0.3146752200148401D+00	0.0000000000000000D+00
21	-0.8224999997764826D-01	0.0000000000000000D+00

for the 23rd order representation is 1.85×10^{-9}. The steady state value of $\frac{\delta P}{P_0}$ for a 1 Hz step input is -0.2953.

A set of three surfaces can be found from the results of this case. The frequency response is found by substituting $j\omega$ for s in the transfer function. The natural log of the magnitude of the frequency response is equal to the Z axis of surface 1. The X axis is equal to the natural log of the frequency ω. The Y axis is equal to the number of pole-zero pairs deleted starting from zero and increasing to 17. Figure 3.3 is a representation of surface 1 as produced by the SURFACE II[36] program available from The University of Tennessee Computing Center. (Instructions for the use of this program are available from The University of Tennessee Computing Center.) Figure E.7 in Appendix E is also surface 1 as seen from another view.

The phase angle, in radians, of the frequency response is equal to the Z axis of surface 2. The X axis is equal to the natural log of the frequency ω. The Y axis is equal to the number of pole-zero pairs deleted. Figure 3.4 is a representation of surface 2. Figure E.8 in Appendix E is also surface 2 as seen from another view.

The time response for a unit step input can be found by multiplying the transfer function through by g(s)=1/s and performing an inverse Laplace transform. The Z axis of surface 3 is equal to the fractional change in nuclear power. The X axis is the time in seconds. The Y axis is the number of pole-zero pairs deleted. Figure 3.5 is a representation of surface 3. Figure E.9 in Appendix E is also surface 3 as seen from another view.

From Figures 3.3, 3.4, 3.5, E.7, E.8, and E.9 it will be possible to estimate the maximum number of pole zero pairs that can be deleted.

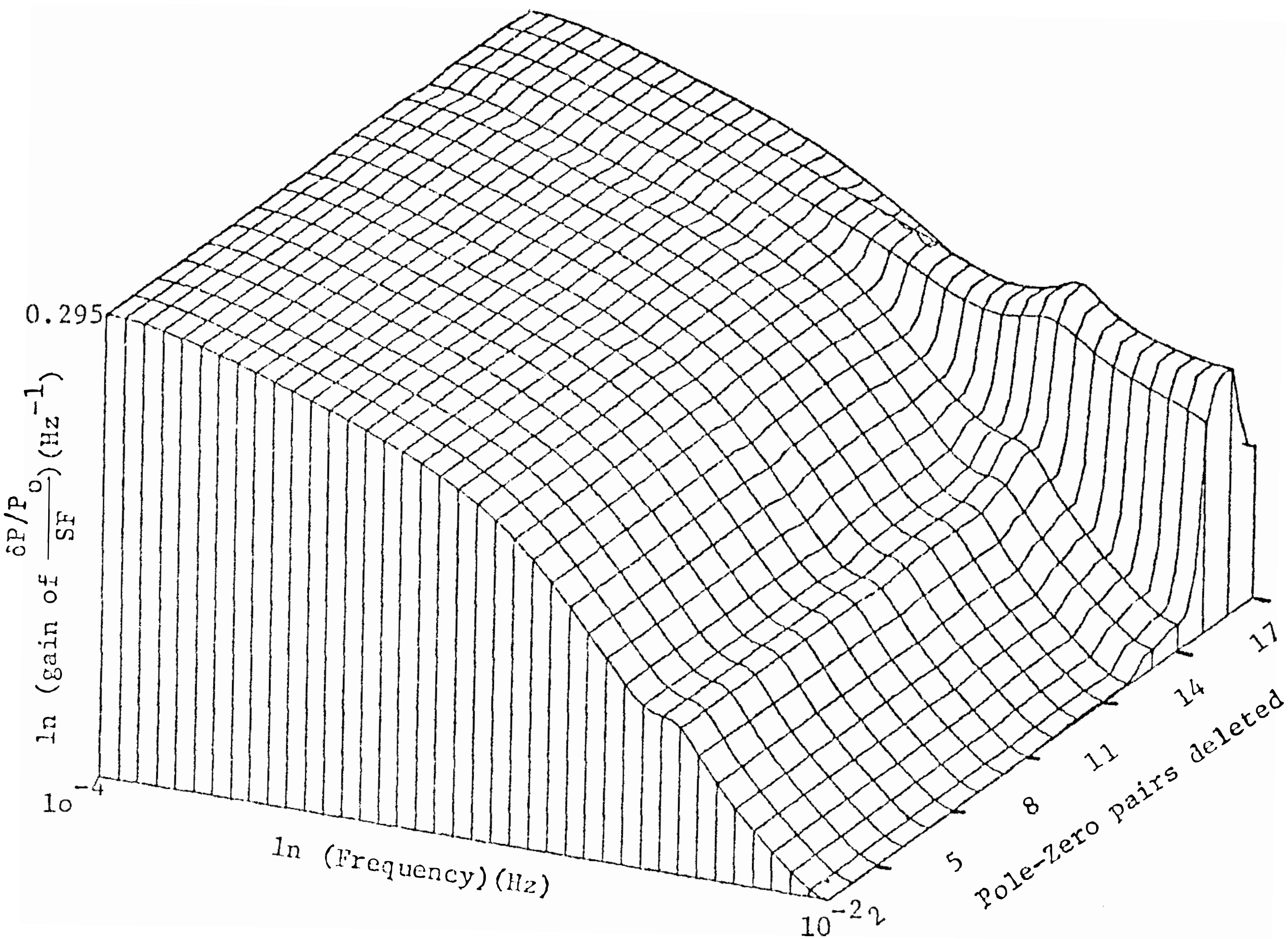

Figure 3.3 Surface of 23rd order gain of fractional nuclear power for a change in electrical system frequency as a function of input frequency and pole-zero pairs deleted.

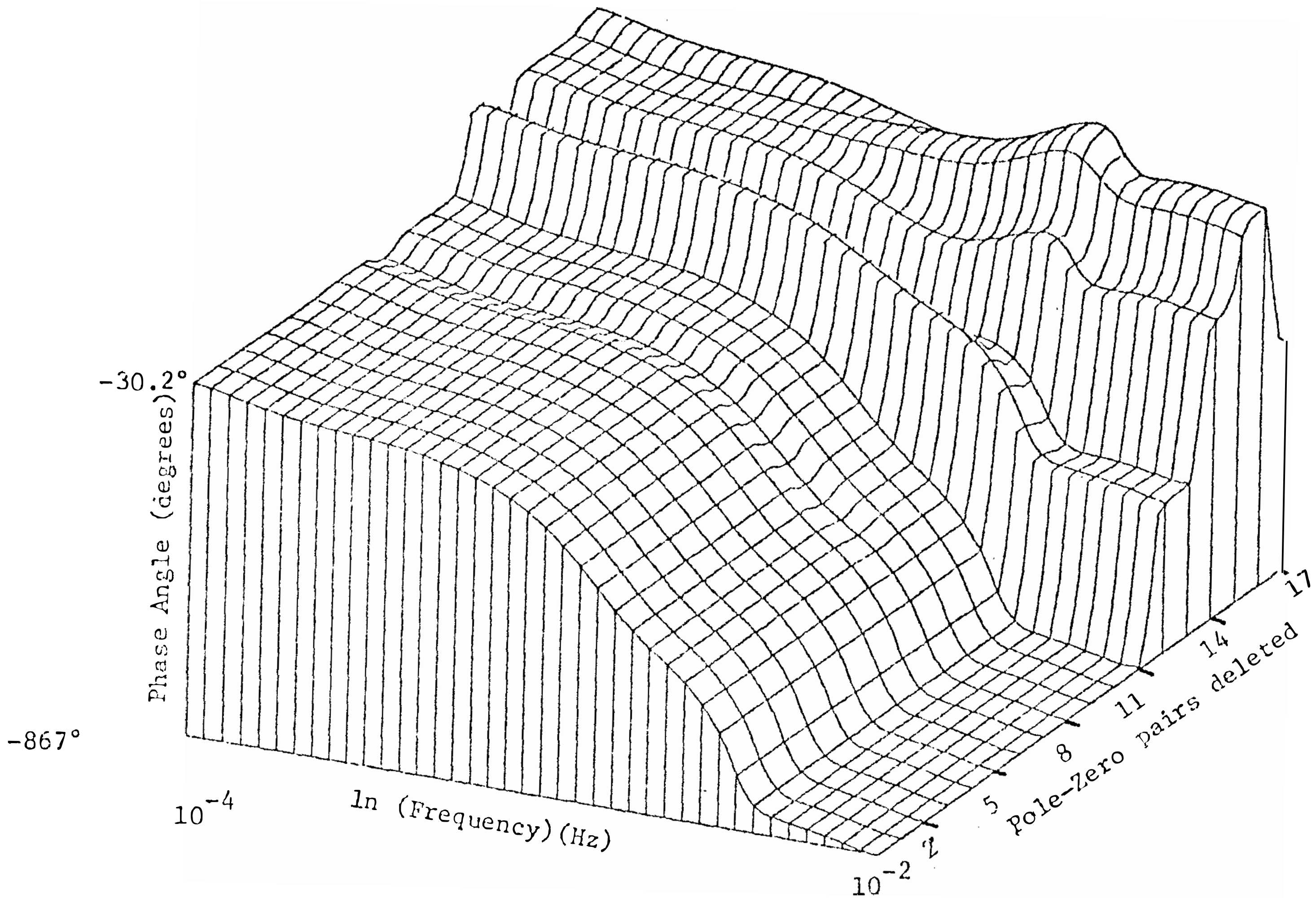

Figure 3.4 Surface of 23rd order phase angle of fractional change in nuclear power for a change in electrical system frequency as a function of input frequency and pole-zero pairs deleted.

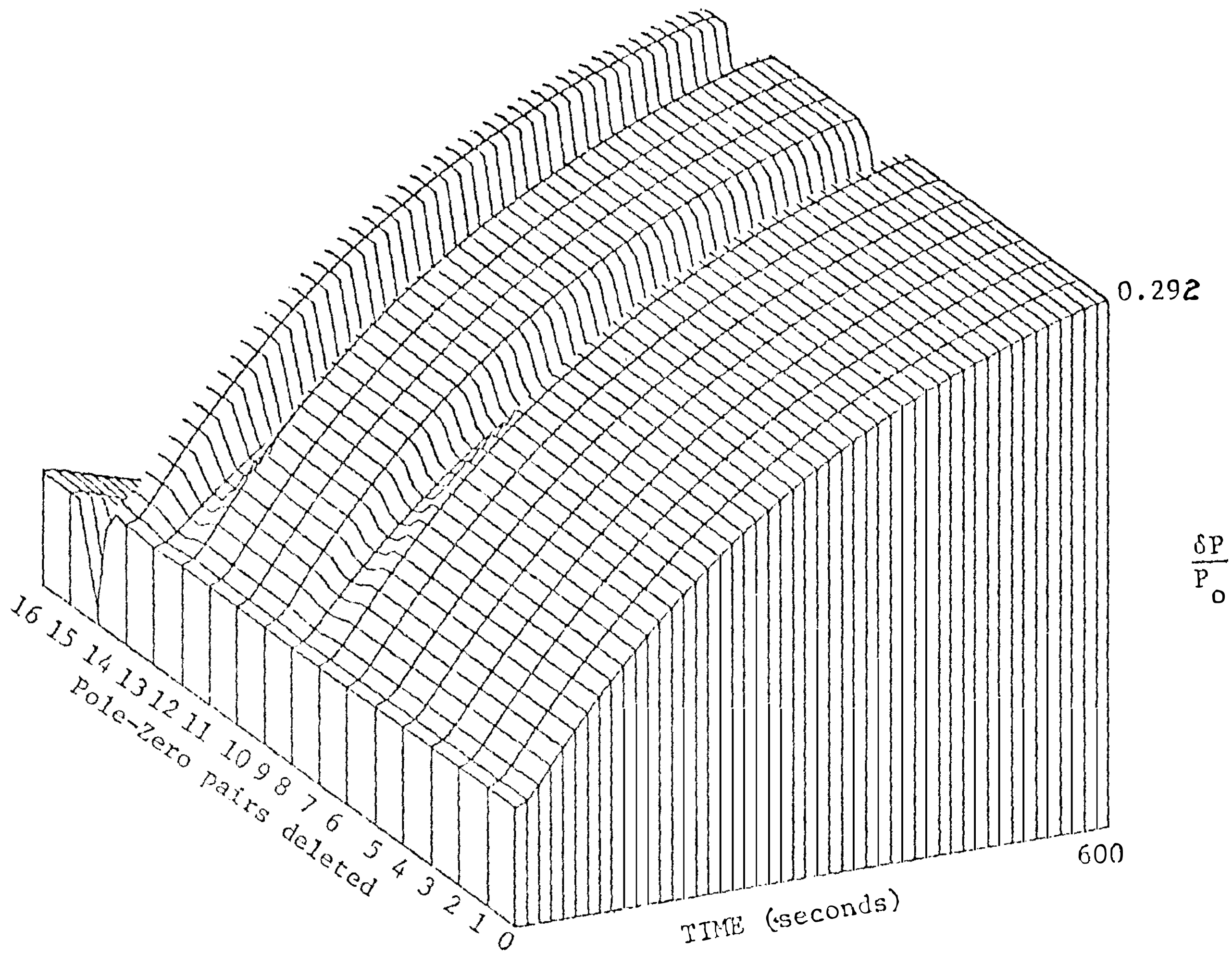

Figure 3.5 Surface of the time response of the fractional change in nuclear power as a function of time and pole-zero pairs deleted for a unit step change in electrical system frequency.

This is equivalent to estimating the minimum order of the transfer function of fractional change in nuclear power for a change in electrical frequency by the pole-zero deletion method.

At low frequencies Figures 3.3 and E.7 indicate there need be no maximum for deletion of pole-zero pairs. This is primarily due to the fact that the gain factor, K, has been recalculated each time a pole-zero pair was deleted. As the surface is examined toward the higher frequencies, it appears that only 14 pole-zero pairs can be deleted before the surface is far from the response of the initial model having no pole-zero pairs deleted.

Figures 3.4 and E.8, which show the phase angle as a function of frequency and number of pole-zero pairs deleted, will not be affected by the recalculation of the gain factor K. Therefore, at low frequencies the inconsistency between the response at no pole-zero pair deletion and the response at higher pole-zero pair deletion happens sooner. From these figures, it appears that the maximum number of pole-zero pairs that should be deleted is 11.

Figures 3.5 and E.9, which show the fractional change in nuclear power for a unit step input of electrical frequency as a function of time and number of pole-zero pairs deleted, shows a dip in the surface in the pole-zero pair deletion ranges of 7 to 9 and 12 to 14. This indicates that this method may give a "bad" response at a point in the pole-zero pair deletion and then obtain a "good" response as more pole-zero pairs are deleted. This can be attributed to the fact that the pole-zero deletion algorithm only considers the real parts of the numerical values of the poles and zeroes. Therefore it is possible that a pole-zero pair could be deleted that have unequal imaginary parts. This can be checked by looking at the printed output of the REDUCE program. However, REDUCE has not been automated to tell the user when this has happened, or to correct itself when this happens. Also it is possible that a pole complex conjugate pair or a zero complex conjugate pair would not be both deleted at the same time. This would leave an imaginary part of either a pole or zero without its complimentary complex conjugate when calculating the time and frequency response.

From the investigation of these surfaces, it appears that the minimum order of the fractional change in nuclear power to a change in electrical frequency transfer function would be about 11. This is if the interest is to match the time and frequency responses as closely as possible. If the interest is only to match the gain of the frequency response or the time response, then the pole-zero deletion method appears to obtain a value of 9 as the minimum order for this transfer function. A list of the numerical values of the poles and zeroes for the reduced 11th order transfer function of fractional change in nuclear power vs electrical system frequency is given in Table XX.

This procedure can be applied to any linear state variable model. Further investigation of other numerical methods might result in further minimization of the system order than what can be obtained by the pole-zero deletion method.

The main disadvantage of this method is that only one state variable response can be obtained. This means that if an algebraic variable needed to be obtained, which might depend upon more than one state variable, then this method would get quite complicated. For

TABLE XX

LIST OF THE NUMERICAL VALUES OF THE POLES AND ZEROES FOR THE REDUCED 11th ORDER TRANSFER FUNCTION OF FRACTIONAL CHANGE IN NUCLEAR POWER vs ELECTRICAL SYSTEM FREQUENCY

	REAL PART	IMAGINARY PART
A. Poles		
1	-0.8161078603294609D+00	-0.6027362789131288D+01
2	-0.8161078603294609D+00	0.6027362789131288D+01
3	-0.4888984254503823D+01	0.0000000000000000D+00
4	-0.4314690614323917D+00	0.2281844295007351D-02
5	-0.2003087512600324D+00	0.0000000000000000D+00
6	-0.2150423998650362D+00	0.0000000000000000D+00
7	-0.1000127856222936D+00	0.4030307367457476D-02
8	-0.2532307050510290D-01	0.0000000000000000D+00
9	-0.1729322606608031D-03	0.0000000000000000D+00
10	-0.9999999962747097D-01	0.0000000000000000D+00
11	-0.5000000000000000D+01	0.0000000000000000D+00
B. Zeroes		
1	0.6594037552966448D+02	0.0000000000000000D+00
2	-0.6922348150124941D+01	-0.1818512956169113D+01
3	-0.6922348150124941D+01	0.1818512956169113D+01
4	-0.3656658346498506D+01	0.0000000000000000D+00
5	0.1538612815401276D+01	-0.2856448344664414D+01
6	0.1538612815401276D+01	0.2856448344664414D+01
7	-0.1316823892945096D+00	0.0000000000000000D+00
8	-0.1443983273816879D+00	0.0000000000000000D+00
9	-0.4422183469784892D-01	0.0000000000000000D+00

example, let it be assumed that it is desired to find the turbine mechanical shaft power change for a change in electrical frequency transfer function. Before the pole-zero deletion method can be used, five state variable transfer functions must be obtained. This is because the mechanical shaft power depends on state variable number 12, 13, 15, 16, and 19 as presented in Section III.2. Then after these transfer functions have been obtained, they must be algebraically combined into one polynomial and then the zeroes must be factored out again before pole-zero pairs can be deleted.

Another disadvantage to the pole-zero deletion method is that it is very easy to obtain the incorrect zeroes. This is due to the uncertainty in choosing the correct input parameter HCRIT. Often the resulting frequency responses and time responses appear to be correct, but they will still be incorrect. Therefore, it is necessary to have a backup method of obtaining frequency response and time response such as MATEXP[25] and SFR3[30] computer codes, so that the correct response is certain.

The system matrix of the 25th order model of Chapter III could not be rearranged so that the final values could be calculated by the REDUCE program for a power demand input signal. In addition, as has been previously pointed out, the turbine mechanical shaft power is calculated from five state variables. REDUCE has been written to calculate only one state variable response at a time. A recommendation for the improvement of the REDUCE program to handle this problem is given in Chapter V. Because of these problems, a transfer function of the turbine mechanical shaft power for a power demand input or electrical system frequency input could not be obtained in this study. However, this chapter has demonstrated the use of the pole-zero deletion method of system reduction.

CHAPTER IV

A COMPARISON OF HIGH AND LOW ORDER PHYSICAL MODELS

IV.1 Introduction

In Chapter III, two methods of reducing the high order model were presented. The first method was called the "physical method." This method resulted in reducing the 57th order PWR system model presented in Chapter II to a 25th order system model. The second method was called the pole-zero deletion method. This method was applied to the transfer function of fractional change in nuclear power for a change in electrical system frequency. This transfer function was originally a 23rd order model and it was found in Chapter III that it could possibly be reduced to a 9th order representation.

The reduced model by the pole-zero deletion method was compared to the original model in Chapter III by developing a three dimensional surface from time and frequency response calculations. As more pole-zero pairs were deleted, a point was attained where the reduced response no longer resembled the full order response.

The physically reduced model has not been compared to the high order model of Chapter II. The intent of this chapter is to compare the 25th order PWR system model of Chapter III with the 57th order PWR system model of Chapter II and make improvements on the low order model if possible. It is desired to have a low order model so that a simpler representation of the PWR system can be achieved.

IV.2 The Basis For Comparison

In order to compare the high order model with the physically reduced low order model, a choice must be made of the state variables and algebraic variables which are common to both models. In this study, the following variables were chosen as a basis for comparison

1. δP_M The change in turbine mechanical shaft power in units of megawatts
2. $\delta \rho_{ext}$ The reactivity change induced by the control rods in units of cents
3. $\% P_N$ The percent of full nuclear power
4. $\% P_S$ The percent of full power delivered by the secondary fluid
5. δT_F The change in fuel temperature in degrees Fahrenheit
6. δP_S The change in steam pressure in units of psi
7. δW_{FW} The change in feedwater flow rate in units of lbm/sec
8. δW_S The change in steam flow rate in units of lbm/sec
9. $\delta \varepsilon/\varepsilon_o$ The fractional change in steam valve coefficient
10. δT_{FW} The change in UTSG inlet feedwater temperature in degrees Fahrenheit
11. δT_{CL} The change in cold leg temperature in degrees Fahrenheit
12. δT_{HL} The change in hot leg temperature in degrees Fahrenheit
13. δP_C The change in the integral of the ACE signal in units of puMw-sec
14. δF The change in electrical system frequency in Hz
15. δT_{HP} The change in the high pressure turbine torque in units of ft-lbf
16. δT_{LP} The change in low pressure turbine torque in units of ft-lbf

In all the figures of this chapter, the high order model response is represented by a solid line. The low order model response is represented by + characters.

IV.3 Discussion of Figure 4.1 and Figure 4.2

The first case presented will be for a -0.05 puMw (-50 Mw) step in the power demand signal. Figure 4.1 shows the response of the 16 basis variables of both the high order and low order models for a -0.05 puMw step in power demand. The solid line in Figure 4.1 is identical with the results shown in on page 120 and the line designated by crosses is identical with the results shown in Figure 3.2.

The turbine shaft power appears to attain the desired power change of 50 Mw almost immediately. A more detailed look at the first 20 seconds of the turbine power is shown in Figure 4.2. It appears that both the high order and low order model give the same result for the turbine power. This is plausible since both models contain the same turbine representation. However, the effect of steam pressure upon the turbine model will be different for the two models.

The control rod reactivity is very different in the two models. This is primarily due to the nonlinear reactor control system representation in the high order model. The high order reactor controller stops moving the rods after the reactivity is reduced by 7.560 cents. This is because the temperature error signal has fallen within the deadband. The low order reactor controller, on the other hand, will remove reactivity until the temperature error signal is zero.

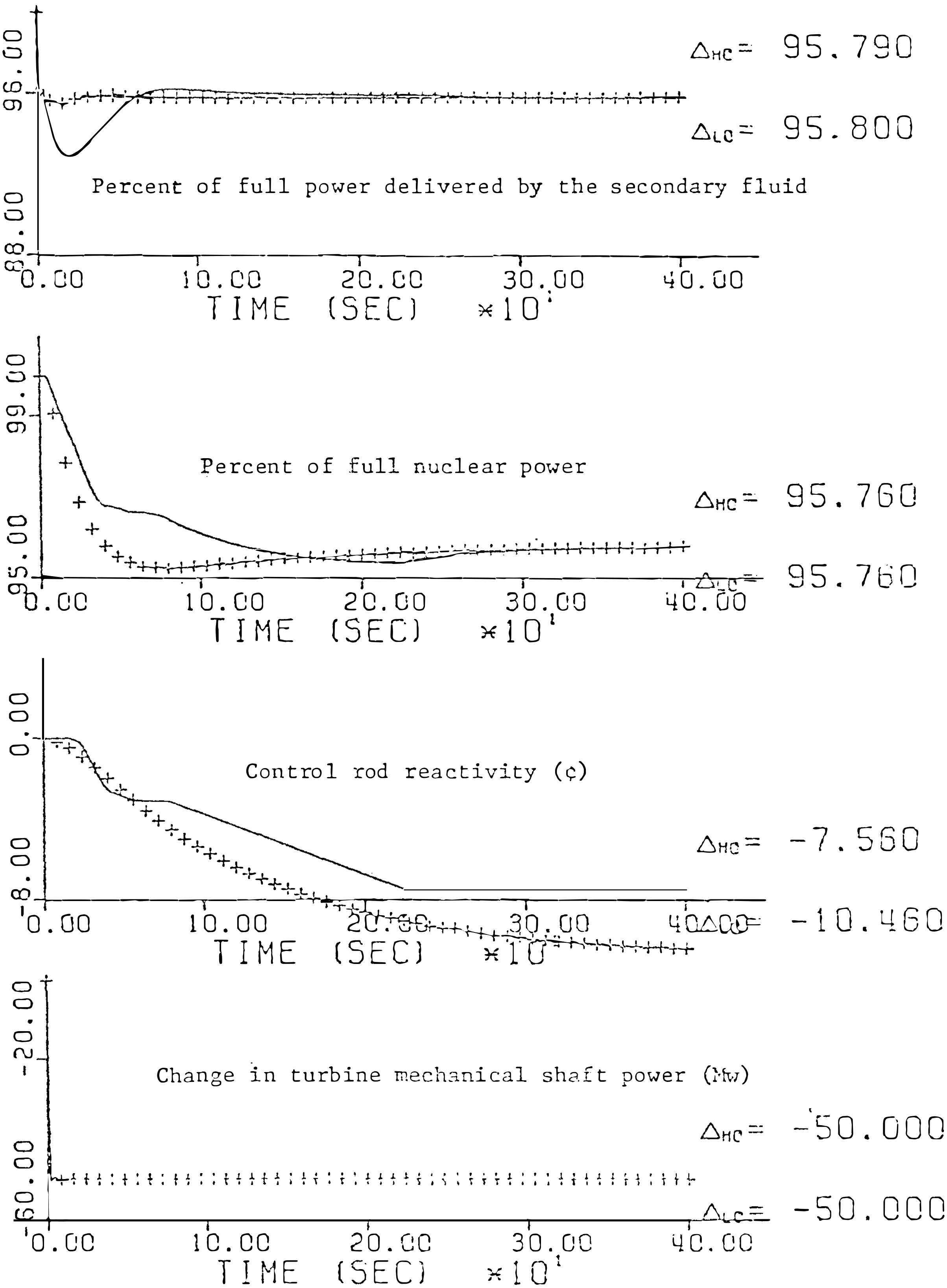

Figure 4.1 Response of high and low order models for a -0.05 puMw step in power demand.

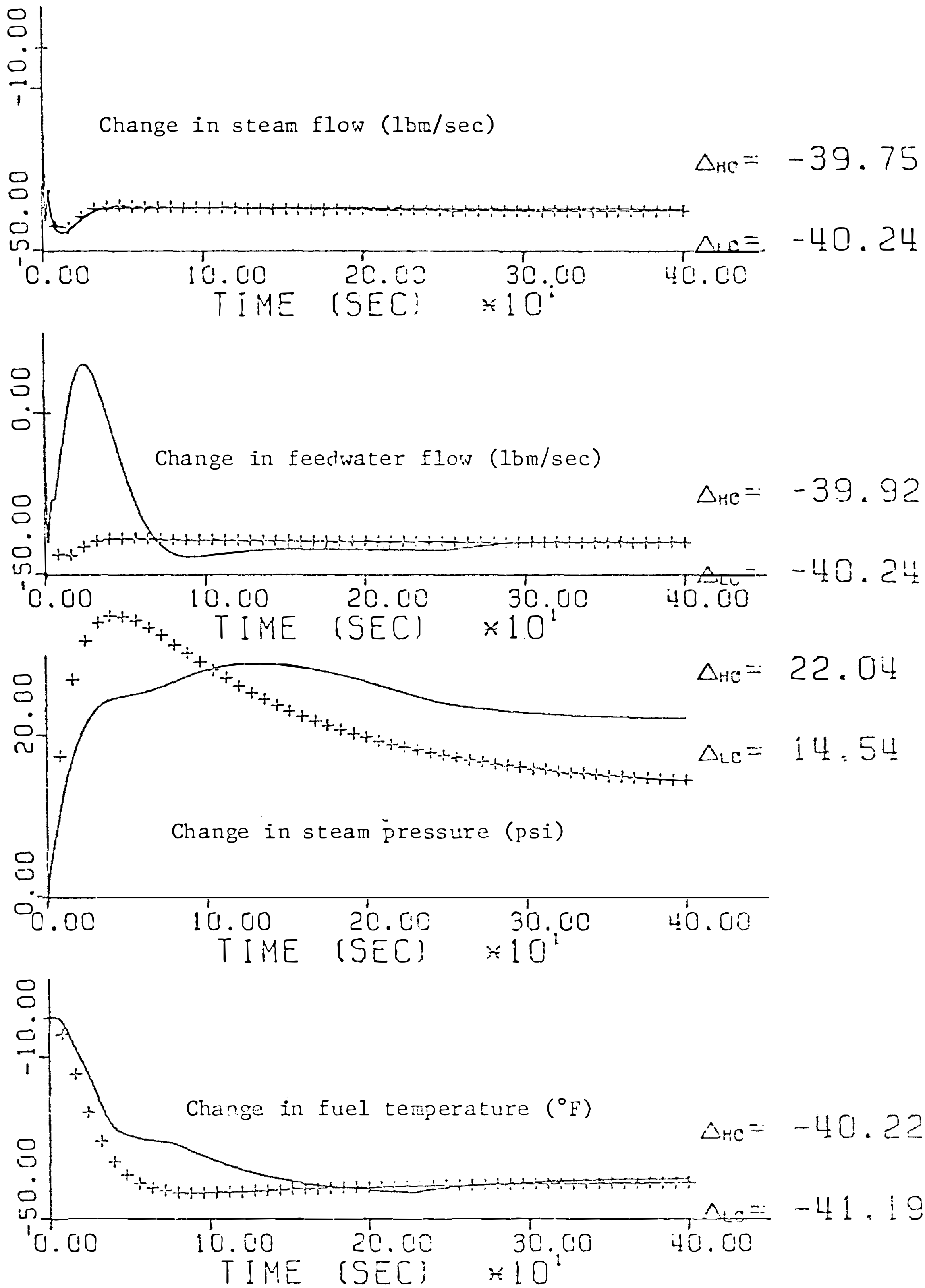

Figure 4.1 (continued)

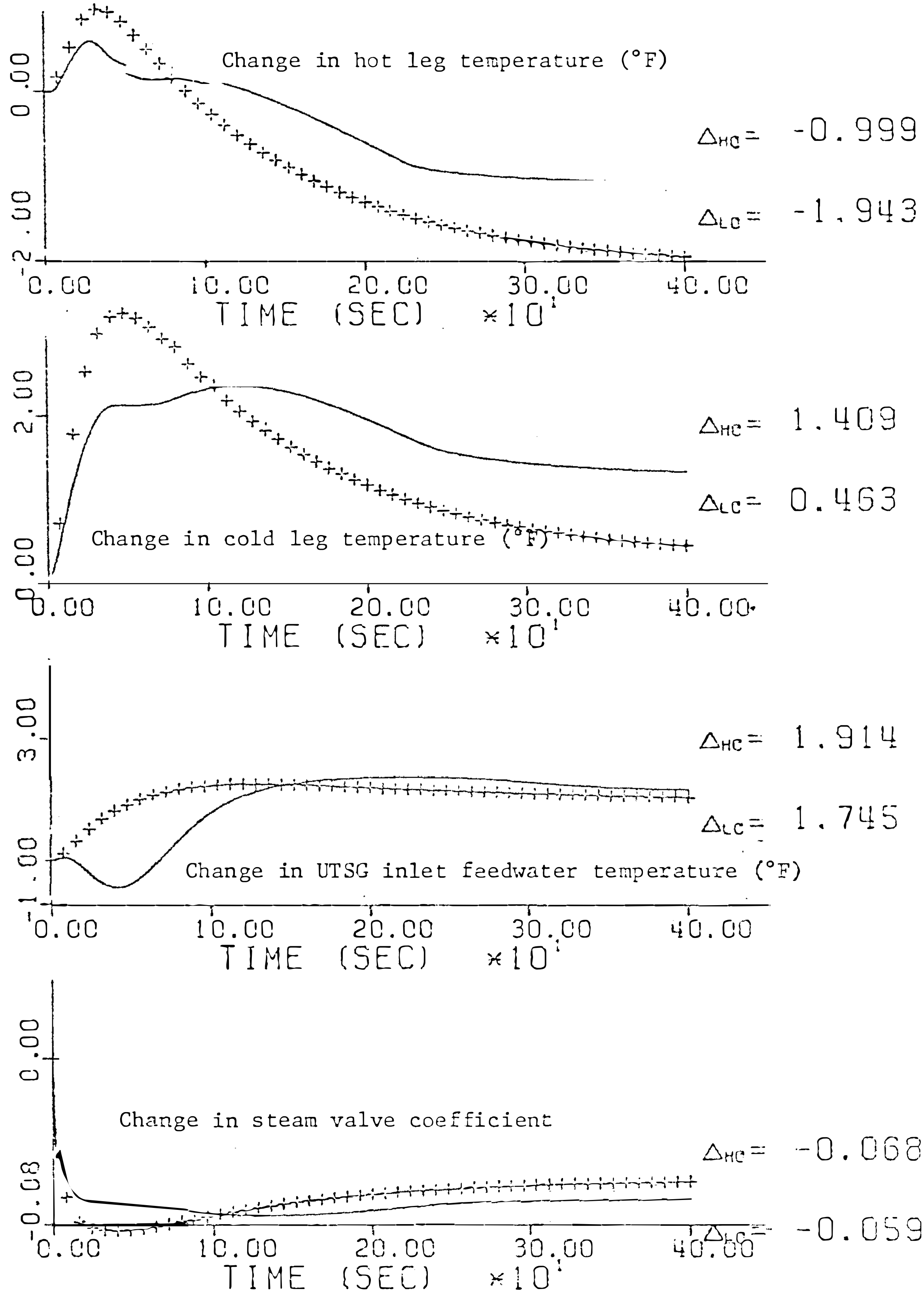

Figure 4.1 (continued)

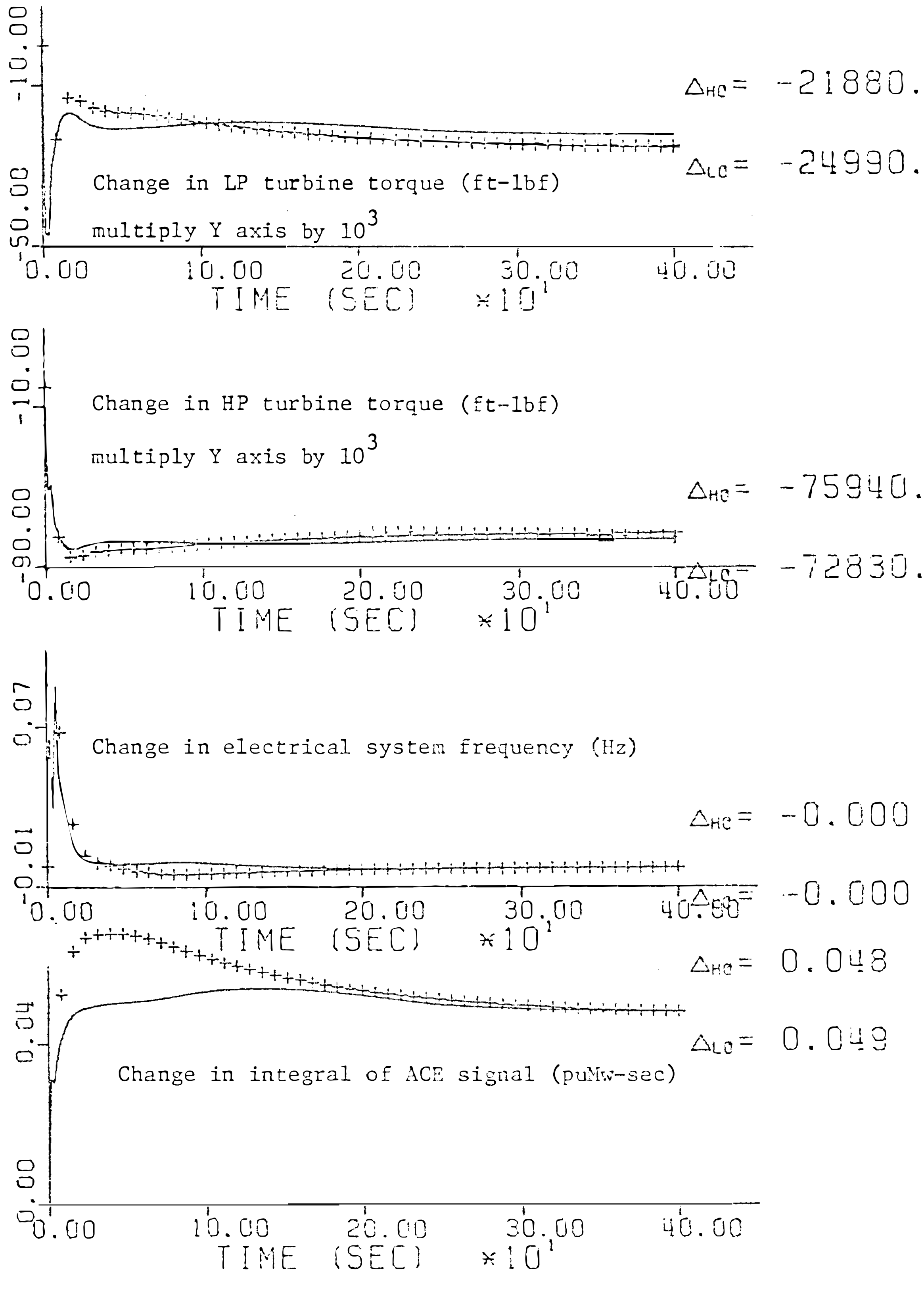

Figure 4.1 (continued)

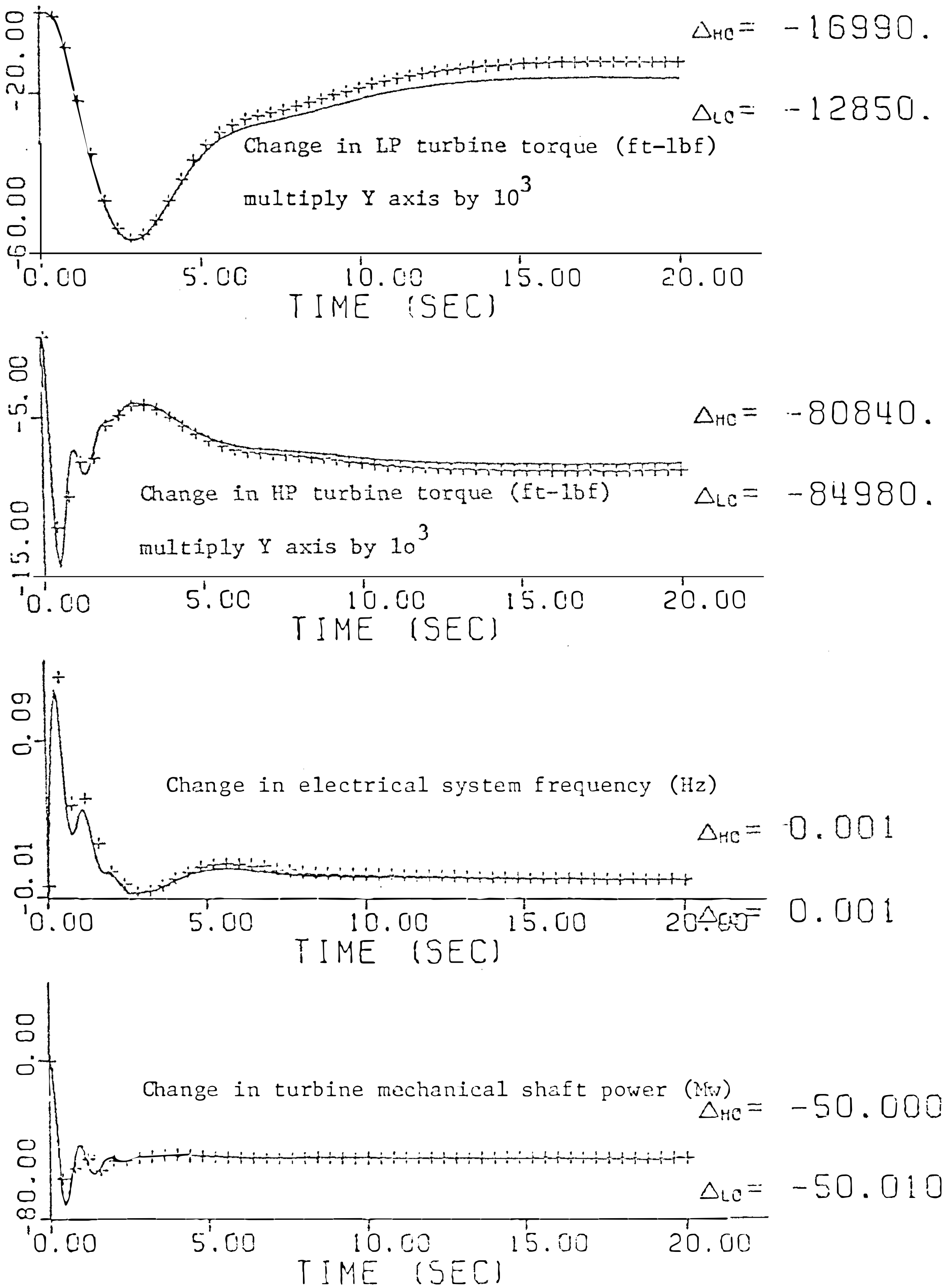

Figure 4.2 First twenty seconds of Figure 4.1.

The percent of full nuclear power response of the low order model is much "smoother" than that of the high order model. This is primarily due to the nonlinear reactor controller of the high order model.

The percent of full power delivered to the secondary fluid response for the low order model is almost identical to the high order model response. The main difference is during the first 100 seconds of the response. The "dip" in the high order response is due to the feedwater flow. This dip arises due to the downcomer level error signal (see Figure 2.10 page 30). Thus the assumption of perfect feedwater flow control for the low order model will not account for changes in controlled feedwater flow due to changes in downcomer level. This will ultimately affect the reactor control system since the percent of full power delivered to the secondary fluid is an input to the reactor control system.

The fuel temperature response for the low order model is very similar to the high order model response. Any inconsistency is again primarily due to the nonlinear reactor control system of the high order model.

The steam pressure response for the low order model is different from the high order model response. This can be attributed to the nonlinear control system of the high order reactor controller, and the Pf controller. The low order model reactor controller is different from the high order model reactor controller because it will drive the average reactor coolant temperature more toward the average temperature set point. This means that if the average reactor coolant temperature is more negative (which it is in this case), the steam pressure deviation will ultimately be less positive at steady state. However, during the transient, the steam pressure inconsistency is largely due to the different rates of reactivity change of the high order model, whereas the low order model has a single rate of reactivity change. The Pf controller will also affect the steam pressure. The output of the Pf controller is the fractional change in the steam valve coefficient. In this case, the fractional change in valve coefficient is larger for the low order model than the high order model during the first 100 seconds of the response. The high order model response of fractional change in valve coefficient becomes greater than the low order model response after approximately 100 seconds. This will cause the response of steam pressure to be greater for the low order model during the first 100 seconds than the high order model response. After approximately 100 seconds, the high order response of steam pressure then becomes greater than the low order model response. Further discussion of the effect of the valve coefficient will follow.

The feedwater flow difference during the first 100 seconds has already been attributed to the assumption of perfect feedwater flow, which does not consider downcomer level deviation as part of the feedwater flow control.

The steam flow rate response for the low order model is very similar to the high order model response. This can be attributed to the Pf controller. The Pf controller will force the steam flow to achieve the desired power level out of the turbine. Because the turbine representation is the same for both models, the steam flow change must be the same to achieve the same turbine power change.

The change in steam valve coefficient is very close for both models. The difference arises from the fact that the steam flow is the same for both cases. The steam flow is proportional to steam pressure and steam valve coefficient (equation II.24). Because the low order model steam pressure deviation is smaller at steady state, the low order model steam valve coefficient deviation must be greater at steady state in order to obtain the same steady state steam flow rate. Notice that the steam pressure deviation for both high and low order models intersect at approximately 100 seconds. Because the steady state steam flow has already been obtained by this time for both models, the steam valve coefficient deviation for both high and low order models should also intersect at approximately 100 seconds.

The inlet UTSG feedwater temperature response for the low order model is similar to the high order model except during the first 100 seconds. This can be attributed to the perfect feedwater flow control assumption of the low order model.

The average temperature deviation of the hot and cold leg for the low order model is approaching the average temperature set point. The average temperature deviation of the hot and cold leg for the high order model will not reach the average temperature set point because of the deadband of the high order model reactor control system.

The integral of the ACE signal response and the electrical system frequency response is almost identical for both the high order and low order models. This is plausible since the representation for the integral of the ACE signal and electrical system frequency is almost identical for both high and low order models. The only difference between the two being the representation of the turbine mechanical shaft power which may be different due to the fact that steam pressure is an input to the turbine model.

The high pressure and low pressure turbine shaft torque response is very close for the high and low order models. Any differences can be attributed to the differences in steam pressure for both models. This is the reason for the intersection of the curves again at approximately 100 seconds. One interesting note is that the turbine shaft torques take almost the full 400 seconds to reach steady state, while the total turbine shaft power (which is the sum of the torques multiplied by a constant) is at steady state after only a few seconds.

Figure 4.2 also shows the response of both the high order and low order models for a -0.05 puMw step in power demand. However, only the first 20 seconds are shown for the turbine shaft power, the electrical system frequency, and the high and low pressure turbine torques. From Figure 4.2, the early part of the transient experiences an oscillatory motion that was not apparent from Figure 4.1. However, the responses of both the high and low order models is almost identical. A small difference between the responses exist for the high and low pressure turbine torques. This again can be attributed to the differences between the steam pressure and steam valve coefficient responses as shown in Figure 4.1. However, the first 5 seconds of the response of the torques is almost identical since the effect of steam pressure has not been felt.

IV.4 Discussion of Figure 4.3

Figure 4.3 shows the response of the 16 basis of comparison variables for both the high order and low order model for a -0.1 step

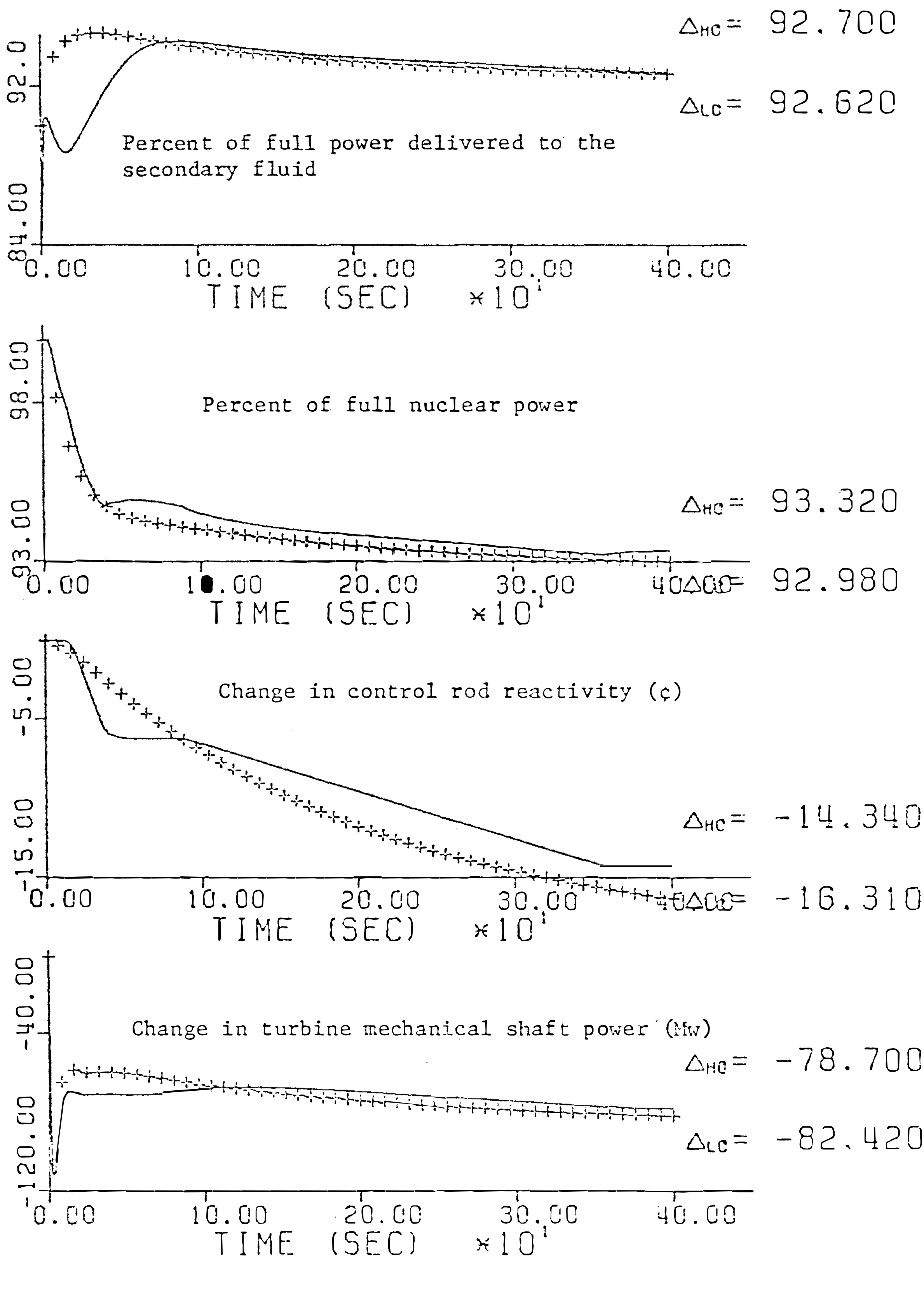

Figure 4.3 Response of the high and low order models for a -0.1 step in steam valve coefficient with Pf controller decoupled.

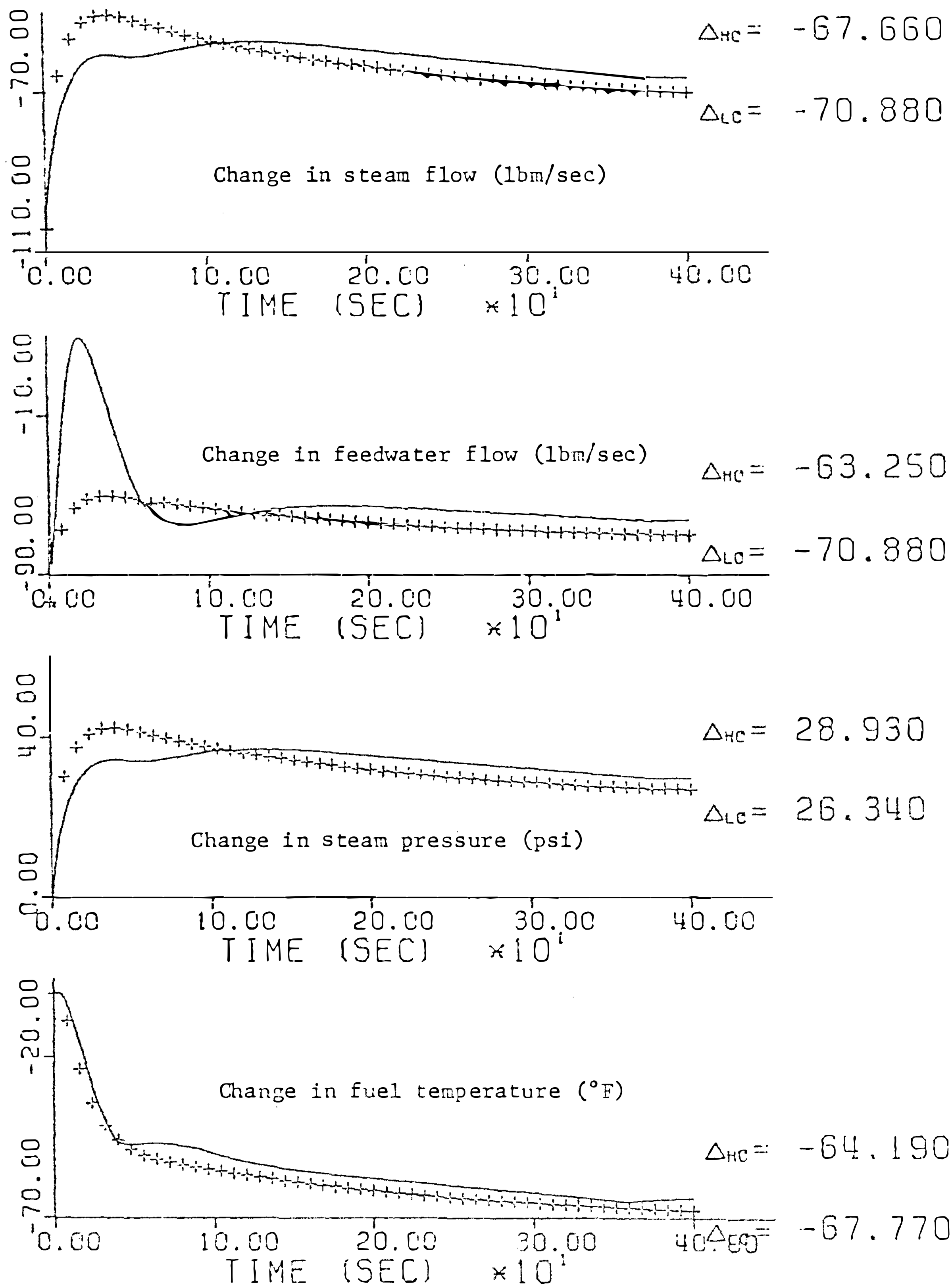

Figure 4.3 (continued)

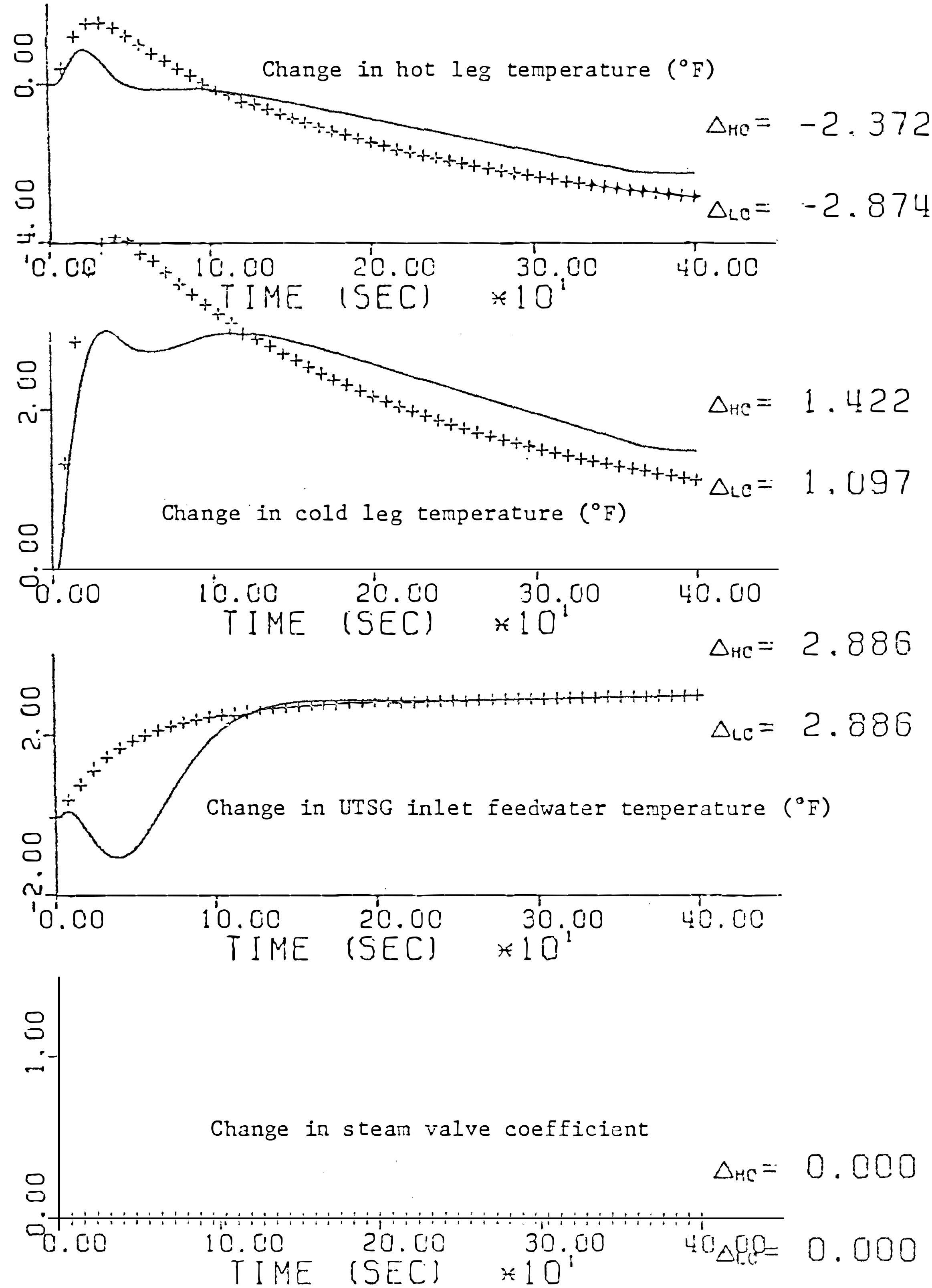

Figure 4.3 (continued)

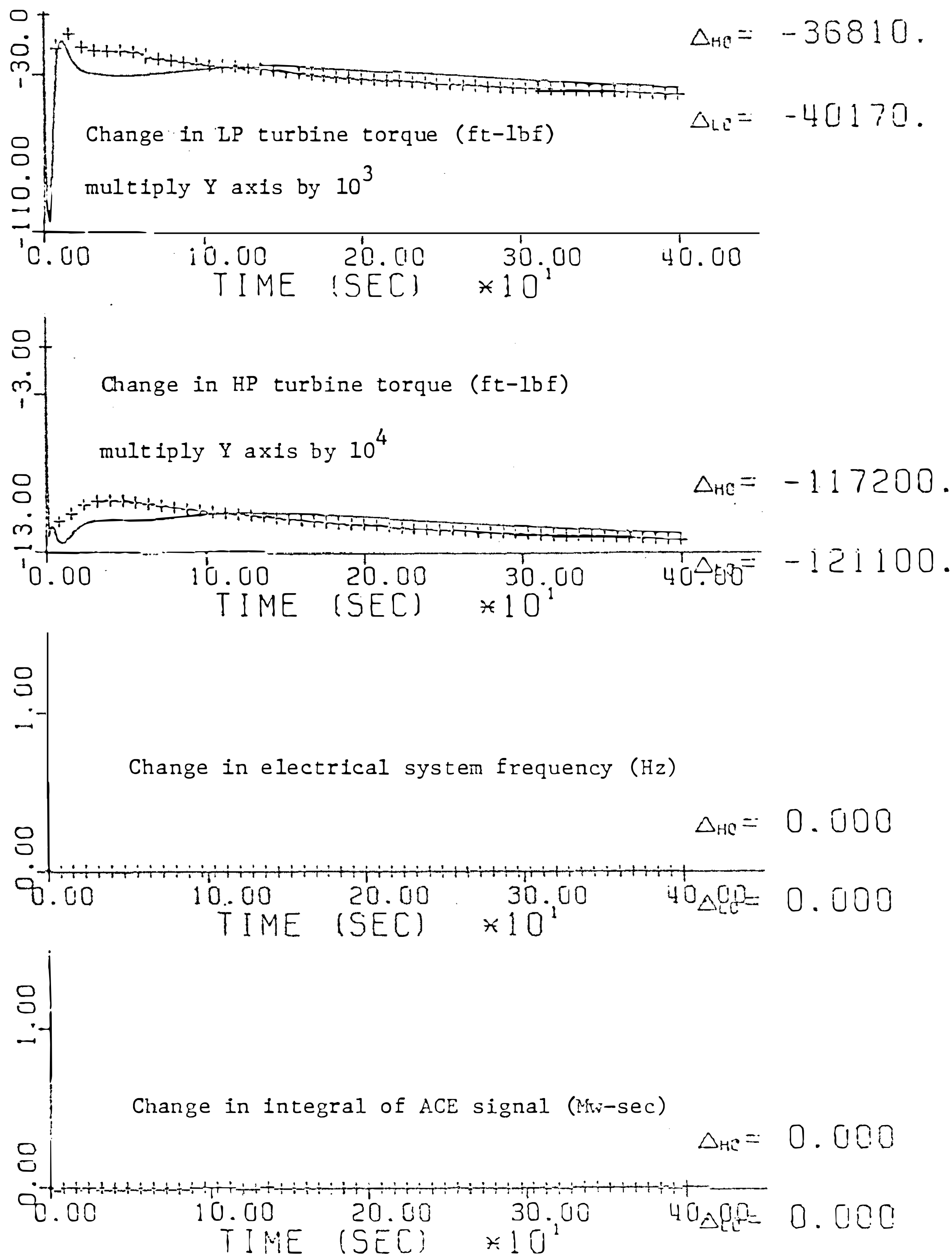

Figure 4.3 (continued)

in fractional steam valve coefficient. In order to obtain Figure 4.3 the following steps were taken

1. Decouple the Pf controller of the high order model by setting the matrix coefficients (55,55) (55,56), and (55,57) equal to zero.
2. Decouple the Pf controller of the low order model by setting the matrix coefficients (23,23), (23,24), and (23,25) equal to zero.
3. Form the forcing vector of the high order model for a unit change in steam valve coefficient. This vector will be identical to matrix coefficients (i,55) for i=1 through 57. Multiply this vector by -0.1 to obtain the forcing vector for a -0.1 step in steam valve coefficient.
4. Form the forcing vector of the low order model for a unit change in steam valve coefficient. This vector will be identical to matrix coefficients (i,23) for i=1 through 25. Multiply this vector by -0.1 to obtain the forcing vector for a -0.1 step in steam valve coefficient.

Referring to Figure 4.3, one sees that the turbine shaft power is not controlled by the Pf controller. Therefore, the turbine power results are slightly different in the high and low order models. The valve coefficient change is the same for both the high order and low order models because it is the forcing function. Since the steam flow to the turbine is proportional to both steam valve coefficient and steam pressure, any differences in turbine shaft power can be attributed to steam pressure.

The response of the reactivity change due to the control rods for the low order model is different from the high order model. This can be attributed, as in Figure 4.1, to the nonlinear reactor control system of the high order model.

The percent of full nuclear power responses from the high and low order models agree well. Only slight differences in the shape of the curves arise because of the different reactor control system representations.

The percent of full power delivered by the secondary fluid response is slightly different between high and low order models during the first 100 seconds of the response. This can be attributed, as in Figure 4.1, to the perfect feedwater flow assumption of the low order model.

The fuel temperature response from the high and low order models also agree well. Again only slight differences in the shape of the curves are present which is primarily due to the nonlinear reactor control system of the high order model.

The steam pressure response is a closer match in this case than in Figure 4.1. Therefore the Pf controller is responsible for a larger portion of the differences of the steam pressure response of Figure 4.1. However, there is still a slight difference between the high and low order model responses. This again can be attributed to the reactor control system since the low order model reactor control system will cause a larger change in the average reactor coolant temperature.

The feedwater flow, as in Figure 4.1, has some slight differences during the first part of the transient. However, in this case the steady state response will also be different. Because the Pf controller has been decoupled, the steam flow will not be controlled. Therefore, it is possible for the steam flow to obtain different values at steady state. This would depend on the steady state value of the steam pressure. Since the feedwater flow rate must be equal to the steam flow rate at steady state, this explains the difference of the high and low order model response of feedwater flow rate at steady state.

The steam flow rate is different in the high and low order models at steady state. This can be attributed to the fact that steam pressure is also different in the high and low order models, and the steam valve coefficient is the same for both models.

The steam valve coefficient response is equal to zero since the Pf controller has been decoupled from the system. The forcing function in this case is a -0.1 step in steam valve coefficient.

The feedwater inlet temperature to the UTSG has a very close match between the high and low order response in this case. The difference in the early part of the transient is due to the perfect flow assumption of the feedwater control system in the low order model.

The average temperature of the hot and cold leg temperatures, as in Figure 4.1, will be closer to the temperature set point in the low order model case. Notice also that the transient peaks of the hot and cold leg temperatures are smaller in the high order model response. This means that the nonlinear reactor control system will cause a reduction in the transient peaks.

The integral of the ACE signal and the electrical system frequency responses will be zero since the Pf controller has been decoupled.

The high pressure and low pressure turbine torques are very close to one another for this case. Any differences in this case can be attributed solely to the steam pressure differences.

IV.5 Discussion of Figure 4.4

In Figure 4.1 through 4.3, the differences between the high and low order model responses have been attributed to the reactor control and Pf controller systems. In Figure 4.3, the Pf controller was decoupled and resulted in a closer response between the high order and low order model. Now it is desired to examine the effect of decoupling the reactor control system (or in the nonlinear case "turning off the reactor control system"). This can be accomplished very easily. For the high order model the reactor control system can be "turned off" by using the value of 4 for the input parameter NTYPE in the SYSTEM-MATEXP program (see Appendix A). For the low order model, the reactor control system is decoupled by setting matrix coefficient (1,11) equal to zero.

Figure 4.4 shows the response of the high and low order models for a -0.1 step in the steam valve coefficient. This is identical to Figure 4.3 except the reactor control system has been decoupled ("turned off") for both the high and low order models. Therefore the Pf controller and reactor control system are both not used in this case. The only remaining control systems are three element control of feedwater flow on the high order model, perfect control of the feedwater flow on the low order model, and pressurizer pressure control on the high order model.

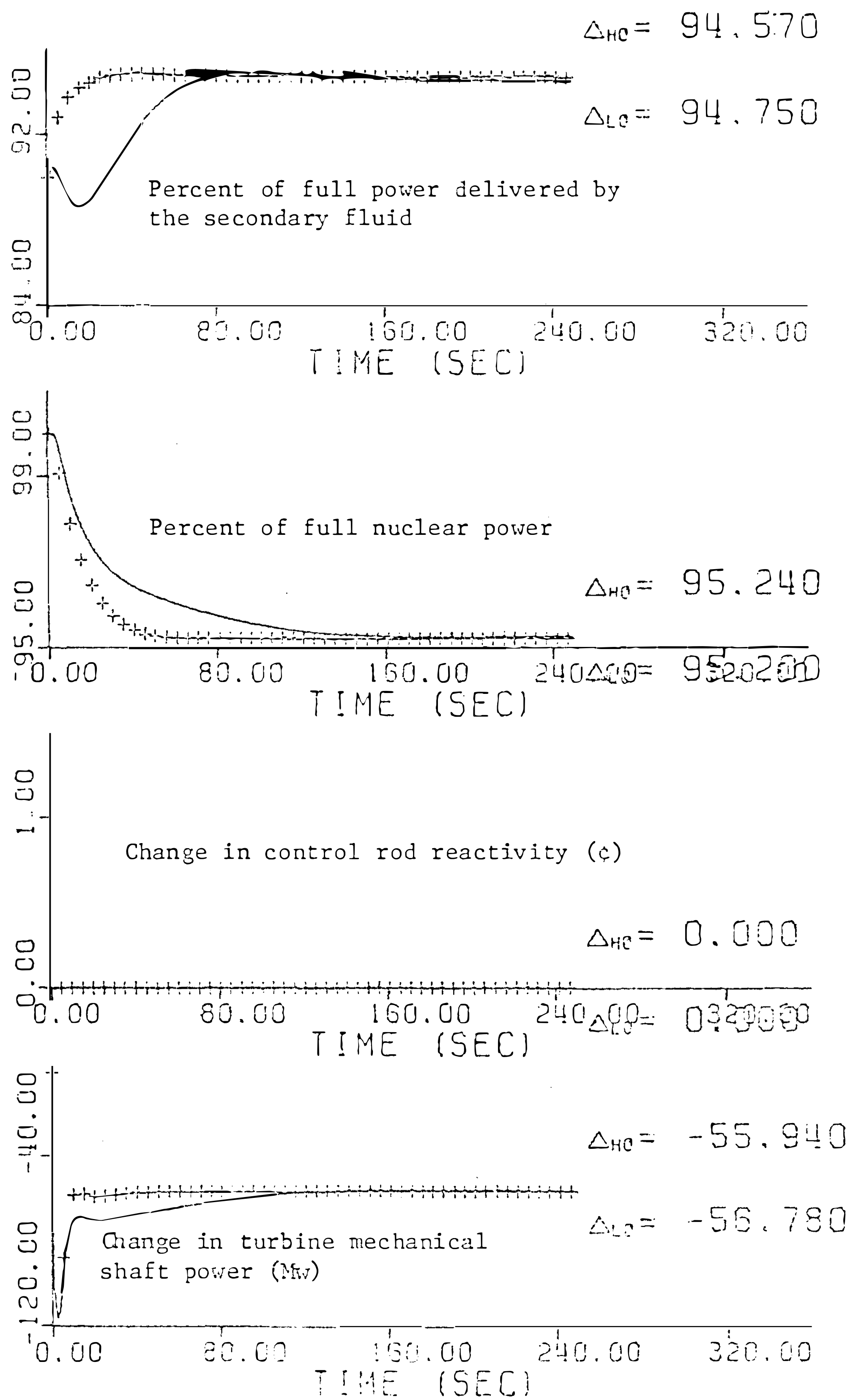

Figure 4.4 Response of high and low order models for a -0.1 step in steam valve coefficient with Pf and reactor controllers decoupled.

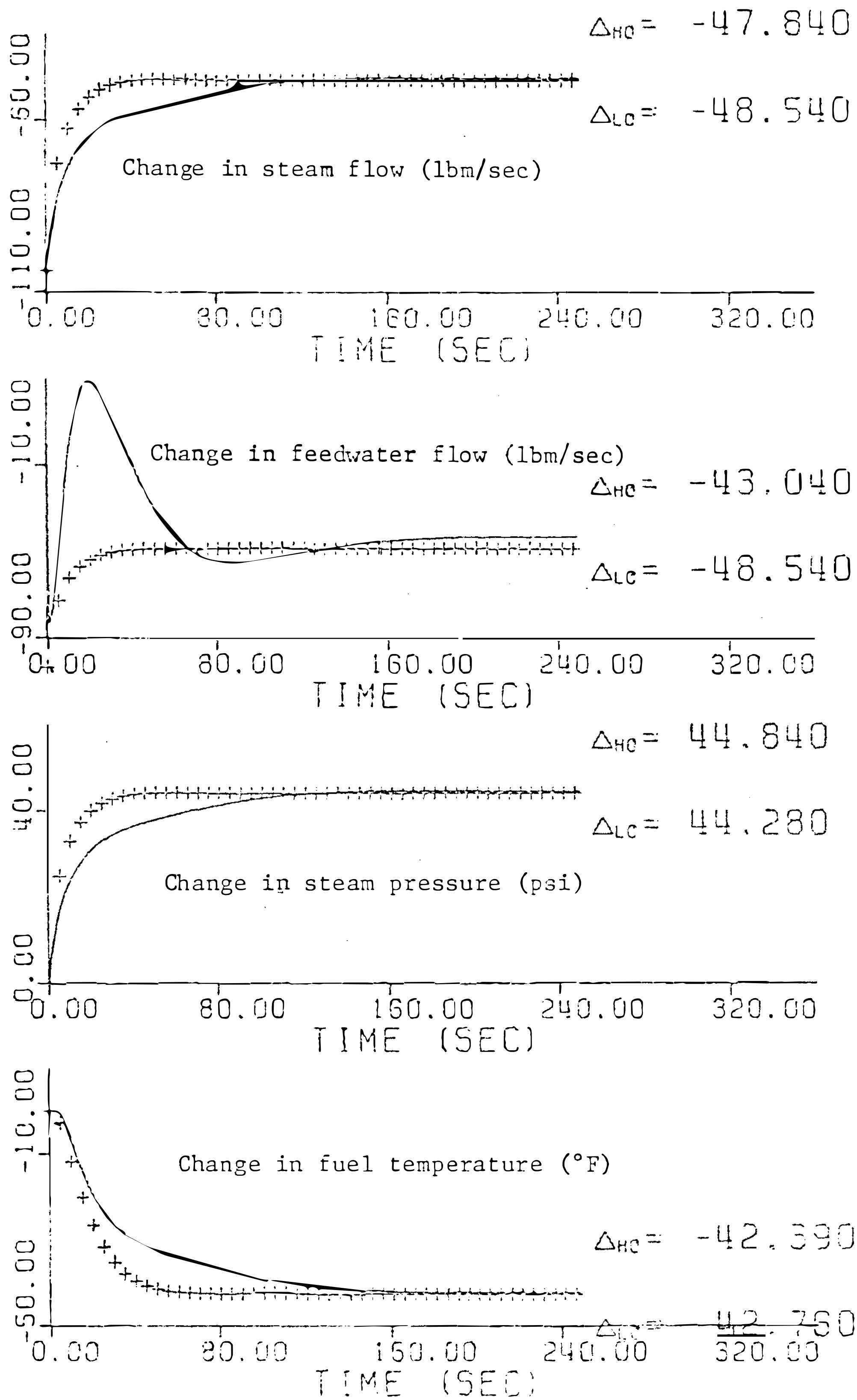

Figure 4.4 (continued)

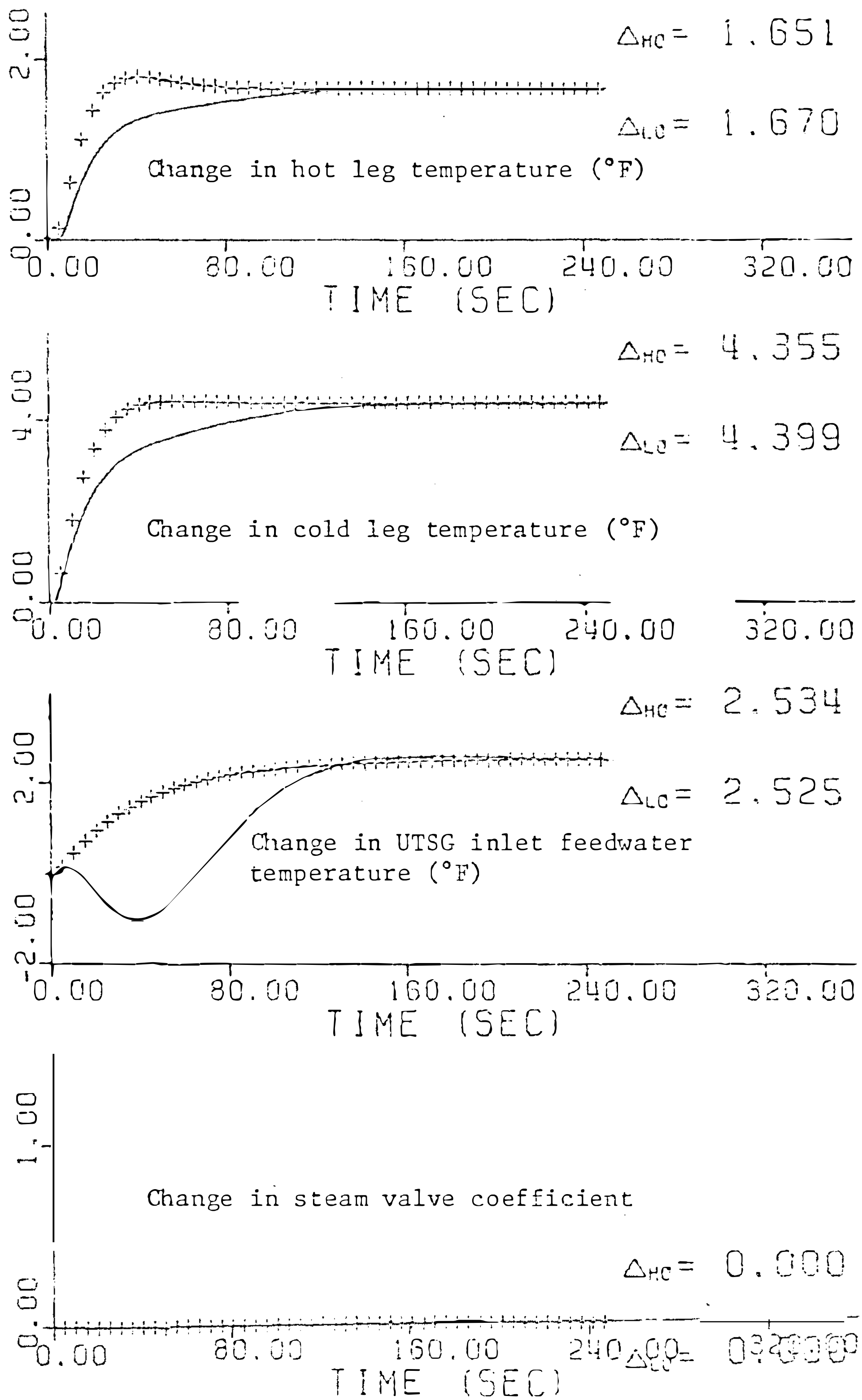

Figure 4.4 (continued)

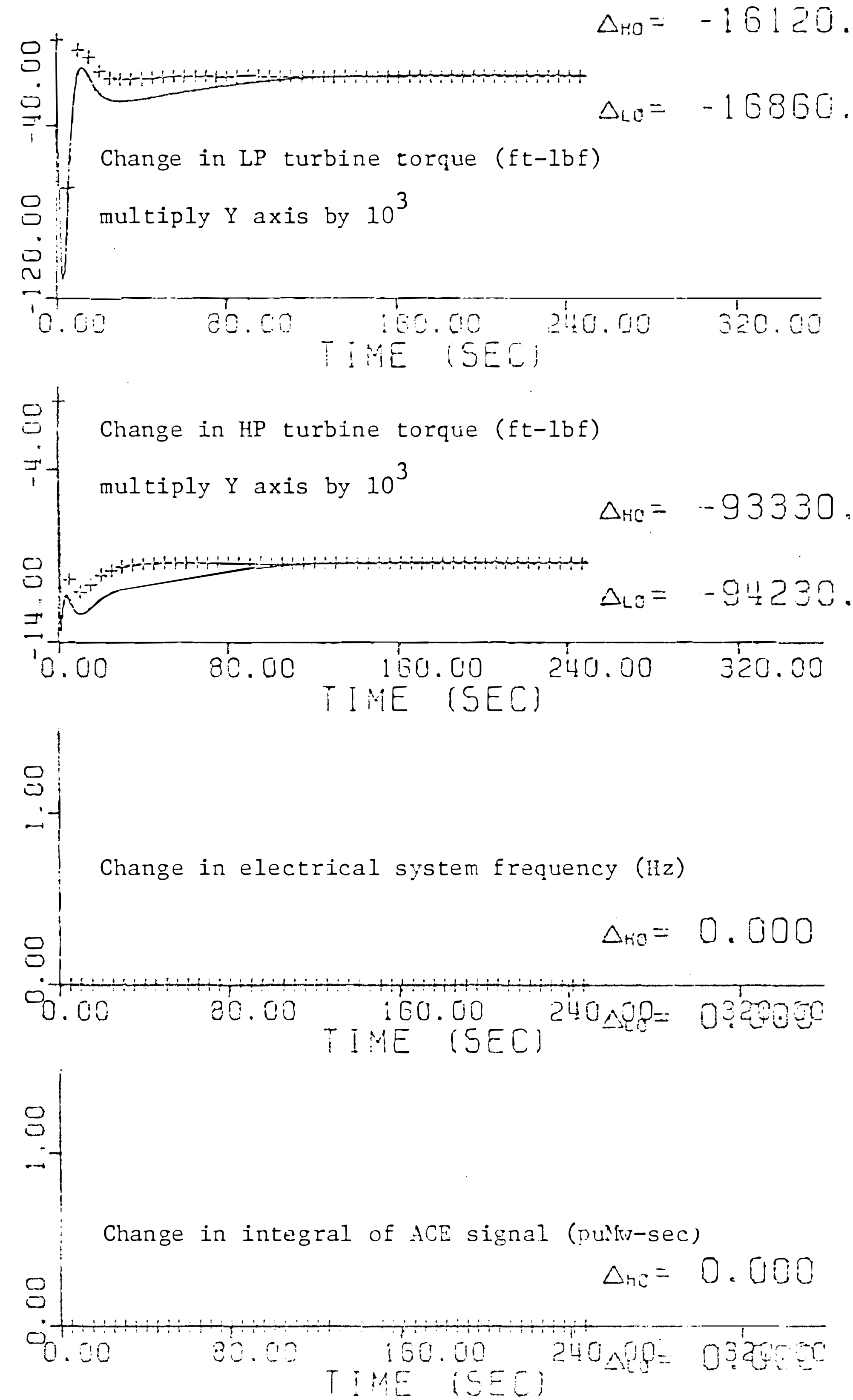

Figure 4.4 (continued)

Referring to Figure 4.4, one sees that all the responses of the 16 basis variables from the high and low order models at steady state are in good agreement. Some differences still exist during the early part of the responses due to the perfect feedwater flow control assumption of the low order model. In addition, because the equations of the low order reactor core and UTSG model are "more lumped," the detailed dynamic effects of the early part of the transient are not as good for the low order model. This is consistent with work done previously (see Ali[2]).

IV.6 Discussion of Figure 4.5

At this point the following question must be asked, "Is there anything that can be done to make the overall low order PWR system model response agree more with the overall high order PWR system model response?" The Pf controller model used in the low order model is exactly the same as the high order model. The only difference between the two Pf controller models is the value of the turbine gain constant K_T. This constant was determined from the steady state response of the turbine mechanical shaft power for a change in valve coefficient forcing function (see Section II.7 and Section III.2).

Let it be assumed that the turbine gain constant is not the main cause of the differences in the high and low order models. Let it also be assumed that the differences of the high and low order models is largely due to the reactor control system. This is plausible since there is a large difference in the representation of the reactor control system of the high and low order models (nonlinear vs. linear).

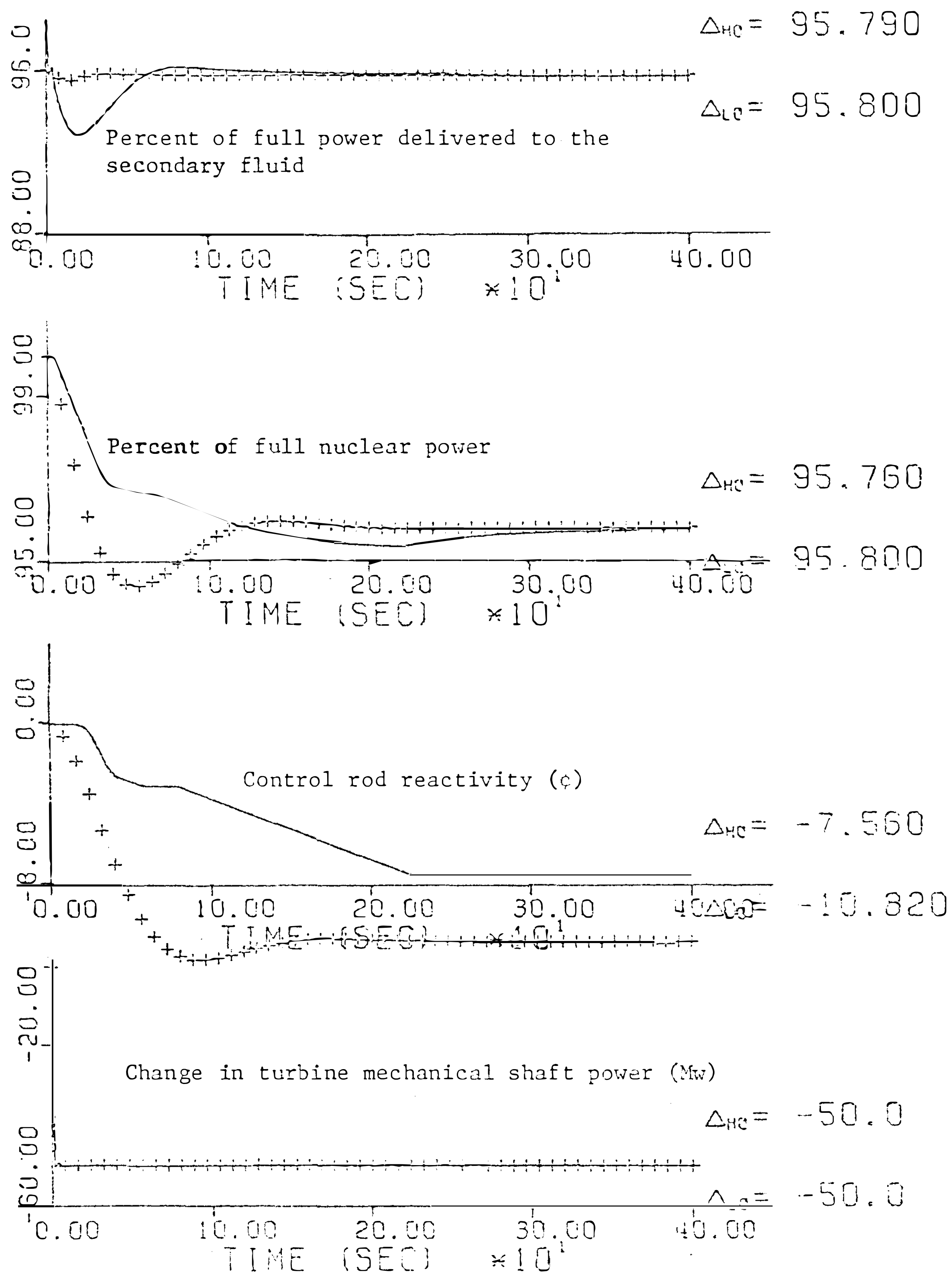

Figure 4.5 Response of high and low order overall PWR system models for a -0.05 puMw step in power demand with the gain of the low order reactor controller multiplied by 4.0.

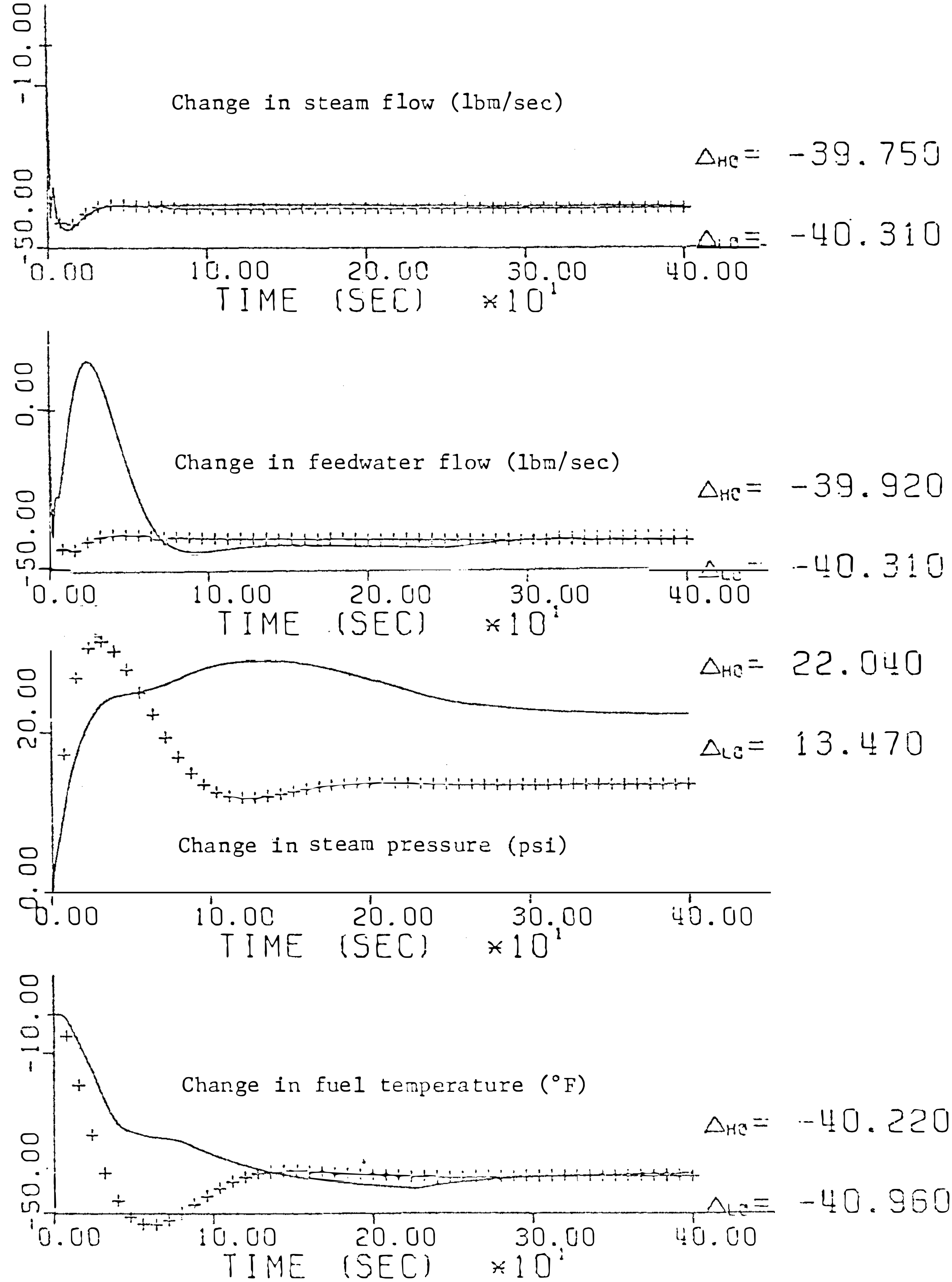

Figure 4.5 (continued)

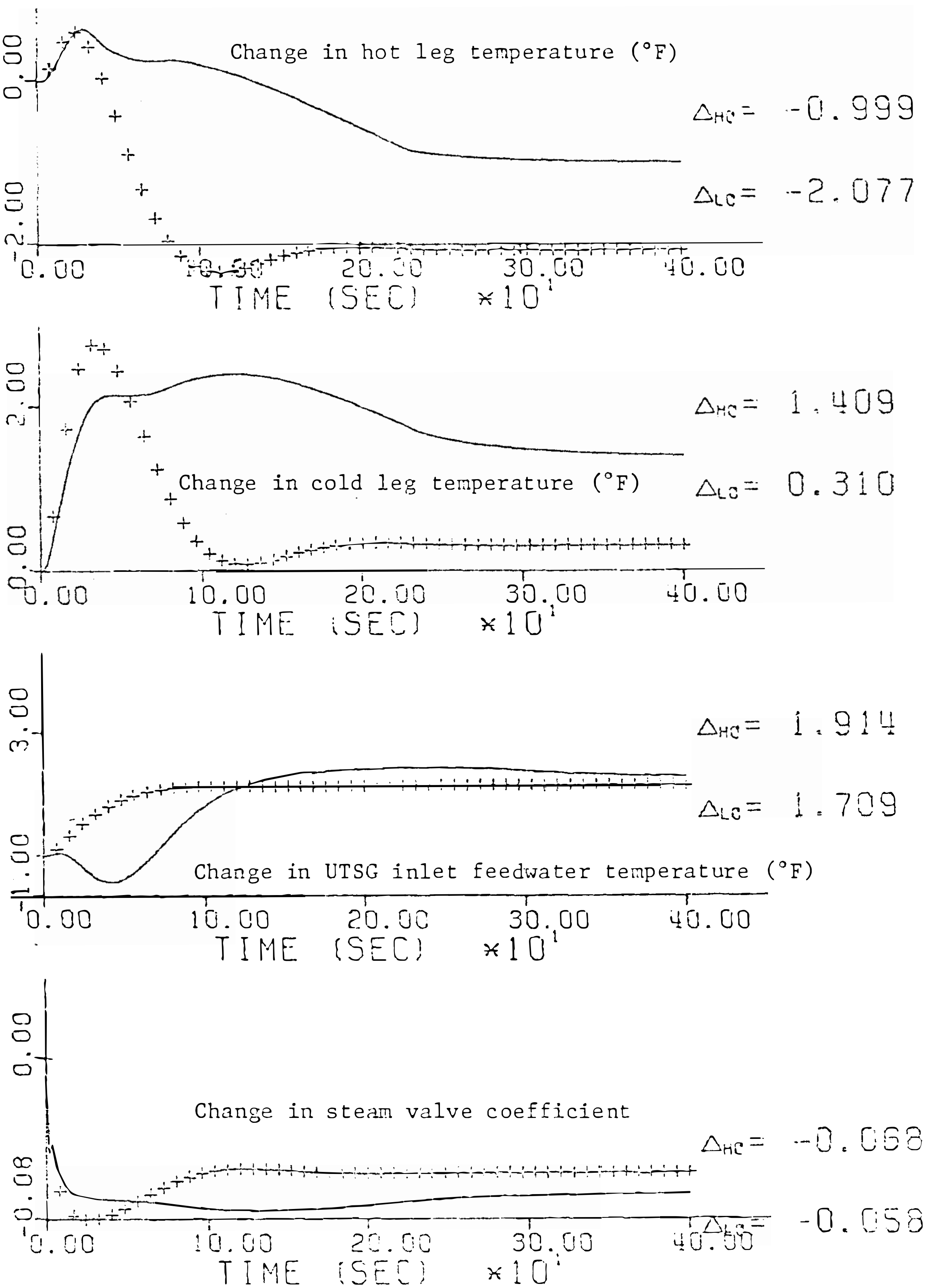

Figure 4.5 (continued)

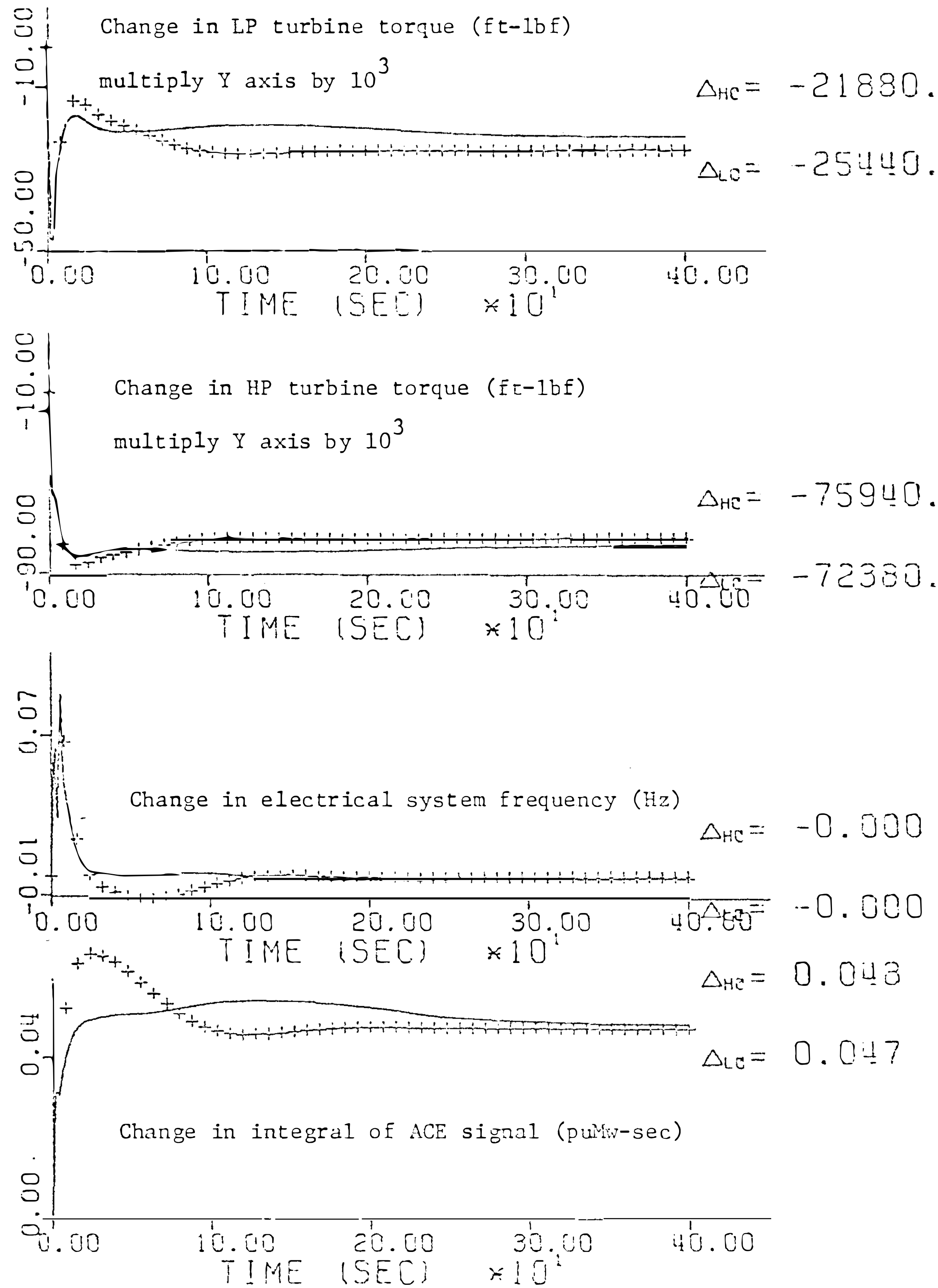

Figure 4.5 (continued)

Therefore, the low order reactor control system model will be changed to attempt to improve the agreement. Recall that the gain of the low order reactor control system model was described by the following equation

(IV.1) $K = K' \times K''$

The value of K" was set equal to 0.1 (steps/sec-F) while the value of K' was defined to be identically equal to the high order model value of ROWSTP. In this thesis, the value of ROWSTP used is 0.00225 (dollars/°F-sec). For this case, K^1 will be multiplied by 4.0. The criterion for choosing this number is to increase the rate at which the control rod reactivity will come to steady state.

Figure 4.5 is identical to Figure 4.1 on page 173 except the gain on the low order reactor control system model has been changed. The result of this change was to multiply row 11 of the low order system matrix by 4.0

Referring to Figure 4.5, one sees that the response of the low order model 16 basis variables of comparison have about the same steady state values as those shown in Figure 4.1. Therefore, it must be concluded that no matter what gain is used in the low order reactor controller, the steady state value of control rod reactivity, and thus steam pressure, will be the same. The only effect that a change in the value of K" will have is the rate at which the new steady state value is reached. This is why the response is oscillatory in Figure 4.5. This is plausible since the low order model reactor control system will always bring the average temperature to the average temperature set point. The average temperature set point for a given power level change will always be the same, therefore the average temperature change will always be the same for a given power level change due to the reactor control action.

Therefore, it is concluded that no improvement can be made on the steady state value of the control rod reactivity for the low order model. However, a change in the gain of the low order model reactor control system could improve on the shape of the response and more closely match the high order model response.

CHAPTER V

CONCLUSIONS AND RECOMMENDATIONS

Assuming that the Pf control system is coupled, the 25th order overall PWR system model will predict the turbine mechanical shaft power equally as well as the 57th high order overall PWR system model. If other output variables of the system are of interest, such as steam pressure, or steam valve coefficient, some small differences exist between the two models. This is primarily due to the nonlinear reactor control system of the high order model.

The pole-zero deletion method can be used for the reduction of the order of the system model. There are some disadvantages to using this method. The system matrix must be in a form such that the final values of the desired state variables can be calculated. The REDUCE program as written produces and reduces only one transfer function at a time. It may be desired to reduce the order of an output variable which is a function of more than one state variable. For example, the mechanical turbine shaft power is a function of five state variables (see Appendix D).

As a possible continuation of this research, the REDUCE program could be modified to handle this multi-state variable problem. Let j be the number of state variables needed to determine some desired output variable y(s). Then the following equation can be written

$$y(s) = \sum_{i=1}^{j} A_i \frac{\left[K \prod_{k=1}^{m} (s - z_k)\right]_i}{\left[\prod_{\ell=1}^{n} (s - p_\ell)\right]_i} = \sum_{i=1}^{j} A_i X_i(s) \tag{V.1}$$

where

A_i = constant coefficient

K_i = gain for the X_i transfer function defined by Equation (III.23)

z_{k_i} = zeroes for the X_i transfer function defined by Equation (III.20)

= poles for the X_i transfer function defined by Equation (III.20)

m_i = the total number of zeroes for the X_i response

n_i = the total number of poles for the X_i response

The poles of each state variable X will be the same. Thus equation (V.1) can be written as

$$Y(s) = \frac{\mathbb{K}}{\prod_{l=1}^{n}(s-p_l)} \sum_{i=1}^{j} A_i \prod_{k=1}^{m}(s-z_k)_i \tag{V.2}$$

where

$$\mathbb{K} = \prod_{i=1}^{j} K_i$$

The product term in the numerator of equation (V.2) can be combined so that equation (V.2) can be written as

$$Y(s) = \frac{\mathbb{K}}{\prod_{l=1}^{n}(s-p_l)} \sum_{i=1}^{j} a_m s^m + a_{m-1}s^{m-1} + \dots + a_1 s + a_0. \tag{V.3}$$

Then the constant coefficients, a_m, of equation (V.3) having the same order as s can be combined to obtain

(V.4) $$y(s) = \frac{K}{\prod_{l=1}^{n}(s-p_l)}\left(b_t s^t + b_{t-1}s^{t-1} + \ldots + b_1 s + b_0\right)$$

where

t = maximum value of m_i for $i = 1, 2, \ldots, j$.

The solution to the polynomial

(V.5) $$b_t s^t + b_{t-1}s^{t-1} + \ldots + b_1 s + b_0 = 0$$

will be defined to be the zeroes of the output variable y(s). This will allow equation (V.4) to be written as

(V.6) $$y(s) = K \frac{\prod_{k=1}^{t}(s-z_k)}{\prod_{l=1}^{n}(s-p_l)}.$$

The pole-zero deletion method could now be applied to equation (V.6).

The 25th order overall PWR system model presented in Chapter III has an 11th order representation of a turbine-feedwater heater system. This model is identical to the turbine-feedwater heater system used in the high order overall PWR system model of Chapter II. In this study, no investigation was made into reducing the order of this model. Elgerd[9] (shown in equation 9-13, page 326) presents an empirical 2nd order transfer function model for a reheat turbine system. The input to this model is a change in steam valve position. The output of this model is the change in turbine shaft power. This model would have no feedback on the other components of the PWR system through changes in feedwater temperature to the UTSG. An investigation should be made into the validity of this model. In addition, it should be possible to determine the parameters of this model from the physical input parameters of the turbine-feedwater heater used in this study. These parameters are listed in Table XI.

The input parameters of the turbine-feedwater heater were obtained from IBM and the SEQUOYAH-FSAR for a typical 1200 MWe nuclear plant. However the values of the nozzle chest volume, V_C, and the reheater shell side volume, V_R, could not be determined exactly in this study. Therefore, the values of V_R and V_C should be determined for a typical 1200 MWe nuclear plant.

The SYSTEM computer code calculates the system matrix coefficients for the reactor core, UTSG, three element controller, and reactor controller models. Subroutine PRESS calculates the pressurizer pressure matrix coefficients after the system coefficients other than the pressurizer pressure model have been read in by MATEXP. The SYSTEM program should be improved to calculate the system coefficients for the turbine-feedwater heater model and the Pf controller model.

As a further improvement, the SYSTEM program should have the option to specify either the high order model or the low order model coefficients to be calculated. The SYSTEM program should also have the capability to develop a more detailed high order model. For example, it may be desirable for some particular applications to have a multi-node representation for the reactor fuel rather than a single lump representation. Ideally, the user of the SYSTEM-MATEXP code would be able to sit at the computer terminal and type in only a few input parameters. Then the computer will calculate the desired system coefficients, in as much detail as desired. The resulting calculations could then be used to simulate the system response for the desired forcing function.

LIST OF REFERENCES

LIST OF REFERENCES

1. Akin, I. E., "A Note on Control System Model Simplification," Int. J. Control, 1971, Vol. 14, No. 5.

2. Ali, M. R. A., "Lumped Parameter, State Variable Dynamic Models for U-Tube Recirculation Type Nuclear Steam Generators," Ph.D. Dissertation, Nuclear Engineering Department, University of Tennessee, August 1976.

3. Arumugan, M. and Ramomoorty, M., "A Method of Simplifying Large Dynamic Systems," Int. J. Control, 1973, Vol. 17, No. 6.

4. Bille, W. and Sinha, N. K., "A New Method of Reduction of Dynamic Systems," Int. J. Control, 1971, Vol. 14, No. 1.

5. Bosley, M. J., Kropholler, H. W., Lees, F. P., and Neale, R. M., "The Determination of Transfer Functions From State Variable Models," Automatica, Vol. 18, Pergamon Press 1972.

6. Cherng, J. C., "An Investigation of Feedwater Control and Nonlinear Effects for a U-Tube Steam Generator Model," M.S. Thesis, Nuclear Engineering Department, The University of Tennessee (December 1978).

7. Cope, J. and Dunphey, J., "RILMAT - A Program for Calculating the Eigenvalues and Eigenvectors of a Matrix," Computing Technology Center, Union Carbide Corporation, Nuclear Division, Oak Ridge, Tennessee.

8. Davison, E. J., "The Numerical Solution of Large Systems of Linear Differential Equations," AIChE Journal, Jan. 1968.

9. Elgerd, O. I., "Electric Energy Systems Theory: An Introduction," McGraw-Hill Inc., 1971.

10. Renesio, R. and Milanese, M., "A Note on the Derivation and Use of Reduced-Order Models," IEEE Transactions on Automatic Control, Feb. 1976.

11. IBM Data Processing Application, "Power Systems Simulator Description of Models," IBM Technical Publications Department, 1133 Westchester Avenue, White Plains, New York 10604, 1970.

12. Jones, J. B. and Hawkins, G. A., "Engineering Thermodynamics - An Introductory Textbook," 1960, John Wiley and Sons, Inc.

13. Katz, E. M., "Planning, Performing and Interpreting Dynamic Measurements in Pressurized Water Reactors," Ph.D. Dissertation, Nuclear Engineering Department, The University of Tennessee (June 1975).

14. Kearton, W. J., "Steam Turbine Theory and Practice," Sir Issac Pitman & Sons LTD., Fifth Edition 1948.

15. Kerlin, T. W., "Frequency Response Testing in Nuclear Reactors," Academic Press, New York (1974).

16. Kerlin, T. W., Nuclear Engineering 5210, 5220, 5230 Class Notes, Nuclear Engineering Department, The University of Tennessee (1977-78 Academic Year).

17. Kerlin, T. W., Upadhyaya, B. R., Zwingelstein, G. C., "Identification of Nuclear Systems," Nuclear Technology, Vol. 36, November 1977.

18. Kiser, E. M., "Investigation of Identifiability of Various Parameters in Pressurized Water Reactors with Application to Millstone 2 and Oconee I Nuclear Power Plants," M.S. Thesis, Nuclear Engineering Department, University of Tennessee (March 1977).

19. Krishnamurthi, V. and Seshadri, V., "A Simple and Direct Method of Reducing Order of Linear Systems and Routh Approximations in the Frequency Domain," IEEE Transactions on Automatic Control, October 1976.

20. Lal, M., Mitra, R., and Jain, A. M., "On Schwarz Canonical Form for Large System Simplification," IEEE Transactions on Automatic Control, April 1975.

21. Lees, F. P. and Bosley, M. J., "A Survey of Simple Transfer-Function Derivations from High-Order State Variable Models," Automatica, Vol. 8, Pergamon Press, 1972.

22. Lees, F. P. and Gibilaro, L. G., "The Reduction of Complex Transfer Function Models to Simple Models Using the Method of Moments," Chemical Engineering Science, 1969, Vol. 24.

23. Machado, E. L., personal communication, undocumented computer programs, 1978.

24. Masche, George, "Systems Summary of a Westinghouse Pressurized Water Reactor Nuclear Power Plant," 1971 Westinghouse Electric Corporation, PWR Systems Division.

25. MATEXP: "A General Purpose Digital Computer Program for Solving Ordinary Differential Equations by the Matrix Exponential Method," S. S. Ballard, R. K. Adams, ORNL-TM-1933, (August 1967).

26. Nagarajan, R., "Optimum Reduction of Large Dynamic Systems," Int. J. Control, 1971, Vol. 14, No. 6.

27. Reddoch, T. W., "Models and Cost Functionals for Optimal Automatic-Generator Controllers," Ph.D. Dissertation, Louisiana State University, 1973.

28. Riggs, J. B. and Edgar, T. F., "Simplification of Large-Scale Linear Dynamic Systems," Dept. of Chemical Engineering, The University of Texas, Austin, Texas.

29. Sequoyah Nuclear Plant - Final Safety Analysis Report, Tennessee Valley Authority, April 1974.

30. SFR3 Code - "A Fortran Program for Calculating the Frequency Response of a Multivariable System and its Sensitivities to Parameter Changes," T. W. Kerlin and J. L. Lucius, USAEC Report ORNL-TM-1575 (1966).

31. Shamash, V., "Linear System Reduction Using Pade Approximation to Allow Retention of Dominant Modes," Int. J. Control, 1975, Vol. 21, No. 2.

32. Shankkar, P. V. G., "Simulation Model of a Nuclear Reactor Turbine," Nuclear Engineering and Design, November 1977, Volume 44 (1977) No. 2.

33. Shieh, L. S. and Wei, Y. J., "A Mixed Method for Multivariate System Reduction," IEEE Transaction on Automatic Control, June 1975.

34. Sinha, N. K. and Bereznai, G. T., "Optimum Approximation of High-Order Systems by Low-Order Models," Int. J. Control, 1971, Vol. 14, No. 5.

35. Strange, J., "Incorporation of Pressurizer Pressure Controller Models into State Variable Models of H. B. Robinson and Oconee Nuclear Power Plants," Research Project for Nuclear Engineering 5980, University of Tennessee, August 1975.

36. SURFACE II Graphics System (Revision One), R. J. Sampson, Revised 1978.

37. Thakkar, J. G., "Correlation of Theory and Experiment for the Dynamics of a Pressurized Water Reactor," M. S. Thesis, Nuclear Engineering Department, The University of Tennessee (March 1975).

38. Westinghouse Electric Corporation, PWR Systems Division, "Precautions, Limitations, and Setpoints for Nuclear Steam Supply Systems," Revision 5, June 1976.

39. Westinghouse Electric Corporation, PWR Systems Division, FA-1-793, December 9, 1977.

40. Wrangham, D. A., "The Theory and Practice of Heat Engines," New York, The Macmillan Co., Cambridge, England: at the University Press, 1942.

41. Meghreblian, R. V., Holmes, D. K., "Reactor Analysis," McGraw-Hill Book Company Inc., 1960.

APPENDIXES

APPENDIX A

DESCRIPTION AND INSTRUCTIONS ON THE USE OF THE SYSTEM-MATEXP PROGRAMMING PACKAGE

A.1 DESCRIPTION OF THE SYSTEM-MATEXP PROGRAMMING PACKAGE

The SYSTEM-MATEXP programming package was developed with the intent of reducing the effort involved in dynamic modeling of PWR systems. Previously, the system matrix coefficients had to be calculated by hand and calculated again for new initial conditions or if a mistake had been made. Then the resulting coefficients were used in the MATEXP code.

Ali[2] developed a code to calculate the matrix coefficients and forcing vector coefficients for a 15th order UTSG model. This program has been modified and is called the SYSTEM program. The SYSTEM program will calculate the matrix coefficients and forcing vector coefficients for the UTSG, reactor core, three-element feedwater controller, and reactor controller of the high order PWR model presented in this thesis.

The output of the SYSTEM program, along with other data, is used as input to the MATEXP program. A version of subroutine DISTRB of the MATEXP program has been written to simulate the nonlinear reactor controller presented in this thesis. DISTRB will also allow the calculation of algebraic variables to be made at each time step in the solution. Subroutine PRES has also been added to MATEXP to calculate the matrix coefficients of the pressurizer pressure model. Subroutines ROD, STEAM, VALVE, FEED1, and FEED2 have been added to MATEXP to vary all the possible forcing functions on the PWR system. These subroutines are called by DISTRB depending on the value of the input parameter ITYPE.

A flowchart of the SYSTEM-MATEXP programming package is given in Figure A.1. A list of the input cards to the SYSTEM program is given in Section A.2. A list of the input cards to the MATEXP program is given in Section A.3. The instructions for the execution of the SYSTEM-MATEXP programming package is given in Section A.4. Figure A.2 is an example of the input file for the SYSTEM program. Figure A.3 is an example of the input file for the MATEXP program. The reader should refer to Figures A.1, A.2, and A.3 to help in understanding the use of this program.

A.2 INPUT FORMAT FOR THE SYSTEM PROGRAM (FOR24.DAT)

Card No. 1 (geometrical parameters)

Column	1-5	6-15	16-25	26-35	36-45	46-55	56-65	66-75
Format	I5	7D10.4						
Input	NT	TOD	TMT	USHD	USHT	LSHD	LSHT	OVHT

NT - number of U-tubes

TOD - tube outside diameter (inches)

TMT - tube metal thickness (inches)

USHD - steam generator upper shell diameter (inches)

USHT - steam generator upper shell thickness (inches)

LSHD - steam generator lower shell diameter (inches)

LSHT - steam generator lower shell thickness (inches)

OVHT - steam generator overall height (ft)

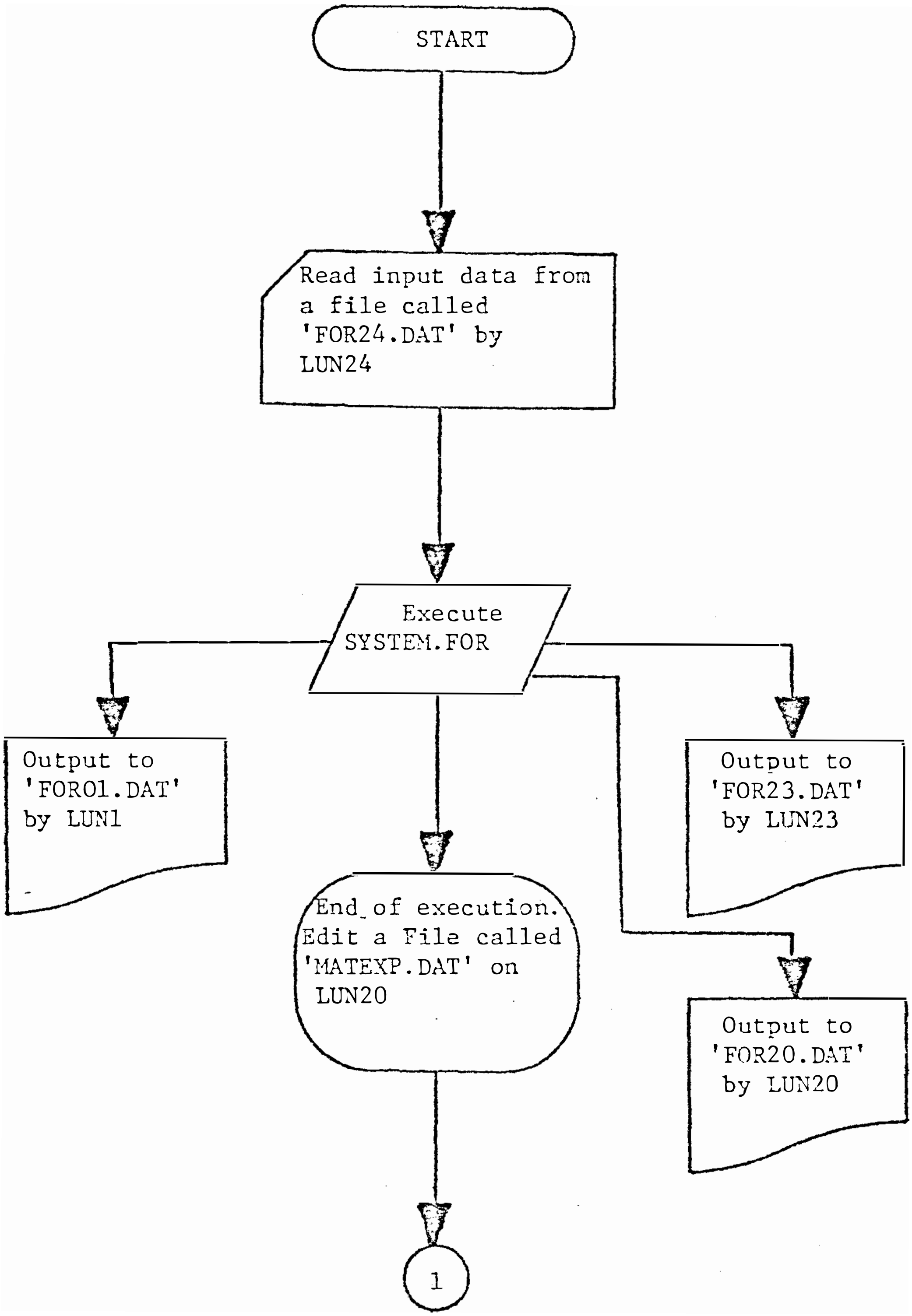

Figure A.1 Flowchart of the SYSTEM-MATEXP computer program.

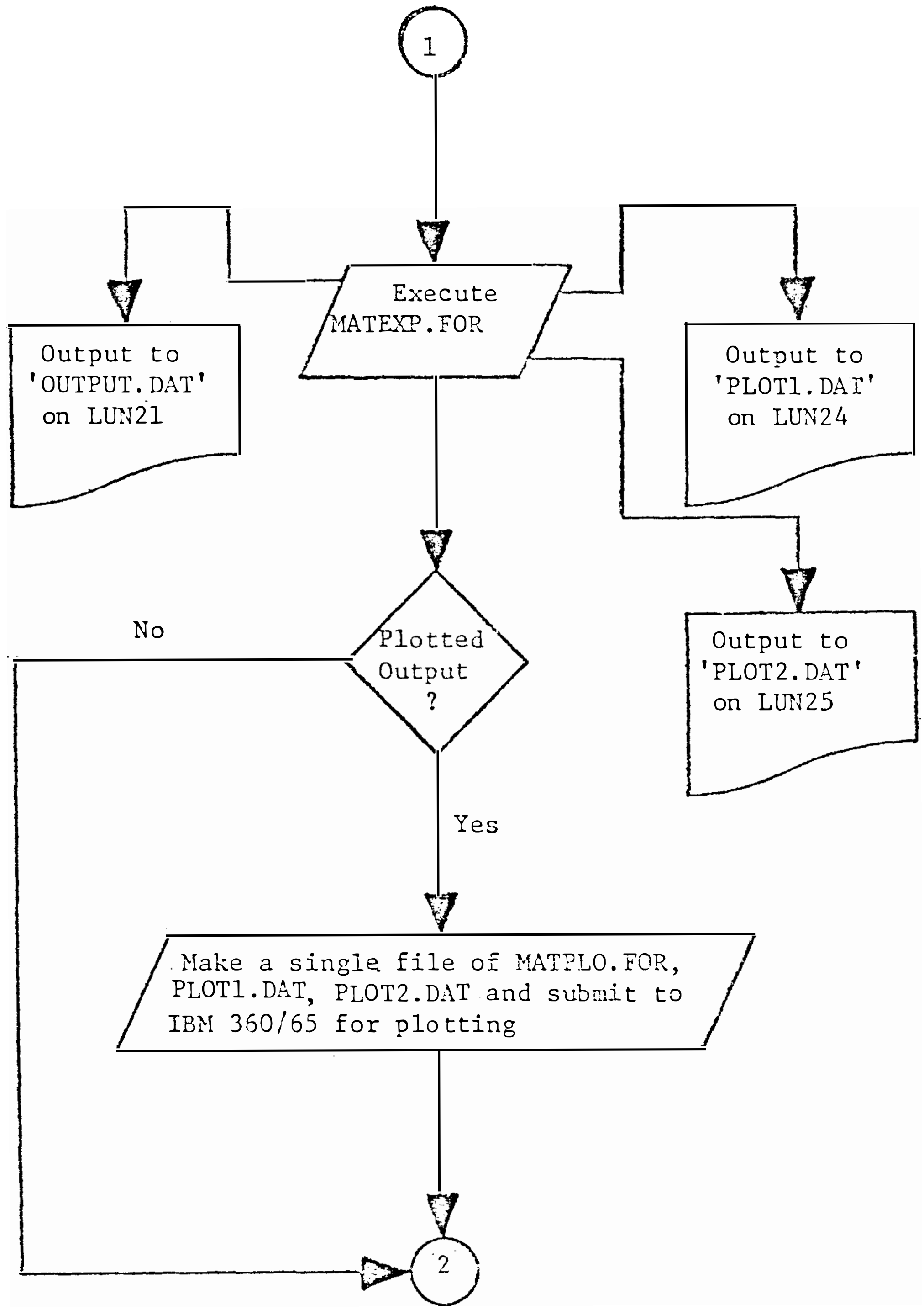

Figure A.1 (continued)

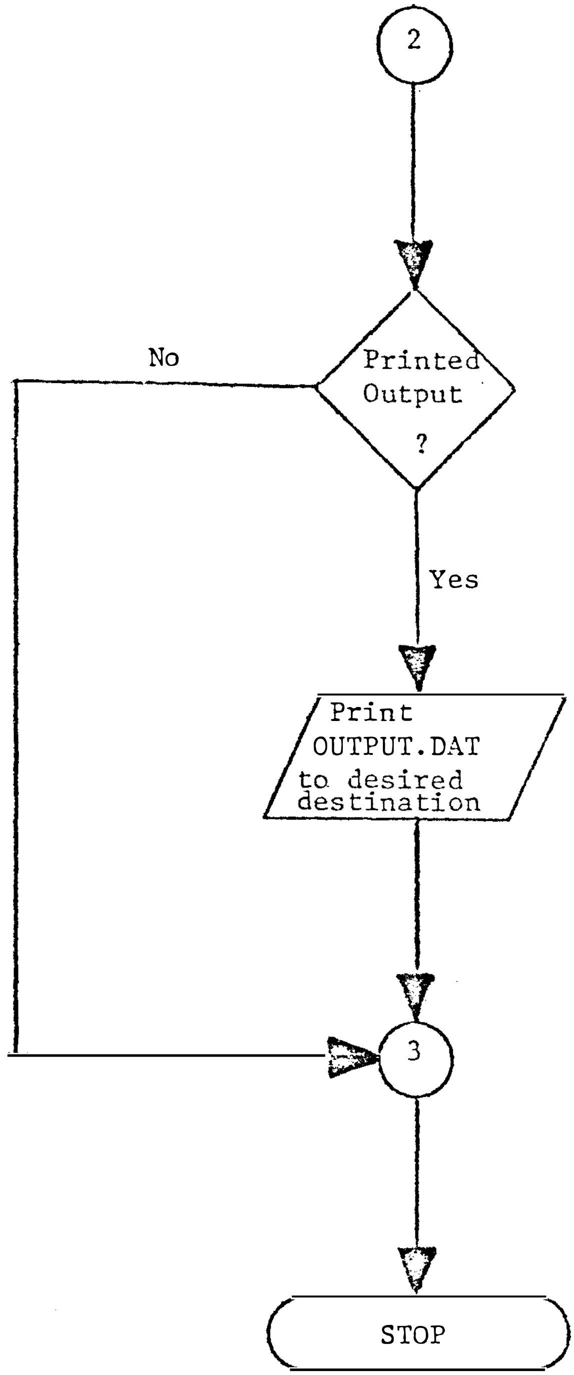

Figure A.1 (continued)

```
 3388      .875   .05      178.0     3.5       135.0    2.36      67.67
60.87      32.0       42.17      9.63
0.3939E+08 .1077E+04 1.31       592.5     542.5      2250.0   45.710     .28  E+08
3.73133E+6  832.0    522.89     434.30    .2         3870.0   52.32      1.1650
 .5150E+05 4500.0    2160.0     1972.0    6000.0     9.0
 530.0     0.11
 515.24    683.1     1198.3     .02098    .52470     .5457
 .14000    .1700     -.2000     -.0350     .35  E-05-.7135E-03-.7100E-03+.2370E-02
    0.200
   8     7     4     1
  0.006898  0.000209  0.001414  0.001309  0.002727  0.000925  0.000314 -0.000011
   17.9E-6    0.0125    0.0308    0.1140    0.3070    1.1900    3.1900 -0.000200
    3436.0  222739.0     0.059   59900.0     0.974     200.0
    1376.0    1791.0    250.00    500.00    540.00
3.73313E+6   1198.30      30.0     0.208      80.0      10.0       5.0       4.0
      40.0       0.3       1.0    .00225
```

Figure A.2 A typical 'FOR24.DAT' data file for the SYSTEM program.

```
NEOD)YAH--57TH ORDER--100% POWER MODEL--LOOK AT TURBINE S.S.
FULL CONTROL EVERYWHERE--10% DECREASE IN VALVE COEFFICIENT
10/16/78--CASE B
   20
         65          66          67          69           8          27          35          59
         55          53          14          12          26          57          63          64
         25          42          70          60
 TURB(PU)    RO CENTS   %N POWER   %S POWER    FUEL (F)   STM PRES   FEED FLW   STM FLOW
 VALVE CF    FEED (F)   COLD LEG   HOT  LEG    INTE ACE   FREQ  HZ   HP  TORQ   LP  TORQ
 DUMP LEV    PRI PRES   HEAT(KW)   ERROR(F)
   1 0.0022500         63.0         1.5         1.0
  61     60     61     59     62     68     69     67     27     35
57       1       0.000100          0.0         0.020        400.0        2.000  3 4 5 751 0 0 8106.
42 42   -5.15197E-2  42 43   +1.71586E-4  43 42   -3.33333E-1  1 42   -5.58659E-2
44 44   -1.62933E+01 44 45   -3.67203E+01 44 47    1.92900E+00 44 27    +0.02492
44 48    5.87490E+00 45 44   -9.95530E+00 45 45   -3.11534E+01 45 27    +0.01487
45 47    1.17850E+00 45 48    3.58920E+00 46 44    3.93000E-01
46 45    8.85830E-01 46 46   -5.00000E-01 46 47   -4.65300E-02
47 48   -1.41760E-01 47 46    1.95320E-01 47 47   -2.71340E-01
47 48   -2.10100E-01 48 46    6.16130E-01 48 47   -1.07470E+00
48 48   -1.27670E+00 48 50    3.76480E-01 49 49   -3.33330E-01
50 48        -1.0102 50 49    7.86240E-03 50 27      8.350E-5
50 50   -2.50000E-01 51 47    1.90200E-01 49 27     4.0064E-4
51 48    1.45900E-01 51 51   -1.00000E-01 52 47    1.35167E+00
52 48    1.03653E+00 52 52   -1.00000E-01 52 54    1.39527E+00
53 44    1.33782E+00 53 45    3.01440E+00 53 46   -1.10060E+00 53 35   -1.27066E-3
53 47   -1.58377E-01 53 48   -3.74300E-01 53 49    4.58180E-01
53 52    2.19300E-02 53 53   -2.50000E-02 54 44    4.37220E-02 52 35   -2.1678E-3
54 45    9.85100E-02 54 46   -3.59700E-02 54 47   -5.17600E-03
54 48   -1.22400E-02 54 49    1.49700E-02 54 54   -1.00000E-01
54 48   -1.22400E-02
17 53   -3.29293E-03 19 53    1.74002E-03
```

Figure A.3 A typical 'MATEXP.DAT' file for the MATEXP program.

21	53	-6.57212E-03	22	53	-1.09817E-03	23	53	2.36510E-04	24	53	1.41542E-03
25	53	-4.73033E-05									
26	53	3.88205E-03	27	53	-2.46112E-03	28	53	1.06875E-04	29	53	1.46608E-02
38	53	-0.0010283	41	53	-0.0011124						
17	55	2.1853	19	55	-0.9436	21	55	3.6122	22	55	0.6056
23	55	-0.1384	24	55	-0.8253	25	55	0.9790	26	55	-2.0363
27	55	-57.0201	28	55	-0.0474	29	55	+0.4112	33	55	989.4940
34	55	384649.7310	38	55	1.0086	41	55	1.0912	44	55	20.7296
45	55	12.6666	55	55	-5.00	55	56	-7.0050	55	57	-2.3350
56	57	0.34167	57	57	-0.10						
55	55		55	56		55	57				
17	58	0.1027	19	58	-0.0443	21	58	0.1698	22	58	0.0285
23	58	-0.0065	24	58	-0.0380	25	58	0.0460	26	58	-0.0957
27	58	-2.6799	28	58	-0.0022	29	58	-0.0193	33	58	46.5060
34	58	18050.2690	38	58	0.0474	41	58	0.0513			
[illegible]	58	0.0131671	40	58	0.3333	58	46	-0.6815	58	47	1.1886
[illegible]	47	1.6360	58	50	-0.4164						
1	1	-3.85363E+02	1	2	1.25000E-02	1	3	3.08000E-02	1	4	1.14000E-01
1	5	3.07000E-01	1	6	1.19000E+00	1	7	3.19000E+00	1	8	-6.14525E-01
1	9	-5.58659E+00	1	10	-5.58659E+00	2	1	1.16760E+01	2	2	-1.25000E-02
3	1	7.89944E+01	3	3	-3.08000E-02	4	1	7.31285E+01	4	4	-1.14000E-01
5	1	1.52346E+02	5	5	-3.07000E-01	6	1	5.16760E+01	6	6	-1.19000E+00
7	1	1.75419E+01	7	7	-3.19000E+00	8	1	2.41373E+02	8	8	-2.53225E-01
9	6	2.53225E-01	9	1	2.61863E+00	9	8	1.02915E-01	9	9	-3.64916E+00
9	13	3.54624E+00	10	1	2.61863E+00	10	8	1.02915E-01	10	9	3.44333E+00
10	10	-3.54624E+00	11	10	6.95847E-01	11	11	-6.95847E-01	12	11	9.57486E-01
12	12	-9.57486E-01	13	13	-5.34613E-01	13	14	5.34613E-01	14	14	-4.78743E-01
14	20	4.78743E-01	15	12	1.40592E+00						
36	14	2.50000E-01	36	36	-2.50000E-01	37	12	2.50000E-01	37	37	-2.50000E-01
38	27	1.23857E-03	38	35	-3.50375E-04	38	38	-3.33333E-02	39	12	2.00000E-01
39	14	2.00000E-01	39	36	-1.90000E-01	39	37	-1.90000E-01	39	39	-3.00000E-01
39	40	-2.00000E-02	40	39	1.00000E+00	41	1	-7.49638E-01	41	27	8.79112E-04

Figure A.3 (continued)

41	35	-3.79011E-04	41	41	-2.50000E-02						
15	15	-1.40592E+00	16	15	4.52644E+00	16	16	-5.17625E+00	16	21	6.49818E-01
16	26	-4.99208E+00	17	16	7.59049E-01	17	17	-1.40887E+00	17	21	4.36060E-02
17	22	5.98782E-01	17	23	-5.10361E-02	17	24	4.36060E-02	17	25	-6.09455E-02
17	26	1.66025E+00	17	27	-1.85048E-02	17	28	-5.41535E-01	17	29	1.69395E-01
18	17	7.59049E-01	18	18	-1.40887E+00	18	23	6.49818E-01	18	26	5.04719E-01
19	18	4.52644E+00	19	19	-5.17625E+00	19	21	-1.88244E-02	19	22	2.20319E-02
19	23	2.20319E-02	19	24	6.30994E-01	19	25	2.63098E-02	19	26	-2.46262E+00
19	27	7.98838E-03	19	28	2.33769E-01	19	29	-7.31266E-02	20	19	1.40592E+00
[illegible]	[illegible]	-1.40592E+00	21	16	2.42955E+00	21	21	-3.97366E+00	21	22	-8.43323E-02
21	23	-8.43323E-02	21	24	7.20548E-02	21	25	-1.00707E-01	21	26	1.39694E+00
21	27	8.25544E-02	21	28	-8.94806E-01	21	29	1.08799E+00	22	17	2.42955E+00
22	21	1.20830E-02	22	22	-5.40182E+00	22	23	-1.41419E-02	22	24	1.20830E-02
22	25	-1.68877E-02	22	26	2.34256E-01	22	27	4.09011E-01	22	28	-1.50051E-01
22	29	4.69386E-02	23	18	2.42955E+00	23	21	-2.76099E-03	23	22	3.23144E-03
23	23	-5.38445E+00	23	24	-2.76099E-03	23	25	3.85887E-03	23	26	-5.35279E-02
23	27	4.15311E-01	23	28	3.42884E-02	23	29	-1.07255E-02	24	19	2.42955E+00
24	21	-1.64646E-02	24	22	1.92700E-02	24	23	1.92700E-02	24	24	-4.06218E+00
24	25	2.30116E-02	24	26	-3.19203E-01	24	27	1.20119E-01	24	28	2.04464E-01
24	29	7.44125E-01	25	21	4.95080E-04	25	22	2.29466E-02	25	23	2.29466E-02
25	24	4.95080E-04	25	25	-4.77932E-02	25	26	5.20583E-03	25	27	-4.87738E-03
25	28	-1.56080E+01	25	29	1.92322E-03	26	21	-4.06200E-02	26	22	4.75413E-02
26	23	4.75413E-02	26	24	-4.06200E-02	26	25	5.67722E-02	26	26	-7.87509E-01
26	27	1.72376E-02	26	28	5.04440E-01	26	29	-1.57795E-01	27	21	2.57583E-02
27	22	1.19388E+00	27	23	1.19388E+00	27	24	2.57583E-02	27	25	-2.01915E-02
27	26	-1.55375E+00	27	27	-4.10183E-01	27	28	4.71541E+00	27	29	1.00062E-01
28	21	-1.11887E-03	28	22	2.21147E-03	28	23	2.21147E-03	28	24	-1.11887E-03
28	25	6.64819E-04	28	26	-2.25310E-02	28	27	2.53168E-04	28	28	-2.72424E-01
28	29	-4.34643E-03	29	21	2.08011E-04	29	22	9.64117E-03	29	23	9.64117E-03
29	24	2.08011E-04	29	25	2.62739E-03	29	26	-1.46117E-02	29	27	5.98218E-03
29	28	-6.57587E+00	29	29	-7.25943E-02						
17	35	2.05721E-04	19	35	-9.88085E-05	21	35	3.39935E-04	22	35	5.70044E-05

Figure A.3 (continued)

```
23 35  -1.30256E-05 24 35  -7.76757E-05 25 35   5.65876E-04 26 35  -1.91634E-04
27 35   2.18450E-03 28 35  -5.58467E-06 29 35  -1.01843E-03 30 25  -2.00000E-01
30 30  -2.00000E-01 31 25  -1.50800E+01 31 30  -1.50750E+01 32 25  -4.62805E+02
32 30  -4.62652E+02 32 31   5.59597E-02 33 27   1.24577E+00 33 35  -1.00000E+00
34 27   4.83309E+02 34 32   1.26413E+01 34 33   7.07402E-01 34 34  -4.00680E+00
34 35  -3.88357E+02 35 34   1.00000E+00

  35
  0.00000E+00   0.00000E+00   0.00000E+00   0.00000E+00   0.00000E+00
  0.00000E+00   0.00000E+00   0.00000E+00   0.00000E+00   0.00000E+00
  0.00000E+00   0.00000E+00   0.00000E+00   0.00000E+00   0.00000E+00
  0.00000E+00   2.28248E+00   0.00000E+00  -9.87920E-01   0.00000E+00
  3.78150E+00   6.34127E-01  -1.44899E-01  -8.64076E-01   1.02461E+00
 -2.13177E+00  -5.96969E+01  -4.96589E-02   4.30498E-01   0.00000E+00
  0.00000E+00   0.00000E+00   1.03648E+03   4.02113E+05   0.00000E+00
  6.20800E-03   1.79000E-05
  12     41     40     38     1
  2.00000E-01   3.00000E-01   1.00000E+00   1.03698E+03   1.03698E+03
  1.19830E+03   1.19830E+03  -3.50000E-02   4.12033E+02   1.16500E+00
  1.24577E+00
```

Figure A.3 (continued)

Card No. 2 (geometrical parameters)

Column	1-10	11-20	21-30	31-40
Format	4D10.4			
Input	AFS	AD	LD	RL

AFS - secondary flow area in the tube region (ft^2)

AD - downcomer level (ft^2)

LD - downcomer level (ft)

RL - riser level (ft)

Card No. 3 (primary side parameters)

Column	1-10	11-20	21-30	31-40	41-50	51-60	61-70	71-80
Format	8D10.4							
Input	WP	VP	CP1	TPID	TPOT	PP	ROP	PHC

WP - primary water (reactor coolant) mass flow rate into the steam generator (lbm/hr)

VP - total steam generator primary water volume (ft^3)

CP1 - specific heat at constant pressure of the primary water (B/lbm-°F)

TPI - primary water inlet temperature (°F)

TPO - primary water outlet temperature (°F)

PP - primary loop average pressure (psia)

ROP - average density of primary water (lbm/ft^3)

PHC - primary side heat content (B)

Card No. 4 (secondary side parameters)

Column	1-10	11-20	21-30	31-40	41-50	51-60	61-70	71-80
Format	8D10.4							
Input	WSO	PSTG	TSAT	TFWI	XE	VSS	ROS1	CP2

WSO - steam flow rate (lbm/hr)

PSTG - steam generator pressure (psig)

TSAT - saturation temperature at PSTG (°F)

TFWI - feedwater inlet temperature (°F)

XE - quality of steam at riser exit

VSS - volume of secondary steam in the drum steam volume (ft^3)

ROS1 - subcooled secondary water average density (lbm/ft^3)

CP2 - specific heat of secondary side subcooled water (B/lbm-°F)

Card No. 5 (heat transfer coefficients)

Column	1-10	11-20	21-30	31-40	41-50	51-60
Format	6D10.4					
Input	HTA	HP	UM	HS1	HS2	KM

HTA - overall heat transfer area of the steam generator U-tubes (ft^2)

HP - primary side film heat transfer coefficient ($B/hr\text{-}ft^2\text{-}°F$)

M - tube metal conductance ($B/hr\text{-}ft^2\text{-}°F$)

HS1 - subcooled secondary film heat transfer coefficient ($B/hr\text{-}ft^2\text{-}°F$)

HS2 - boiling secondary film heat transfer coefficient (B/hr-ft^2-°F)

KM - conductivity of the tube metal (B/hr-ft-°F)

Card No. 6 (tube metal properties)

Column	1-10	11-20
Format	2D10.4	
Input	ROM	CM

ROM - density of tube metal (lbm/ft^3)

CM - tube metal heat capacity (B/lbm-°F)

Card No. 7 (steady state thermodynamic properties)

Column	1-10	11-20	21-30	31-40	41-50	51-60
Format	6D10.4					
Input	HF	HFG	HG	VF	VFG	VG

HF - enthalpy of saturated water (B/lbm)

HFG - latent heat of vaporization (B/lbm)

HG - enthalpy of saturated steam (B/lbm)

VF - specific volume of saturated water (ft^3/lbm)

VFG - difference between specific volumes of saturated steam and water (ft^3/lbm)

VG - specific volume of saturated steam (ft^3/lbm)

Card No. 8 (thermodynamic property gradients)

Column	1-10	11-20	21-30	31-40	41-50	51-60	61-70	71-80
Format	8D10.4							
Input	DTSAT	DHF	DHFG	DHG	DVF	DVFG	DVG	DROG

DTSAT - $\frac{\partial T_{sat}}{\partial P_s}$ (°F/psi)

DHF - $\frac{\partial h_f}{\partial P_s}$ (B/lbm-psi)

DHFG - $\frac{\partial h_{fg}}{\partial P_s}$ (B/lbm-psi)

DHG - $\frac{\partial h_g}{\partial P_s}$ (B/lbm-psi)

DVF - $\frac{\partial v_f}{\partial P_s}$ (ft^3/lbm-psi)

DVFG - $\frac{\partial v_{fg}}{\partial P_s}$ (ft^3/lbm-psi)

DVG - $\frac{\partial v_g}{\partial P_s}$ (ft^3/lbm-psi)

DROG - $\frac{\partial \rho_g}{\partial P_s}$ (lbm/ft^3-psi)

Card No. 9 (SYSTEM control card)

Column	1-5	6-10	11-15	16-20
Format	4I5			
Input	ITYPE	NC	NUTSG	NCNTRL

ITYPE - specification of forcing vector

1 1°F primary inlet temperature - no feedwater flow control

2 Unit change in fractional steam flow - no feedwater flow control

3 Unit change in steam valve coefficient - no feedwater flow control

4 1°F feedwater inlet temperature - no feedwater flow control

5 Unit change in fractional feedwater flow - no feedwater flow control

6 1°F primary inlet temperature - perfect feedwater flow control

7 Unit change in fractional steam flow - perfect feedwater flow control

8 Unit change in steam valve coefficient - perfect feedwater flow control

9 1°F feedwater inlet temperature - perfect feedwater flow control

10 1°F primary inlet temperature - three element feedwater flow control

11 Unit change in fractional steam flow - three element feedwater flow control

12 Unit change in steam valve coefficient - three element feedwater flow control

13 1°F inlet feedwater temperature - three element feedwater flow control

NC - The number of state variable equations which will be used to describe the reactor core. If NC=0, the UTSG will be treated as an isolated model.

NUTSG - The number of UTSG's per reactor unit

NCNTRL - A non-zero entry will cause the reactor control system matrix to be calculated. A zero entry will not calculate the reactor control system matrix. NCNTRL should be set equal to zero for NC equal to zero.

Card No. 10 (include only for NC > 0)

neutronics data for the reactor core model

Column	1-10	11-20	21-30	31-40	41-50	51-60	61-70	71-80
Format	8F10.0							
Input	BETAT	BETA1	BETA2	BETA3	BETA4	BETA5	BETA6	ALPHAF

BETAT - total delayed neutron fraction

BETA1 - 1st delayed neutron group fraction

BETA2 - 2nd delayed neutron gruop fraction

BETA3 - 3rd delayed neutron group fraction

BETA4 - 4th delayed neutron group fraction

BETA5 - 5th delayed neutron group fraction

BETA6 - 6th delayed neutron group fraction

ALPHAF - fuel coefficient of reactivity (1/°F)

Card No. 11 (include only for NC > 0)

neutronics data for the reactor core model

Column	1-10	11-20	21-30	31-40	41-50	51-60	61-70	71-80
Format	8F10.0							
Input	GEN	LAMDA	LAMDA2	LAMDA3	LAMDA4	LAMDA5	LAMDA6	ALPHAC

GEN - neutron generation time (seconds)

LAMDA1 - 1st group decay constant (1/sec)

LAMDA2 - 2nd group decay constant (1/sec)

LAMDA3 - 3rd group decay constant (1/sec)

LAMDA4 - 4th group decay constant (1/sec)

LAMDA5 - 5th group decay constant (1/sec)

LAMDA6 - 6th group decay constant (1/sec)

ALPHAC - coolant coefficient of reactivity (1/°F)

Card No. 12 (include only for NC > 0)

heat transfer data for the reactor core model

Column	1-10	11-20	21-30	31-40	41-50	51-60
Format	6F10.0					
Input	POWER	FUELM	CPF	AREA	FRACF	H

POWER - initial reactor power level (Mw)

FUELM - mass of fuel (lbm)

CPF - specific heat of the fuel (B/lbm-°F)

AREA - total heat transfer area from fuel to coolant (ft^2)

FRACF - fraction of the total power produced in the fuel

H - overall heat transfer coefficient from fuel to coolant ($B/hr\text{-}ft^2\text{-}°F$)

Card No. 13 (include only for NC > 0)

reactor coolant volumes

Column	1-10	11-20	21-30	31-40	41-50
Format	5F10.0				
Input	UPPERV	LOWERV	HOTV	COLDV	COOLV

UPPERV - volume of coolant in upper plenum (ft^3)

LOWERV - volume of coolant in lower plenum (ft^3)

HOTV - volume of coolant in hot let piping (ft^3)

COLDV - volume of coolant in cold leg piping (ft^3)

COOLV - volume of coolant surrounding the reactor core (ft^3)

Card No. 14 (include only for NCNTRL > 0)

reactor control system data

Column	1-10	11-20	21-30	31-40	41-50	51-60	61-70	71-80
Format	8F10.0							
Input	WMAX	HGMAX	SET1	RK1	LEAD	LAG1	LAG2	TAU

WMAX - maximum flow rate of steam leaving the UTSG (lbm/hr)

HGMAX - the enthalpy of the steam leaving the UTSG at maximum flow conditions (B/lbm)

SET1 - time constant of average temperature set point transfer function (sec)

RK1 - gain of average temperature set point transfer function (°F/%Power)

LEAD - lead time constant of lead-lag compensated average temperature transfer function (sec)

LAG1 - first lag time constant of lead-lag compensated average temperature transfer function (sec)

LAG2 - second lag time constant of lead-lag compensated average temperature transfer function (sec)

TAU - time constant of RTD transfer function (sec)

Card No. 15 (include only for NCNTRL > 0)

reactor control system data

Column	1-10	11-20	21-30
Format	3F10.0		
Input	SET3	RK2	RK3

SET3 - time constant of power mismatch transfer function (sec)

RK2 - nonlinear gain of power mismatch transfer function (°F/%Power)

RK3 - variable gain of power mismatch transfer function (unitless)

A.3 MATEXP INPUT INSTRUCTIONS

Card No. 1 (title card)

Column	1-80
Format	20A4
Input	TITLE1

TITLE1 - 80 alphanumeric characters on one card may be used for a title. A blank is considered to be an alphanumeric character.

Card No. 2 (title card)

Column	1-80
Format	20A4
Input	TITLE2

TITLE2 - 80 alphanumeric characters on one card may be used for a title. A blank is considered to be an alphanumeric character.

Card No. 3 (title card)

Column	1-16
Format	4A4
Input	TITLE3

TITLE3 - 16 alphanumeric characters on one card may be used for a title. A blank is considered to be an alphanumeric character.

Card No. 4 (plotting information)

Column	1-5
Format	I5
Input	NPLOT

NPLOT - The total number of plots to be made. Include a blank if no plots are desired. NPLOT must be $\leq$ 24.

Card No. 5 (plotting information)

Column	1-80
Format	8(5X,I5)
Input	NSPTV(I)

NSPTV(I) - A vector of the state variable numbers to be plotted. If necessary, repeat card No. 5 until NPLOT entries for NSPTV(I) have been made.

Card No. 6 (plotting information)

Column	1-80
Format	8(2X,A8)
Input	DY(I)

DY(I) - A vector of the names of the state variables, corresponding with NSPTV(I), to be plotted. Each name can be up to 8 alpha-numeric characters in length. If necessary, repeat card No. 6 until NPLOT entries for DY(I) have been made.

Card No. 7 (Reactor control system input data not previously input to the SYSTEM program)

Column	1-5	6-15	16-25	26-35	36-45
Format	I5	E10.3	E10.3	E10.3	E10.3
Input	NTYPE	ROWSTP	TRIP	DBOUT	DBIN

NTYPE - The type of temperature error signal which will be used by the reactor control system.

1 = $\delta T_{s1} - \delta T_{s2} + \delta T_{s3}$

2 = δT_{s3}

3 = $\delta T_{s1} - \delta T_{s2}$

4 = 0

ROWSTP - The amount of reactivity induced by the control rods per step change. Note that control rods move in discrete steps rather than continuously.

TRIP - The temperature error signal that will trip the plant. When this temperature error signal is reached, the execution of the MATEXP program will cease.

DBOUT - The absolute value of the temperature error signal deadband upon leaving (going out of) steady state conditions. Westinghouse[38] recommends 1.5°F.

DBIN - The absolute value of the temperature error signal deadband upon entering (going in to) steady state conditions. Westinghouse[38] recommends 1.0°F.

Card No. 8 (Locations in the solution vector for algebraic and state variables needed by the reactor control system and for plotting capabilities)

Column	1-5	6-10	11-15	16-20	21-25	26-30	31-35	36-40
Format	I5	I5	I5	I5	I5	I5	I5	I5
Input	NREAC	NTBAR	NDQ	NSTM	NK3	NK2	NPT	NPN

Column	41-45	46-50
Format	I5	I5
Input	NPRES	NFLOW

NREAC - Solution vector location for the reactivity induced by the control rods. Must be greater than the number of state variable equations and $\leq$ 70.

NTBAR - Solution vector location for the temperature error signal. Must be greater than the number of state variable equations and $\leq$ 70.

NDQ - Solution vector location for the difference in percent of full power delivered to the secondary fluid and the percent of full nuclear power ($\%P_S$ - $\%P_N$). Must be greater than the nimber of state variable equations and $\leq$ 70.

NSTM - Solution vector location for the steam flow out of the UTSG. Must be greater than the number of state variable equations and $\leq$ 70.

NK3 - Solution vector location for the variable gain of the power mismatch transfer function. Must be greater than the number of state variable equations and $<$ 70.

NK2 - Solution vector location for the nonlinear gain of the power mismatch transfer function. Must be greater than the number of state variable equations and $<$ 70.

NPT - Solution vector location for the percent of full power delivered to the secondary fluid. Must be greater than the number of state variable equations and $\leq$ 70.

NPN - Solution vector location for the percent of full nuclear power. Must be greater than the number of state variable equations and $<$ 70.

NPRES - Solution vector location of the UTSG steam pressure.

NFLOW - Solution vector location of the UTSG feedwater flow rate.

Card No. 9 (MATEXP control card)

Column	1-2	3-5	6-7	8-10	11-20	21-30	31-40	41-50
Format	I2	3X	I2	3X	F10.0	F10.0	F10.0	F10.0
Input	NE		LL		P	TZERO	T	TMAX

Column	51-60	61-62	63-64	65-66	67-69	70	71-72	73-74
Format	F10.0	I2	I2	I2	I3	I1	I2	I2
Input	PLINTC	MATYES	ICSS	JFLAG	ITMAX	LASTCC	I1Z	ICONTR

Column	75-80
Format	F6.0
Input	VAR

NE - number of equations, must be < 70

LL - matrix tag number

P - precision, recommend 10^{-6} or less

TZERO - zero time

T - computational time interval

TMAX - maximum time

PLTINC - printing time increment

MATYES - matrix control flag

1 = use previous A and T

2 = read new coefficient to alter A

3 = read entire new A (nonzero values)

4 = CALL DISTRB to calculate entire new A

5 = read some, DISTRB to calculate others

6 = DISTRB to alter some A elements

ICSS - initial condition vector (XIC) flag

1 = read in all new nonzero values

2 = read new values to alter previous vector

3 = use previous vector

4 = vector = 0

5 = use last value of solution vector (X) from previous run

JFLAG - forcing function (Z) flag

1 through 4 = same as ICSS for constant Z

5 = Call DISTRB at each time step for variable Z. (Use this for the reactor control system.)

ITMAX - maximum number of terms in series approximation of exp (AT)

LASTCC - nonzero for last case

I1Z - row of Z is only one nonzero, otherwise = 0

ICONTR - for internal control options

0 = read new control card for next case

1 = go to 212, call DISTRB for new A or T

-1 = go to 215, call DISTRB for new initial conditions

VAR - maximum allowable value of largest coefficient matrix element *T (recommend VAR = 1.0)

Card No. 10 (nonzero elements of system matrix)

Column	1-3	4-6	7-20	Repeat, 4 per card
Format	I3	I3	E14.5	
Input	I1	J1	D1	I2, J2, D2, I3, J3, D4, I4, J4, D4

I1 - row number, zero for last entry

J1 - column number

D1 - A matrix coefficient

Note: A value of zero for I1 must be included to stop the reading of the matrix coefficients. This is equivalent to including a blank card for the last entry of Card No. 10. Repeat Card No. 10 until all matrix coefficients have been read in.

Note: The SYSTEM program can be used to calculate the matrix coefficients. One output from SYSTEM is FOR01.DAT and will contain these coefficients. However, matrix coefficients not calculated by SYSTEM must be included here.

Option A for JFLAG = 1 through 4

(as per the original MATEXP program)

Card No. 11 (initial condition vector) Include if ICSS = 1 or 2

Column	1-2	3-5	6-17	
Format	I2	I3	E12.3	Repeat columns 3-17 5 per card
Input	MM	Row No.	I.C. Value	

Note: Insert blank card to stop reading in the initial condition vector.

Card No. 12 (disturbance vector) Include if JFLAG = 1 or 2

Column	1-2	3-5	6-17	
Format	I2	I3	E12.3	Repeat columns 3-7 5 per card
Input	KK	Row No.	Z Value	

Note: Insert blank card to stop reading in the disturbance vector.

Option B for JFLAG = 5 (reactor control system or non-constant disturbance vector)

Card No. 11 (number of forcing vector elements calculated by the SYSTEM program)

Column	1-5
Format	I5
Input	NCOFX

NCOFX - The number of forcing vector elements calculated by SYSTEM. If more than NCOFX forcing vector elements are needed, they must be input in DISTRB. NCOFX must be $\geq$ 1.

Card No. 12 (forcing vector coefficients calculated by SYSTEM)

Column	1÷70
Format	5E14.5
Input	COFX(I)

COFX(I) - The forcing vector elements calculated by SYSTEM. Card No. 12 is repeated until NCOFX elements have been input. If more than NCOFX elements are needed, include their input in DISTRB.

Card No. 13 (data used by the reactor control system which has already been input into the SYSTEM program)

Column	1-14	15÷28
Format	E14.5	E14.5
Input	BETAT	GEN

BETAT - total delayed neutron fraction

GEN - neutron generation time (sec)

Note: If subroutine DISTRB is being used, but the reactor model is not, SYSTEM will not automatically calculate this card, therefore, include a blank card for this case.

<u>Card No. 14</u> (data used by the reactor control system which has already been input into the SYSTEM program)

Column	1-5	6-10	11-15	16-20	21-25
Format	5I5				
Input	ITYPE	NSET3	NSET2	NSET1	NROW1

ITYPE - The type of forcing function. See Card No. 9 of Section A.2 of the SYSTEM program instructions.

NSET3 - The state variable number of the power mismatch temperature signal.

NSET2 - The state variable number of the lead-lag compensated temperature signal.

NSET1 - The state variable number of the temperature set point signal.

NROW1 - The row number in which the reactivity induced by the control rods is

<u>Card No. 15</u> (data used by the reactor control system which has already been input into the SYSTEM program)

Column	1-14	15-28	29-42	43-56	51-70
Format	5E14.5				
Input	RK1	RK2	RK3	WMAX	WSO

See Card No. 14 and 15 of Section A.2 of the SYSTEM program instructions.

Card No. 16 (data used by the reactor control system which has already been input into the SYSTEM program)

Column	1-14	15-28	29-42	43-56	57-70
Format	5E14.5				
Input	HG	HGMAX	DHG	HFW	CP2

See Card Nos. 4, 7, 8, and 14 of Section A.2 of the SYSTEM program instructions.

Card No. 17 (data used by the reactor control system which has already been input into the SYSTEM program)

Column	1-14
Format	E14.5
Input	VCOF

See Card No. 4 of Section A.2 of the SYSTEM program instructions.

Note: Card Nos. 10 through 17 can be calculated and placed in the data files FOR01.DAT and FOR23.DAT by the SYSTEM program. See Section A.4 on how to execute the SYSTEM-MATEXP programming package.

A.4 EXECUTION OF THE SYSTEM-MATEXP PROGRAMMING PACKAGE

The SYSTEM-MATEXP programming package was executed on the Dec-System 10 at the University of Tennessee for this thesis. However, this program could be executed on other computer systems depending on the input-output devices available. Referring to Figure A.1, the abbreviation LUN stands for "logical unit number". Each LUN corresponds to an input-output device. The Fortran statement WRITE (1, 100) will cause the contents of the format statement labeled by 100 to be written into device 1. For this program, the following LUN's were used

1 - DSKC of the user's disk space

3 - line printer

5 - teletype

20 - DSKC of the user's disk space

21 - DSKC of the user's disk space

23 - DSKC of ther user's disk space

24 - DSKC of the user's disk space

25 - DSKC of the user's disk space

In order to execute the SYSTEM-MATEXP program, the following steps must be taken,

1. Assemble the data file FOR24.DAT by creating card numbers 1 through 14 as per the instructions of Section A.2.
2. Execute the SYSTEM program by typing the following command.

   ```
   .EX SYSTEM.FOR,FOR:IMSLIB/LIB
   ```

   In order to execute the SYSTEM program for the input parameter ITYPE=10 through 13, the user must first specify ITYPE=5 and perform steps 1 and 2 beforehand.
3. Assemble the data file MATEXP.DAT by creating card numbers 1 through 9 as per the instructions of Section A.3.
4. Add to the end of the MATEXP.DAT file the matrix coefficients

not calculated by the SYSTEM program (if any) as per card No. 10 of the instructions of Section A.3.

5. If subroutine DISTRB is called in MATEXP, but the reactor core (and thus the reactor controller) is not being considered, add a blank card to the front of the data file FOR23.DAT which has already been formed from step 2 (see card No. 13 of Section A.3).

6. Combine data files by typing the following command

   .COPY MATEXP.DAT=MATEXP.DAT,FOR01.DAT,FOR23.DAT

7. Program the forcing vector. This is done by modifying subroutine ROD for ITYPE = 1, 6, 10, subroutine STEAM for ITYPE = 2, 7, 11, subroutine VALUE for ITYPE = 3, 8, 12, subroutine FEED1 for ITYPE = 4, 9, 13, and subroutine FEED2 for ITYPE = 5.

8. Execute the MATEXP program by typing the following command.

   .EX MATEXP.FOR

9. If printed output is desired, two options can be made. The first option would be to type the following command.

   .PRINT OUTPUT.DAT

   The second option would be to change all the fortran statements WRITE (20, to WRITE (3, throughout the MATEXP program before performing step number 8 then skip step number 9 after performing step number 8.

10. If plotted output is desired, type the following commands.

    .COPY SEND.FOR=MATPLO.FOR,PLOT1.DAT,PLOT2.DAT

    .HSUBMIT SEND.FOR

APPENDIX B

CALCULATION OF THE THREE ELEMENT CONTROLLER MODEL WITH WESTINGHOUSE PARAMETERS

The following block diagram was given by Westinghouse[39] for the three element controller transfer function model:

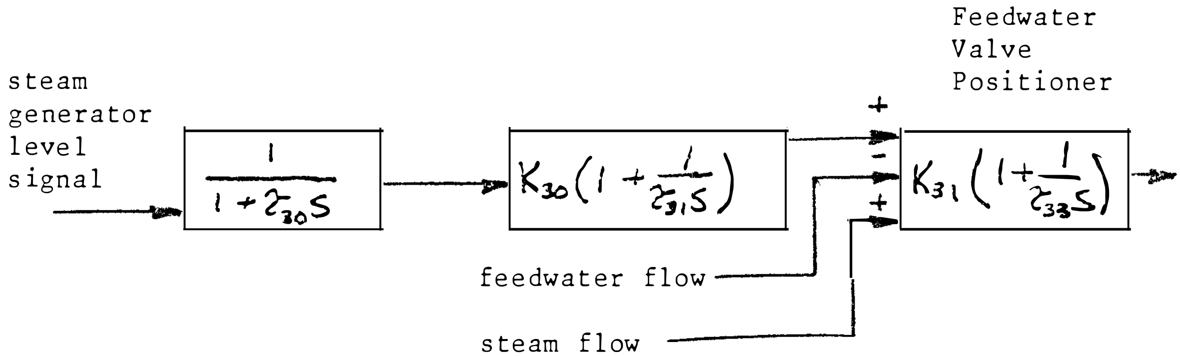

The values of the time constants and gains were also given to be

τ_{30} = 5 seconds

τ_{31} = 1800 seconds

τ_{33} = 200 seconds

K_{30} = 3% Full Flow/% Level Span

K_{31} = 1% Valve Lift/% Full Flow

It is desired to calculate the equivalent parameters for the three element controller block diagram of Figure 2.10 on page 30. The parameters will be calculated for the Sequoyah 100 percent power model used throughout this thesis. The following data are needed to evaluate the parameters

1. Nominal steam flow rate = maximum steam flow rate

   = 3.731×10^6 lbm/hr = 1036.389 lbm/sec

2. Assume that at 100 percent flow, the feedwater valves are 100 percent open

3. Westinghouse[39] has indicated that 1 percent span is equivalent to 0.12 ft of the downcomer level.

With this information the Westinghouse gains can be calculated

$$K_{30} = 3\ \frac{\%\ \text{Full Flow}}{\%\ \text{Level Span}} \times \frac{10.3639\ \text{lbm/sec}}{\%\ \text{Full Flow}} \times \frac{1\%\ \text{Level Span}}{0.12\ \text{ft}}$$

$$= 259.097\ \text{lbm/sec-ft}$$

$$K_{31} = 1\ \frac{\%\ \text{Valve Lift}}{\%\ \text{Full Flow}} \times \frac{100\%\ \text{Full Flow}}{100\%\ \text{Valve Lift}} = 1.0$$

It is easily seen that the equivalent three element controller parameters of Figure 2.10 on page 30 are

$$\tau = \tau_{30} = 5.0\ \text{sec}$$

$$\tau_1 = \frac{\tau_{31}}{K_{30}} = \frac{1800.0}{259.097} = 6.947\ \text{sec}$$

$$\tau_2 = \frac{\tau_{33}}{K_{31}} = \frac{200.0}{1.0} = 200.0\ \text{sec}$$

$$K_1 = K_{30} = 259.097\ \frac{\text{lbm}}{\text{ft-sec}}$$

$$K_2 = K_{31} = 1.0$$

APPENDIX C

DERIVATION OF THE HIGH ORDER PWR REACTOR CONTROL SYSTEM MODEL

From Westinghouse documentation on PWR control systems[38], equation (II.32) can be written for the average temperature set point for a change in power transfer function. Equation (II.32) is rearranged to obtain

$$\text{(C.1)} \quad (1 + \tau_{set1} s)\,\delta T_{S1}(s) = K_1\,\delta \%P_S(s).$$

An energy balance can be done on the secondary fluid in the steam generator to obtain

$$\text{(C.2)} \quad P = \frac{dE}{dt} = W_s h_s - W_{FW} h_{FW}.$$

Equation (C.2) is linearized to obtain

$$\text{(C.3)} \quad \delta P = W_s\,\delta h_s + h_s\,\delta W_s - W_{FW}\,\delta h_{FW} - h_{FW}\,\delta W_{FW}.$$

The percent power delivered by the secondary fluid is defined to be

$$\text{(C.4)} \quad \%P_s = \frac{P_s}{P_{max}}\,100 = \frac{W_s (h_g - h_{FW})\,100}{W_{max}(h_g - h_{FW})_{max}}.$$

At steady state, the feedwater flow will equal the steam flow. Let it be assumed that saturation conditions exist, which allows the following equation to be written

$$\text{(C.5)} \quad \delta\%P_s = \frac{100}{W_{max}(h_g - h_{FW})_{max}}\left[W_s \frac{\partial h_g}{\partial P_s}\,\delta P_s + h_g\,\delta W_s - W_s C_{PZ}\,\delta T_{FW} - h_{FW}\,\delta W_{FW}\right].$$

Substituting equation (C.5) into equation (C.1) will yield

(C.6) $$\left(1+\tau_{set1}s\right)\delta T_{s1}(s) = \frac{K_1 100}{W_{max}(h_g - h_{FW})_{max}} \times$$

$$\left[W_s \frac{\partial h_g}{\partial P_s}\delta P_s + h_g \delta W_s - W_s C_{PZ}\,\delta T_{FW} - h_{FW}\,\delta W_{FW}\right](s).$$

The inverse Laplace transform of equation (C.6) is

(C.7) $$\frac{d\,\delta T_{s1}}{dt} = -\frac{\delta T_{s1}}{\tau_{set1}} + \frac{K_1 100}{W_{max}(h_g - h_{FW})_{max}\tau_{set1}}\left[W_s \frac{\partial h_g}{\partial P_s}\delta P_s\right.$$

$$\left. + h_g \delta W_s - W_s C_{PZ}\,\delta T_{FW} - h_{FW}\,\delta W_{FW}\right].$$

Also from reference 38, equation (II.33) defines the lead-lag compensated average temperature transfer function. Equation (II.33) can be rearranged to obtain

(C.8) $$\left(1+\tau_{LAG1}s\right)\left(1+\tau_{LAG2}s\right)\delta T_{s2}(s) = \left(1+\tau_{LEAD}s\right)\left[\frac{\delta T_H' + \delta T_C'}{2}\right](s).$$

Equation (C.8) can again be rearranged, and an inverse Laplace transform will yield

(C.9) $$\tau_{LAG1}\tau_{LAG2}\frac{d^2\,\delta T_{s2}}{dt^2} + \left(\tau_{LAG1}+\tau_{LAG2}\right)\frac{d\,\delta T_{s2}}{dt} + \delta T_{s2} =$$

$$+\frac{1}{2}\left[\delta T_H' + \delta T_C'\right] + \frac{\tau_{LEAD}}{2}\left[\frac{d\,\delta T_H'}{dt} + \frac{d\,\delta T_C'}{dt}\right].$$

Equations (II.35) and (II.36) define the transfer functions of the hot and cold leg temperatures as measured by the resistance temperature detectors. Equations (II.35) and (II.36) can be rearranged and an inverse Laplace transform performed to obtain

$$\frac{d\,\delta T_H'}{dt} = \frac{1}{\tau_{RTD}}\left[\delta T_{HL} - \delta T_H'\right] \tag{C.10}$$

$$\frac{d\,\delta T_c'}{dt} = \frac{1}{\tau_{RTD}}\left[\delta T_{CL} - \delta T_c'\right]. \tag{C.11}$$

A dummy temperature variable will now be defined by the following equation

$$\frac{d\,\delta T_{s2}}{dt} = \delta T_{dummy}. \tag{C.12}$$

Thus, equations (C.12), (C.11), and (C.10) can be substituted into equation (C.9) to obtain

$$\frac{d\,\delta T_{dummy}}{dt} = \frac{-(\tau_{LAG1}+\tau_{LAG2})}{\tau_{LAG1}\tau_{LAG2}}\,\delta T_{dummy} - \frac{\delta T_{s2}}{\tau_{LAG1}\tau_{LAG2}} + \frac{1}{2}\left[1 - \frac{\tau_{LEAD}}{\tau_{RTD}}\right]\left[\delta T_c' + \delta T_H'\right] + \frac{\tau_{LEAD}}{2\tau_{RTD}}\left[\delta T_{CL} + \delta T_{HL}\right]. \tag{C.13}$$

Again from reference 38, equation (II.34) defines the temperature equivalent of a power mismatch transfer function. Equation (II.34) is rearranged to obtain

$$(C.14)\quad (1+\tau_{set3}s)\,\delta T_{s3}(s) = K_2 K_3 \left[\delta\%P_s - \delta\%P_N\right](s) .$$

$\%P_s$ has been defined previously by equation (C.5). $\frac{\delta P}{P_o}$ is the fractional change in nuclear power and is state variable number 1 in both the high order and low order PWR models (see Table II on page 10 and Table XVI on page 137).

The percent change in nuclear power is defined by the following equation

$$(C.15)\quad \delta\%P_N = \frac{100\,P_o}{P_{max}}\left(\frac{\delta P}{P_o}\right) = \frac{100\,W_s(h_g - h_{FW})}{W_{max}(h_g - h_{FW})_{max}}\frac{\delta P}{P_o} .$$

The gains K_2 and K_3 of the power mismatch transfer function are not constant (see Figures 2.16 on page 47 and 2.17 on page 48). The following equation will then be used to express K_2 and K_3

$$(C.16)\quad K_2 = K_{2_o} + \delta K_2$$

$$(C.17)\quad K_3 = K_{3_o} + \delta K_3$$

Substituting equations (C.17), (C.16), (C.15) and (C.5) into equation (C.14) and performing an inverse Laplace transform will yield

$$(C.18)\quad \frac{d\,\delta T_{s3}}{dt} = -\frac{\delta T_{s3}}{\tau_{set3}} + \frac{100}{\tau_{set3}\,W_{max}(h_g - h_{FW})_{max}}\, X$$

equation (C.18) continued

$$\left[K_{2_0}K_{3_0} + K_{2_0}\delta K_3 + K_{3_0}\delta K_2 + \delta K_2 \delta K_3\right] \times$$

$$\left[W_s \frac{\partial h_g}{\partial P_s}\delta P_s + h_g \delta W_s - C_{P2} W_s \delta T_{FW} - h_{FW}\delta W_{FW} - W_s (h_g - h_{FW})\frac{\delta P}{P_0}\right].$$

Equations (C.18), (C.13), (C.12), (C.11), (C.10) and (C.7) are the final form of the state variable equations for the reactor control system of the high order PWR model. Subroutine DISTRB is used to simulate the nonlinear gain of equation (C.18). The values of the parameters used to calculate the coefficients were obtained from reference 38 and are given in Table VIII on page 45.

APPENDIX D

DERIVATION OF THE TURBINE-FEEDWATER HEATER SYSTEM MODEL

D.1 Introduction

This appendix is written with the intent of deriving a turbine and feedwater heater model as presented in reference 11. The derivation of the model is not shown in reference 11, therefore the equations are derived in this appendix. The models represented here for the turbine and feedwater heaters attempt to follow the developments that led to the documented IBM model. This model proved very useful and convenient in giving a balance-of-plant model within the time schedule available for this study. However, some of the approaches differ from the author's preferred choices. Nevertheless, the model was used to expedite the present work. The equations as they appear in reference 11 consist of a set of nonlinear algebraic and differential equations. The computer code, MATEXP, solves a set of first order linear differential equations. In order to use MATEXP with this model, it is necessary to linearize the nonlinear equations. However, these equations can also be solved in their nonlinear form if desired (see Shankhar[32], IBM[11]).

Table XI on page 85 gives a listing and description of all the parameters used in this model. Table XI on page 85 also gives a value of these parameters at steady state initial conditions. These values were obtained for a typical 1200 MWe plant at 100 percent power from references 11 and 29. Figure 2.28 on page 84 shows a block diagram of the turbine-feedwater heater model. This figure shows all the differential and algebraic variables presented in this appendix. The reader should refer to page 85 and page 84 while reading this appendix.

Section D.2 of this appendix presents the derivation of the differential equations. Section D.3 presents the derivation of the turbine shaft power. Section D.4 presents all the algebraic equations needed to describe the system in a state variable form. Section D.5 presents the final form of both the linear and non-linear form of the equations. Section D.5 also gives the final calculated linear equations used in this study.

The isolated turbine-feedwater heater model can be perturbed by four forcing functions as presented in Chapter II. The results of these four cases are shown on pages 95, 287, 290 and 293.

D.2 Differential Equations

i) Nozzle chest

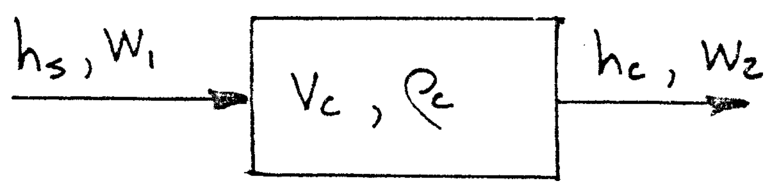

A mass balance over the constant nozzle chest volume V_c will result in the following equation

$$\frac{dM}{dt} = W_1 - W_2 . \tag{D.1}$$

Because the volume is constant the mass, M, can be expressed as $\rho_c V_c$. After rearranging equation (D.1) and performing a linearization, the following equation will result

$$\frac{d\delta\rho_c}{dt} = \frac{1}{V_c}\left[\delta W_1 - \delta W_2\right]. \tag{D.2}$$

An energy balance on the nozzle chest will result in the following equation

(D.3) $$\frac{dE}{dt} = W_1 h_s - W_2 h_c$$

The energy stored in the volume V_c can be expressed as $E=Mu_c$. The mass, as before, can be expressed as $M=\rho_c V_c$. Thus equation (D.3) can be written as

(D.4) $$V_c \rho_c \frac{du_c}{dt} + V_c u_c \frac{d\rho_c}{dt} = W_1 h_s - W_2 h_c .$$

Callender's empirical state equation[11,14,40], which relates enthalpy, specific volume, and pressure can be used to eliminate u_c from equation (D.4). This expression is reasonably valid for superheated steam. The complete Callender's relation is given by

(D.5) $$p_c v_c = \frac{J}{g_c}\left[k_1 h_c - k_2 - k_3 p_c\right]$$

where k_1, k_2, and k_3 are constants given on page 85 for h_c units of B/lbm, v_c units of ft^3/lbm, and p_c units of lbf/ft^2. The product $k_3 p_c J$ is much smaller than the other products of equation (D.5), therefore this product will be assumed equal to zero. Then, after differentiation, equation (D.5) can be expressed as

(D.6) $$p_c dv_c + v_c dp_c = \frac{J k_1}{g_c} dh_c .$$

By definition, the enthalpy h_c can be expressed as

(D.7) $$h_c \equiv u_c + \frac{p_c v_c}{J} .$$

Upon differentiation and rearranging, equation (D.7) can be written as

$$du_c = dh_c - \frac{p_c dv_c}{J} - \frac{v_c dp_c}{J} \tag{D.8}$$

Substituting equation (D.6) into equation (D.8) will result in

$$du_c = dh_c - \frac{k_1}{g_c} dh_c \tag{D.9}$$

After rearranging and division by dt, equation (D.9) can be written as

$$\frac{dh_c}{dt} = \frac{1}{1 - \frac{k_1}{g_c}} \frac{du_c}{dt} \tag{D.10}$$

Then equations (D.10), (D.7) and (D.2) can be substituted into equation (D.4), resulting in

$$\frac{dh_c}{dt} = \frac{1}{1 - \frac{k_1}{g_c}} \left[\frac{W_1 h_s}{V_c \rho_c} - \frac{W_2 h_c}{V_c \rho_c} + \left(\frac{P_c}{J \rho_c^2} - \frac{h_c}{\rho_c} \right) \left(\frac{W_1 - W_2}{V_c} \right) \right]. \tag{D.11}$$

Then after linearization and division by h_{c_0}, equation (D.11) will become

$$\frac{d \frac{\delta h_c}{h_{c_0}}}{dt} = \frac{1}{1 - \frac{k_1}{g_c}} \left[\frac{P_c}{J V_c \rho_c^2 h_c} \delta W_1 + \frac{W_1}{V_c \rho_c h_c} \delta h_s - \frac{P_c}{J \rho_c^2 V_c} \delta W_2 - \frac{W_1}{\rho_c V_c} \frac{\delta h_c}{h_{c_0}} \right]. \tag{D.12}$$

ii) High Pressure Turbine

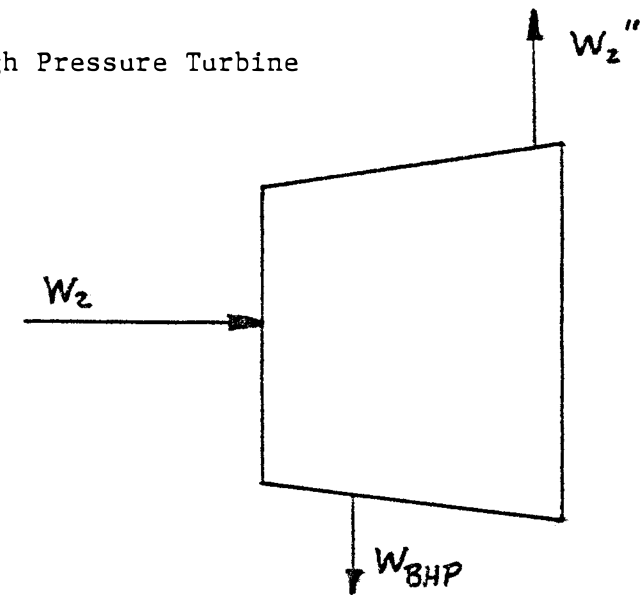

A mass balance on this system will result in

$$\frac{dM}{dt} = W_2 - W_2'' - W_{BHP} \tag{D.13}$$

It will be assumed that the regenerative bleed flow, W_{BHP}, is equal to $K_{BHP}\, W_2$. "Let T_{W2} be the time constant associated with volume of the bleed lines".[11] This will allow the approximate differential equation for the exiting flow to the reheater to be obtained from equation (D.13). In addition, equation (D.13) will be linearized and divided by W_{2_0}'' to obtain

$$\frac{d\,\frac{\delta W_2''}{W_{2_0}''}}{dt} = \frac{1}{T_{W2}}\left[\frac{1-K_{BHP}}{W_{2_0}''}\,\delta W_2 - \frac{\delta W_2''}{W_{2_0}''}\right]. \tag{D.14}$$

iii) Reheater and Moisture Separator

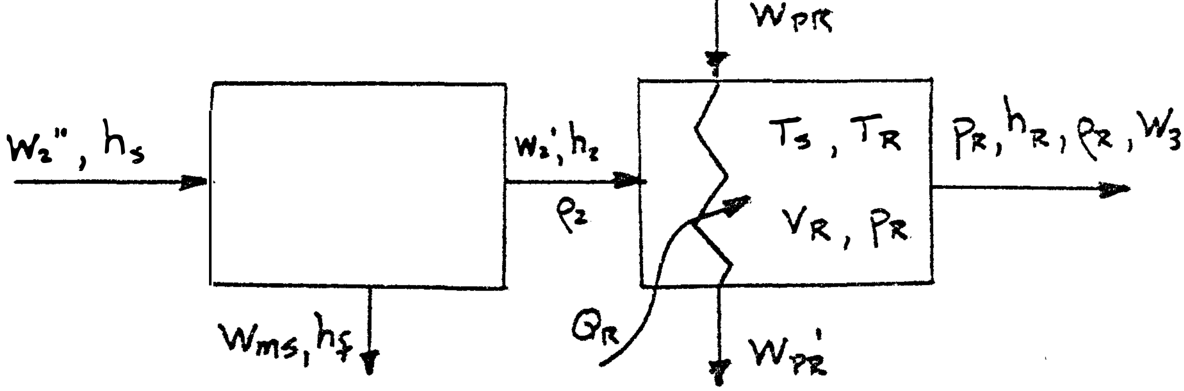

If one performs a mass balance on the reheater shell side, the following equation will result

$$\frac{dM}{dt} = W_2' - W_3 \tag{D.15}$$

Because the reheater volume remains constant, the mass can be written as $M=V_R\rho_R$. Thus, after linearization, equation (D.15) can be written as

$$\frac{d\delta\rho_R}{dt} = \frac{1}{V_R}\left[\delta W_2' - \delta W_3\right] \tag{D.16}$$

An energy balance can be made on the shell side of the reheater, which will result in the following equation

$$\frac{dE}{dt} = Q_R + W_2' h_2 - W_3 h_R \tag{D.17}$$

The internal energy of this control volume can be written as $E=Mu_R$. This can also be written as $E=V_R\rho_R u_R$. Substituting this expression for energy into equation (D.17) will result in the following equation

$$V_R \rho_R \frac{du_R}{dt} + V_R u_R \frac{d\rho_R}{dt} = Q_R + W_2' h_2 - W_3 h_R \tag{D.18}$$

Because the steam leaving the reheater of the shell side is superheated, a substitution can be made for the $\frac{du_R}{dt}$ term of equation (D.18) similar to that of equation (D.10) except the subscript c is replaced with subscript R. This expression, along with equation (D.16) can be substituted into equation (D.18) and rearranged to obtain

$$\frac{dh_R}{dt} = \frac{1}{1-\frac{k_1}{g_0}} \left[\frac{Q_R + W_2' h_2 - W_3 h_R}{V_R \rho_R} + \left(\frac{P_R}{J\rho_R^2} - \frac{h_R}{\rho_R}\right)\left(\frac{W_2' - W_3}{V_R}\right)\right]. \tag{D.19}$$

A linearization of the above equation and division by h_{RO} will yield

$$\frac{d\frac{\delta h_R}{h_{R_0}}}{dt} = \frac{1}{1-\frac{k_1}{g_0}} \left[\left(\frac{h_2}{h_R V_R \rho_R} + \frac{P_R}{J V_R h_R \rho_R^2} - \frac{1}{\rho_R V_R}\right)\delta W_2' \right. \tag{D.20}$$

$$+ \frac{W_2}{V_R \rho_R h_R}\delta h_2 - \frac{P_R}{J\rho_R^2 V_R}\delta W_3$$

$$\left. - \frac{W_2'}{\rho_R V_R}\frac{\delta h_R}{h_{R_0}} + \frac{\delta Q_R}{V_R \rho_R h_R}\right].$$

If a mass balance is now performed on the tube side of the reheater, the following equation can be written

$$\frac{dM}{dt} = W_{PR} - W_{PR}' \tag{D.21}$$

Let it be assumed that the control volume for the reheater tube side is a "well mixed tank." Thus, the mass M can be written as $M = W_{PR}' T_{R1}$ where T_{R1} is a constant. After linearization and division by W_{PR_o}', the following equation is obtained

$$\frac{d \dfrac{\delta W_{PR}'}{W_{PR_o}'}}{dt} = \frac{1}{T_{R1}} \left[\frac{\delta W_{PR}}{W_{PR_o}'} - \frac{\delta W_{PR}'}{W_{PR_o}'} \right]. \tag{D.22}$$

In equation (D.20), the heat transfer across the reheater tubes, δQ_R, is given as a state variable. IBM[11] uses an approximation to obtain the reheater heat transfer. Basically, two assumptions are made: (1) the dynamic heat transfer is assumed to be equal to the steady state heat transfer modified by a time constant, (2) the heat transfer coefficient for heat transfer across the reheater tubes is assumed to vary as the tube side flow rate to the first power. These assumptions are not correct. A proper dynamic heat balance will avoid assumption (1). Assumption (2) is incorrect because the overall heat transfer coefficient depends on surface effects on both sides of the tubes and on tube conduction effects. The IBM[11] equation is

$$T_{R2} \frac{dQ_R}{dt} + Q_R = H_R \left[\frac{W_{PR} + W_{PR}'}{2} \right] \left[T_S - T_R \right] \tag{D.23}$$

where

T_S = main steam temperature

T_R = reheat steam temperature

H_R = overall heat transfer coefficient/flow

If the flow does not change much, then equation (D.23) should still give good results. However, it is just as easy to model it correctly, and future modifications should incorporate a change in equation (D.23). However, due to the time schedule of this research, and the necessity to obtain a usable model, the IBM[11] model was not changed for this thesis. Upon linearization, equation (D.23) will become

$$\frac{d\,\delta Q_R}{dt} = \frac{1}{T_{RZ}}\Big[\frac{H_R}{2}(T_S - T_R)(\delta W_{PR} + \delta W_{PR}') + \frac{H_R}{2}(W_{PR} + W_{PR}')(\delta T_S - \delta T_R) - \delta Q_R\Big]. \tag{D.24}$$

iv) Low Pressure Turbine

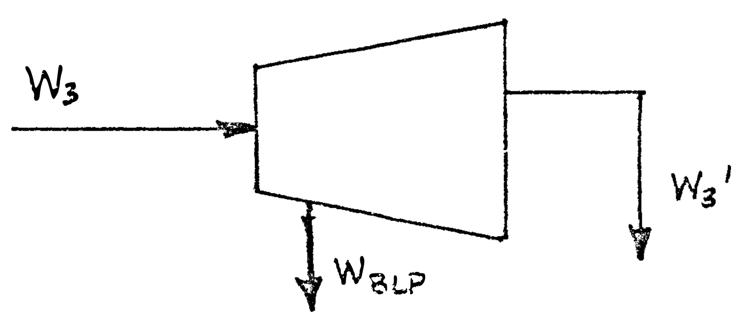

A mass balance of the control volume for the LP turbine will result in the following equation

$$\frac{dM}{dt} = W_3 - W_{BLP} - W_3'. \tag{D.25}$$

It will be assumed that the regenerative bleed flow, W_{BLP}, is equal to $K_{BLP}\, W_3$. If T_{W3} is defined to be the time constant associated with the volume of the bleed lines, the approximate differential equation for the flow to the condenser can be obtained from equation (D.25). In addition, equation (D.25) will be linearized and divided by W_{3_0}' to obtain

$$\frac{d\,\frac{\delta W_3'}{W_{3_0}'}}{dt} = \frac{1}{T_{W3}}\left[\frac{1-K_{BLP}}{W_{3_0}'}\,\delta W_3 - \frac{\delta W_3'}{W_{3_0}'}\right] \tag{D.26}$$

v) Feedwater Heater #1

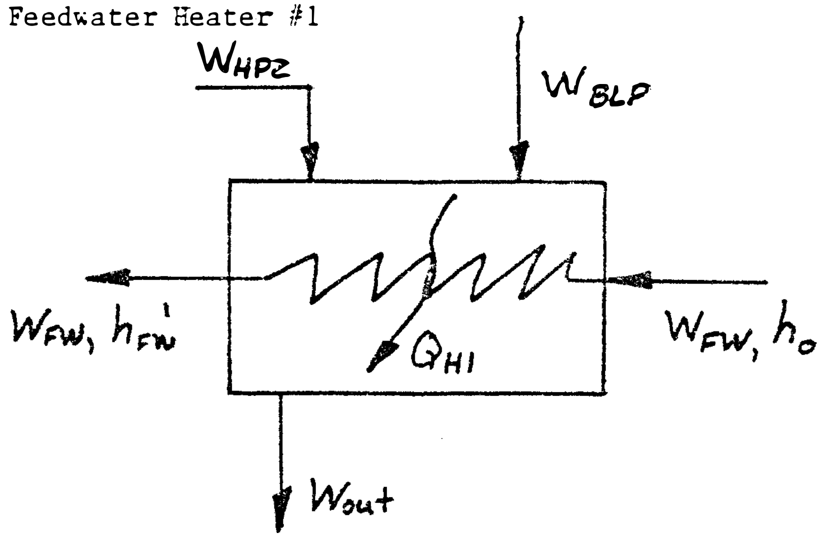

The following equation can be obtained by performing an energy balance on the tube side of feedwater heater #1

$$\frac{dE}{dt} = Q_{H1} + h_o W_{FW} - h_{FW}' W_{FW} \tag{D.27}$$

The energy in this control volume can be expressed as $E=Mu_{FW}'$. If it is assumed that the control volume is a "well mixed tank" then the mass can be expressed as $M=T_{H1}W_{FW}$ where T_{H1} is a constant. This will result in

$$(D.28)\quad T_{H1} W_{FW} \frac{du_{FW}'}{dt} + T_{H1} u_{FW}' \frac{dW_{FW}}{dt} = Q_{H1} + W_{FW}(h_o - h_{FW}')$$

The internal energy term can be expressed as $u_{FW}' = h_{FW}' - (pv)_{FW}'$. Because this fluid is in a liquid state, it will be essentially incompressible. Therefore, the change in the $(pv)_{FW}'$ term will be small compared to the change in the enthalpy term. This will allow the internal energy to be expressed as $u_{FW}' \approx h_{FW}'$. Then equation (D.28) can be written as

$$(D.29)\quad \frac{dh_{FW}'}{dt} = \frac{Q_{H1}}{T_{H1} W_{FW}} + \frac{(h_o - h_{FW}')}{T_{H1}} - \frac{h_{FW}'}{W_{FW}} \frac{dW_{FW}}{dt}$$

The heat transfer from the shell side to the tube side will be expressed as an effective flow on the shell side multiplied by a constant. If it is assumed that the effective flow rate is equal to $W_{HP2} + W_{BLP} = W_{HP2} + K_{BLP}W_3$, the heat transfer from the shell side to the tube side can be written as

$$(D.30)\quad Q_{H1} = H_{FW}(K_{BLP}W_3 + W_{HP2})$$

The constant H_{FW} could be called the latent heat removed from the steam entering the shell side of feedwater heater #1 as it condenses across the feedwater heater tubes. The only comment that the IBM[11] report has made is "the proportionality constant H_{FW} is calculated during the initialization phase."[11] Therefore one must assume that given the steam flows W_3 and W_{HP2}, and the initial heat transfer Q_{H1}, the constant H_{FW} is determined. However, the numerical value of H_{FW} used by IBM and for this thesis (given on page 85) is the same for feedwater heater #1 and feedwater heater #2. Equation (D.29) will now be written as

$$\text{(D.31)} \quad \frac{dh'_{FW}}{dt} = \frac{H_{FW}}{T_{H1} W_{FW}} \left[K_{BLP} W_3 + W_{HP2} \right] + \frac{(h_o - h'_{FW})}{T_{H1}} - \frac{h'_{FW}}{W_{FW}} \frac{dW_{FW}}{dt}$$

Assuming that the inlet enthalpy change is zero ($\delta h_o = 0$), linearization of the above equation will result in

$$\text{(D.32)} \quad \frac{d\,\delta h'_{FW}}{dt} = \frac{H_{FW}}{T_{H1} W_{FW}} \left[K_{BLP} \delta W_3 + \delta W_{HP2} \right] - \frac{\delta h'_{FW}}{T_{H1}} - \frac{h'_{FW}}{W_{FW}} \frac{d\,\delta W_{FW}}{dt} - \frac{H_{FW}}{T_{H1} W_{FW}^2} \left(K_{BLP} W_3 + W_{HP2} \right) \delta W_{FW}$$

The high order PWR model presented in Chapter II has a representation for the feedwater flow rate entering the UTSG. It will be assumed that the feedwater flow rate and its derivative are the same through the complete feedwater heater system. Thus the feedwater flow rate, W_{FW}, will become a coupling term if the turbine-feedwater heater model is coupled to the UTSG model. The feedwater flow derivative term in equation (D.32) can be expressed by equation (II.30). This equation resulted from the three-element feedwater flow controller model. Equation (II.30) is repeated here for clarity

$$\text{(D.33)} \quad \frac{d\delta W_{FW}}{dt} = \delta r$$

If the turbine-feedwater heater odel is coupled to the physical low order PWR model of Chapter III, then the feedwater flow will be controlled perfectly. If the steam flow out of the UTSG is expressed as in equation (II.24), then the following equation will result

$$\text{(D.34)} \quad \frac{d\delta W_{FW}}{dt} = \epsilon_o \frac{d\delta P_s}{dt} + W_{s_o} \frac{d\,\delta\epsilon/\epsilon_o}{dt}$$

where $\frac{d\delta P_s}{dt}$ and $\frac{d\,\delta\epsilon/\epsilon_o}{dt}$ are expressed in state variable equations 10 and 23 respectively.

vi) Feedwater Heater #2

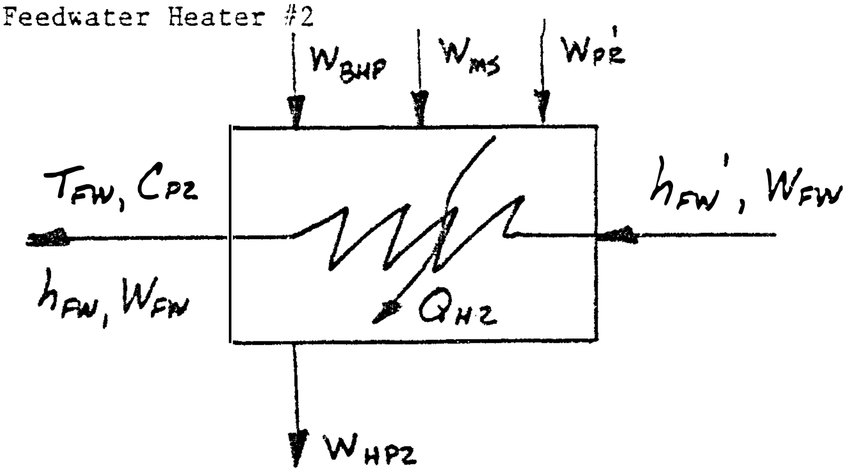

An energy balance similar to the energy balance done on feedwater heater #1 is done for feedwater heater #2 which will result in

(D.35) $$\frac{dE}{dt} = Q_{H2} + W_{FW}h'_{FW} - W_{FW}h_{FW}$$

By analogy with the derivation of the feedwater heater #1 equations, the following equations can be written

(D.36) $$E = T_{H2}W_{FW}h_{FW}$$

(D.37) $$Q_{H2} = H_{FW}(K_{BHP}W_2 + W_{ms} + W'_{PR})$$

Substitution of equations (D.36) and (D.37) into equation (D.35), linearization of the resulting equation, and letting δh_{FW} be set equal to $C_{P2}\,\delta T_{FW}$ (incompressible fluid), will obtain the following equation

$$\text{(D.38)} \quad \frac{d\,\delta T_{FW}}{dt} = \frac{1}{C_{p2} T_{H2}} \left[\frac{H_{FW}}{W_{FW}} \left(K_{BHP}\, \delta W_2 + \delta W_{ms} + \delta W_{PR}' \right) \right.$$

$$\left. - \frac{H_{FW}}{W_{FW}^2} \left(K_{BHP} W_2 + W_{ms} + W_{PR}' \right) \delta W_{FW} + \delta h_{FW}' \right]$$

$$- \frac{\delta T_{FW}}{T_{H2}} - \frac{h_{FW}}{W_{FW}} \frac{d\,\delta W_{FW}}{dt} .$$

A mass balance on feedwater heater #2 will give

$$\text{(D.39)} \quad \frac{dM}{dt} = W_{BHP} + W_{ms} + W_{PR}' - W_{HP2} .$$

If the control volume is assumed to be a "well mixed tank," then the mass can be expressed as $M = T_{HP2} W_{HP2}$, where T_{HP2} is a constant. Again $W_{BHP} = K_{BHP} W_2$ as before. Upon linearization and divison by W_{HP2o}, equation (D.39) will become

$$\text{(D.40)} \quad \frac{d \frac{\delta W_{HP2}}{W_{HP2o}}}{dt} = \frac{1}{T_{HP2} W_{HP2o}} \left[K_{BHP}\, \delta W_2 + \delta W_{ms} \right.$$

$$\left. + \delta W_{PR}' \right] - \frac{1}{T_{HP2}} \frac{\delta W_{HP2}}{W_{HP2o}} .$$

D.3 Derivation of the Turbine Shaft Power

The mechanical shaft power is given in Chapter II by equation (II.51) to be $P = F\tau$ where F equals the rotational frequency (60 Hz) and

τ is the torque applied to the generator shaft. This can also be written as

$$P_m = \Omega \left[T_{HP} + T_{LP} \right] \quad \text{(D.41)}$$

where Ω is the nominal frequency, usually equal to 60 Hz, and T_{HP} and T_{LP} are the high pressure turbine torque and the low pressure turbine torque respectively.

The flow entering the HP turbine, W_2, "is assumed totally available to produce torque since the regeneration bleed flow from the HP turbine is typically tapped right after the HP turbine."[11] This will allow the following equation to be written

$$T_{HP} = \frac{1}{J\Omega} W_2 \left(h_c - h_2 \right) \quad \text{(D.42)}$$

where h_c is the nozzle chest enthalpy of the steam entering the HP turbine and h_2 is the enthalpy of the steam as it leaves the HP turbine to the reheater.

Let it be assumed for the moment that the steam exhaust from the HP turbine has been expanded isentropically. If we define the exhaust enthalpy of the HP turbine for an isentropic process to be h_2', then the following equation can be written[12]

$$\eta_{HP} = \frac{h_c - h_2}{h_c - h_2'} . \quad \text{(D.43)}$$

The following empirical relationship has been developed[11] for the isentropic endpoint enthalpy of the HP turbine for nuclear power plants

$$h_2' = 1080.3 + 0.37\,(p_{R1} - 200) - 0.0011\,(p_{R1} - 200)^2 - 0.10\,(p_c - 1000.0) \tag{D.44}$$

where p_{R1} and p_c are the reheater entrance pressure (psia) and the nozzle chest pressure respectively (in psia). This empirical relationship given by equation (D.44) was applied to a 1000 Mwe BWR nuclear plant. This expression could be different for a PWR nuclear plant of a different power rating. However, for this thesis, no changes were made on the IBM[11] model. The pressures p_{R1} and p_c can be related by the following equation assuming an ideal gas relationship for saturated steam

$$\frac{p_{R1}}{\rho_2'^{\gamma}} = \frac{p_c}{\rho_c^{\gamma}} \tag{D.45}$$

Let W_3'' be defined to be the effective flow through the turbine. In equation form this will be $W_3'' = \frac{1}{2}(W_3 + W_2')$. This definition "arises from the assumption that one-half of the bleed flow (for regeneration purposes) produces torque, or alternatively, that the average bleed flow passes one half way through the LP turbine."[11] This will allow the following equation to be written

$$T_{HP} = \frac{\eta_{HP}}{J\Omega} W_2 (h_c - h_2') \tag{D.46}$$

where h_c and h_2 are the inlet and outlet enthalpies of the HP pressure turbine respectively. An analagous relationship exists for the LP turbine assuming isentropic expansion which allows the following equation to be written

$$\text{(D.47)} \quad T_{LP} = \frac{\eta_{LP}}{J\Omega} W_3'' \left(h_R - h_4' \right)$$

Upon linearization, and assuming that $\delta h_4'=0$, equations (D.41) through (D.47) will become

$$\text{(D.48)} \quad \delta P_m = \Omega \left(\delta T_{HP} + \delta T_{LP} \right)$$

$$\text{(D.49)} \quad \delta T_{HP} = \frac{\eta_{HP}}{J\Omega} \left[W_2 \delta h_c - W_2 \delta h_2' + (h_c - h_2') \delta W_2 \right]$$

$$\text{(D.50)} \quad \delta T_{LP} = \frac{\eta_{LP}}{J\Omega} \left[\left(\frac{W_3 + W_3'}{2} \right) \delta h_R + \left(\frac{h_R - h_4'}{2} \right) \left(\delta W_3 + \delta W_3' \right) \right]$$

$$\text{(D.51)} \quad \delta h_2' = 0.3678 \, \delta P_R - 0.10 \, \delta P_c$$

$$\text{(D.52)} \quad \delta \rho_2' = \left[\frac{P_R}{P_c} \right]^{1/\gamma} \delta \rho_c + \left[\frac{P_R}{P_c} \right]^{1/\gamma} \frac{\rho_c}{\gamma P_R} \delta P_R - \left[\frac{P_R}{P_c} \right]^{1/\gamma} \frac{\rho_c}{\gamma P_c} \delta P_c \, .$$

Equations (D.48) through (D.52) are combined to describe the mechanical shaft power. In this study subroutine DISTRB was used to calculate P_m at each time step in the solution. However, P_m could be incorporated as part of a constant coefficient system matrix by substituting equations (D.48) through (D.52) into the expression of P_m of a Pf controller model (see equation (II.56)). For this thesis the final calculated form of P_m is given in equation (D.88).

D.4 Algebraic Equations

The state variables of the turbine-feedwater heater model are given by Table XII on page 90. There are many algebraic variables in equations (D.1) through (D.52) which need to be described. W_1, can be related to the steam flow leaving the UTSG, W_s by the following equation

$$W_1 = (NUTSG)\, W_s = (NUTSG)\, \epsilon P_s \qquad \text{(D.53)}$$

where NUTSG is the number of UTSG's in the total plant, is the valve coefficient, and P_s is the steam pressure leaving the UTSG. This equation can be linearized to obtain

$$\delta W_1 = NUTSG \left[\epsilon_0 \, \delta P_s + W_{s_0} \frac{\delta \epsilon}{\epsilon_0} \right]. \qquad \text{(D.54)}$$

The steam flow entering the nozzle chest can be expressed by the following empirical relationship[11]

$$W_2 = \sqrt{g_c}\, A_{K2} \left[P_c \rho_c - P_2 \rho_2 \right]^{0.5} \qquad \text{(D.55)}$$

where A_{K2} is a constant given on page 85. Equation (D.55) is linearized to obtain

$$\delta W_2 = \frac{\sqrt{g_c}\, A_{K2}}{2\left[P_c\rho_c - P_2\rho_2\right]^{0.5}} \left[P_c\,\delta\rho_c + \rho_c\,\delta P_c - P_2\,\delta\rho_2 - \rho_2\,\delta P_2\right]. \tag{D.56}$$

The steam flow leaving the moisture separator and into the reheater can be obtained by performing an energy balance at steady state over the moisture separator as the control volume

$$W_2''\,h_2 - W_2'\,h_g - W_{ms}\,h_f = 0 = \frac{dE}{dt} \tag{D.57}$$

It is assumed that $W_{ms} = W_2'' - W_2'$. This will allow equation (D.57) to be rearranged and linearized to obtain

$$\delta W_2' = \left[\frac{h_2 - h_f}{h_{fg}}\right]\delta W_2'' - \frac{W_2''}{h_{fg}}\,\delta h_2\,. \tag{D.58}$$

The steam flow leaving the reheater and into the LP turbine can be described by the following empirical relationship[11]

$$W_3 = \sqrt{g_c}\,K_3\left[P_R\rho_R\right]^{0.5} \tag{D.59}$$

where K_3 is a constant. Equation (D.59) is linearized to obtain

$$\delta W_3 = \frac{K_3\sqrt{g_c}}{2\left[P_R\rho_R\right]^{0.5}}\left[P_R\,\delta\rho_R + \rho_R\,\delta P_R\right]. \tag{D.60}$$

The steam flow from the bypass line to the reheater shell side will follow the "critical flow"[2] assumption which will allow the following equation to be written

$$W_{PR} = \epsilon_2 P_s \tag{D.61}$$

Where ϵ_2 is the valve coefficient and P_s is the steam pressure of the UTSG. Linearization of equation (D.61) will yield

$$\delta W_{PR} = \epsilon_{2_0} \delta P_s + W_{PR_0} \frac{\delta \epsilon_2}{\epsilon_{2_0}} \tag{D.62}$$

Callender's empirical relationship[11] for superheated steam can be used on the nozzle chest and reheater outlet pressures to obtain

$$p_c = \frac{J\rho_c}{g_c}\left[k_1 h_c - k_2\right] \tag{D.63}$$

$$p_R = \frac{J\rho_R}{g_c}\left[k_1 h_R - k_2\right] \tag{D.64}$$

Equations (D.63) and (D.64) are linearized to obtain

$$\delta p_c = \frac{J}{g_c}\left[\rho_c k_1 \delta h_c + (k_1 h_c - k_2)\delta\rho_c\right] \tag{D.65}$$

$$\delta p_R = \frac{J}{g_c}\left[\rho_R k_1 \delta h_R + (k_1 h_R - k_2)\delta\rho_R\right]. \tag{D.65}$$

It will be assumed that the quality of the steam entering the nozzle chest and entering the reheater shell side is approximately 1.0. Therefore the following equations are obtained

(D.67) $$\delta h_s = \left(\frac{\partial h_s}{\partial P_s}\right) \delta P_s$$

(D.68) $$\delta T_s = \left(\frac{\partial T_{sat}}{\partial P_s}\right) \delta P_s$$

It is assumed that the steam on the tube side of the reheater behaves as an ideal gas (superheated). Thus the following equation is obtained

(D.69) $$p_R = R \rho_R T_R$$

Differentiating equation (D.69) yields

(D.70) $$dT_R = \frac{1}{R}\left[\frac{dp_R}{\rho_R} - \frac{p_R}{\rho_R^2}\, d\rho_R\right]$$

By definition, the enthalpy of the steam on the reheater tube side can be written as $h_R = u_R + \frac{p_R}{\rho_R J}$. Differentiating this equation will yield

(D.71) $$dh_R = du_R + \frac{dp_R}{J\rho_R} - \frac{p_R}{J\rho_R^2}\, d\rho_R \, .$$

Substituting equation (D.71) into equation (D.70) will give

(D.72) $$dT_R = \frac{J}{R}\left[dh_R - du_R\right].$$

Because the ideal gas law has been assumed, the internal energy can be written as $du_R = C_v dT_R$ where C_v is defined to be $C_v = \left[\frac{\partial u}{\partial T}\right]_{\substack{\text{constant}\\ \text{volume}}}$. Therefore, the temperature on the shell side of the reheater can be expressed as

(D.73) $$\delta T_R = \frac{\delta h_R}{\left[\frac{R}{J} + C_v\right]}$$

The steam leaving the moisture separator and entering the reheater is saturated. Thus the following equations can be obtained

(D.74) $$\delta h_z = \frac{\partial h_z}{\partial P_R}\,\delta P_R$$

(D.75) $$\delta \rho_z = \frac{\partial \rho_z}{\partial P_R}\,\delta P_R \approx \delta \rho_z'$$

D.5 Final Form of the Non-linear and Linear Differential Equations

The final form of the model will have 11 state variables. These state variables are described in Table XII on page 90. If it is desired to analyze the model in its nonlinear form, the following differential equations will be needed: (D.1), (D.11), (D.13), (D.15), (D.19), (D.21), (D.23), (D.25), (D.31), (D.35), (D.39).

In addition, the following assumptions which have been previously discussed are made

- mass of nozzle chest fluid = $V_c \rho_c$
- mass of HP turbine fluid = $W_2'' T_{w2}$
- mass of shell side reheater fluid = $V_R \rho_R$
- mass of tube side reheater fluid = $W_{PR}' T_{R1}$
- mass of LP turbine fluid = $W_3' T_{w3}$
- mass of shell side feedwater heater fluid = $W_{HP2} T_{HP2}$
- mass flow = $W_{BHP} = K_{BHP} W_2$
- mass flow = $W_{BLP} = K_{BLP} W_3$
- energy storage in feedwater heater #2 = $T_{H2} W_{FW} h_{FW}$
- heat transfer from shell to tube side of feedwater heater #2

  $= Q_{H2} = H_{FW}(K_{BHP} W_2 + W_{ms} + W_{PR}')$

  where V_c, T_{W2}, V_R, T_{R1}, T_{W3}, T_{HP2}, K_{BHP}, K_{BLP}, T_{H2}, and H_{FW} are constants.

The following algebraic equations would also be needed: (D.53), (D.55), (D.57), (D.59), (D.61), (D.63), and (D.64).

The mechanical shaft power would also be described by equations (D.41), (D.42), (D.43), (D.44), (D.45), (D.46), and (D.47). In addition, for a nonlinear solution, it will be assumed that a table of steam properties are available to update the thermodynamic properties at each step in the solution.

If it is desired to obtain a linear solution to the model, the following differential equations must be used: (D.2), (D.12), (D.14), (D.20), (D.22), (D.24), (D.26), (D.32), (D.38), (D.40), and (D.16).

In addition, the following algebraic equations should be substituted into the differential equations to obtain a state variable formulation: (D.54), (D.56), (D.58), (D.60), (D.62), (D.65), (D.66), (D.67), (D.68), (D.73), (D.74), and (D.75).

In addition, the mechanical shaft turbine power can be found by applying equations (D.48) through (D.52).

In this study, the linear solution to these equations was obtained. The data from page 85 was substituted into the algebraic equations. The resulting calculated algebraic equations were then substituted into the differential equations plus any remaining data from Table XI which has not been used in the algebraic equations, to obtain the final calculated equations in a state variable form. The final equations used in this study are

$$\frac{d\delta\rho_c}{dt} = +0.025\,\delta P_s + 20.73\,\frac{\delta\epsilon}{\epsilon_0} - 16.29\,\delta\rho_c + 1.93\,\delta\rho_R - 36.72\,\frac{\delta h_c}{h_{c_0}} + 5.88\,\frac{\delta h_R}{h_{R_0}} \tag{D.76}$$

$$\frac{d\frac{\delta h_c}{h_{c_0}}}{dt} = +0.015\,\delta P_s + 12.67\,\frac{\delta\epsilon_2}{\epsilon_{2_0}} - 31.15\,\frac{\delta h_c}{h_{c_0}} - 9.96\,\delta\rho_c + 1.18\,\delta\rho_R + 3.59\,\frac{\delta h_R}{h_{R_0}} \tag{D.77}$$

(D.78) $$\frac{d\,\frac{\delta W_z''}{W_{z_o}''}}{dt} = +0.393\,\delta\rho_c + 0.886\,\frac{\delta h_c}{h_{c_o}} - 0.047\,\delta\rho_R - 0.142\,\frac{\delta h_R}{h_{R_o}} - 0.5\,\frac{\delta W_z''}{W_{z_o}''}$$

(D.79) $$\frac{d\,\delta\rho_R}{dt} = +0.195\,\frac{\delta W_z''}{W_{z_o}''} - 0.271\,\delta\rho_R - 0.21\,\frac{\delta h_R}{h_{R_o}}$$

(D.80) $$\frac{d\,\frac{\delta h_R}{h_{R_o}}}{dt} = +0.616\,\frac{\delta W_z''}{W_{z_o}''} - 1.075\,\delta\rho_R - 1.277\,\frac{\delta h_R}{h_{R_o}} + 0.377\,\delta Q_R$$

(D.81) $$\frac{d\,\frac{\delta W_{PR}'}{W_{PR_o}'}}{dt} = -0.33\,\frac{\delta W_{PR}'}{W_{PR_o}'} + (4.0\times10^{-4})\,\delta P_s + 0.33\,\frac{\delta\epsilon_z}{\epsilon_{z_o}}$$

(D.82) $$\frac{d\,\delta Q_R}{dt} = -1.01\,\frac{\delta h_R}{h_{R_o}} + 0.008\,\frac{\delta W_{PR}'}{W_{PR_o}'} + (8.5\times10^{-5})\,\delta P_s - 0.25\,\delta Q_R + 0.013\,\frac{\delta\epsilon_z}{\epsilon_{z_o}}$$

(D.83) $$\frac{d\,\frac{\delta W_3'}{W_{3_0}'}}{dt} = +0.19\,\delta\rho_R + 0.146\,\frac{\delta h_R}{h_{R_0}} - 0.1\,\frac{\delta W_3'}{W_{3_0}'}$$

(D.84) $$\frac{d\,\delta h_{FW}'}{dt} = +1.352\,\delta\rho_R + 1.037\,\frac{\delta h_R}{h_{R_0}} - 0.01\,\delta h_{FW}'$$
$$+1.395\,\frac{\delta W_{HPZ}}{W_{HPZ_0}} - 0.0022\,\delta W_{FW} - 0.063\,\frac{d\,\delta W_{FW}}{dt}$$

(D.85) $$\frac{d\,\delta T_{FW}}{dt} = +1.338\,\delta\rho_c + 3.0144\,\frac{\delta h_c}{h_{c_0}} - 1.1\,\frac{\delta W_2''}{W_{2_0}''}$$
$$-0.16\,\delta\rho_R - 0.374\,\frac{\delta h_R}{h_{R_0}} + 0.46\,\frac{\delta W_{PR}'}{W_{PR_0}'}$$
$$+0.022\,\delta h_{FW}' - 0.025\,\delta T_{FW}$$
$$-0.0013\,\delta W_{FW} - 0.0997\,\frac{d\,\delta W_{FW}}{dt}$$

(D.86) $$\frac{d\,\frac{\delta W_{HPZ}}{W_{HPZ_0}}}{dt} = +0.044\,\delta\rho_c + 0.099\,\frac{\delta h_c}{h_{c_0}} - 0.036\,\frac{\delta W_2''}{W_{2_0}''}$$
$$-0.0052\,\delta\rho_R - 0.0122\,\frac{\delta h_R}{h_{R_0}}$$
$$+0.015\,\frac{\delta W_{PR}'}{W_{PR_0}'} - 0.1\,\frac{\delta W_{HPZ}}{W_{HPZ_0}}.$$

The final form of the turbine torque in ft-lbf is

(D.87) $$\delta T_{HP} = +1{,}184{,}187.03\ \delta\rho_c + 11{,}076{,}434.76\ \frac{\delta h_c}{h_{co}} - 140{,}272.02\ \delta\rho_R - 1{,}657{,}726.72\ \frac{\delta h_R}{h_{Ro}}$$

(D.88) $$\delta T_{LP} = +938955.00\ \delta\rho_R + 6{,}456{,}187.70\ \frac{\delta h_R}{h_{Ro}} + 386{,}305.53\ \frac{\delta W_3'}{W_{3o}'} .$$

Thus the final form of the total turbine power in units of Mw is

(D.89) $$\delta P_m = 605.28\ \delta\rho_c + 5661.52\ \frac{\delta h_c}{h_{co}} - 408.28\ \delta\rho_R - 2452.65\ \frac{\delta h_R}{h_{Ro}} + 197.45\ \frac{\delta W_3'}{W_{3o}'} .$$

From equation (D.86), the power produced by the HP turbine can be found by determining the thermodynamic state of the fluid in the nozzle chest and the reheater (input-output characteristics). From equation (D.87), the power produced by the LP turbine can be found by deter mining the thermodynamic state of the fluid in the reheater and the fluid flow entering the LP turbine. Therefore, this model assumes that the power delivered by the LP turbine is a function of input characteristics only. This is equivalent to saying that the thermodynamic state of the fluid in the condenser remains constant.

APPENDIX E

SOME FIGURES PLACED IN THE APPENDIX FOR CLARITY

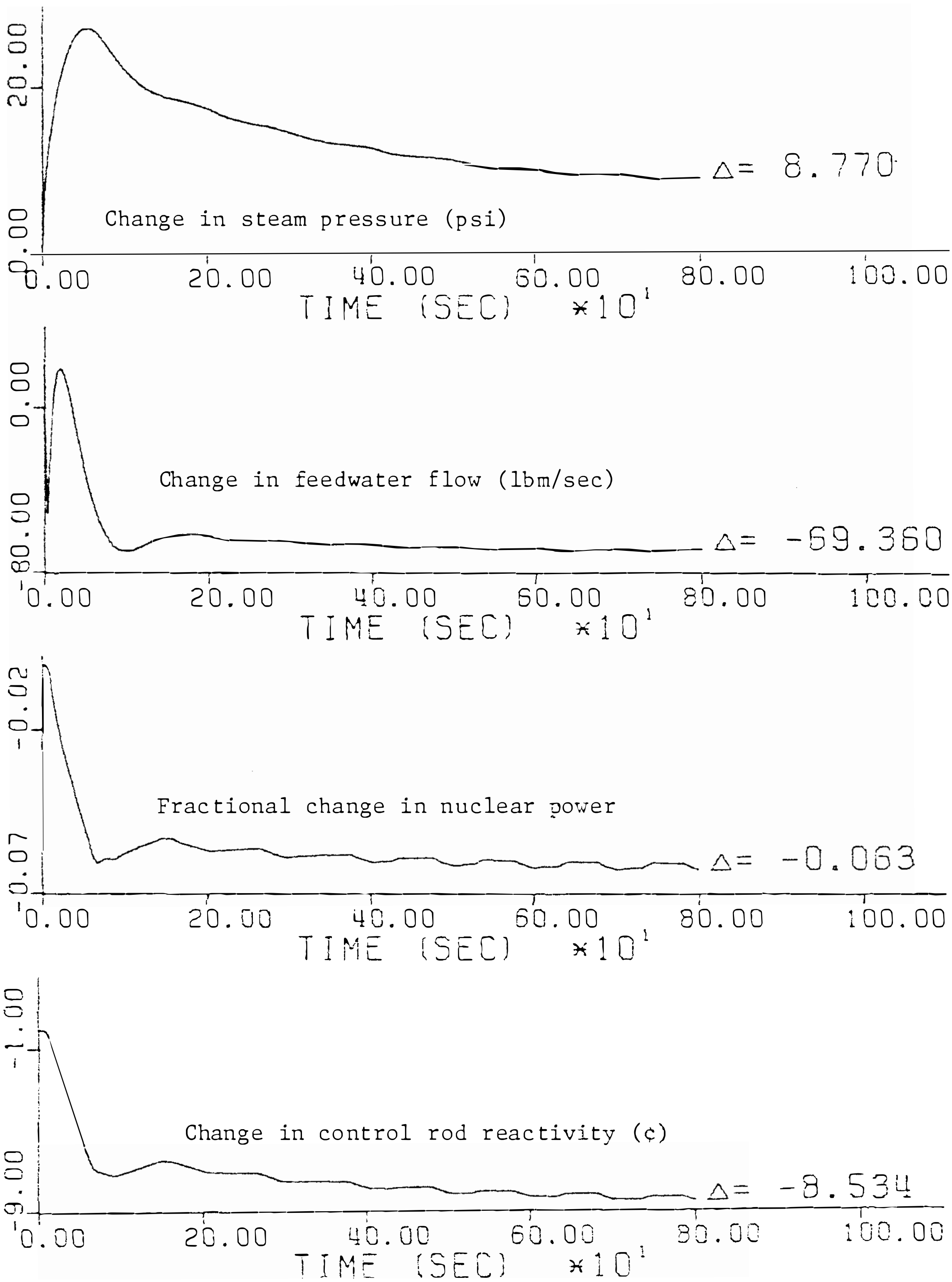

Figure E.1 Response of high order coupled reactor, three element controller, core, UTSG, and reactor controller models for a +10 percent step in valve coefficient showing the effect of making DBOUT and DBIN too small on the reactor control system (0.50°F and 0.25°F respectively).

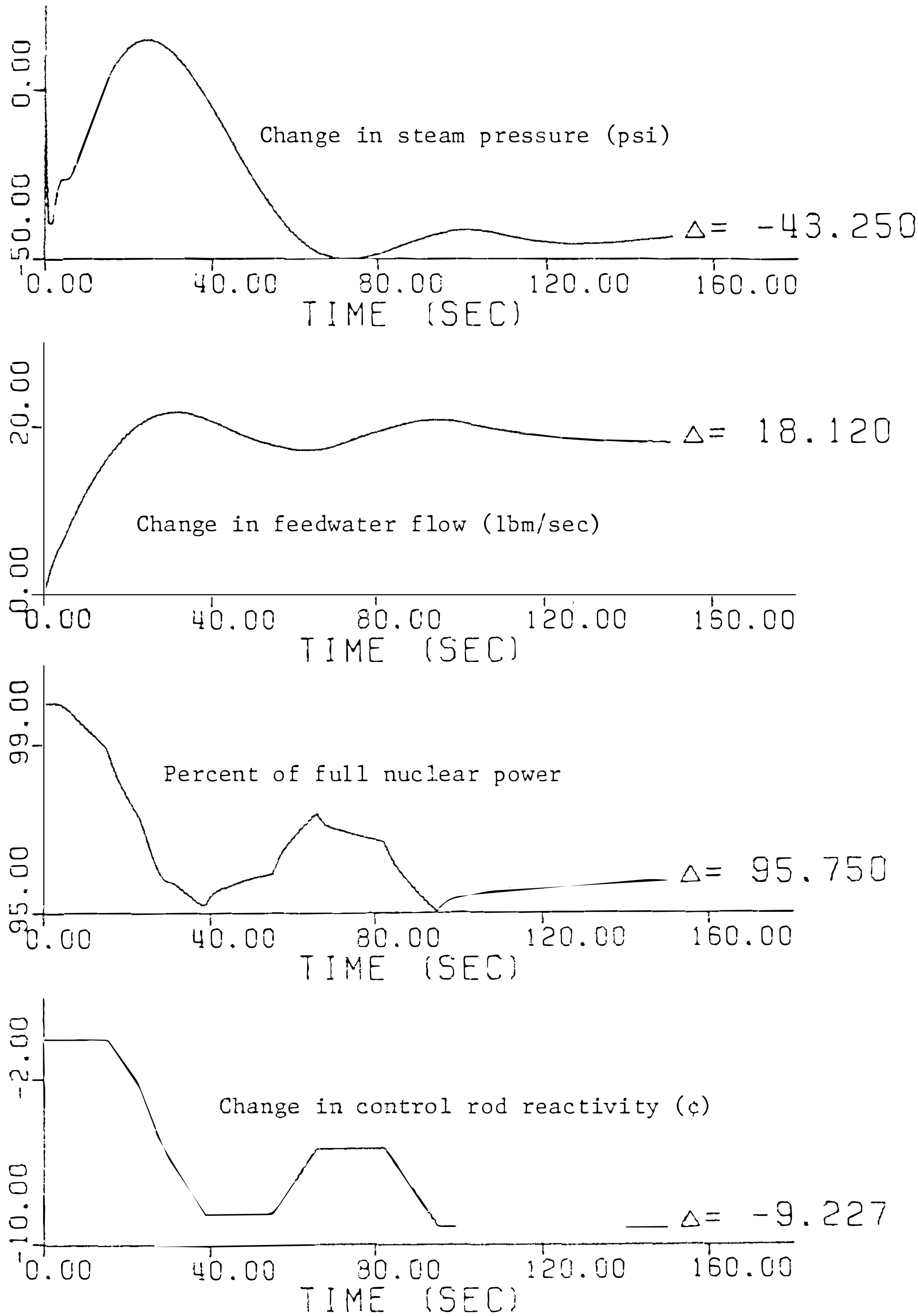

Figure E.2 Response of overall high order PWR system model for a -0.05 puMw (-50 Mw) step in tie line power flow showing the effect of making ROWSTP too large on the reactor control system (ROWSTP = 0.0225 [dollars/step]).

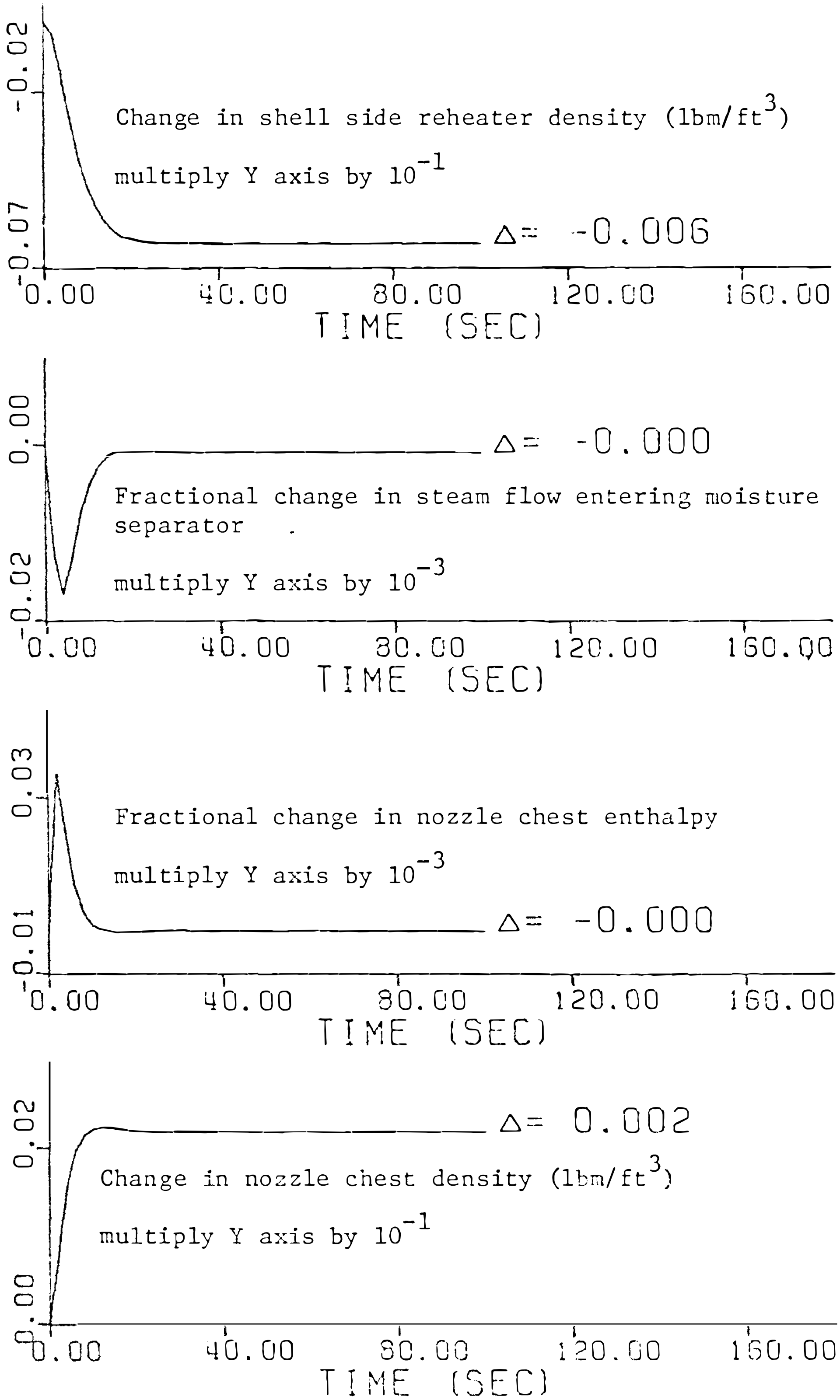

Figure E.3 Response of isolated turbine-feedwater heater model for a +10 percent step in the bypass steam valve coefficient.

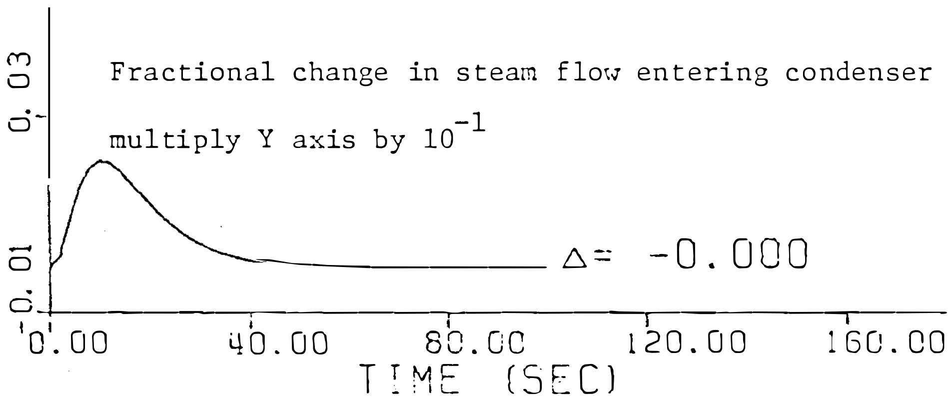

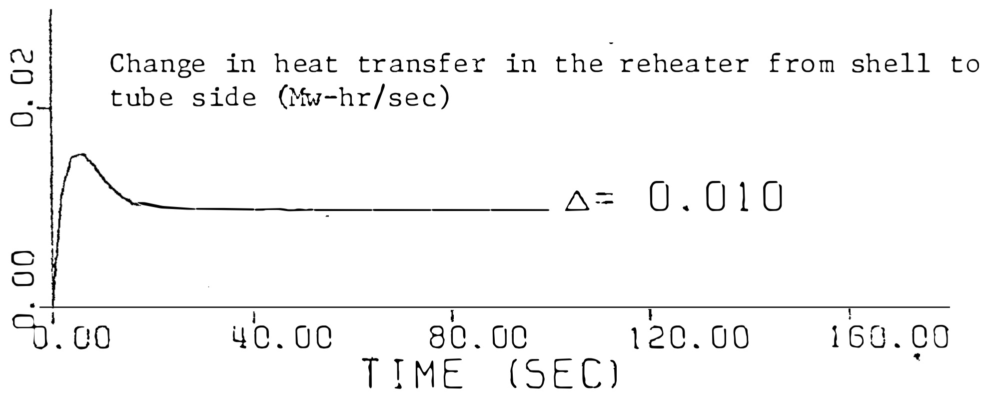

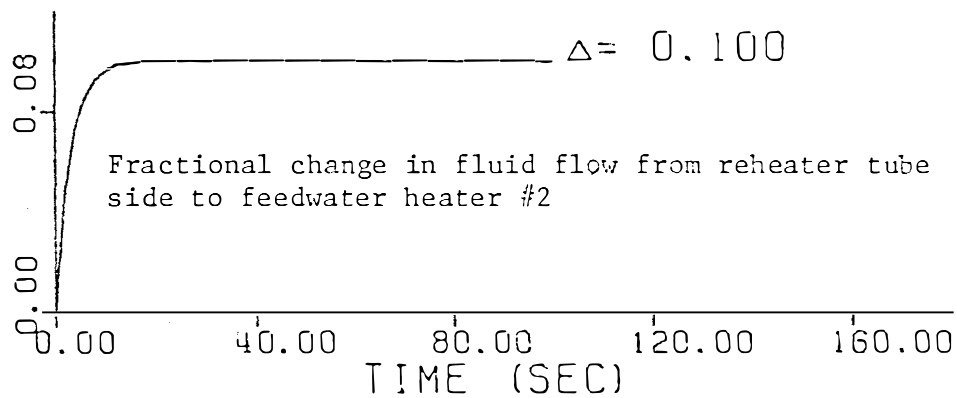

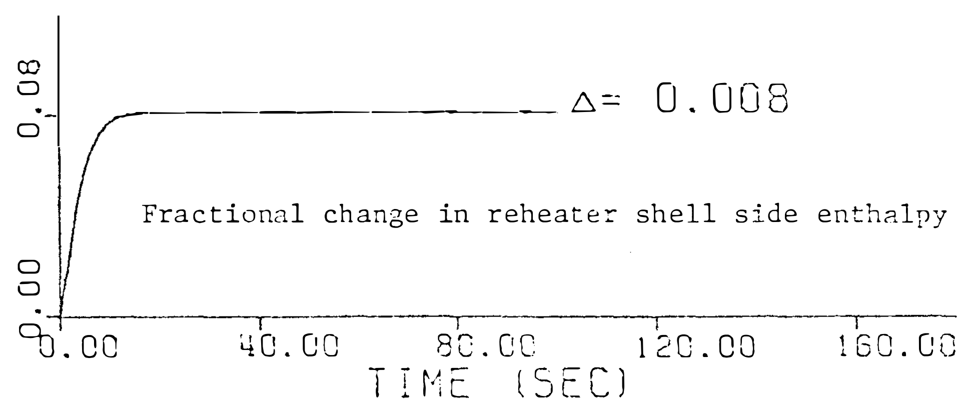

Figure E.3 (continued)

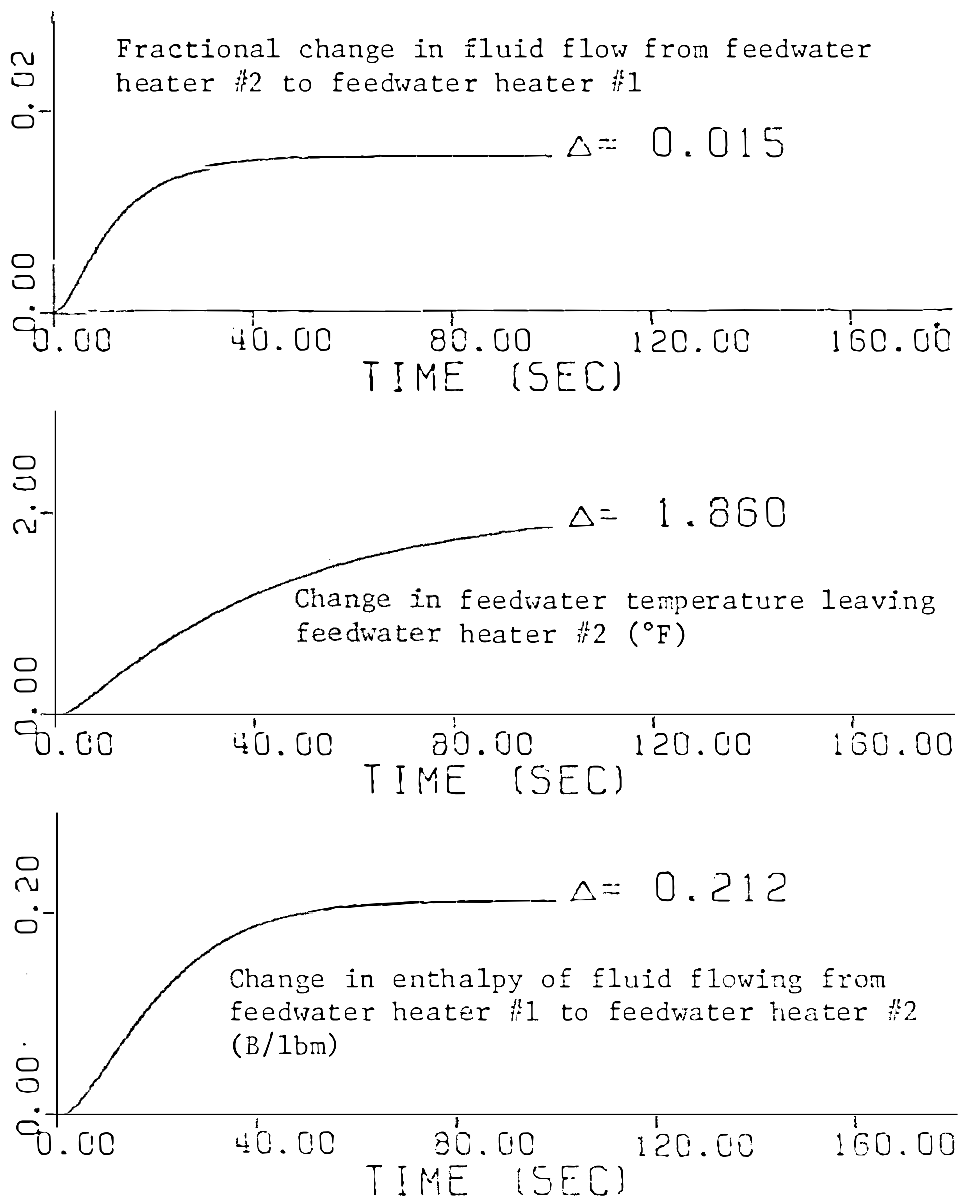

Figure E.3 (continued)

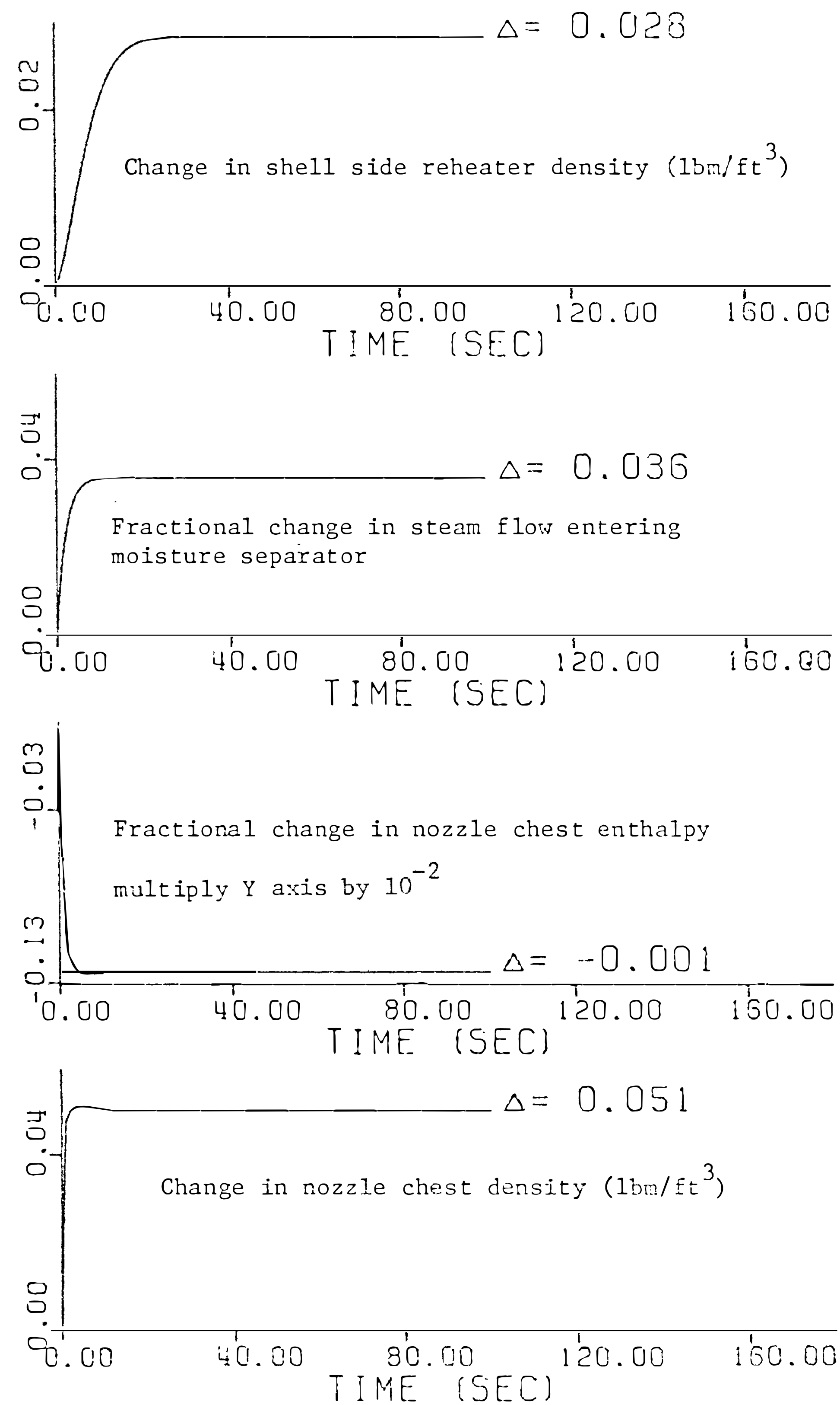

Figure E.4 Response of isolated turbine-feedwater heater model for a +30 psi step in inlet steam pressure.

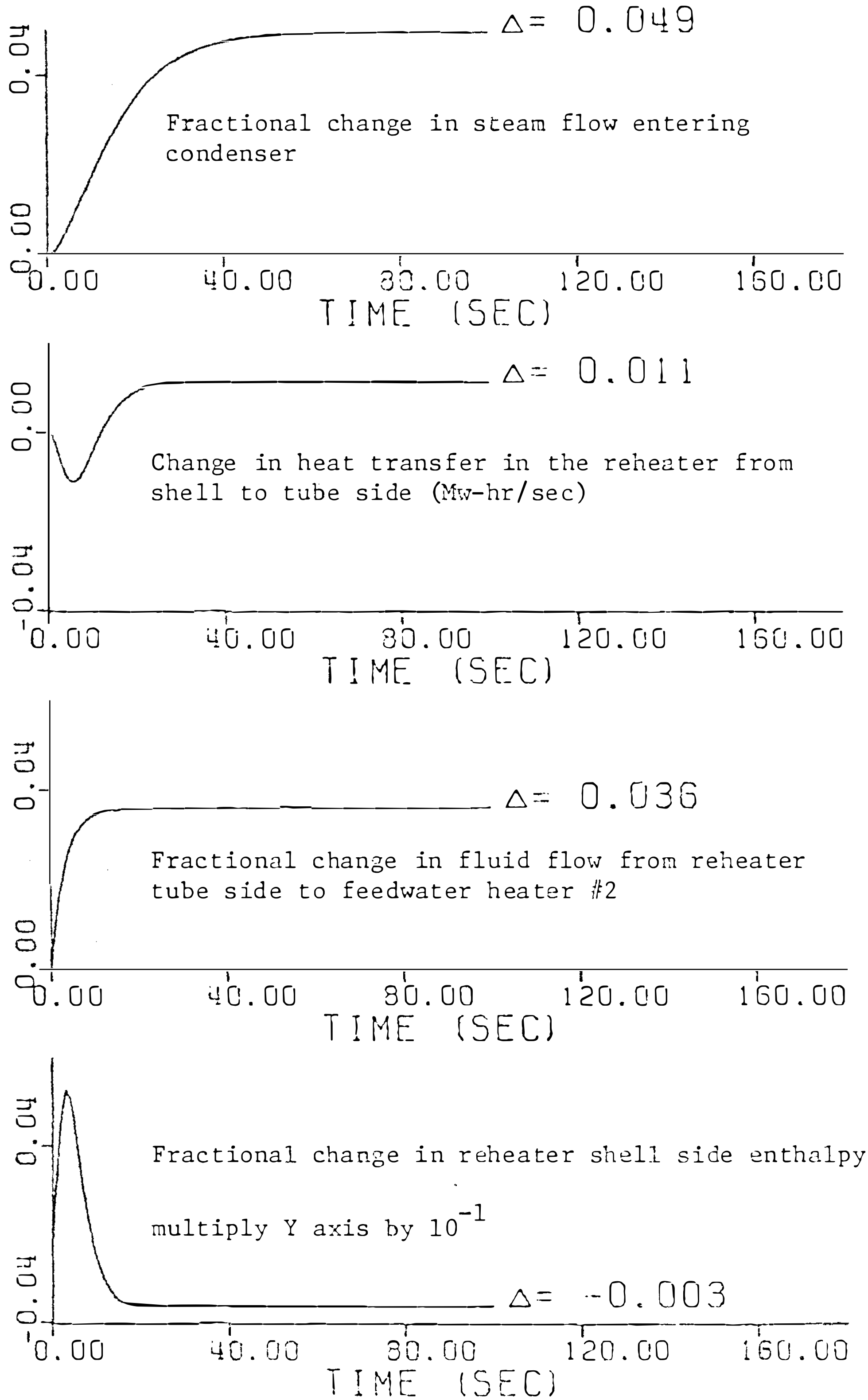

Figure E.4 (continued)

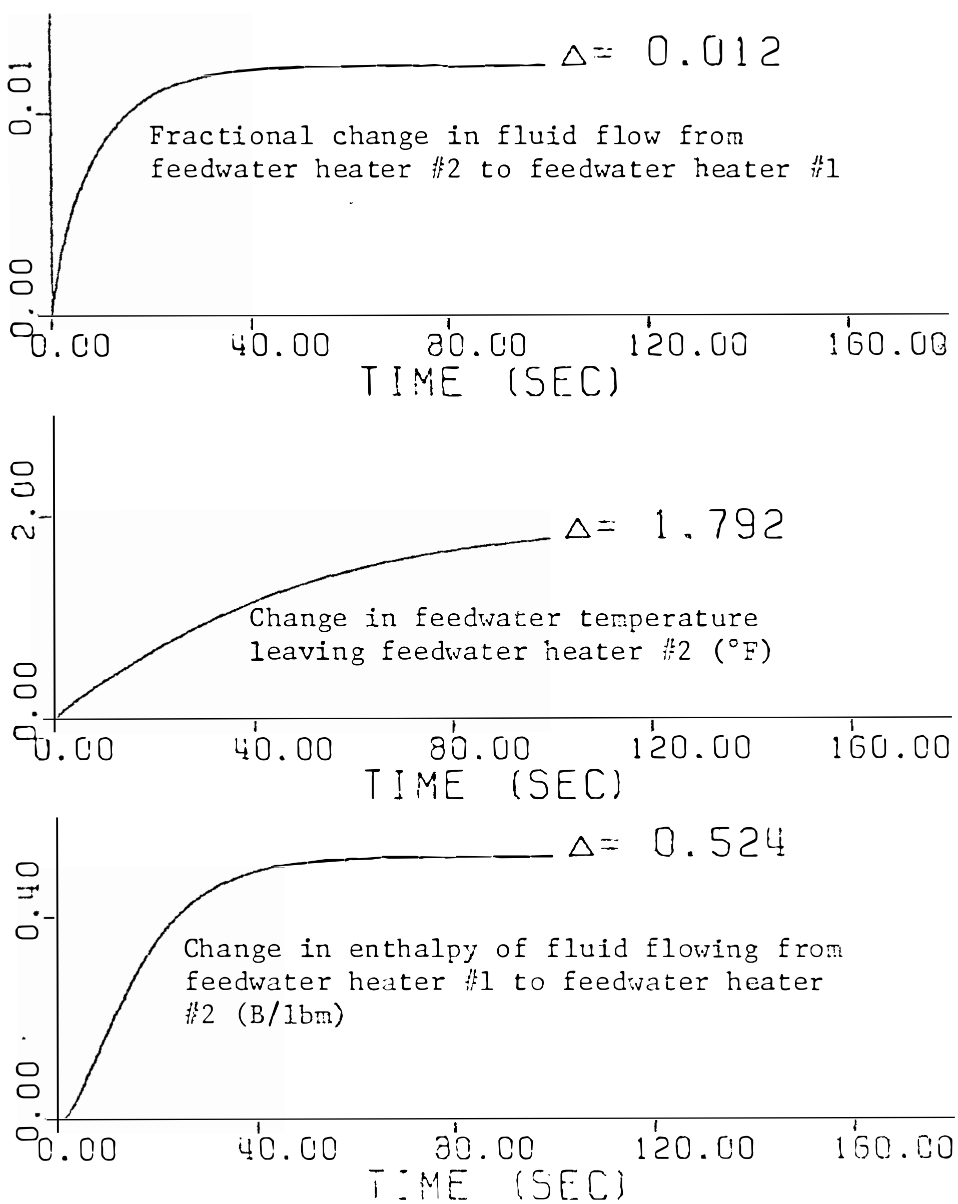

Figure E.4 (continued)

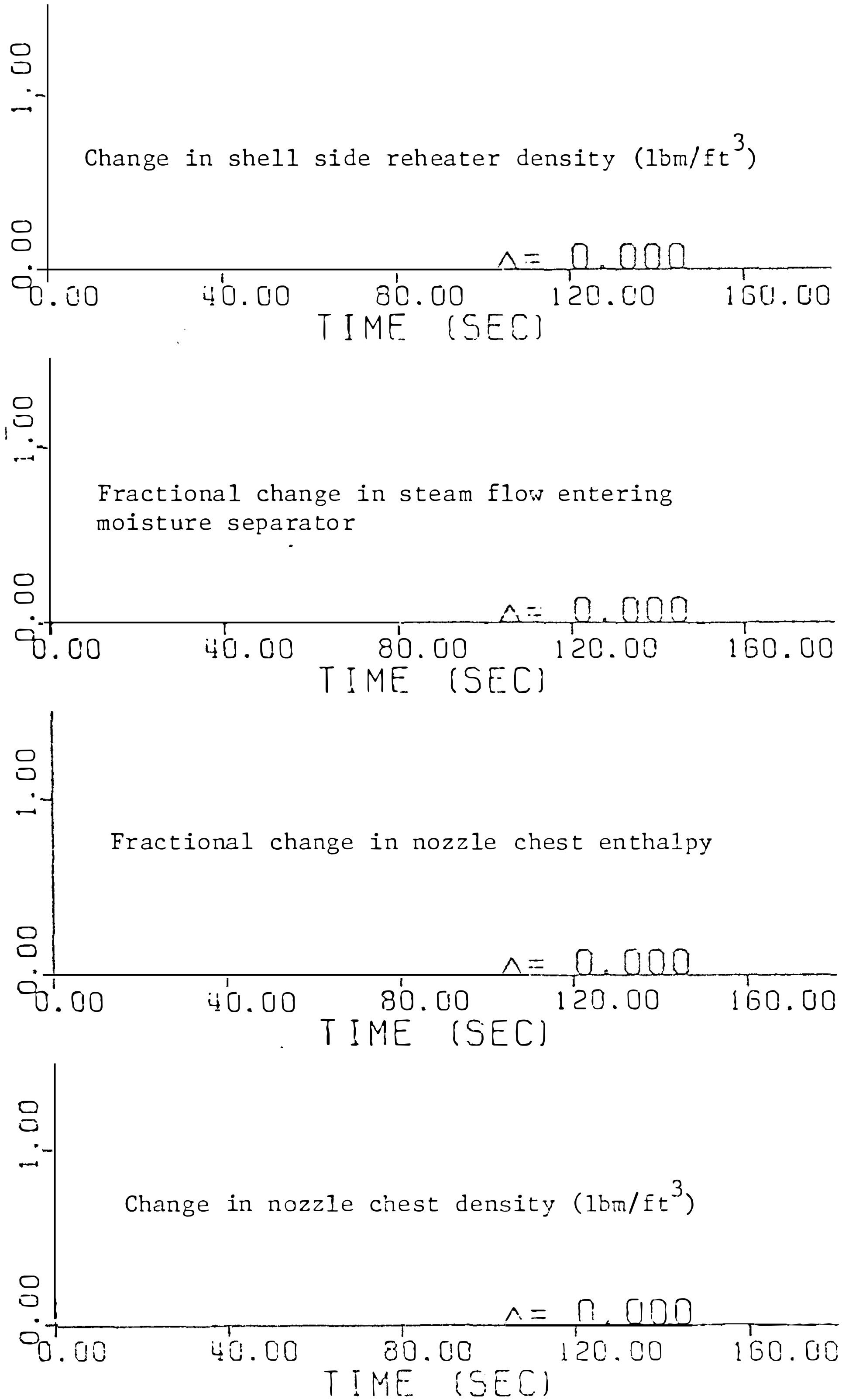

Figure E.5 Response of isolated turbine-feedwater heater model for a +100 lbm/sec step in feedwater flow rate.

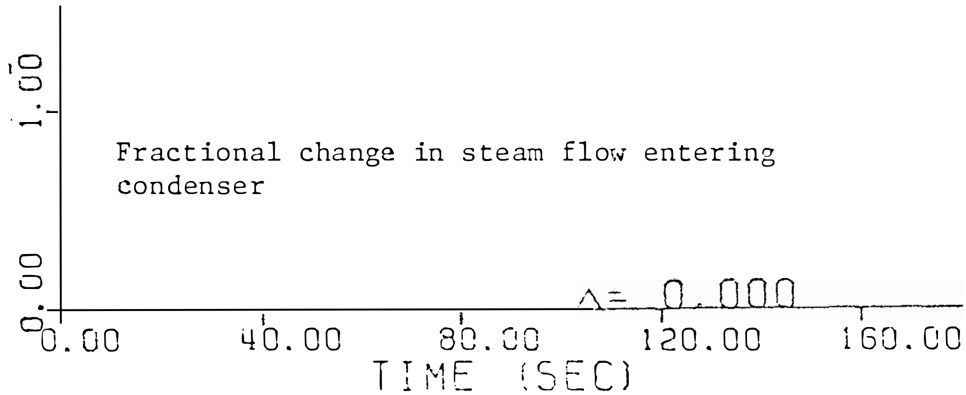

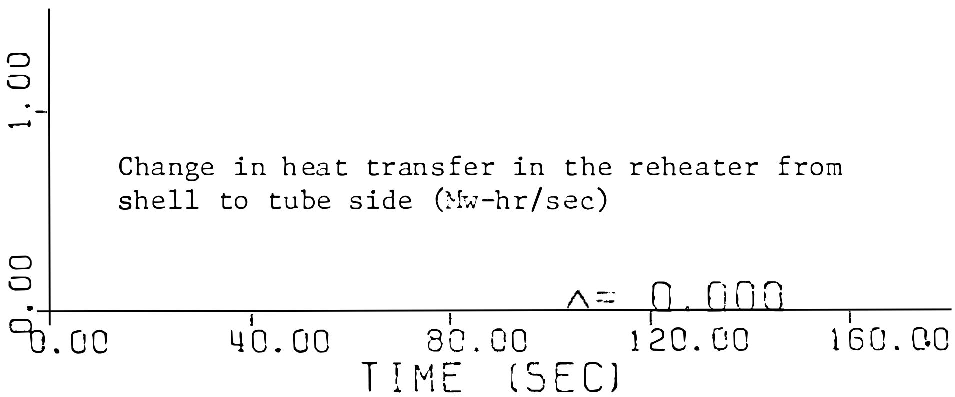

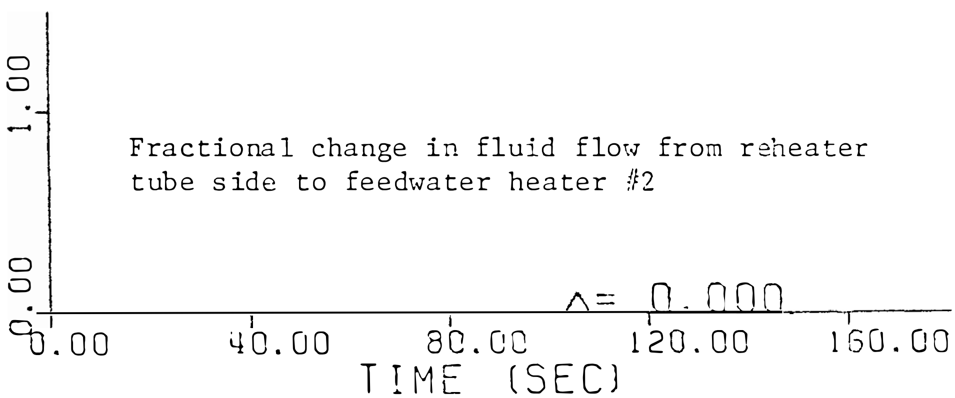

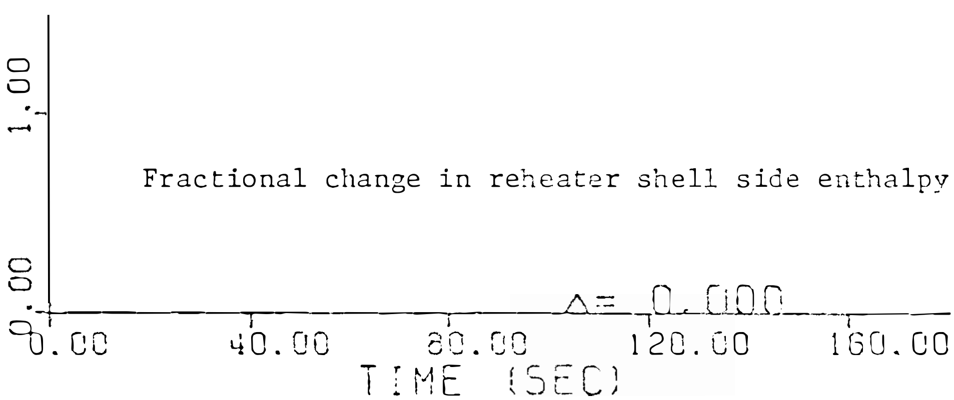

Figure E.5 (continued)

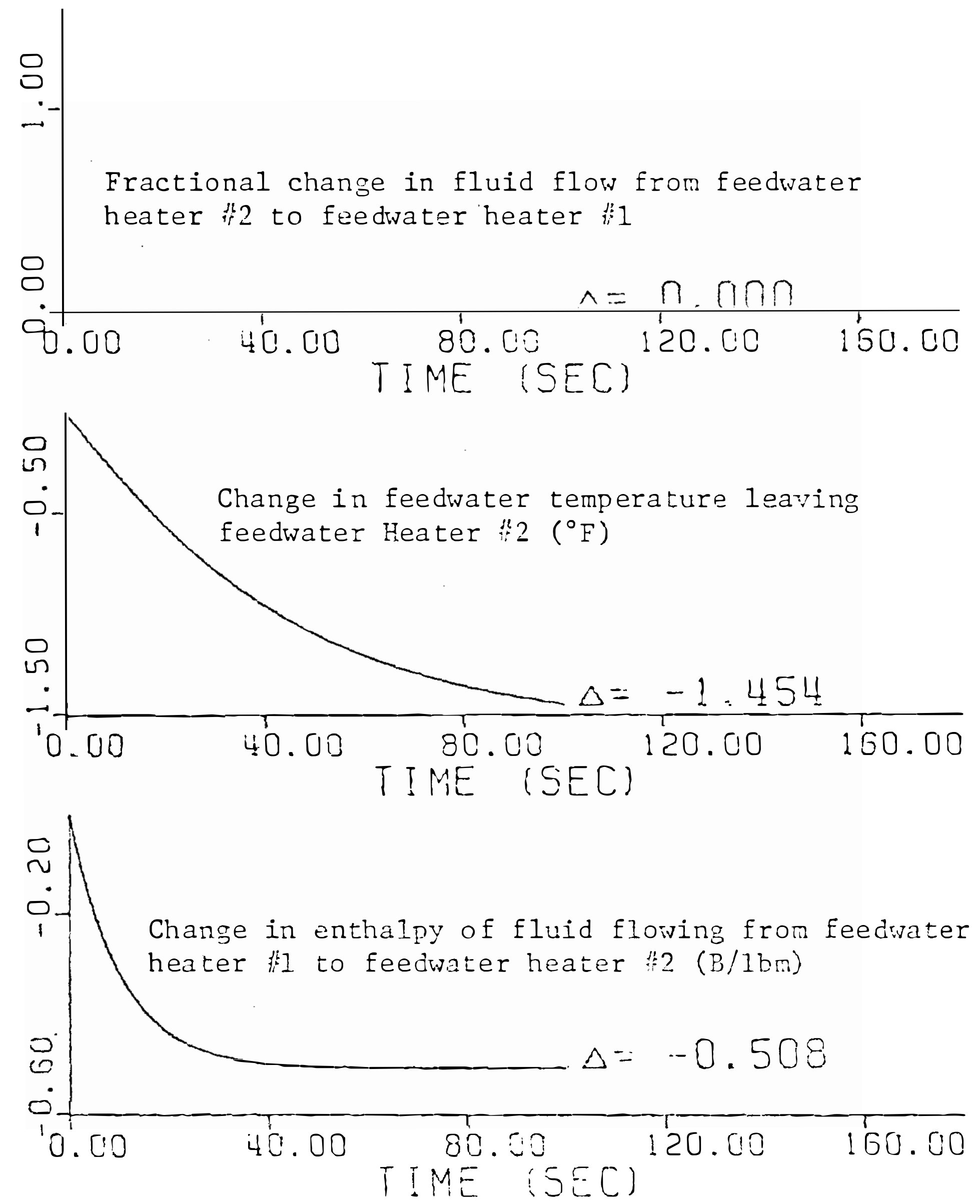

Figure E.5 (continued)

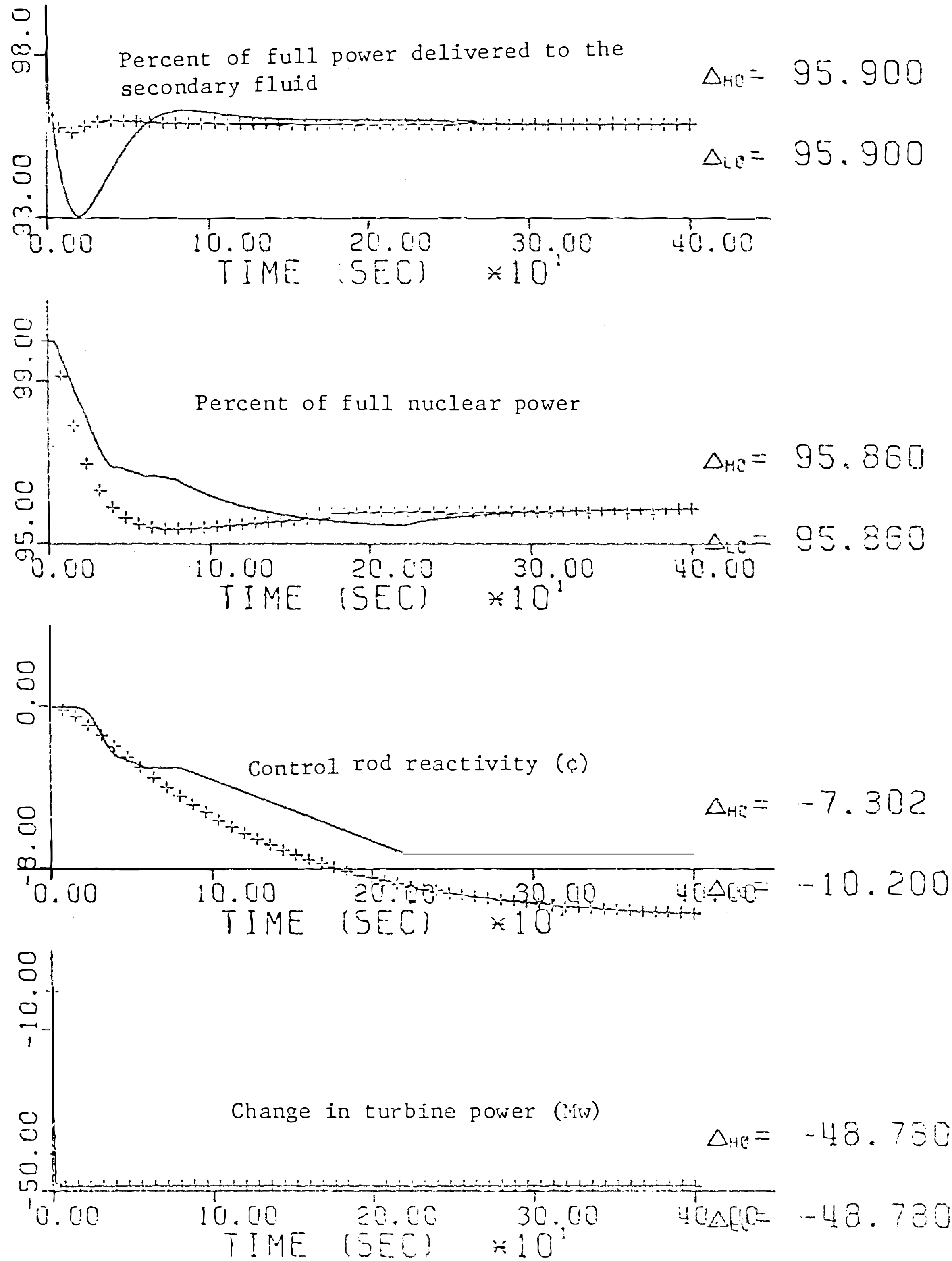

Figure E.6 Response of the low order and high order PWR models for a -0.05 puMw step in tie line power flow.

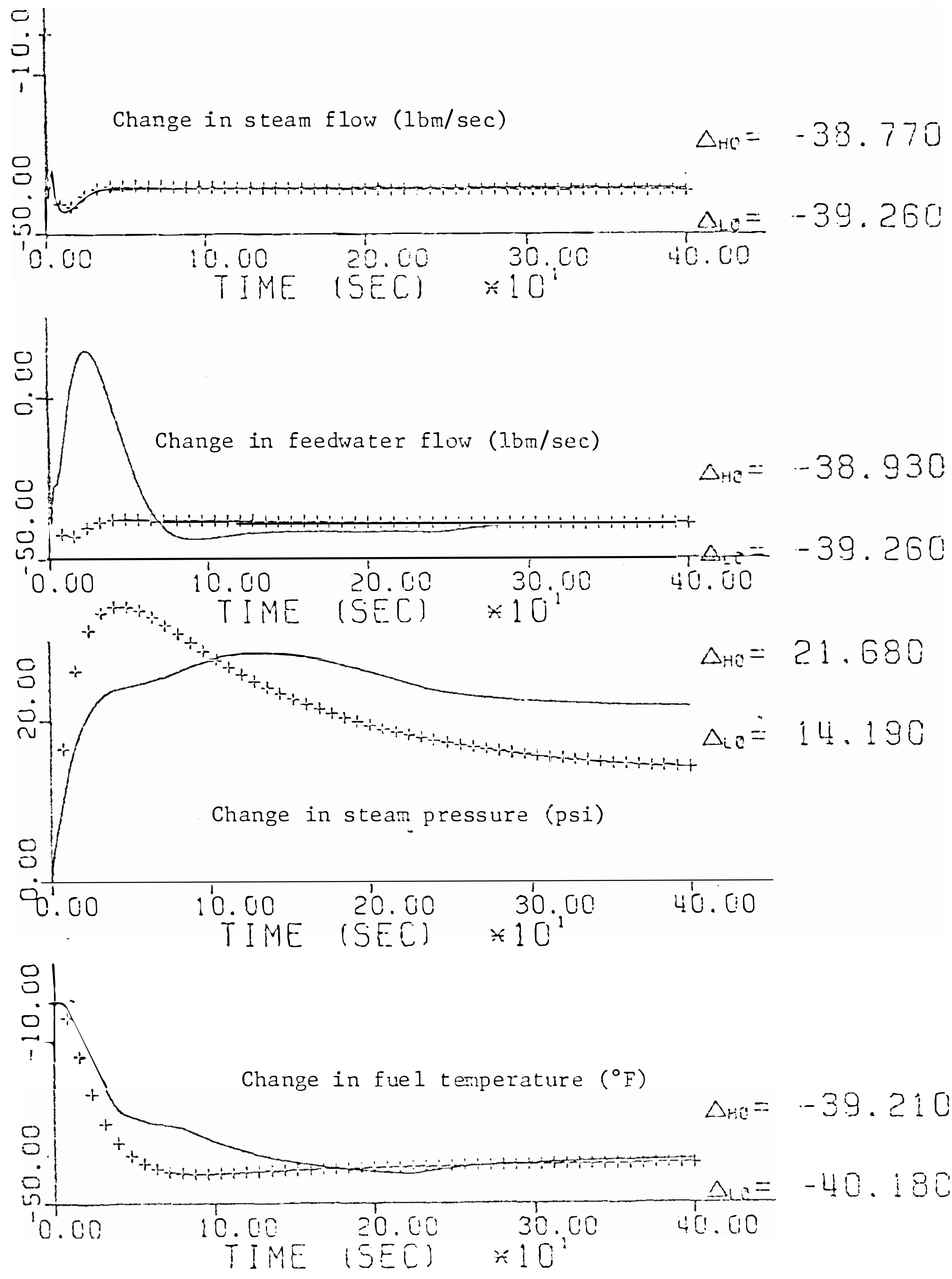

Figure E.6 (continued)

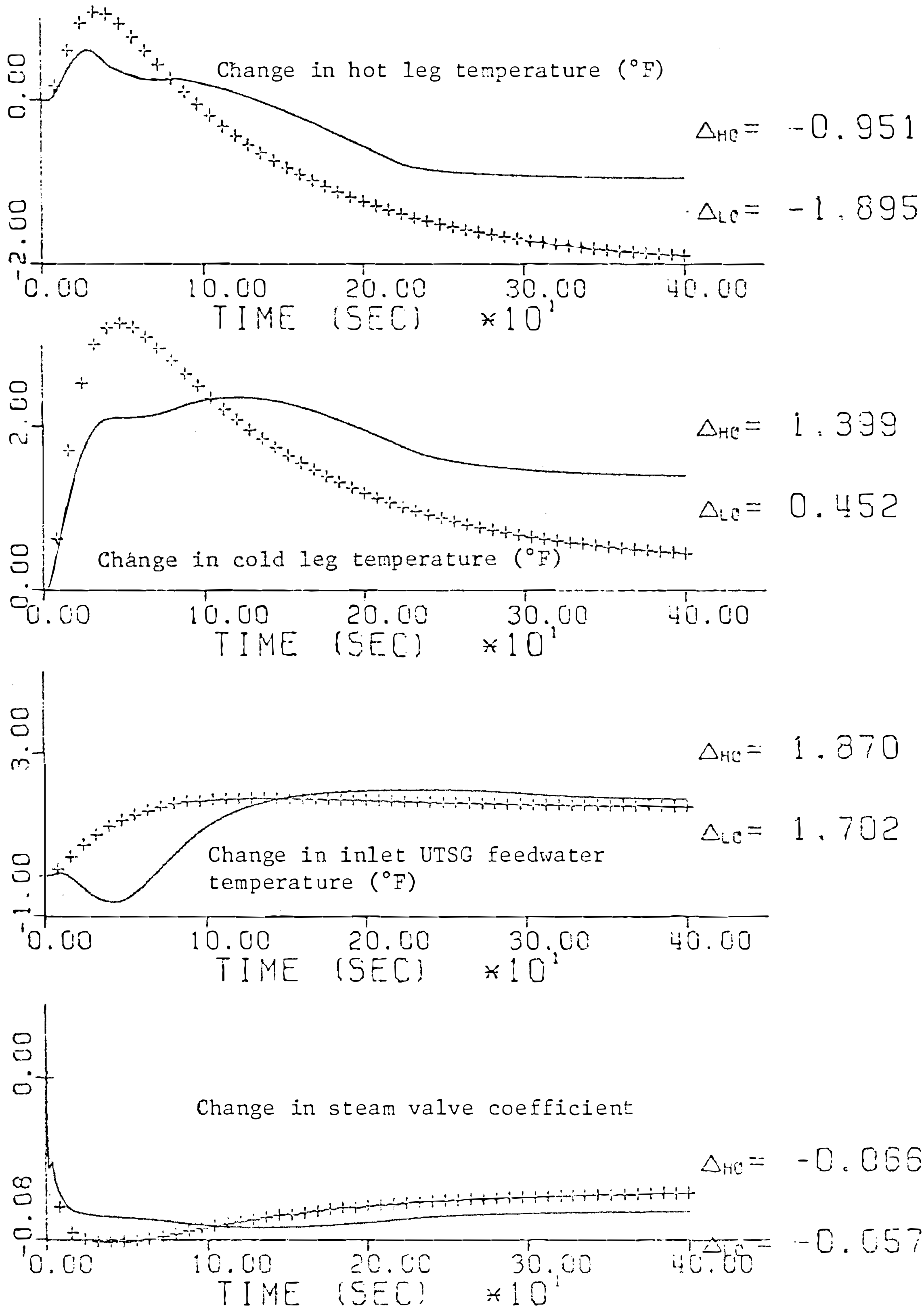

Figure E.6 (continued)

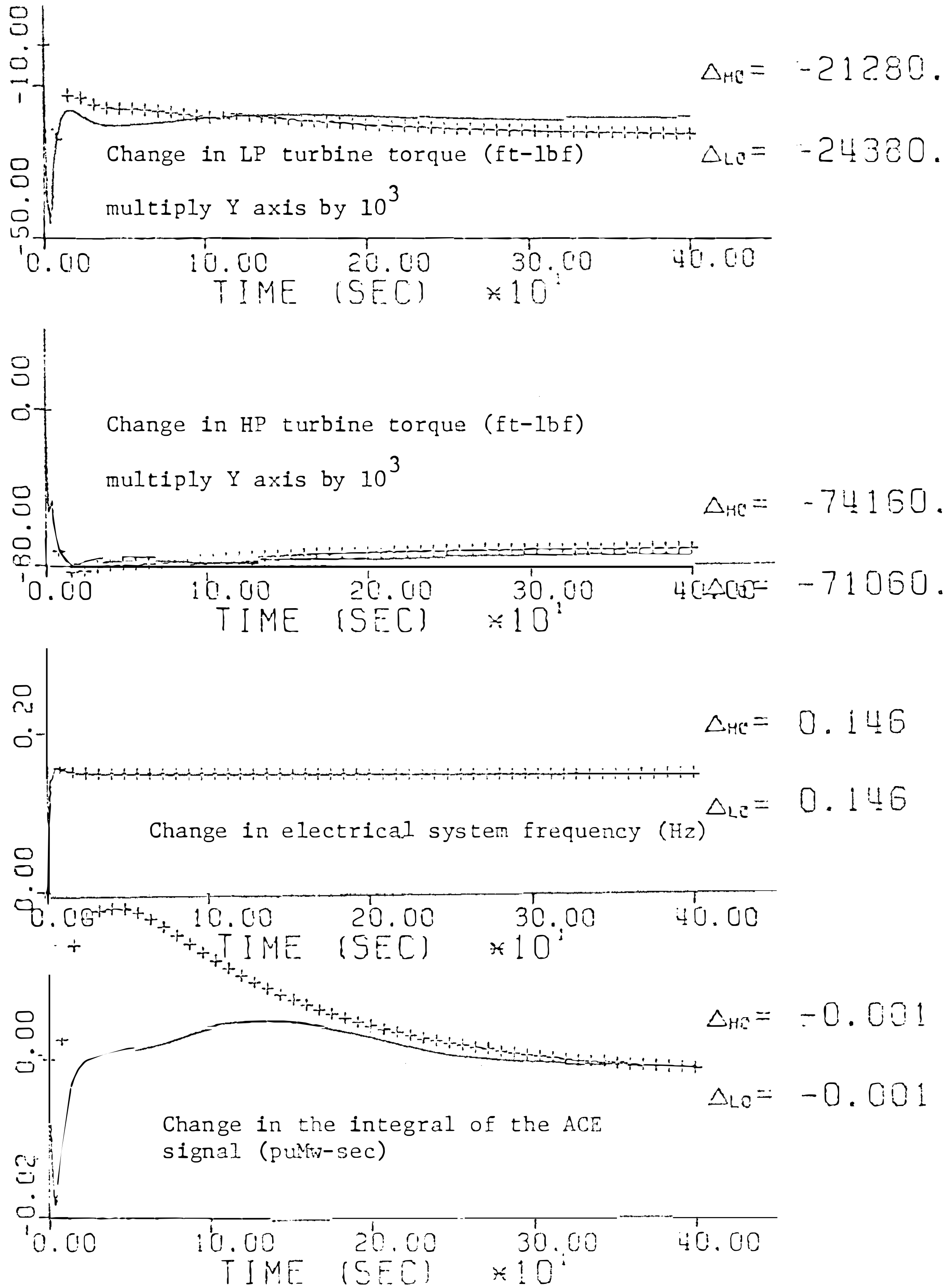

Figure E.6 (continued)

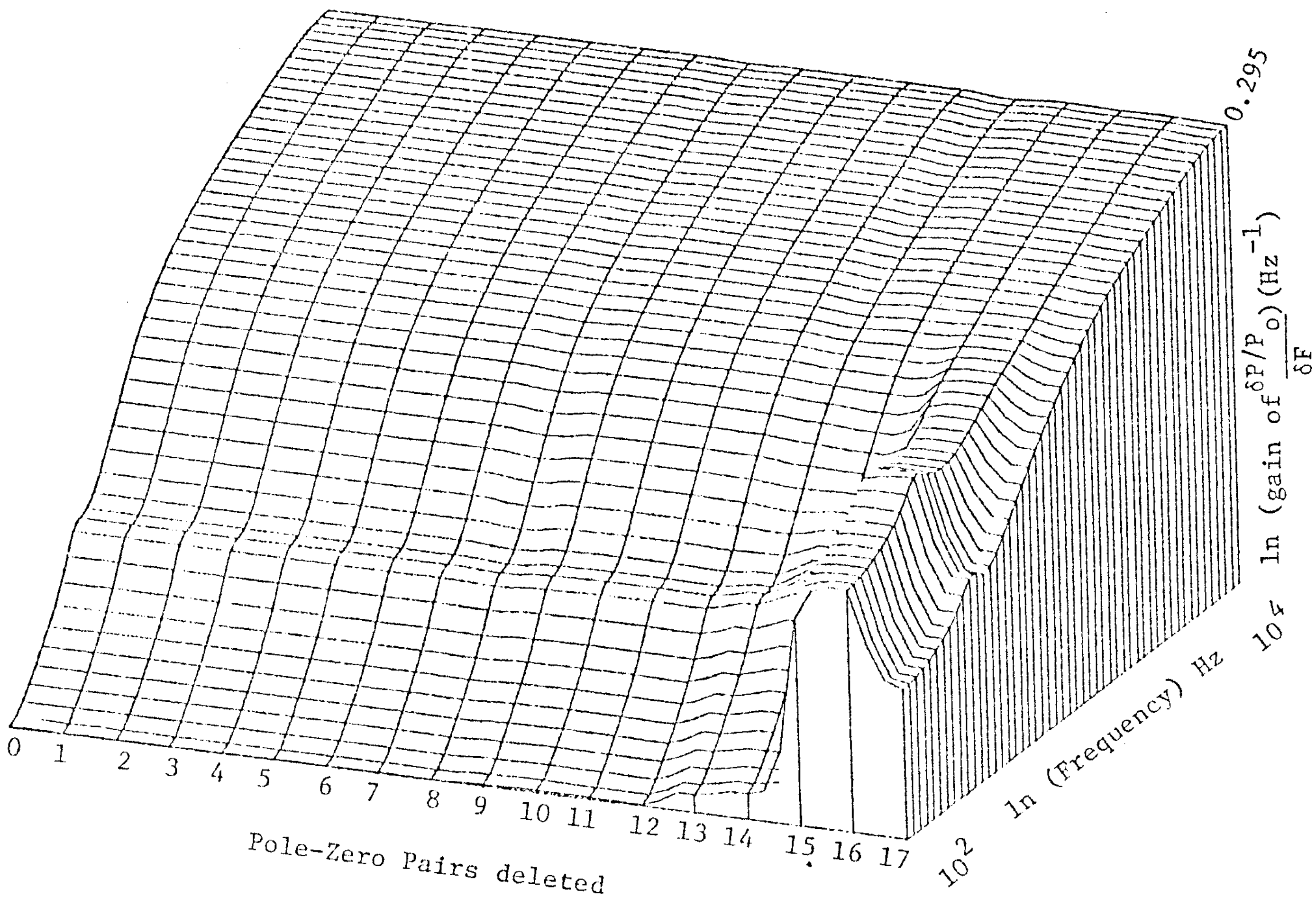

Figure E.7 Surface shown in Figure 3.3 rotated 115° about the Z axis.

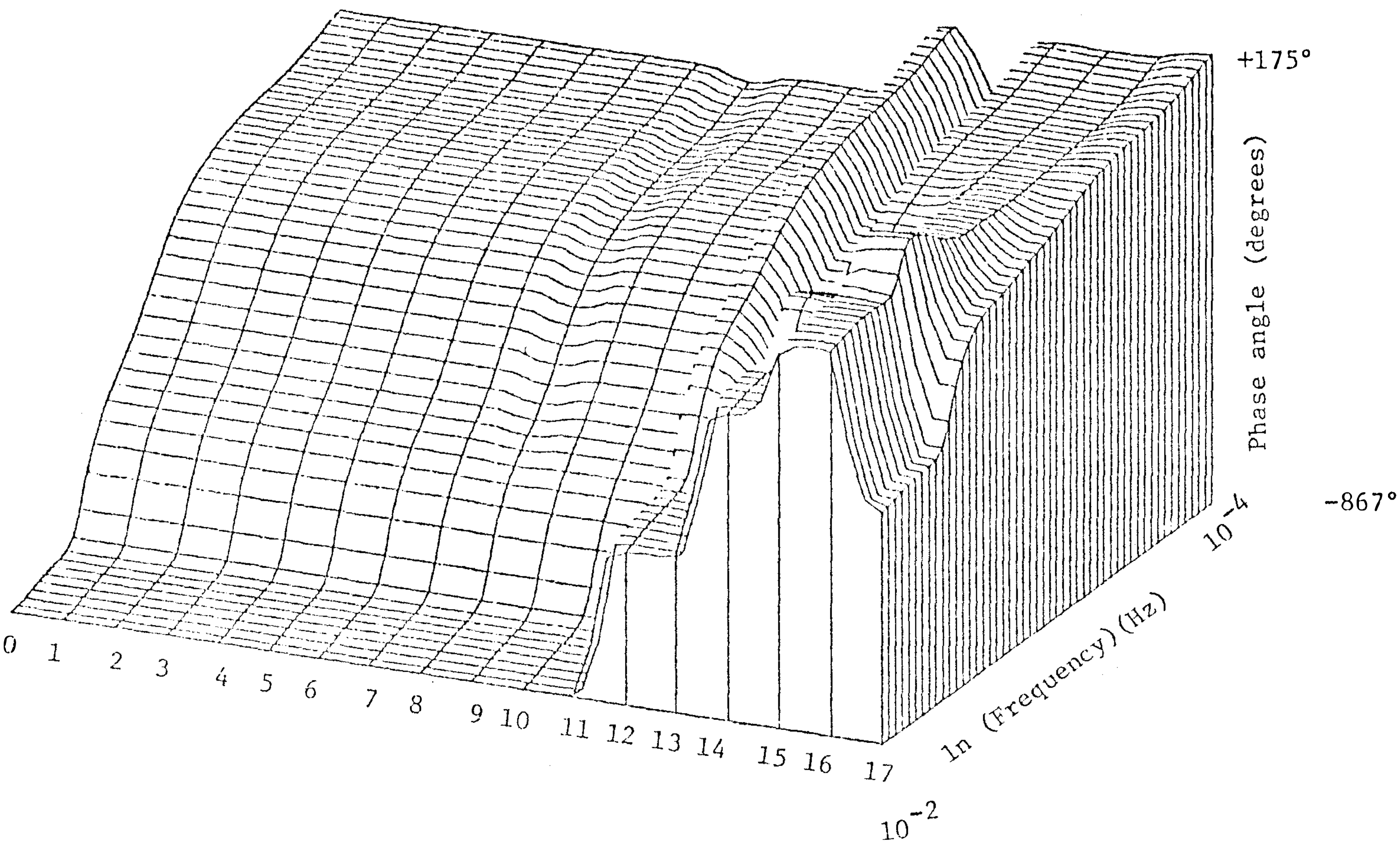

Figure E.8 Surface shown in Figure 3.4 rotated 115° about the Z axis.

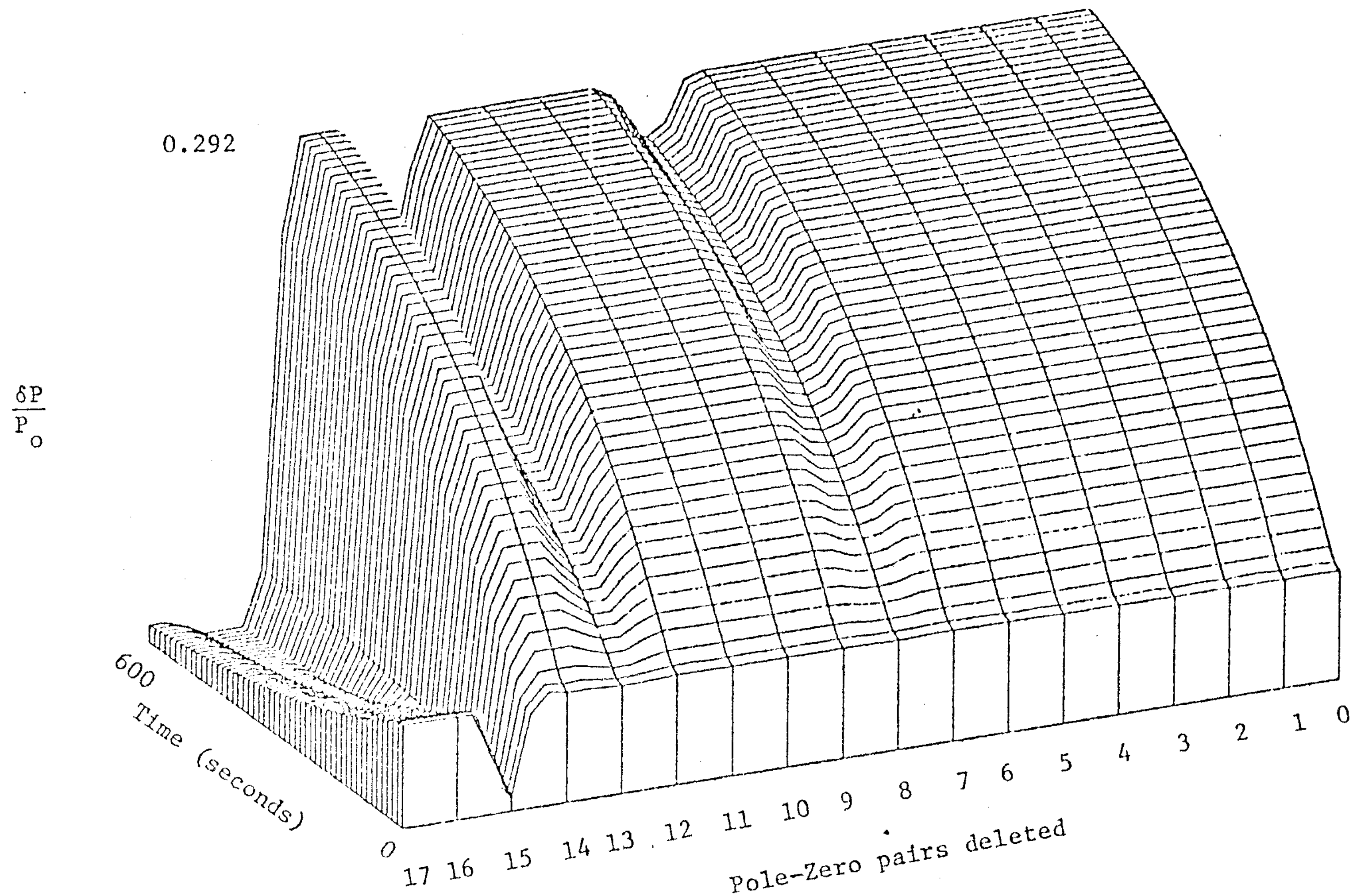

Figure E.9 Surface shown in Figure 3.5 rotated -115° about the Z axis.

APPENDIX F

DERIVATION OF THE PF OR MEGAWATT FREQUENCY CONTROLLER MODEL.[9,27]

The real power in a power system is controlled by controlling the driving torques of the individual turbines of the system. It is important for the further discussions of Pf control to understand the workings of the individual power regulators. Figure F.1 shows a schematic of the operating features of a speed-governing system.

The model developed here[27] applies to small deviations around a nominal steady state. The following chain of events are assumed to take place

1. The system is initially in a constant steady state, characterized by a constant nominal speed or frequency $f°$, a constant prime mover valve setting $X_E°$, and a constant generator output power $P_G°$.
2. By means of the speed changer, we command a power increase P_C. As a result of this command, the linkage point A moves downward a small distance X_A proportional to P_C.
3. The movement of linkage point A causes small position changes X_C and X_D of the linkage points C and D. At this time no speed changes have taken place, which means that point B is fixed. Points C and D therefore move upward. As oil flows into the hydraulic motor, the steam valve will move a small distance X_E, resulting in increased turbine torque and, consequently, a power increase P_G.
4. The increased power output causes a momentary surplus, or accelerating, power in the system. If the system is very large ("infinite"), the increased generator power will not noticeably effect the speed or frequency. However, if the system is of finite size, the speed and frequency will

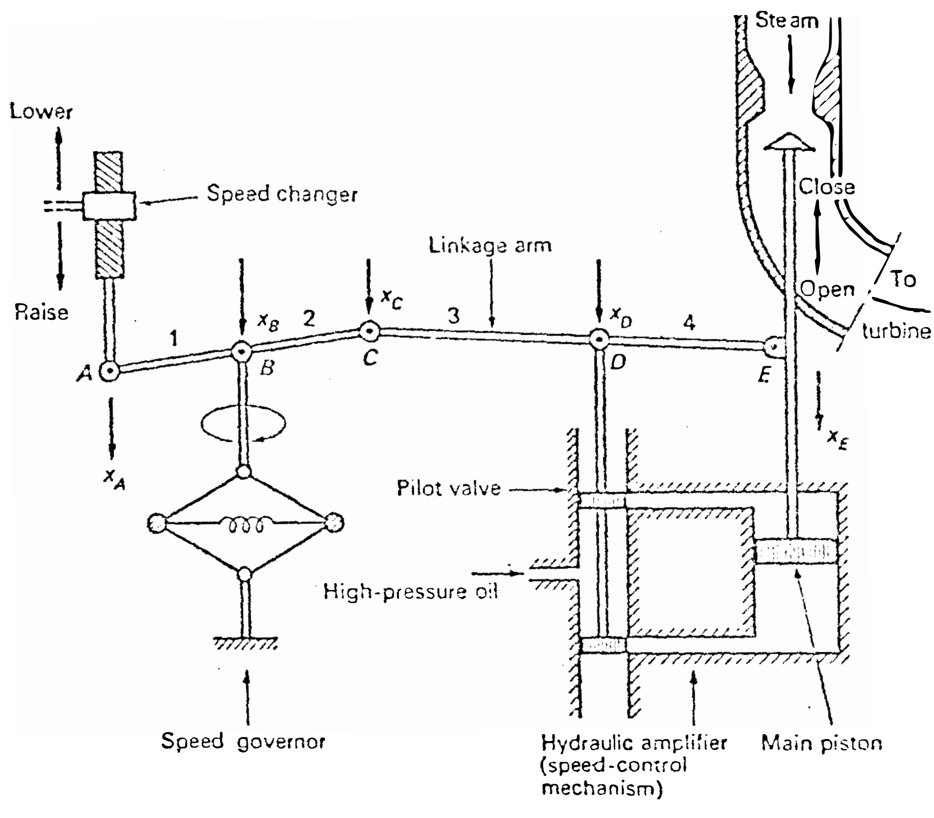

Figure F.1 Typical real-power control mechanism.

experience a slight increase that will cause the linkage point B to move downward a small distance ΔX_B proportional to Δf. The speed governor being fast, we neglect any time delay in it. Consequently, we set ΔX_B proportional to Δf.

All incremental movements $\Delta X_A, \ldots, \Delta X_E$ are assumed positive in the directions indicated in Figure F.1. Since all linkage movements are small, we have the following linear relationships

$$\Delta X_C = k_1 \Delta f - k_2 \Delta P_c \tag{F.1}$$

$$\Delta X_D = k_3 \Delta X_C + k_4 \Delta X_E \tag{F.2}$$

The positive constants k_1, and k_2 depend upon the lengths of the linkage arms 1 and 2 and upon the proportional constants of the speed changer and the speed governor. The positive constants k_3 and k_4 depend upon the lengths of the linkage arms 3 and 4.

If we assume that the oil flow into the hydraulic motor is proportional to position ΔX_D of the pilot valve, we obtain the following relationship for the position of the main piston

$$\Delta X_E = k_5 \int (-\Delta X_D)\, dt \tag{F.3}$$

The positive constant k_5 depends upon orifice and cylinder geometrics and fluid pressure.

By taking the Laplace transform of equations (F.1), (F.2), and (F.3), and eliminating the variables ΔX_C and ΔX_D, we obtain the following equation

$$\Delta X_E(s) = \frac{k_2 k_3 \Delta P_c(s) - k_1 k_3 \Delta F(s)}{k_4 + \dfrac{s}{k_5}} \tag{F.4}$$

where

(F.5) $$\Delta F(s) \equiv \mathcal{L}\left[\Delta f\right]$$

(F.6) $$\Delta X_E(s) \equiv \mathcal{L}\left[\Delta X_E\right]$$

(F.7) $$\Delta P_c(s) \equiv \mathcal{L}\left[\Delta P_c\right].$$

Equation (F.4) can be rewritten as follows

(F.8) $$\Delta X_E(s) = \frac{K_G}{1+\tau_T s}\left[\Delta P_c(s) - \frac{\Delta F(s)}{R}\right]$$

where

$R \equiv \dfrac{k_2}{k_1}$ = speed "regulation" due to governor action

$K_G \equiv \dfrac{k_2 k_3}{k_4}$ = static gain of speed-governing mechanism

$\tau_T = \dfrac{1}{k_4 k_5}$ = time constant of speed-governing mechanism.

The value of these constants used in this study are given on page 105. One additional assumption will be made. The incremental change in steam valve position, ΔX_E, will be assumed to be directly proportional to the fractional change in steam valve coefficient. In addition, a more generalized form of equation (F.8) can be written by adding a subscript i to each variable. The subscript i denoting the ith control area as given on page 102. In equation form, this can be written as

(F.9) $$\Delta X_{E_i} \propto \frac{\Delta \epsilon_i}{\epsilon_{i_o}}$$

Thus, the static gain K_G will now be change to K_2. In this study, the power control error signal, ΔP_{Ci} will always be set equal to the ACE signal. ACE or "area control error" is defined to be

$$ACE_i = \Delta P_{TIE_i} + \left(D + \frac{1}{R}\right)\Delta F_i \tag{F.10}$$

where

ΔP_{TIE} = the tie line power flow a power flowing into the ith control area from outside the ith control area (see Figure 2.31) in puMw units

D = constant damping coefficient (puMw/Hz).

R and F_i have been defined previously. In this study, only one control area will be considered, that of a single 1200 Mwe PWR nuclear power plant. Therefore the i subscripts will be dropped. In addition, in order to be consistent with the symbols used previously in this thesis, the Δ symbol used by Elgerd will be changed to δ. Thus the following equation can be written for the fractional change in valve coefficient

$$\frac{\delta \epsilon}{\epsilon_0}(s) = \frac{K_2}{1 + \tau_T s}\left[-ACE(s) - \frac{\delta F(s)}{R}\right]. \tag{F.11}$$

Performing an inverse Laplace transform, equation (F.11) becomes

$$\frac{d\,\delta\epsilon/\epsilon_0}{dt} = -\frac{\delta\epsilon/\epsilon_0}{\tau_T} - \frac{K_2}{\tau_T}\int ACE\,dt - \frac{K_2}{R\tau_T}\,\delta F \tag{F.12}$$

Let $\delta P_C = \int ACE(t)\,dt$. This will allow equation (F.12) to be written as two first order linear differential equations.

$$\text{(F.13)} \quad \frac{d\,\delta P_c}{dt} = ACE = \delta P_{TIE} + \left(D + \frac{1}{R}\right)\delta F$$

$$\text{(F.14)} \quad \frac{d\,\delta \epsilon/\epsilon_o}{dt} = -\frac{\delta\epsilon/\epsilon_o}{\tau_T} - \frac{K_2}{\tau_T}\delta P_c - \frac{K_2}{\tau_T R}\delta F$$

From page 102, the following equation can be written

$$\text{(F.15)} \quad \frac{\delta F(s)}{\delta P_{sum}(s)} = \frac{1}{Ms + D}$$

where

δP_{SUM} = sum of all power signal into the ith control area (puMw)

= $\delta P_M - \delta P_{TIE} - \delta P_D$

M = generator inertia constant (puMw-sec/Hz)

δP_M = mechanical shaft power produced by the generator (puMw)

δP_D = the power demand signal for the ith control area (puMw)

δP_{TIE}, δF, and D have been previously defined. After performing an inverse Laplace transform, equation (F.15) becomes

$$\text{(F.16)} \quad \frac{d\,\delta F}{dt} = -\frac{D}{M}\delta F + \frac{1}{M}\left[\delta P_M - \delta P_{TIE} - \delta P_D\right].$$

Equations (F.13), (F.14), and (F.16) make up the state variable model for the Pf controller. The values of the parameters used in this study are given on page 105.

APPENDIX G

INSTRUCTIONS FOR THE USE OF THE

REDUCE COMPUTER PROGRAM

G.1 INTRODUCTION

The REDUCE computer code is a program which will reduce the order of a state variable system model by the pole-zero deletion method. The theory used to develop the pole-zero deletion method is given in Section III.4 of this thesis. The time response and frequency response of both the full and reduced representation are also evaluated by REDUCE. The printed output from REDUCE can be used to compare the accuracy of the low order representation. Additional output can be used to develop plots if desired.

Figure G.1 is a flow chart of the REDUCE program. From Figure G.1, the input and output, as well as internal characteristics of REDUCE, can be determined.

In Figure G.1, the abbreviations LUN stand for "logical unit number." The fortran statement WRITE (20,100) will cause the contents of the format statement labeled by 100 to be written into the LUN 20. The various LUN's used by REDUCE are shown in Figure G.1.

The computer used to run this program for this thesis was the Dec System 10 at the University of Tennessee. For this computer system, the following devices were used with the corresponding LUN's

3 line printer

20 DSKC of the user's disk space

21 DSKC of the user's disk space

22 DSKS of the user's disk space

23 DSKC of the user's disk space

In Section G.2, the instructions for the input data file used to run REDUCE is given. Then the data file called 'FILE.DAT' used in this thesis is given in Figure G.2.

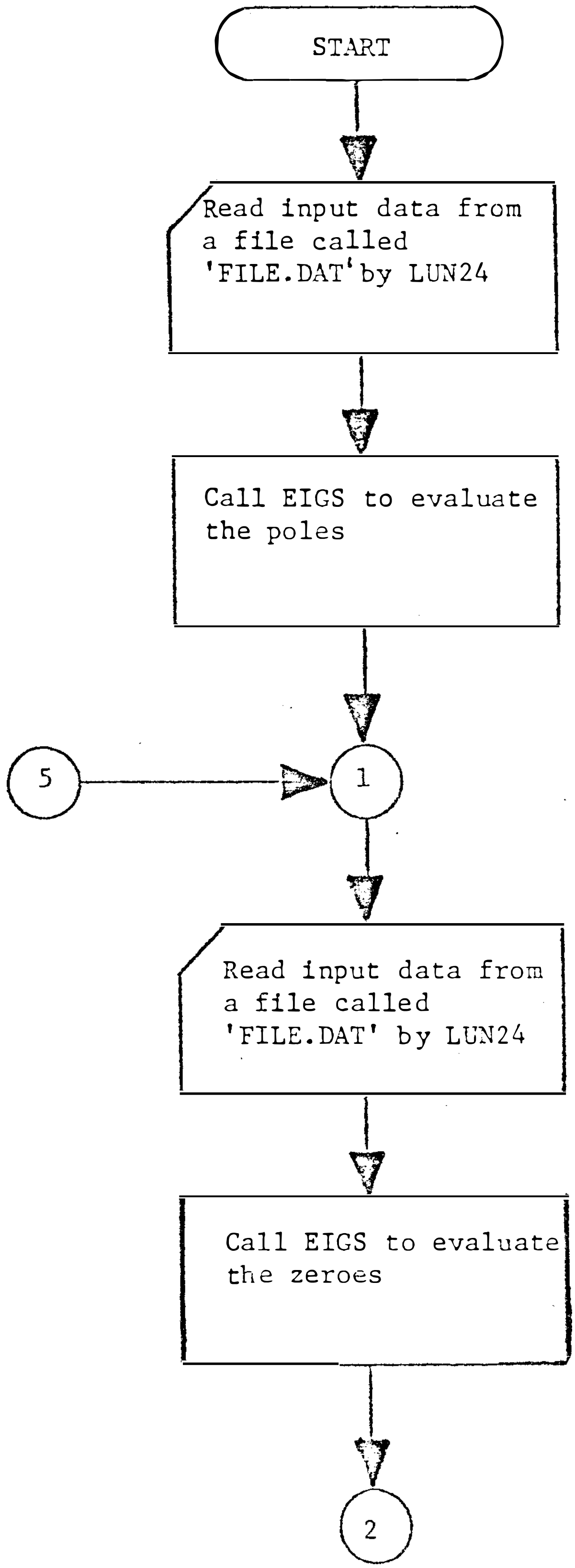

Figure G.1 Flow chart of the REDUCE computer program.

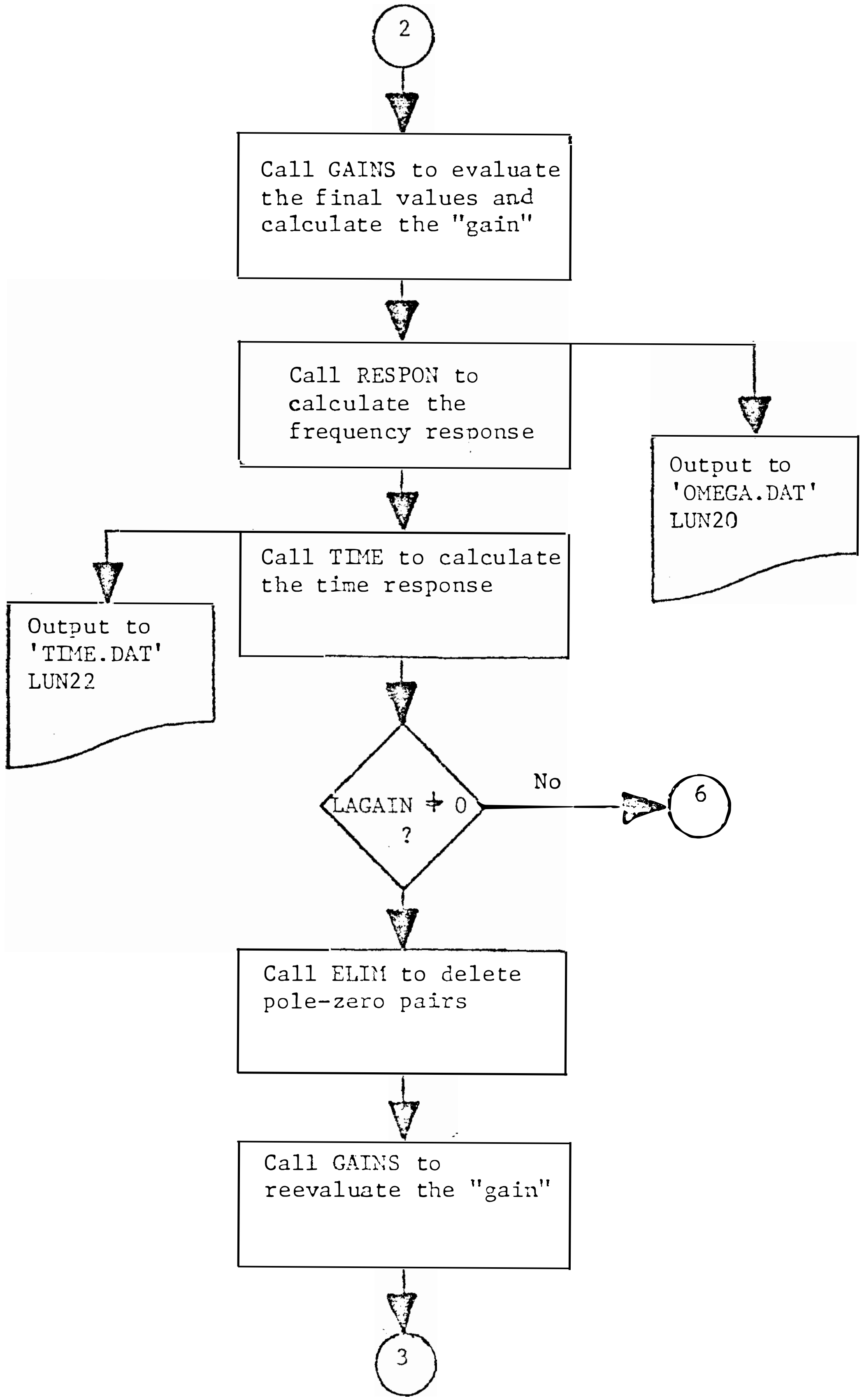

Figure G.1 (continued)

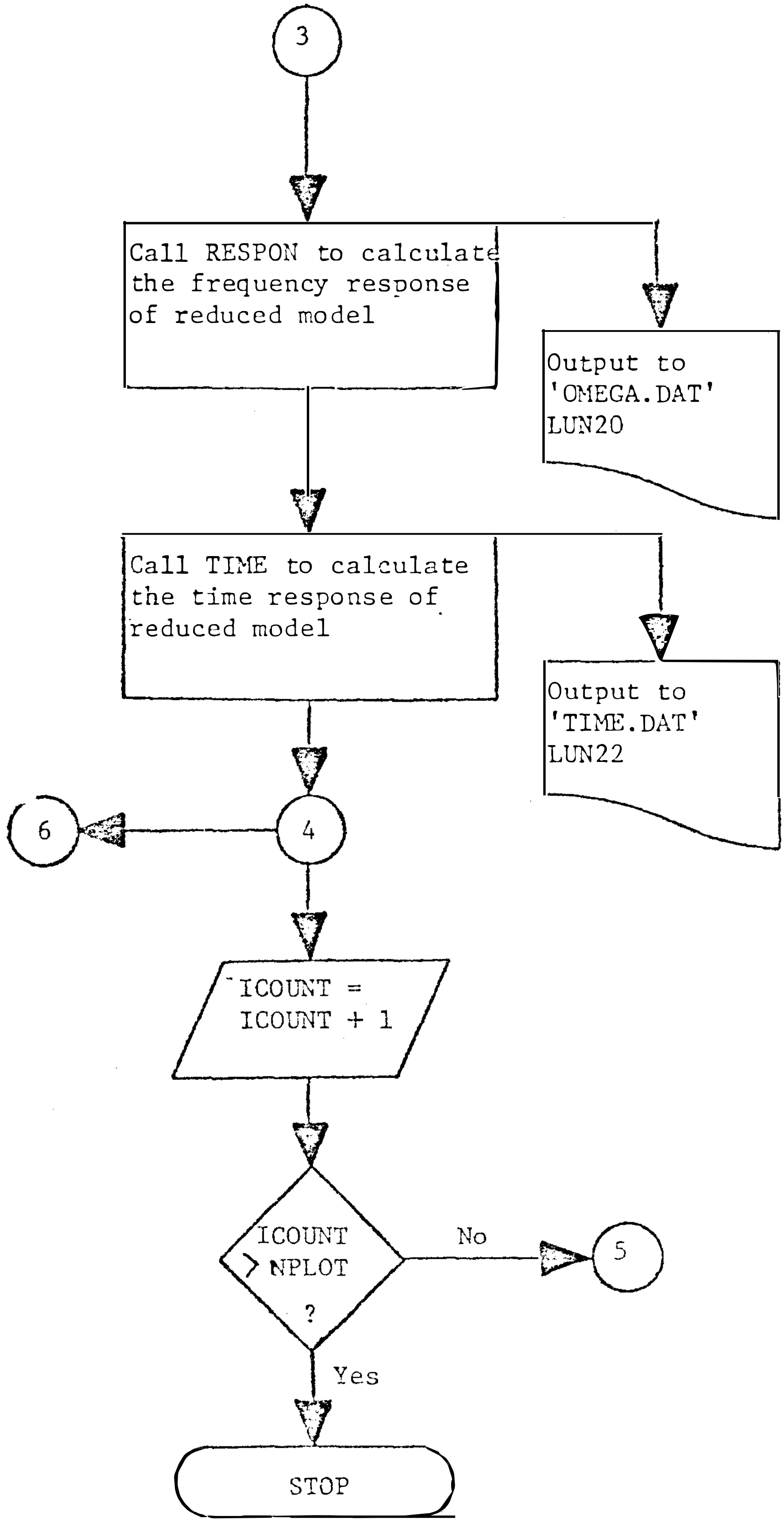

Figure G.1 (continued)

```
23TH ORDER SEQUOYAH LOW ORDER MODEL FOR POWER DEMAND PERTURBATION
   23   61   17  100    100.0  +1.000D-10
    1    1    1    1    1    1    1    1    1    1    1    1    1    1    1    1
    1    1
 POWR POWR POWR POWR POWR POWR POWR POWR POWR POWR POWR POWR POWR POWR POWR POWR
 POWR POWR
1.0000D-041.2600D-041.5800D-042.0000D-042.5200D-043.1700D-044.0000D-04
5.0600D-046.3800D-048.0000D-041.0000D-031.2600D-031.5800D-032.0000D-03
2.5200D-033.1700D-034.0000D-035.0600D-036.3800D-038.0000D-031.0000D-02
1.2600D-021.5800D-022.0000D-022.5200D-023.1700D-024.0000D-025.0600D-02
6.3800D-028.0000D-021.0000D-011.2600D-011.5800D-012.0000D-012.5200D-01
3.1700D-014.0000D-015.0600D-016.3800D-018.0000D-011.0000D+001.2600D+00
1.5800D+002.0000D+002.5200D+003.1700D+004.0000D+005.0600D+006.3800D+00
8.0000D+001.0000D+011.2600D+011.5800D+012.0000D+012.5200D+013.1700D+01
4.0000D+015.0600D+016.3800D+018.0000D+011.0000D+02
    1     1-2.619E+00     1     3 1.029E-01     1     4 3.443E+00
    1     5 3.546E+00     2     1-3.854E+02     2     2-8.225E-02
    3     1-2.414E+02     3     3-2.532E-01     3     4 2.532E-01
    4     1-2.619E+00     4     3 1.029E-01     4     4-3.649E+00
    4     7 3.546E+00     5     5-3.132E-01     5     6-3.132E-01
    6     6-1.125E-04     6     7-1.125E-04     6    10 5.382E-06
    6    21-8.013E-06     6    23 4.470E-03     7     7-2.141E-01
    7     8 2.141E-01     8     6 3.250E-01     8     8-1.605E+00
    8     9 1.280E+00     9     8 4.787E+00     9     9-7.782E+00
    9    10 4.192E-01    10     9 5.599E+00    10    10-9.333E-01
   10    21 1.914E-01    10    23-1.234E+02    11     1-3.854E+02
   11     2-8.225E-02    11     3 6.145E-01    11     4 5.587E+00
   11     5-5.587E+00    11    11-3.854E+02    12    10 2.492E-02
   12    12-1.629E+01    12    13-3.672E+01    12    15 1.929E+00
   12    16 5.875E+00    12    23 2.073E+01    13    10 1.487E-02
   13    12-9.955E+00    13    13-3.115E+01    13    15 1.178E+00
   13    16 3.589E+00    13    23 1.267E+01    14    12 3.930E-01
```

Figure G.2 Data file used by the REDUCE program to produce Figures 3.3, 3.4, 3.5, E.7, E.8, and E.9.

```
14    13 8.858E-01   14    14-5.000E-01   14    15-4.653E-02
14    16-1.418E-01   15    14 1.953E-01   15    15-2.713E-01
15    16-2.101E-01   16    14 6.161E-01   16    15-1.075E+00
16    16-1.277E+00   16    18 3.765E-01   17    10 4.006E-04
17    17-3.333E-01   18    10 8.350E-05   18    16-1.010E+00
18    17 7.862E-03   18    18-2.500E-01   19    15 1.902E-01
19    16 1.459E-01   19    19-1.000E-01   20    10-2.701E-03
20    15 1.352E+00   20    16 1.037E+00   20    20-1.000E-01
20    22 1.395E+00   20    23-2.146E+00   20    26-1.000E-01
21    10-1.583E-03   21    12 1.338E+00   21    13 3.014E+00
21    14-1.101E+00   21    15-1.584E-01   21    16-3.743E-01
21    17 4.582E-01   21    20 2.193E-02   21    21-2.500E-02
21    23-1.258E+00   21    26-5.912E-02   22    12 4.372E-02
22    13 9.851E-02   22    14-3.597E-02   22    15-5.176E-03
22    16-1.224E-02   22    17 1.497E-02   22    22-1.000E-01
23    23-5.000E+00

23      -2.025

 1+3.0000D+0  0.000005  +5.000D+20
23      -2.025

 1+3.0000D+0  .005      +5.000D+20
23      -2.025

 1+3.0000D+0  .008      +5.000D+20
23      -2.025

 1+3.0000D+0  .0099     +5.000D+20
23      -2.025

 1+3.0000D+0  .01       +5.000D+20
```

Figure G.2 (continued)

```
23      -2.025

 1+3.0000D+0  .013       +5.000D+20
23      -2.025

 1+3.0000D+0  .02        +5.000D+20
23      -2.025

 1+3.0000D+0  .08        +5.000D+20
23      -2.025

 1+3.0000D+0  .15        +5.000D+20
23      -2.025

 1+3.0000D+0  .20        +5.000D+20
23      -2.025

 1+3.0000D+0  .21        +5.000D+20
23      -2.025

 1+3.0000D+0  .30        +5.000D+20
23      -2.025

 1+3.0000D+0  .40        +5.000D+20
23      -2.025

 1+3.0000D+0   .6        +5.000D+20
23      -2.025

 1+3.0000D+0  1.0        +5.000D+20
23      -2.025
```

Figure G.2 (continued)

```
 1+3.0000D+0  1.1        '+5.000D+20
23     -2.025

 1+3.0000D+0  1.25        +5.000D+20
```

Figure G.2 (continued)

G.2 INSTRUCTIONS FOR THE INPUT DATA FOR REDUCE

Card No. 1 (title)

Column	1-80
Format	20A4
Input	TITLE

TITLE - a title of 80 alphanumeric characters to be used to identify the case being run

Card No. 2 (REDUCE control parameters)

Column	1-5	6-10	11-15	16-20	21-30	31-40
Format	I5	I5	I5	I5	D10.2	D10.2
Input	N	NO	NPLOT	NINT	DT	LCRIT

N - Number of differential equations. Must be $\leq$ 50

NO - Number of frequencies to be used in calculating the frequency responses. Must be $\leq$ 100

NPLOT - Number of cases to be run. (Or the number of plots to be made.) Must be $\leq$ 16.

NINT - The number of time intervals to be evaluated in performing the time response. Must be $\leq$ 1000.

DT - The value of the individual time intervals. No restrictions. DT x NINT + 1 = the time at the end of observation of the desired time response.

LCRIT - The low critical value for deleting poles and zeroes. If any pole-zero pair is found which is less than this value, that pair will be deleted. 1×10^{-10} is a recommended value.

Card No. 3 (state variables to be examined)

Column	1-80
Format	16I5
Input	ISTATE

ISTATE - The vector of state variables to be examined. The total number of state variables to be evaluated must be equal to NPLOT $\leq$ 16.

Card No. 4 (name of the state variables to be examined)

Column	1-80
Formt	16(1X,A4)
Input	NAME(I)

NAME(I) - The vector of the names of the state variables to be examined. Each name can be made of four alphanumeric characters. The total number of names must be equal to NPLOT $\leq$ 16.

Card No. 5 (frequencies to be evaluated)

Column	1-70
Format	7(D10.3)
Input	W(I)

W(I) - Vector of frequencies to be used in evaluating the frequency responses. The total number of frequency points must be equal to NO $\leq$ 100. Repeat this card until all frequency points have been read in (seven points per card).

Card No. 6 (non-zero system matrix coefficients

Column	1-5	6-10	11-20	21-25	26-30	31-40	41-45	46-50	51-60
Format	I5	I5	D10.4	I5	I5	D10.4	I5	I5	D10.4
Input	I1	J1	D1	I1	J2	D2	I3	J3	D3

I1 - row number $\leq$ 50 and $\geq$ 0

J1 - column number $\leq$ 50 and $>$ 0

D1 - value of the matrix coefficient at location (I1, J1)

I2 - row number $\leq$ 50 and $>$ 0

J2 - column number $\leq$ 50 and $>$ 0

D2 - value of the matrix coefficient at location (I2, J2)

I3 - row number $\leq$ 50 and $>$ 0

J3 - column number $\leq$ 50 and $>$ 0

D3 - value of the matrix coefficient at location (I3, J3)

Repeat this card until all the non-zero matrix coefficients have been read in. Make the value of the input parameter I1=0 for the last card of matrix coefficients. This will stop the reading of the system matrix coefficients.

Card No. 7 (non-zero forcing vector coefficients

Column	1-5	6-15	16-20	21-30	31-35	36-45	46-50	51-60
Format	I5	D10.3	I5	D10.3	I5	D10.3	I5	D10.3
Input	I1	F1	I2	F2	I3	F3	I4	F4

I1 - row number $\leq$ 50 and $\geq$ 0

F1 - value of the forcing coefficient at row I1

I2 - row number $\leq$ 50 and $>$ 0

F2 - value of the forcing coefficient at row I2

I3 - row number $\leq$ 50 and $>$ 0

F3 - value of the forcing coefficient at row I3

I4 - row number $\leq$ 50 and $>$ 0

F4 - value of the forcing coefficient at row I4

Repeat this card until all the non-zero forcing coefficients have been read in. Make the value of the input parameter I1=0 for the last card of the forcing coefficients. This will stop the reading of the forcing coefficients.

Card No. 8 (REDUCE control card)

Column	1-5	6-15	16-25	26-35
Format	I5	D10.2	D10.2	D10.2
Input	LAGAIN	RNEST	EPIL	HCRIT

LAGAIN - Non-zero value will cause the time response and frequency response to be repeated again for the reduced model representation (after pole-zero pairs have been deleted). A value of zero will not allow the time response and frequency response to be done for the reduced representation. Must be either zero or non-zero integer number.

RNEST - The estimated difference between the number of poles and number of zeroes. The number of poles by definition is equal to N. RNEST is approximately equal to the number of non-zero system matrix coefficients in the row corresponding to the state variable number being examined. Must be $\leq$ 50.

EPIL - The critical value for deciding whether a pole-zero pair will be deleted. If a pole-zero pair has the same exponent, and if the absolute value of the difference of the mantissas of that pole-zero pair is less than EPIL, then that pole-zero pair will be deleted. Must be $\geq$ 0.

HCRIT - The high critical value for determining the zeroes of the desired state variable transfer function. The forcing vector is multiplied by HCRIT before using Cramer's rule to determine the zeroes. The "bad" eigenvalues are thrown away if they have an absolute value greater than $(\mathrm{HCRIT})^{\mathrm{RNEST}}$.

Repeat card number 7 and 8 (NPLOT-1) times to complete the input data for REDUCE.

The data file which was used to produce Figures 3.3, 3.4, 3.5, E.7, E.8, and E.9 on pages 162, 163, 164, 301, and 302 respectively is given in Figure G.2 on page 315. The SURFACE II[36] computer code was used to produce the 3-D plots from the output data files OMEGA.DAT and TIME.DAT.

VITA

James Downing Freels was born in Morristown, Tennessee, on December 1, 1954 the son of James C. and Patricia Freels. After graduating from Morristown-Hamblen High School East in June 1972, he received his first experience in the engineering field through a summer job with Culley Engineering and Manufacturing Company of Whitesburg, Tennessee.

In the fall of 1972, he started his college education as a Mechanical Engineering major at Virginia Polytechnic Institute and State University in Blacksburg, Virginia. During his stay at V.P.I. & S.U., he participated in the co-op work study program with Tennessee Eastman Company of Kingsport, Tennessee. He completed four work quarters as an M.E. student with T.E.C.

In the spring of 1975, he transferred to the University of Tennessee in Knoxville. He obtained the Bachelor of Science degree in Nuclear Engineering on June 10, 1977. During his undergraduate study at U.T., he worked as a part time employee of the Tennessee Valley Authority in Knoxville from August 1975 to June 1977 on the design of principal piping systems for the Sequoyah-Watts Bar design projects.

In June 1977, he was awarded a graduate research assistantship from the Nuclear Engineering Department of the University of Tennessee. He obtained the M.S. degree in Nuclear Engineering in March 1979.

He is currently employed with Science Applications Incorporated in Oak Ridge, Tennessee.

Jim is married to the former Elizabeth Gilmore Little of Morristown, Tennessee. They currently reside in Clinton, Tennessee.